AD NUMBER
AD875741
LIMITATION CHANGES

TO:

Approved for public release; distribution is unlimited.

FROM:

Distribution authorized to U.S. Gov't. agencies and their contractors; Critical Technology; JUL 1970. Other requests shall be referred to U.S. Army Aviation Materiel Laboratories, Fort Eustis, VA 23604. This document contains export-controlled technical data.

AUTHORITY

USAAMRDL, ltr Jun 1971

USAAVLABS TECHNICAL REPORT 70-32A

2400°F UNCOOLED TURBINE/MATERIAL PROGRAM

VOLUME I

MATERIALS INVESTIGATION

By

M. S. Roush

F. Weber

July 1970

U. S. ARMY AVIATION MATERIEL LABORATORIES

FORT EUSTIS, VIRGINIA

U. S. ARMY
MATERIEL COMMAND

DISCLAIMERS

The research described herein was conducted by
the AiResearch Manufacturing Company, Phoenix,
Arizona, under U. S. Army Contract DA 44-177-
AMC- 83 (T). The work was performed under the
technical management of Lawrence E. Bell, Jr.,
Propulsion Division, U. S. Army Aviation Materiel
Laboratories.

Appropriate technical personnel of this Command
have reviewed this report and concur with the
conclusions and recommendations contained herein.

This document is Volume I of a three-volume
report and covers the materials investigation
conducted under the above-mentioned contract.
Volume II covers the turbine design portion of
the contract, and Volume III deals with the
evaluation of a fluidic temperature sensor system.

2400°F UNCOOLED TURBINE/MATERIAL PROGRAM

Final Report

VOLUME I

MATERIALS INVESTIGATION

By

M. S. Roush
F. Weber

Prepared by

AiResearch Manufacturing Company
A Division of The Garrett Corporation
Phoenix, Arizona

for

U. S. ARMY AVIATION MATERIEL LABORATORIES
FOR EUSTIS, VIRGINIA

BLANK PAGE

ABSTRACT

This volume of the uncooled-turbine program final report describes a materials investigation that was conducted to select, test-evaluate, and further develop materials that would be suitable for fabrication of high-temperature turbine components.

It has long been acknowledged within the turbomachinery field that one of the most advantageous achievements that could be realized in small gas-turbine engine technology would be the development of an uncooled turbine capable of operation in the 2400°F turbine inlet temperature (TIT) range. In 1964, a turbine design and materials research program was initiated with this specific goal. Design objectives included a TIT of 2400°F, a rotational speed of 38,000 rpm, an airflow rate of 5 lbs per sec, a compressor pressure ratio of 10:1, and a predicted total-to-total turbine efficiency of 88 percent.

The materials investigation included both company-sponsored and USAAVLABS-sponsored programs. The initial activities were conducted under company sponsorship and consisted of studies to determine the most desirable intermetallic composition for high-temperature (2400°F range) uncooled turbine components. These activities resulted in the development of a beryllide intermetallic composition, identified as Composition 1.

Specimen-type testing was then conducted under USAAVLABS sponsorship to evaluate the mechanical and physical properties of Composition 1 and those of high-temperature alloys, IN-100 and AiResist 13. Results from this test program showed that (a) IN-100 was suitable material for rotating turbine components in the 2000°F range, (b) AiResist 13 was suitable material for stationary turbine components in the 2000°F range, and (c) Composition 1, while believed to be the most feasible 2400°F uncooled-turbine component material available, had two major deficiencies that required resolution. These deficiencies were insufficient stress-rupture strength at 2400°F for stator or rotor application, and insufficient ductility below 2000°F.

Parallel activities were then conducted, which consisted of (a) cascade rig testing of Composition 1 under USAAVLABS sponsorship and (b) intermetallic composition studies under company sponsorship to improve the low-temperature ductility and high-temperature stress-rupture strength characteristics of Composition 1.

During the time that the specimen test program was being conducted, an activity under USAAVLABS sponsorship was initiated to design and develop a high-temperature (2400°F) cascade test rig. The purpose of this rig was to facilitate engine-environmental testing of a cascade of first-stage stator vanes fabricated from Composition 1 and having the geometry that resulted from the turbine design activities reported in Volume II.

Composition 1 rod-type specimens and first-stage stator vanes were subjected to oxidation and mechanical-integrity-type testing, respectively, in the cascade test rig. Test conditions simulated actual turbine operation, including temperature transients and steady-state temperatures in excess of 2400°F. The test results established that under engine conditions, Composition 1 did not have sufficient low-temperature ductility or high-temperature stress-rupture strength qualities to be adequate for either the uncooled-turbine rotor or stator components.

The composition studies, directed to develop an improved beryllide composition (Composition 2), did not achieve the degree of success that was required. While the Composition 2 material exhibited high-temperature stress-rupture strengths that exceeded the minimum requirement for stator application, it was still insufficient for rotor application. In addition, the low-temperature ductility qualities of Composition 2 were not improved over those of Composition 1.

In view of the cascade-test results and Composition 2 study products, it was decided that without extensive experimental research, it was not expedient to further pursue the use of beryllide compositions as turbine component materials for the subject application.

iv

FOREWORD

In May of 1964, a 4-year uncooled-turbine program was initiated in compliance with Contract DA 44-177-AMC-183(T) Task 1G162204A01409. The program was conducted under the control of the United States Army Aviation Materiel Laboratories (USAAVLABS), Fort Eustis, Virginia, by the AiResearch Manufacturing Company of Arizona, a division of The Garrett Corporation.

The overall program objective was to advance 1964 turbine component technology to a level that would facilitate the development of an uncooled turbine capable of operation at a TIT of 2400°F and a pressure ratio of 10:1. The turbine was to have application in a small gas turbine engine in the 5.0-pound-per-second-airflow class. The design of the uncooled turbine was based on the feasibility of developing an intermetallic beryllide composition with material properties sufficient for the turbine components. Benefits to be derived from such a turbine include significant improvements in power-to-weight ratio and specific fuel consumption (SFC) over those demonstrated by 1964 gas turbine engines of comparable size.

The analytical, experimental, and developmental efforts that were conducted during the subject program are described in the three volumes of the final report.

Volume I presents the results of material investigations (both USAAVLABS- and company-sponsored) that were conducted to develop a material that would be suitable for the turbine components of a 2400°F uncooled turbine.

Volume II presents the results of the aerodynamic, thermodynamic, and mechanical design activities that were conducted for the design of a 2400°F uncooled turbine.

Volume III presents the results of a test-evaluation program that was conducted to determine the feasibility of a fluidic temperature-sensing system for the measurement of TIT's in a 2400°F gas turbine engine.

The manager of the small gas turbine engine project was Mr. J. R. Parsons, and the program manager of this uncooled-turbine program was Mr. F. Weber. Principal contributing engineers were R. P. Craig, R. W. Elliott, J. L. Helmbrecht, R. F. Kirby, G. E. Lindstrom, J. J. Rebeske, C. R. Wheeler and A. E. Wilson. The principal engineering consultants were R. O. Bullock, M. S. Roush, and E. L. Wheeler. The overall

TABLE OF CONTENTS

ix

LIST OF ILLUSTRATIONS

x

xiii

xvii

LIST OF TABLES

LIST OF SYMBOLS

A	area
A_{lm}	log mean area
d	diameter
E	modulus of elasticity
f	resonant frequency
H	energy
I	current
K_S	thermal conductivity
L	gauge length
ℓ	length of specimen
m	mass
Q	heat flow
R	resistance
T	temperature
t	time
ε	emissivity
ΔP	pressure drop
ΔT	temperature gradient
ΔX	distance between thermocouples
Y	calculation constant
λ	wavelength
ρ	density of material

1. INTRODUCTION

This document describes the investigation that was conducted to develop a suitable material for the fabrication of un-cooled high-temperature turbine components. The uncooled turbine was designed for a small gas turbine engine in the 5.0-pound-per-second-airflow class, as reported in Volume II. The design objectives for turbine inlet temperature (TIT) and pressure ratio were 2400°F and 10:1.

1.1 PROBLEM STATEMENT AND OBJECTIVE

In addition to design complexities, the program objective of designing a small uncooled high-temperature turbine imposed a major materials problem. To resolve this problem, preliminary examinations of various types of high-temperature materials were made. It was immediately apparent that present-day high-temperature advanced alloys (SM 200, SM 302, IN-100, AiResist 13) were incapable of sustaining temperatures as high as 2400°F without use of cooling airflow. Therefore, consideration of present-day alloys for the fabrication of first- and second-stage turbine components was abandoned, and other materials were sought and examined for this application.

High-temperature materials that were considered for detailed research included refractory metals, ceramics, and inter-metallics. Certain advantages and disadvantages of each material group are presented in subsequent paragraphs.

1.1.1 Refractory Metals

The refractory metals include those metals with a melting point equal to or higher than that of chromium, namely, 3405°F.

Advantages of these materials include a high melting point, high temperature strength qualities, and use of conventional fabrication techniques.

However, the disadvantages of these materials--primarily the centrifugal stresses that result from the high material density and the poor resistance to oxidation--precluded further consideration for their use in the subject program.

1

1.1.2 Ceramics

Refractory ceramic groups that were examined were the borides, carbides, nitrides, silicides, and oxides.

Advantages of these inorganic nonmetallic materials include a high melting point, chemical and thermal stability, low thermal and electrical conductivity, and high strength-to-density ratios.

However, the disadvantage(s) of poor resistance to oxidation, lack of ductility, poor thermal shock resistance, or excessive creep, which were revealed in each group examined, precluded further consideration for their use in the subject program.

1.1.3 Intermetallics

Examination of the intermetallics and their properties revealed that the beryllides--a series of intermetallic compounds of beryllium and transition-element metals--offered considerable potential as materials for the subject application. The beryllide compounds that appeared to have the most advantageous characteristics were those consisting of zirconium, hafnium, niobium, molybdenum, columbium, and tantalum.

High-temperature strength, light weight, good oxidation resistance, and good thermal shock resistance are some of the advantages offered by the beryllides for the subject application.

The only undesirable feature revealed in the beryllides was their low ductility at room temperature. It was thought that this problem could be resolved by improvement of the processing procedures, reduction of impurities, and addition of alloying elements. Therefore, it was believed that development of the beryllides for use in the subject application would, indeed, contribute to the significant advancement of small gas turbine component technology, and efforts of the material investigation were directed toward accomplishing this objective.

Table I presents an activity flow chart that portrays the scope of the overall material investigation in sequential order, shows the interrelationship of the turbine design and material research activities, and, in addition, lists the paragraph numbers where appropriate discussion can be found in this document.

2

TABLE I. MATERIALS-RESEARCH ACTIVITY FLOW CHART

INITIAL HIGH-TEMPERATURE MATERIAL STUDIES TO SELECT CANDIDATE MATERIALS FOR 2400°F UNCOOLED-TURBINE COMPONENTS*

BERYLLIDE COMPOSITION STUDIES THAT DEVELOPED COMPOSITION 1, INTENDED FOR HIGH-TEMPERATURE STATORS*

USAAVLABS CONTRACT

COMPOSITION 1 TEST SPECIMEN DESIGN AND FABRICATION (2.2)

ESTIMATED MATERIAL PROPERTIES OF COMPOSITION 1

AIRESIST 13 AND IN-100 MATERIAL SPECIMEN TEST EVALUATIONS, INTENDED FOR EXIT-STAGE COMPONENTS

- ALLOY PREPARATION AND TEST SPECIMEN FABRICATION (5.2)
- TENSILE (5.4.1)
- STRESS RUPTURE (5.4.2)
- NOTCH RUPTURE (5.4.3)
- CREEP (5.4.4)
- OXIDATION (5.4.5)
- OXIDATION SULFI-DATION (5.4.6)
- MECHANICAL FATIGUE (5.4.7)
- THERMAL FATIGUE (5.4.8)

BERYLLIDE COMPOSITION STUDIES TO DEVELOP A COMPOSITION 2 MATERIAL FOR ROTOR APPLICATION (4.2)*

COMPOSITION 1 SPECIMEN TEST EVALUATIONS
- TENSILE (2.3)
- IMPACT (2.4)
- STRESS RUPTURE (2.5)
- CREEP (2.6)
- THERMAL FATIGUE (2.7)
- OXIDATION (2.8)
- OXIDATION SULFI-DATION (2.9)
- SPECIFIC HEAT (2.10)
- THERMAL EXPAN-SION (2.11)
- RADIANT EMIS-SIVITY (2.12)
- THERMAL CON-DUCTIVITY (2.13)
- MODULUS OF ELASTICITY (2.14)

MATERIAL REQUIREMENTS
- STRESS-RUPTURE
- TENSILE STRENGTH
- ELONGATION
- OXIDATION RESISTANCE

ACTUAL MATERIAL PROPERTIES DEMONSTRATED

UNCOOLED-TURBINE DESIGN (VOL. II)
PRELIMINARY DESIGN (2. IN VOL. II)
FINAL DESIGN (3. IN VOL. II)

TEST-RIG REQUIREMENTS
- TEMPERATURE
- AIRFLOW RATE
- PRESSURE RATIO
- TURBINE-COMPONENT GEOMETRY

CASCADE TEST RIG DESIGN AND DEVELOPMENT (3.2)
- CASCADE TEST SECTION (3.2.1)
- COMBUSTOR (3.2.2)
- CONTROL SYSTEM (3.2.3)
- TEST INSTRUMENTA-TION (3.4)
- RIG CHECKOUT AND HOT-CORROSION TESTING OF THREE BERYLLIDE COMPOSI-TIONS -- ROD SPECIMENS (3.5.2)

3-PIECE STATOR GEOMETRY

FABRICATION OF COMPOSITION 1 STATOR VANES (3.3)

TEST EQUIPMENT, INSTRUMENTATION, AND SPECIMEN DESIGNS

SPECIMEN TEST EVALUATION OF COMPOSITION 2 CANDIDATES -- STRESS-RUPTURE, OXIDATION, AND TENSILE ELONGATION TESTS (4.3)*

CASCADE TESTING OF COMPOSITION 1 STATOR VANES -- TWO TESTS AT 2400°F (3.5.3)

CONCLUSIONS:
- IN-100 WAS DETERMINED TO BE A SUITABLE MATERIAL FOR ROTATING TURBINE COMPONENTS IN THE 2000°F RANGE.
- AIRESIST 13 WAS DETERMINED TO BE A SUITABLE MATERIAL FOR STATIONARY TURBINE COMPONENTS IN THE 2000°F RANGE.

- COMPOSITION 1 HAD INSUFFICIENT STRESS-RUPTURE STRENGTH AT 2400°F AND INSUFFICIENT DUCTILITY BELOW 2000°F FOR STATOR OR ROTOR APPLICATION.
- COMPOSITION 2 CANDIDATES SHOWED STRESS-RUPTURE STRENGTH IMPROVEMENTS (SUFFICIENT FOR STATOR) BUT LACKED DUCTILITY BELOW 2000°F.

*COMPANY-SPONSORED ACTIVITIES

3

1.2 PERSONNEL HEALTH CONSIDERATIONS

Because of the known toxicity of beryllium metal and its compounds (e.g., beryllides), the prevention of illness due to contact with the beryllides required adherence to certain environmental control procedures:

1. Collecting samples of beryllide dust or fumes in the laboratory atmosphere periodically at the breathing level of personnel on Whatman No. 44 filter papers by use of a small vacuum air sampler. The beryllium in the dust collected was determined by colorimetric procedures. The in-plant atmospheric concentration of beryllium was not allowed to exceed 2 $\mu g/m^3$ of air as an average concentration throughout an 8-hour day.

2. Wearing a respirator and rubber gloves at all times when beryllide specimens were handled.

3. Performing all preparatory handling procedures under a hood with proven ventilation and appropriate filters.

4. Washing hands thoroughly with ample quantities of soap and water after handling beryllide materials. Eating, smoking, or otherwise touching the hands to the mouth after handling beryllides was strictly avoided before washing.

5. Using plastic bags for storage and packaging of beryllide waste prior to disposal.

6. Thorough rinsing of all equipment used for the fabrication of beryllide specimens with water.

7. Limiting areas where beryllide specimens were handled or processed to authorized personnel indoctrinated in safe handling practices.

All personnel working full time on the beryllide test program were required to undergo a medical examination every 6 months. In addition to the mandatory examinations, the company doctor performed other examinations as necessary to determine whether an illness or injury of these personnel had any connection with the beryllide work. During the term of the contract, no illness or injury of these personnel could be attributed to the beryllium material.

4

2. BERYLLIDE COMPOSITION 1 SPECIMEN TESTING

2.1 GENERAL

The beryllide composition designated as Composition 1 was established during a company-sponsored materials research program. Composition 1, identified as $CbBe_{10.6}$ plus 0.5-percent Al, was a mixture of the intermetallic compounds $CbBe_{12}$ and $Cb_2 Be_{17}$ with additional minor alloying elements. It was intended that this material would be used in the high-temperature stators of the subject turbine design.

The Composition 1 material was evaluated under USAAVLABS sponsorship to establish base-line mechanical and physical properties to which modified beryllide materials could be compared. The USAAVLABS-sponsored test evaluations included tensile, impact, stress-rupture, creep, thermal-fatigue, oxidation, oxidation-sulfidation, specific heat, thermal expansion, radiant emissivity, thermal conductivity, and modulus of elasticity type specimen testing.

All Composition 1 testing was accomplished at temperatures in excess of 2000°F for two major reasons: (a) attempts were being made to establish reliable tensile elongation values for ductility comparison purposes; and (b) previous work had shown that beryllides in general showed no measurable plastic deformation below temperatures of approximately 2000°F.

The test specimens, test procedures, and results are described in subsequent paragraphs.

2.2 TEST SPECIMENS

In general, fabrication techniques consisted of melting the required composition by the vacuum-induction technique, with alloying additions at various stages during the melt cycle. The ingot produced was mechanically reduced to -400 mesh powder. The powder was chemically cleaned to remove any contaminants accrued during the process procedure. The powder was then hot-pressed and sintered into shapes from which the various test specimens could be machined.

Preparation of the test specimens was accomplished by diamond sawing, grinding, and electrochemical machining. To prevent surface cracking of the test specimens during the grinding procedures, it was necessary to make a series of light grinding passes in lieu of heavy grinding loads.

Table II indicates the number and configuration of the test specimens machined.

The tensile, stress-rupture, and creep test specimens, Configuration 1D-1, were machined in accordance with Figure 1. This test specimen evolved after a number of trial specimens. A double reduced section was required, as shown in Figure 1, to allow gauge marks to be machined into the brittle material (circular groove) without resulting failure at the marks. No undercutting was allowed in transition regions of tapered sections to straight sections.

The impact test specimens, Configuration 1D-2, were machined in accordance with Figure 2.

The thermal-fatigue test specimens, Configuration 1D-3, were machined in accordance with Figure 3. Initially, the thermal-fatigue test specimen design was for a wedge-shaped specimen with a relatively large base by which it could be positioned. However, thermal shock failures occurred that were attributable to the large section change. Therefore, a specimen (shown in Figure 3) was designed that would endure a reasonable number of thermal cycles in order to obtain a comparison of thermal resistance. The specimens were cut from pressed and sintered test bars and finished to the required shape and dimensions by grinding procedures. During the testing, the specimens were held in a test fixture fabricated from Lava, the trade name for a high talc (magnesium silicate) material.
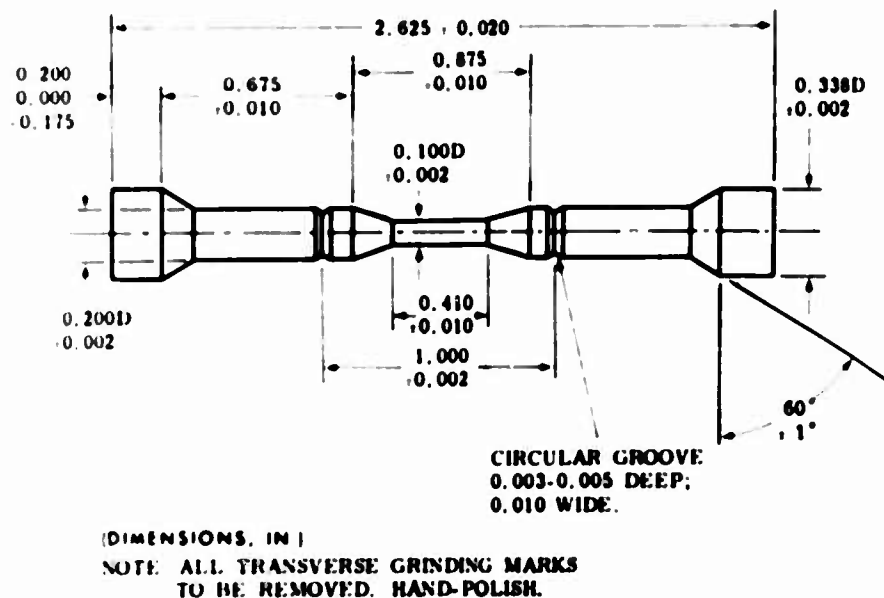
Figure 1. Tensile, Stress-Rupture, and Creep Test Specimen Design.

6

TABLE II. BERYLLIDE COMPOSITION 1 TEST SPECIMENS

Test	Test Temperature (°F)	No. of Specimens at Each Temp	Total	Test Specimen
Short-Time Tensile	2200 2400 2600 2800	3 3 3 3	12	1D-1
Stress Rupture	2400 2800	4 4	8	1D-1
Creep, 1% in Air	2200 2400 2800	4 4 4	12	1D-1 (See Above)
Impact	2200 2400 2600	2 2 2	6	1D-2
Thermal Fatigue	RT-2400-RT* RT-2800-RT	4 4	8	1D-3
Static Oxidation	To 2400	9	9	1D-4
Static Oxidation-Sulfidation	2400	18	18	1D-4
		TOTAL	73	

* RT is Room Temperature

7

0.250
±0.005

0.250
±0.005
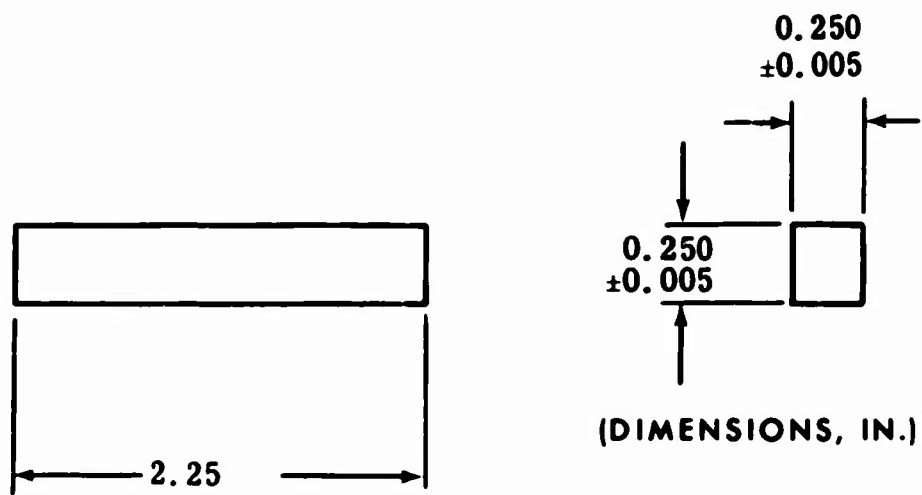
(DIMENSIONS, IN.)

Figure 2.   Impact Test Specimen Design.

0.750

0.250   0.750
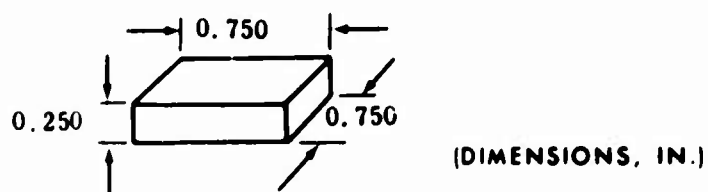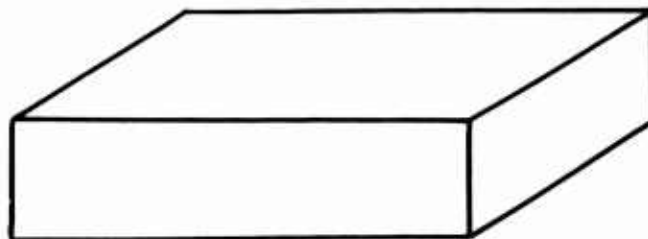
(DIMENSIONS, IN.)

Figure 3.   Thermal-Fatigue Test Specimen
Design.

8

The oxidation and oxidation-sulfidation test specimens, Configuration 1D-4, were cut from pressed and sintered test bars to the dimensions shown in Figure 4.
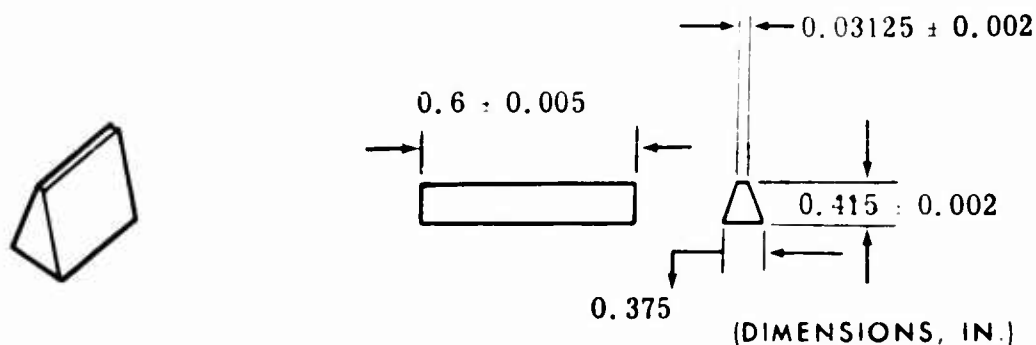
NOTE: SPECIMEN ANGLE IS 45°

Figure 4. Oxidation and Oxidation-Sulfidation Test Specimens.

2.3 TENSILE TESTS

Tensile tests were conducted at 2000°, 2200°, 2400°, 2600°, and 2800°F. The tests were conducted in an argon atmosphere to prevent destruction of the molybdenum grips at the high test temperature. Three specimens were tested at each temperature. The following subparagraphs describe the procedure and results of these tests.

2.3.1 Test Procedure

Elevated-temperature tensile testing was accomplished by conventional techniques with the exception of the requirements for specimen alignment. Testing of brittle materials in tension requires that good axial alignment of the specimen with the direction of load application be maintained. This prevents an unequal stress distribution across the test area and the resulting failure at an apparent stress lower than the actual. The "button head" ends of the specimen were held in a matching seat, in which they were free to rotate. Thus,

there was an opportunity for the specimen to align itself, in addition to the alignment permitted by the rotation of the joints in the testing fixtures. To prevent point or line contacts of the ends with the seat due to improper match, a thin slurry of beryllia powder in water was applied to the seat prior to installation of the specimen into the testing machine. A slight tension was then applied, and the specimen was allowed to align itself and form its own seating surface against the beryllia slurry, which subsequently dried to form a good contact area.

A constant head speed of 0.010 ±0.002 inch per minute was used during application of the load. The gauge length of the test specimens was 0.4 inch.

The 0.2-percent offset yield strength was determined from the stress-strain curve. The circular grooves around each shoulder of each specimen permitted attachment of an extensiometer and prevented slippage during test. For measuring elongation, the ends of the fractured specimen were fitted together, and the distance between gauge marks was measured. The elongation was reported as the increase in length of the gauge section expressed as a percentage of the original gauge length. The test temperatures were measured by two Pt-Pt, 10-percent Rh thermocouples positioned 1/16 inch from the gauge section surface. The test temperatures were also monitored by an optical pyrometer. The accuracy of the test specimen temperature measurements was estimated at ±20°F. Precautions were taken to prevent the thermocouples from contacting the beryllide specimen surface. At the elevated test temperatures, a chemical reaction would occur between the thermocouple point and the beryllium-containing specimen material. Therefore, thermocouple temperature measurements were only possible without physical contact. The test temperature was maintained for 15 minutes prior to performance of each tensile test.

2.3.2 Test Results

Ultimate strength and percent elongation results are tabulated and plotted versus temperature in Table III and Figure 5. The shape of the stress-strain curves produced during the tests made it difficult to establish a yield-strength value because of an indefinite yield-point indication.

TABLE III. BERYLLIDE COMPOSITION 1 TENSILE TEST RESULTS			
Test Temperature (°F)	Ultimate Strength (psi)	Yield Strength (psi)	Elongation (%)
2000	41,250	-	5.1
	40,300	-	5.5
2200	32,500	-	4.95
	36,800	35,600	4.95
	34,600	34,100	4.94
2400	19,800	19,400	7.5
	20,400	20,100	9.92
	22,400	-	10.05
2600	8950	8900	15.0
	10,000	9800	17.1
	8300	8000	17.5
2800	4880	-	31.4
	4125	-	32.7
	4125	-	33.1

Figure 6, ultimate tensile strength/density ratio versus temperature, was prepared to allow comparison of the strength of the beryllides (the density of Composition 1 was 3.02 g per cc) with the strength of other more common materials. Similar data for IN-100, a popular nickel-base superalloy, is also included in this figure for comparative purposes.

11
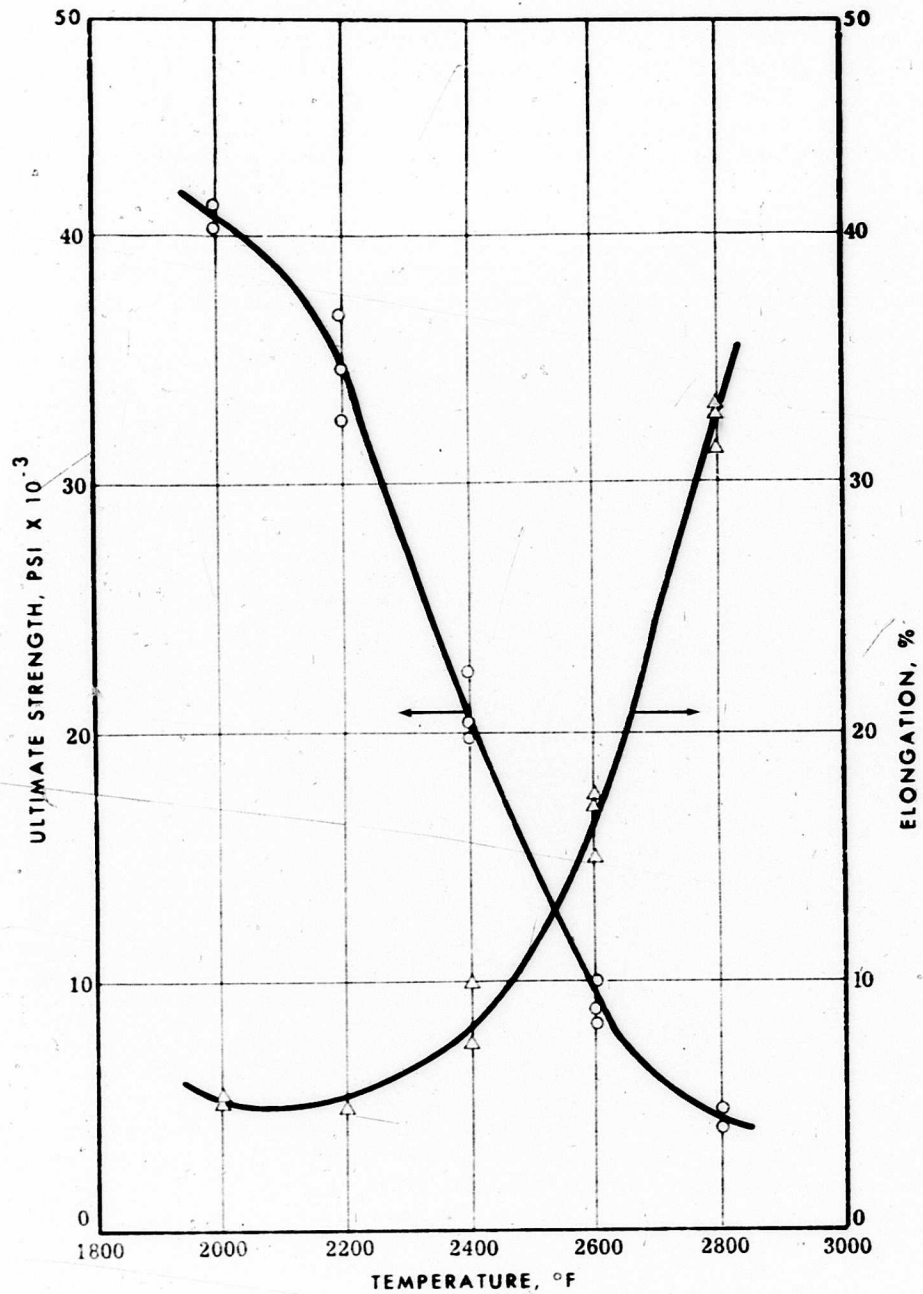
Figure 5. Beryllide Composition 1 Ultimate
Tensile Strength and Elongation.

12
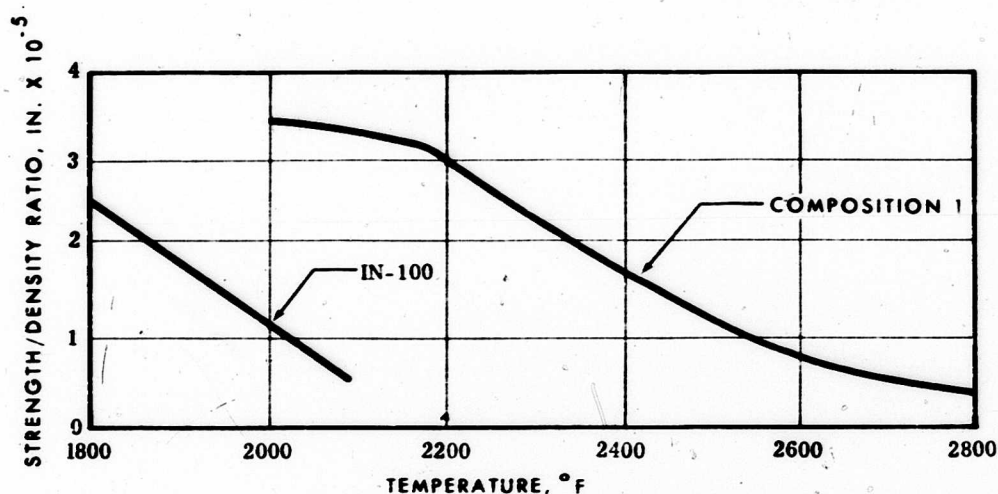
Figure 6.   Tensile Strength/Density Ratio for
IN-100 and Beryllide Composition 1.

2.4   IMPACT TESTS

Impact tests were conducted to define the toughness of beryl-
lide Composition 1. A minimum of two specimens each was
tested at 2200°, 2400°, and 2550°F. The following sub-
paragraphs describe the procedure and results of these tests.

2.4.1   Test Procedure

The impact testing was conducted by heating the test bar 50°
to 75°F above the required test temperature in a furnace.
The test specimen temperature was measured by an optical
pyrometer. The specimen then was removed from the furnace,
quickly placed in the impact fixture, and struck. The time
required to place the specimen in the fixture was measured
with a stopwatch, and the respective impact temperatures were
measured by plotting the measured time against a previously
determined time/temperature-loss graph. The impact values
were recorded in foot-pounds by a TMI impact tester with a
head speed of 11 feet per second.

13

2.4.2 Test Results

The impact test results are presented in Table IV and Figure 7. It is believed that the abnormal data scatter produced at 2400°F may have been the result of the test technique employed.

TABLE IV. BERYLLIDE COMPOSITION 1 IMPACT TEST RESULTS		
Test Temperature (°F)	Head Weight (lb)	Impact Strength (ft-lb)
2150	2	0.8
2160	2	0.28
2180	2	0.365
2185	2	0.25
2185	2	0.405
2350	2	1.25
2360	2	0.32
2520	2	0.345
2550	2	0.225
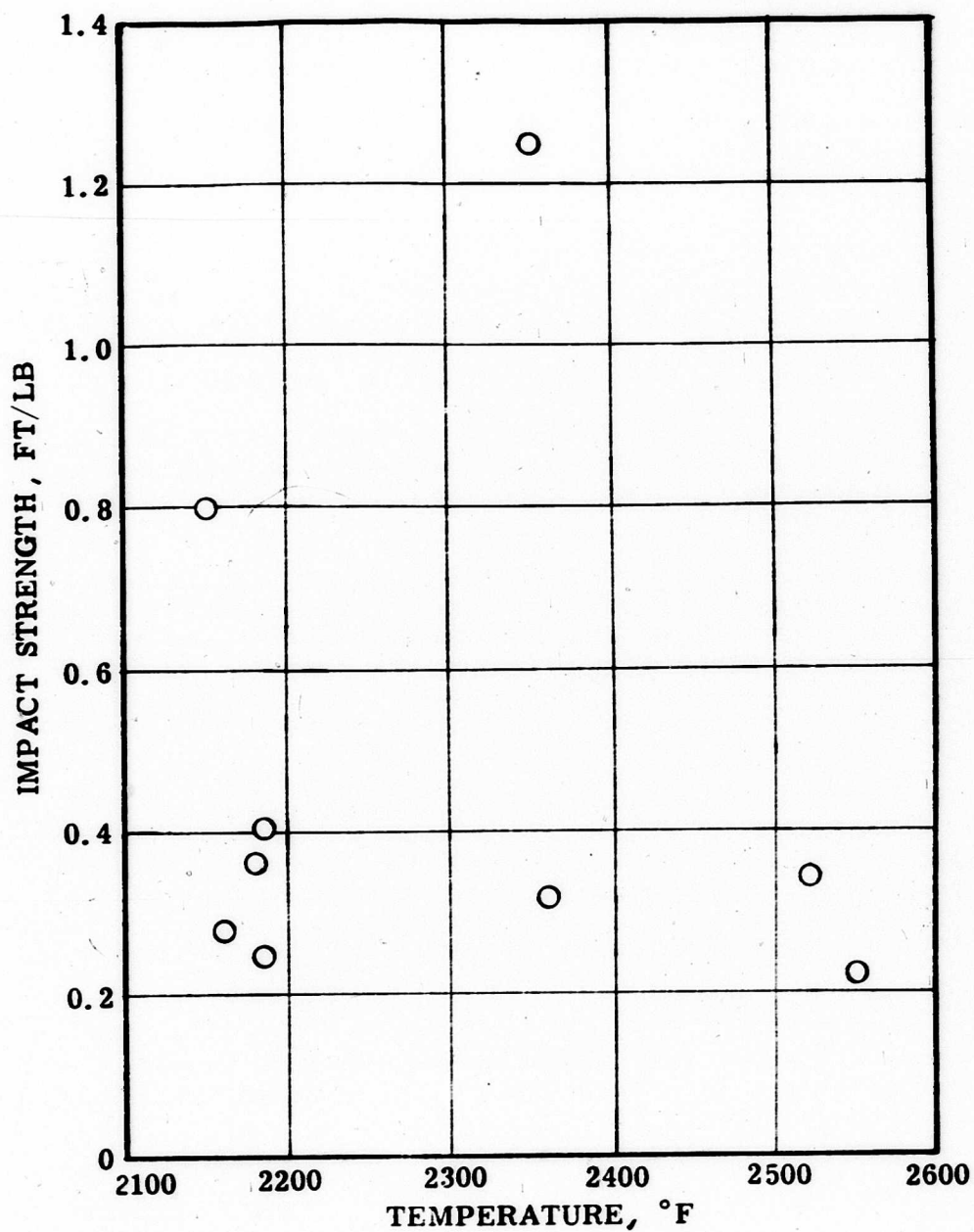
Figure 7. Beryllide Composition 1
Impact Strength.

15

2.5 STRESS-RUPTURE TESTS

Tests were conducted to determine the stress-rupture proper-
ties of beryllide Composition 1. The tests were conducted in
air at 2100°, 2300°, 2400°, 2500°, 2600°, and 2800°F. Eight
specimens were tested: two at 2400°F, two at 2600°F, and one
at each of the other temperatures. The following subpara-
graphs describe the procedure and results of these tests.

2.5.1 Test Procedure

For the lower temperature stress-rupture tests, Inconel 702
test fixtures were used. Chemical reaction with the metallic
fixture was prevented by coating the fixture with a beryllium
oxide slurry which, when dry, formed a boundary layer.

For the higher temperature stress-rupture tests, ceramic test
fixtures and a high-temperature tube furnace were used. To
obtain the desired stress application, the test specimens
were deadweight-loaded.

The test temperature was measured by Pt-Pt, 10-percent Rh
thermocouples positioned 1/16 inch from the gauge length sur-
face. Accuracy of the temperature measurement was estimated
to be ±20°F. An optical pyrometer was used to spot-check the
recorded temperatures. The elongation was determined as the
percentage of increase in length of the gauge section of each
specimen.

The applied stresses used during the stress-rupture tests
were selected to be in agreement with the anticipated stator
stress levels that were determined in the turbine design
studies reported in Volume II. At the completion of each
test, the rupture time and percentage of elongation were re-
corded, along with the applied stress and test temperature.

2.5.2 Test Results

The stress-rupture test results showed a good degree of cor-
relation and are tabulated (Table V) and graphically depicted
on a Larson-Miller curve (Figure 8).

16

Figure 8 depicts the stress-rupture failure points. In addition, the beryllide stress-rupture requirements for a three-piece stator design are shown for 2400°F. These requirements are a maximum stress of 2500 psi at 2400°F for 200 hours for a three-piece stator design, as determined in the design studies reported in Volume II. As can be seen on Figure 8, beryllide Composition 1 does not meet the stress-rupture requirements for the stator design.

Figure 9 presents stress-rupture/density ratio data of Composition 1, IN-100, and TZM (a molybdenum-base alloy) for comparison purposes. The density advantage of Composition 1 is not as important for stator application as it would be for rotor application.

	TABLE V. BERYLLIDE COMPOSITION 1 STRESS-RUPTURE TEST RESULTS			
Specimen No.	Test Temperature (°F)	Stress (psi)	Time to Failure (hr)	Elongation After Rupture (%)
PS 11A	2100	8000	35.7	6.25
PS 7A	2300	5000	32.6	9.6
PS 33B	2400	1500	26.4	-*
PS 34A	2400	2500	41.7	25.0
PS 15B	2500	3500	3.5	N/D
PS 36A	2600	1000	2.2	60
PS 36B	2600	500	46.4	67 **
PS 27B	2800	500	-	- ***

*Premature failure due to alloying with grips.

**Bar tested for 15.7 hr, power failure, bar reloaded and tested for 30.7 hr; total time 46.4 hr.

***Thermocouple failure; test bar broke during realignment.
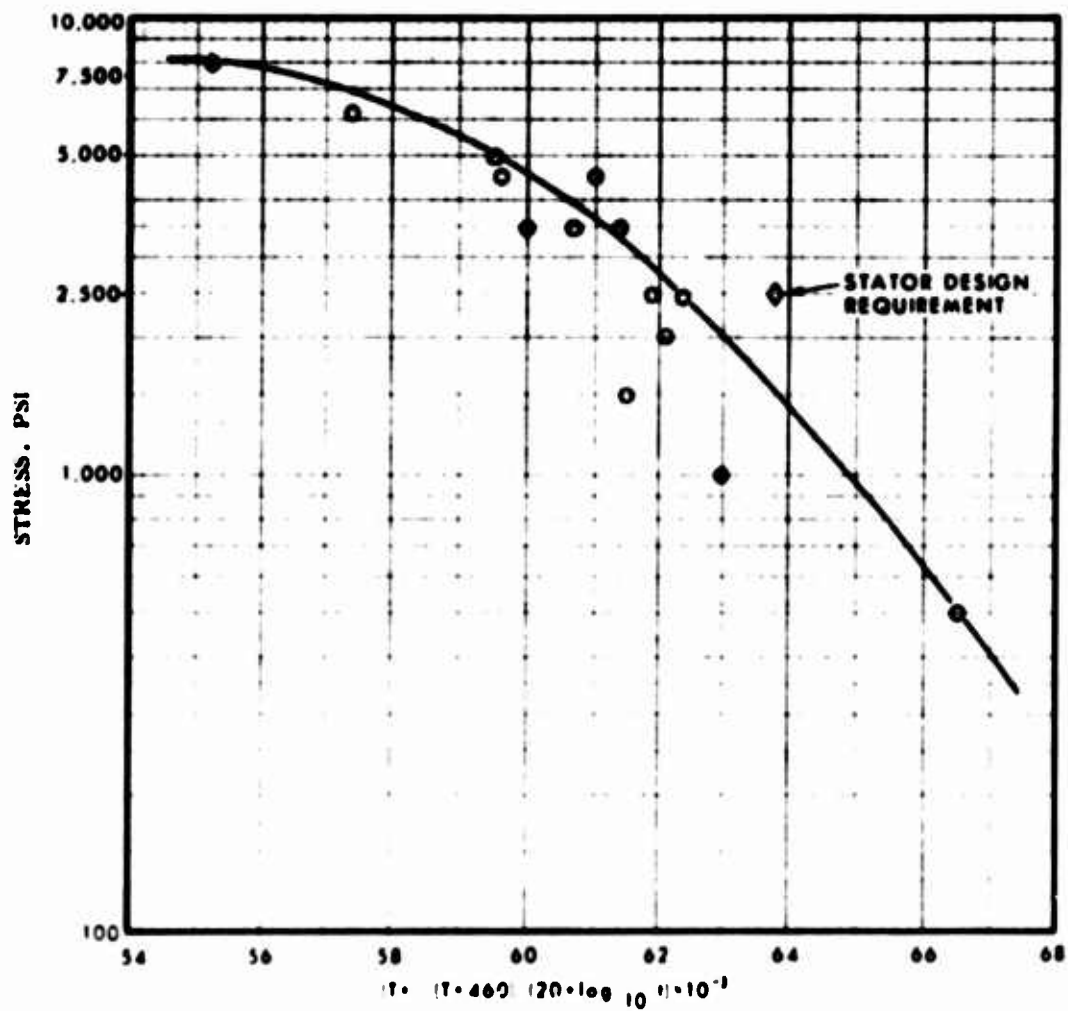
Figure 8.   Larson-Miller Stress-Rupture Curve
for Beryllide Composition 1.

18
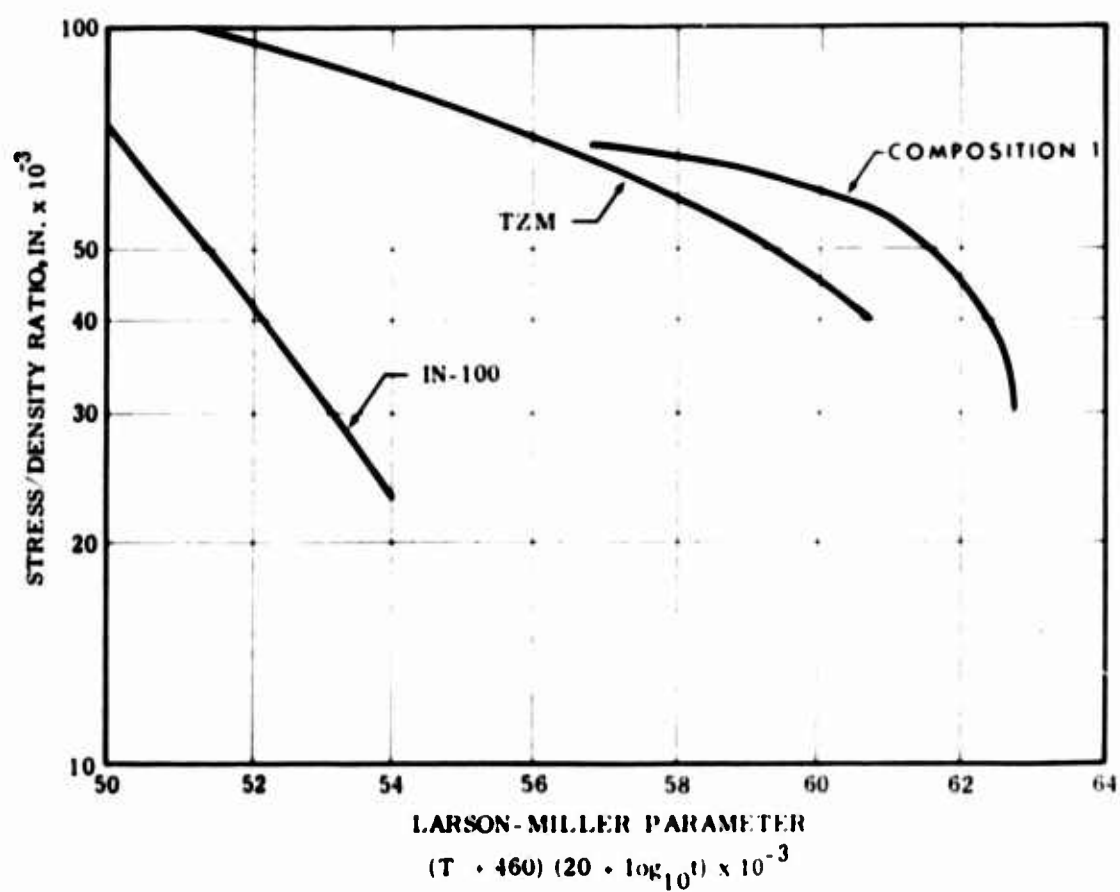
Figure 9. Stress-Rupture/Density Ratio of Beryllide Composition 1, IN-100, and TZM.

19

2.6 CREEP TESTS

Creep tests were conducted in air at 2200°, 2400°, and 2550°F. Nine specimens were tested: four at 2200°, four at 2400°, and one at 2550°F. The following subparagraphs describe the procedure and results of these tests.

2.6.1 Test Procedure

Ceramic test fixtures were used to conduct the Composition 1 test specimen creep testing. During each test the creep was measured by a dial indicator attached to the test fixture. The data were manually and automatically recorded.

Temperature control and recording were maintained by Pt-Pt, 10-percent Rh thermocouples and a Leeds and Northrup recorder. The accuracy of the temperature measurement was estimated to be ·20°F. An optical pyrometer was used to check the test temperatures periodically.

2.6.2 Test Results

Creep testing data were tabulated and are presented as curves (time versus percent elongation for various stress levels at each test temperature) in Figures 10, 11, and 12. Where possible, l-percent creep time was determined and is presented in the l-percent Larson-Miller curve shown on Figure 13.
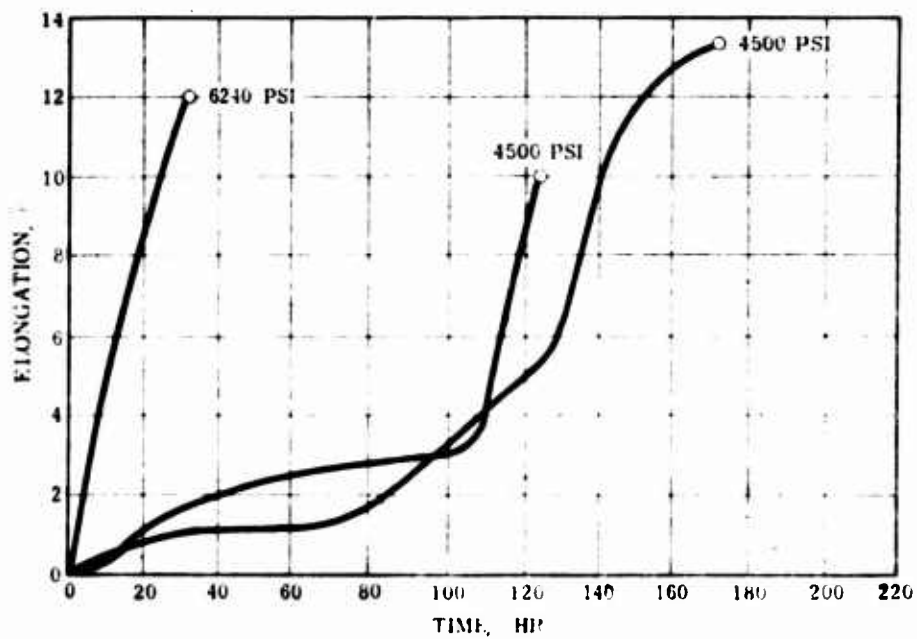
Figure 10.   Creep-Rupture Curve for Composition 1
             at 2200°F.
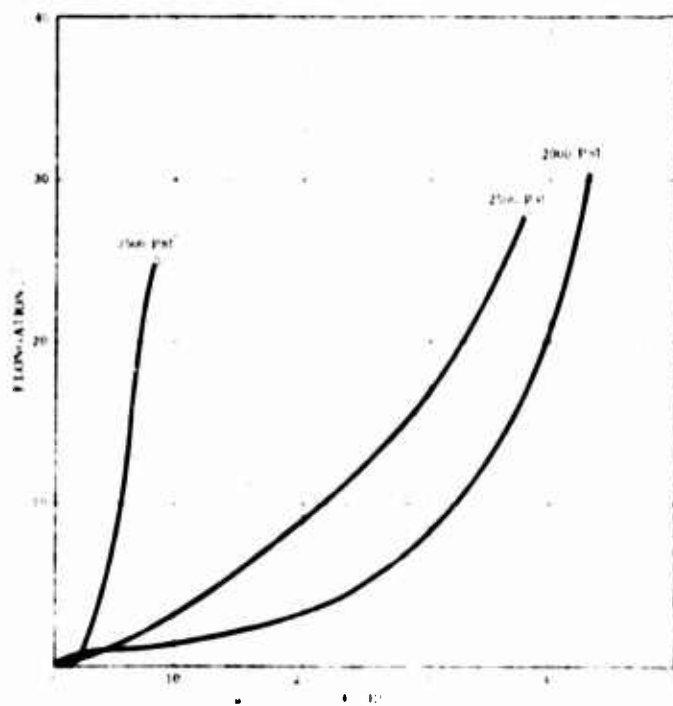
Figure 11.   Creep-Rupture Curve for Composition 1
             at 2400°F.

21
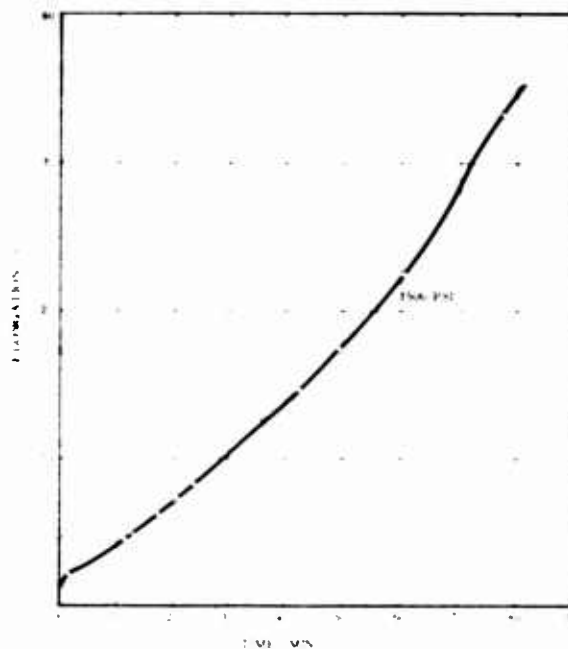
Figure 12. Creep-Rupture Curve for Composition 1
            at 2550°F.

STRESS, PSI

L-M PARAMETER

(T+460) (20+log 10 t) ×10⁻³
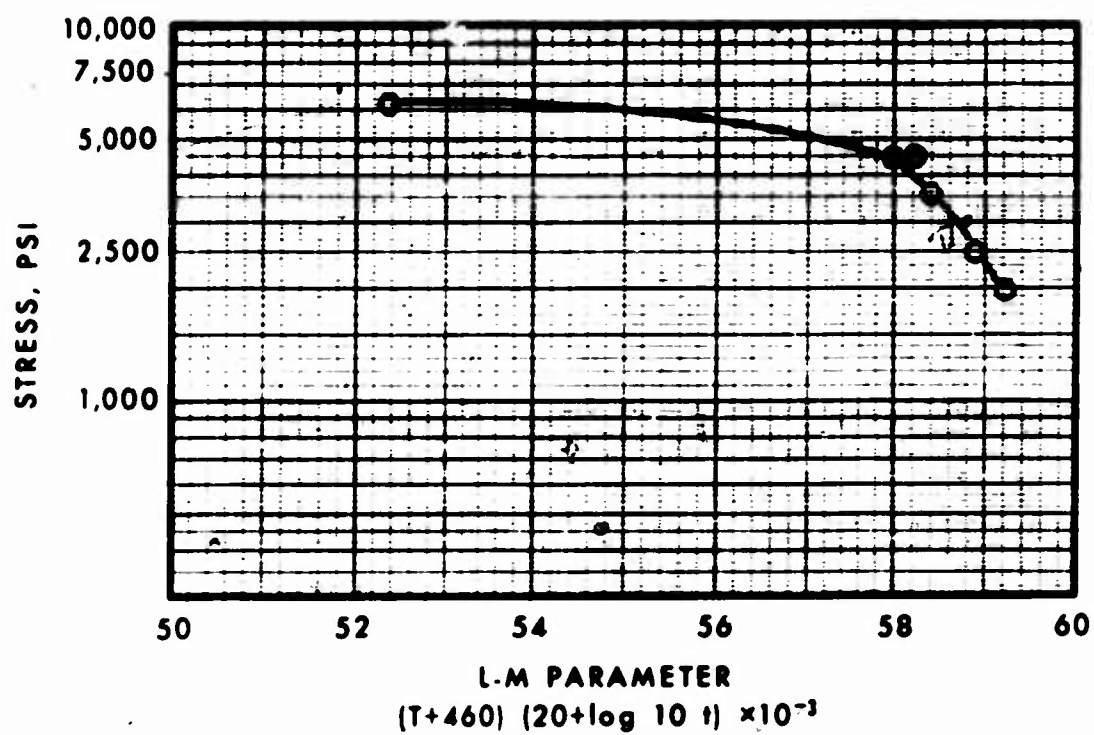
Figure 13. Larson-Miller 1-Percent Creep Curve.

22

2.7 THERMAL-FATIGUE TESTS

Thermal-fatigue properties of Composition 1 were determined by appropriate testing consisting of temperature cycles of 600° to 2400° to 600°F and 800° to 2600° to 800°F. Four specimens were subjected to each cycle until fracture occurred. The following subparagraphs describe the procedure and results of these tests.

2.7.1 Test Procedure

The thermal-fatigue testing was conducted in accordance with the procedure outlined in an ASTM paper* published in 1957.

The test specimens were heated by an oxygen-acetylene flame, shown in Figure 14, for approximately 25 sec, followed by an air blast directed at the leading edge of the specimen for 23 sec. The time/temperature cycle is shown in Figure 15. It was apparent from the tests that the test-cycle cooling time was the most critical control variable.

The leading edges of the specimens were immersed in the torch flame and were brought to temperature uniformly. The temperature was measured by an optical pyrometer. A gradient of approximately 600°F was experienced from the leading edge to the back of each specimen. No time was allowed for stabilization at the test temperature.

Four specimens were subjected to temperature cycles of 600° to 2400° to 600°F and to cycles of 800° to 2600° to 800°F until fracture occurred. The number of cycles was then recorded.

---

*Muscatell, Reynolds, Dyrkacz, and Dolkeim, THERMAL SHOCK RESISTANCE OF HIGH-TEMPERATURE ALLOYS, ASTM, 1957.
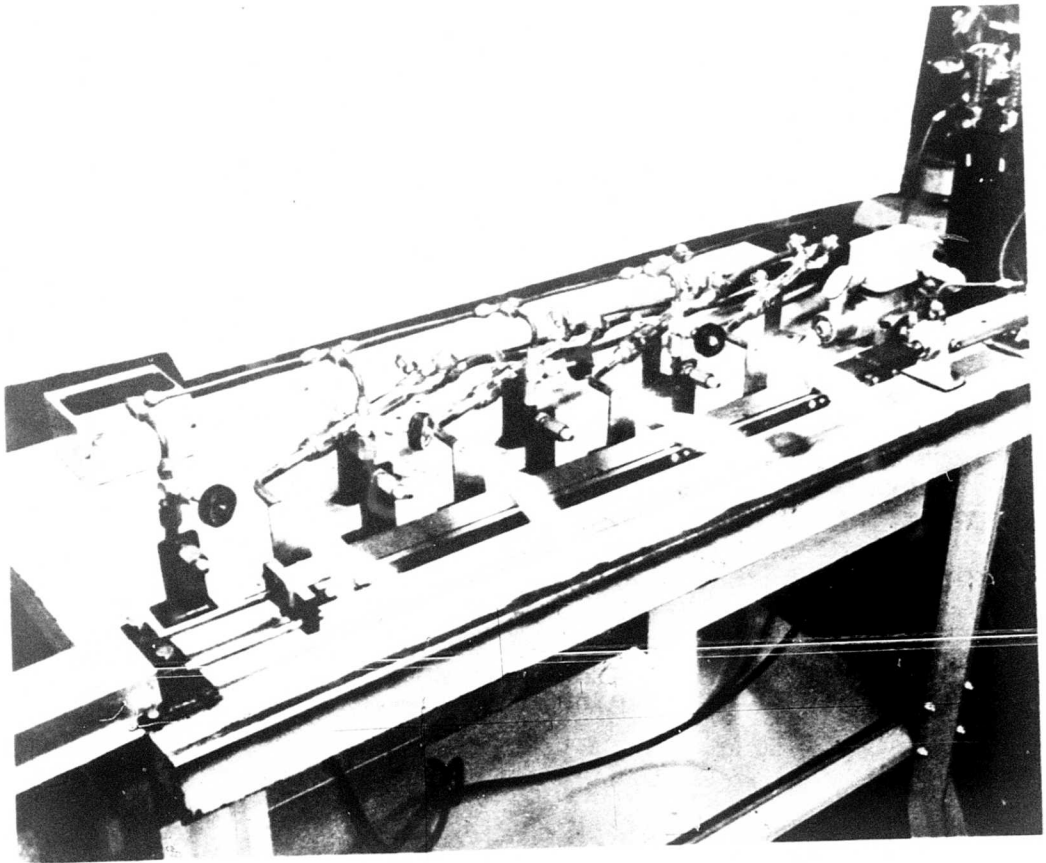
Figure 14. Oxygen-Acetylene Test Flame Rig.
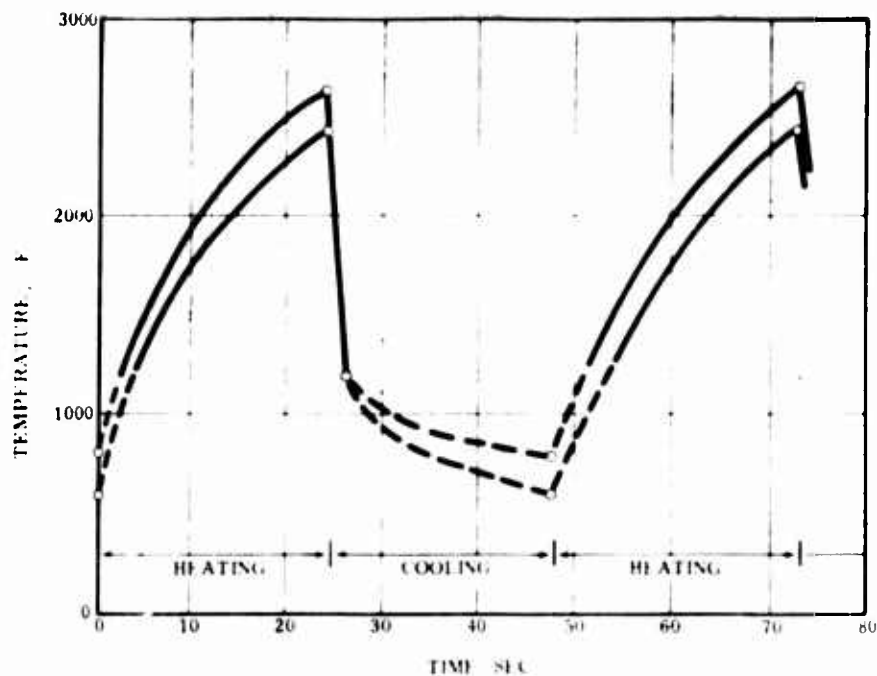
Figure 15.   Composition 1 Thermal-Fatigue Test
Specimen Time/Temperature Cycle.

2.7.2   Test Results

The thermal-fatigue test results are listed in Table VI and
are presented graphically in Figure 16. Figure 17 shows the
test specimens after completion of the test. It was found
that the thermal-fatigue properties increased with rising
temperature in the range tested. Some data scatter was
observed but was not considered to be abnormal. Conventional
materials were not included in the thermal-fatigue testing.

			Cooling Time (sec)		
			TABLE VI. COMPOSITION 1 THERMAL-FATIGUE TEST RESULTS		

Specimen No.	Temperature (°F)	Heating Time (sec)	Leading Edge to Black Heat	Total Time	Cycles to Fracture
AV-PS 42A	2400	25	2	23	25
AV-PS 42B	2400	25	2	23	8
AV-PS 42C	2400	25	2	23	11
AV-PS 42D	2400	25	2	23	10
AV-PS 35	2600	25	2	23	72
AV-PS 41A	2600	25	2	23	80
AV-PS 41B	2600	25	2	23	40
AV-PS 42E	2600	25	2	23	79
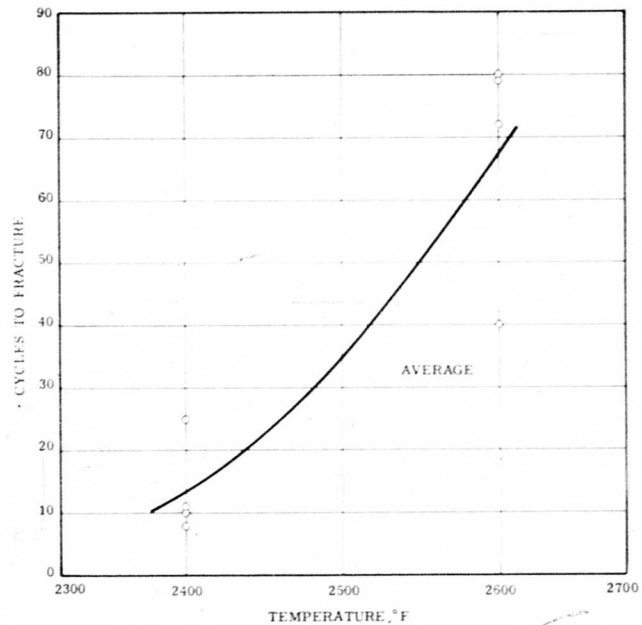
Figure 16.   Thermal-Fatigue Properties
of Composition 1.
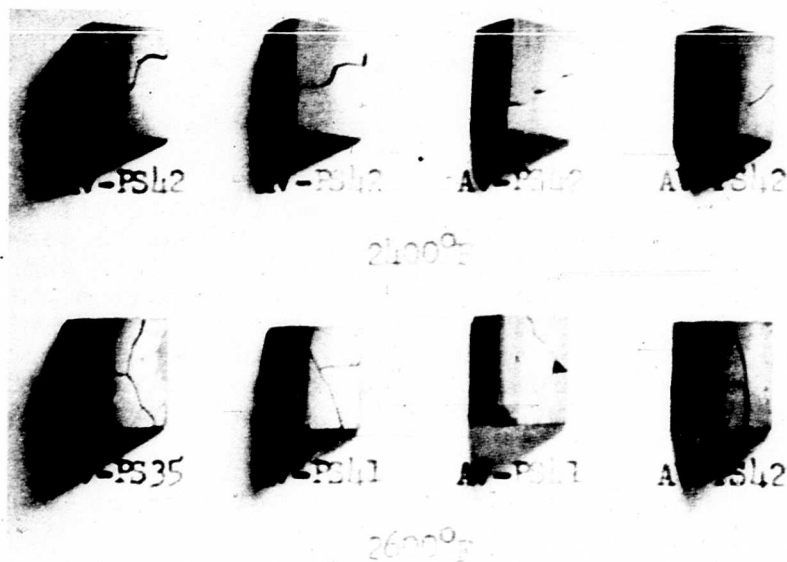
Figure 17.   Thermal-Fatigue Test Specimens
After Test Completion.

27

2.8 OXIDATION TESTS

Composition 1 test specimens were subjected to oxidation
tests in static air at 1700°, 1900°, 2100°, 2300°, and
2400°F. Five specimens were tested, one at each tempera-
ture. The following subparagraphs describe the procedure
and results of these tests.

2.8.1 Test Procedure

Prior to oxidation testing, each of the five test specimens
was weighed, and its surface area was accurately determined.
Each specimen was then cleaned by vapor-honing and was rinsed
in acetone. The cleaned specimens were placed in combustion
boats made of a zircon ($ZrO_2.SiO_2$) and alumina (Al_2O_3)
ceramic, which were then placed in a gradient furnace. The
specimens were arranged in the gradient furnace for the
desired exposure temperatures (1700°, 1900°, 2100°, 2300°,
and 2400°F).

The test was interrupted after 140 and 230 hours during the
300-hour test duration. At these intervals, the test speci-
mens were removed from the furnace, allowed to cool to room
temperature, and without cleaning, were weighed. The oxida-
tion corrosion per initial unit was calculated and plotted
versus time. The specimens showed first a gain, and then a
loss, in weight. The reason for this weight cycle is that
initially the oxide builds up (weight gain), and when it
reaches a sufficient thickness it begins to spall off (weight
loss).

2.8.2 Test Results

The oxidation test data are presented in Table VII and are
graphically illustrated in Figure 18. As can be seen in
Figure 18, specimens exposed to 1700° and 2400°F tempera-
tures exhibited the least resistance to oxidation. It was
believed that the problem at 1700°F was associated with the
"pest" phenomenon frequently observed in such compounds as
the beryllides, silicides, borides, and aluminides; that
is, the degeneration to a powder at some intermediate tem-
perature.

The oxidation test specimens after completion of the test are
shown in Figure 19.

28

TABLE VII. COMPOSITION 1 OXIDATION TEST RESULTS			
Test Temperature (°F)	Exposure Time (hr)	Weight Change (mg/in.^{2})	Cumulative Weight Change (mg/in.^{2})
1700	140	1.5	1.5
	230	36	37.5
	300	-5	32.5
1900	140	7	7
	230	0	7
	300	-3	4
2100	140	3	3
	230	0	3
	300	-4	-1
2300	140	-4	-4
	230	-2	-6
	300	0	-6
2400	140	125	125
	230	-83	42
	300	-41	1
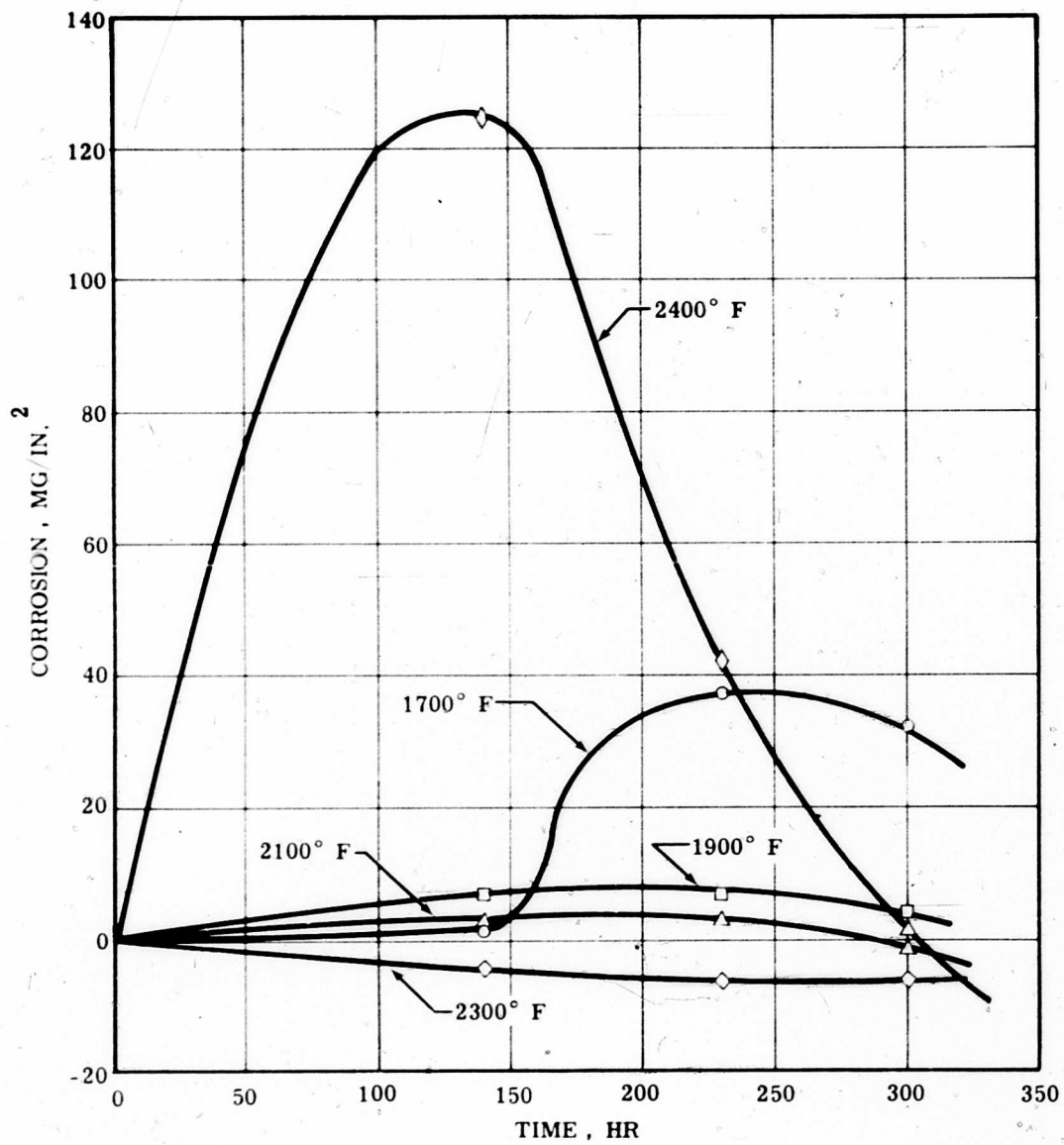
Figure 18. Beryllide Composition 1 Oxidation Tests.
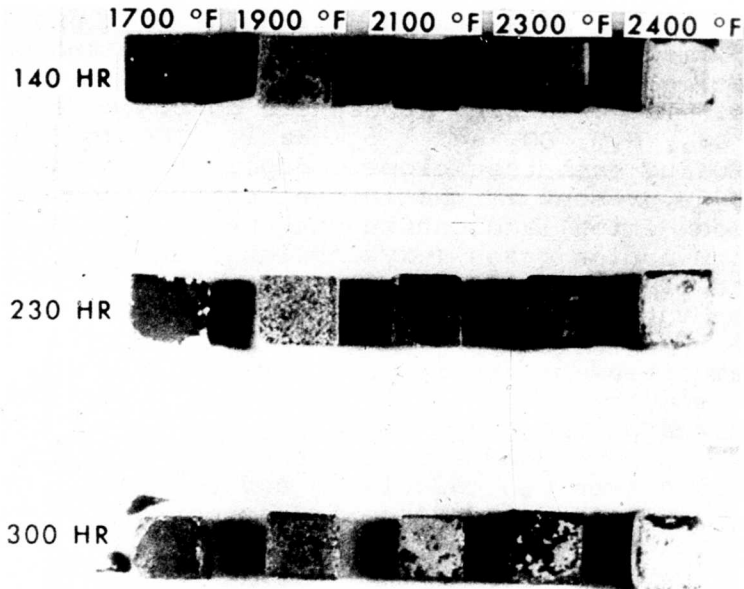
Figure 19. Composition 1 Test Specimens
After Oxidation Testing.

2.9 OXIDATION-SULFIDATION TESTS

Composition 1 test specimens were exposed to synthetic atmo-
spheres containing gaseous sulfur compounds to establish the
resistance of the material to oxidation-sulfidation corrosion.
The tests were conducted at 1600°, 1700°, 1800°, 2000°, 2200°,
and 2400°F. Three specimens were tested at each temperature.
Prior to testing, each specimen was weighed and its surface
area was determined. The following subparagraphs describe
the procedure and results of these tests.

2.9.1 Test Procedure

A special silica retort, used as the test chamber, was in-
stalled in a muffle furnace and was held in place by fire-
brick. Cubic test specimens were cut from previously pressed
and sintered beryllide test bars. The test specimens were
placed in Alundum "combustion boats" and were positioned in
the controlled hot zone of the silica retort. The specimens
then were exposed to an atmosphere that simulated JP-4 gas-
turbine combustion products in a marine-air environment,
which consisted of N_2, O_2, CO_2, H_2O, SO_2, H_2S, and NaCl. The
H_2S and SO_2 gas contents were increased to 100 times the
normal turbine combustion-product contents to obtain an ac-
celerated test.

31

Initially, the specimens were exposed to a reducing atmosphere consisting of N_2, CO_2, H_2O, H_2S, and 1 ppm NaCl for 2 hours. Immediately following the reducing atmosphere, the test specimens were subjected to an oxidizing atmosphere for 20 hours. The oxidizing atmosphere consisted of a mixture of N_2, O_2, CO_2, H_2O, SO_2 and 1 ppm NaCl. The use of these two cycles during each test closely duplicated a gas-turbine start when H_2S is present in the initial combustion gases (oxygen-starved condition) and continuous operation when SO_2 is found in the combustion gases (oxygen-rich condition). Both cycles were conducted with 1 ppm NaCl in the test gases to simulate operation in a marine environment.

After completion of the two test cycles, the specimens were removed from the retort, allowed to cool, cleaned by boiling in concentrated HNO_3, and wire-brushed. After cleaning, the specimens were weighed, and the net weight change per initial unit surface area was calculated and recorded. The data obtained were plotted and presented as corrosion-versus-temperature curves.

2.9.2 Test Results

The test specimens showed very little attack from the corrosive atmosphere. This same test is used to evaluate the resistance to sulfidation corrosion of superalloys, and the test specimens normally exhibit severe attack at 1600° to 2000°F. The beryllides showed good resistance to oxidation-sulfidation attack at every temperature tested.

Table VIII lists the results at each test temperature in weight change per unit area. Figure 20 graphically depicts the average weight change per unit area versus temperature. The oxidation-sulfidation test specimens after completion of the test are shown in Figure 21.

2.10 SPECIFIC HEAT TESTS

To support the design activities reported in Volume II, tests were conducted to determine the physical properties of Composition 1. Specific heat testing was conducted at temperatures from 500° to 2300°F. The following subparagraphs describe the procedure and results of these tests.

2.10.1 Test Procedure

The temperature-enthalpy curve for Composition 1 samples was determined from the temperature rise of a water calorimeter following the introduction of heated samples in a drop tube. Segments of tensile bar specimens, ranging in mass from 0.81 to 1.21 grams, were heated in a resistance furnace and were

32

TABLE VIII. COMPOSITION 1 OXIDATION-SULFIDATION TEST RESULTS		
22 Hours at Temperature		
Temperature (°F)	Weight Change (mg/in.^{2})	Average Weight Change (mg/in.^{2})
1600	0	+0.3
1600	+1	
1600	0	
1700	+4	
1700	+5	
1700	+2	+3.7
1800	0	
1800	0	
1800	0	0
2000	-2	
2000	-3	
2000	-3	-2.7
2200	+7	
2200	+7	
2200	+10	+8
2400	-23	
2400	-24	
2400	-20	-22.3
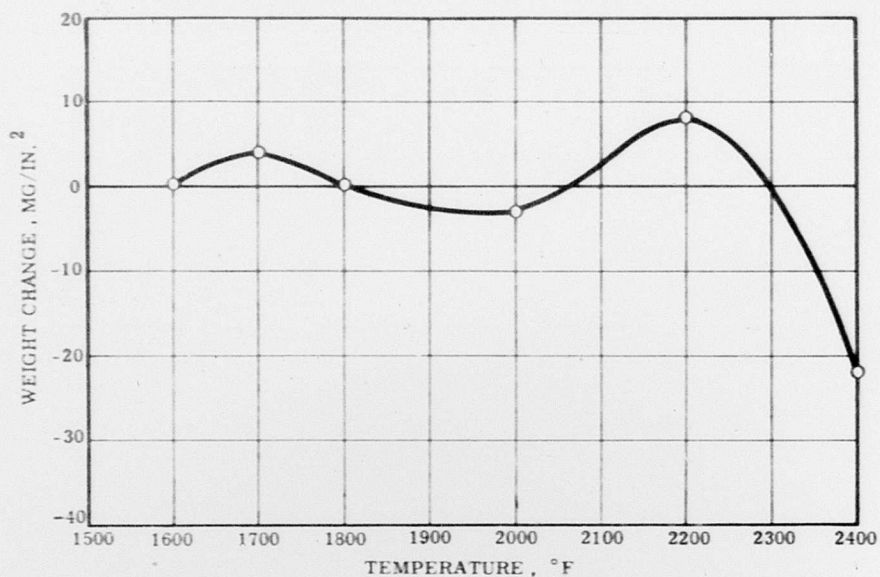
Figure 20. Average Weight Change per Unit Area Versus Temperature for Composition 1 Oxidation-Sulfidation Test Specimens.

1600°F

1700°F

1800°F

2000°F

2200°F

2400°F
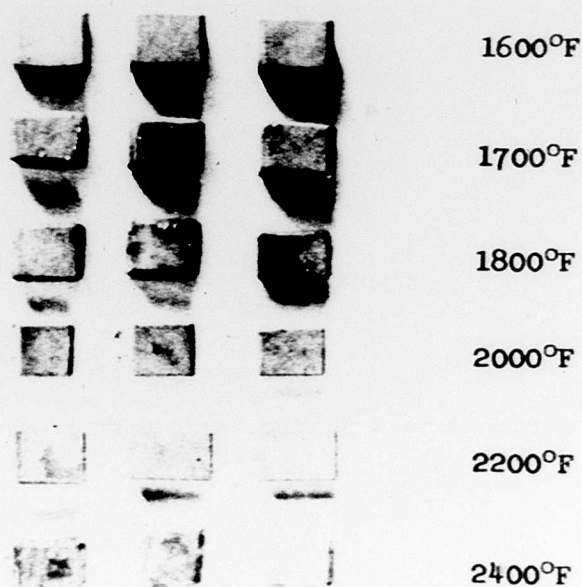
Figure 21. Composition 1 Test Specimens After Oxidation-Sulfidation Testing.

34

dropped through a stainless-steel tube into a nickel-plated, brass calorimeter cup immersed in water. The cup included a boron nitride liner and two shutters to minimize radiation and hot-air transfer.

Prior to testing the Composition 1 samples, the heat capacity of the test apparatus was determined from the temperature rise of the water calorimeter following introduction of a timed electrical current in a constantan coil of known resistance. The specific heat-test apparatus is shown in Figure 22. Testing was conducted at temperatures from 500° to 2300°F.

2.10.2 Test Results

The specific heat of beryllide Composition 1 was determined. Table IX summarizes the test results and the measurements; thus,

$$\Delta T = \text{experimentally measured temperature rise of the water calorimeter}$$

$$\Delta H_{total} = \text{amount of energy introduced to the constantan coil for a known time and resistance, } I^2Rt$$

This was calibrated directly by using a 4.08°F temperature increase and supplying a ΔH_{total} = 2880.

Therefore,

$$\frac{\Delta H}{\Delta T} = 706 \text{ joules/°F}$$

For each sample, ΔH_{total} was calculated by knowing the

$$\Delta H = \Delta H_{total} \text{ divided by the sample weight}$$

$$\text{Mean } \frac{\Delta H}{\Delta T} = \frac{Btu}{lb \text{ °F}} = \text{mean specific heat between ambient temperature and test temperature}$$

The reliability of sample F (Table IX) may be somewhat questionable, since the normal operating temperature of the boron nitride liner was exceeded. The last two lines of Table IX indicate an experimental check on the validity of

35
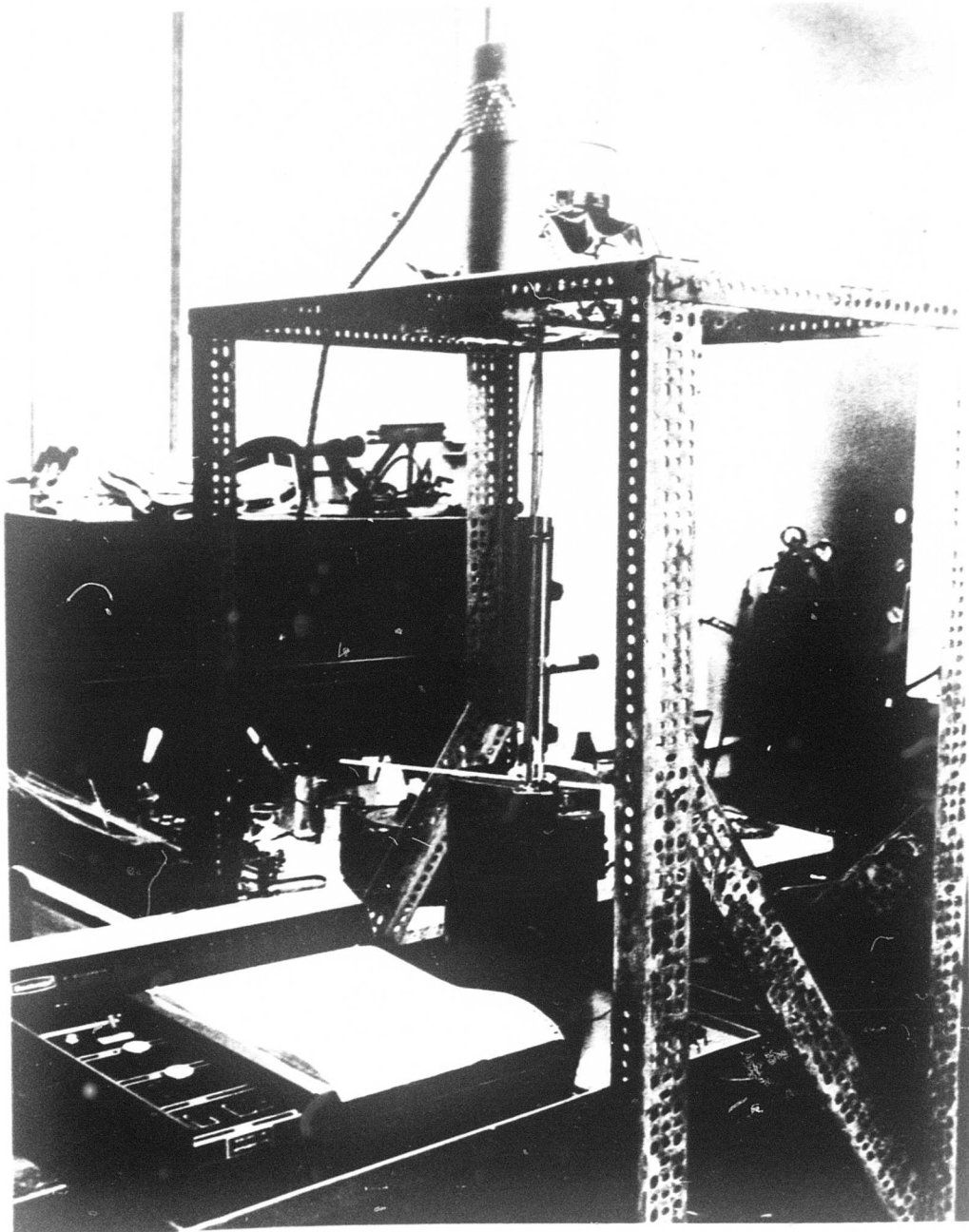
Figure 22. Specific Heat Test Apparatus.

TABLE IX. THERMAL PROPERTIES OF BERYLLIDE COMPOSITION 1

Sample	Weight (gm)	Temperature (°F)	$\frac{\Delta T}{°F}$	ΔH_{total} joules	ΔH j/g (per unit weight)	ΔH cal/g	ΔH Btu/lb	Mean $\Delta H/\Delta T$ (Btu/lb °F)
A	1.2109	491	0.52	367	303	72.5	130.3	0.314
B	1.2109	493	0.52	367	303	72.5	130.3	0.312
C	1.2109	1008	1.16	819	676	161.5	291	0.312
D	0.8134	1456	1.22	860	1057	253	454	0.329
E	0.8740	1922	1.765	1246	1428	341	614	0.333
F	0.9700	2300	2.62	1850	1910	457	820	0.369
G(Al)	1.2105	895	0.78	551	456	109	196	(experimental)
(Al) indirect calibration					459	109.7	197.7	(calculated)

37

the equipment using an aluminum specimen. A ΔH value of 196 was determined experimentally, which compared to a calculated value of 197.5 with the thermodynamic properties of the element known. This was less than 1 percent error.

Figure 23 shows a graph of ΔH versus temperature for beryllide Composition 1. The differential specific heat, dH/dT, was calculated for the intervals between drop temperatures, and the results are summarized in Table X. The last entry is of questionable reliability, as previously stated.
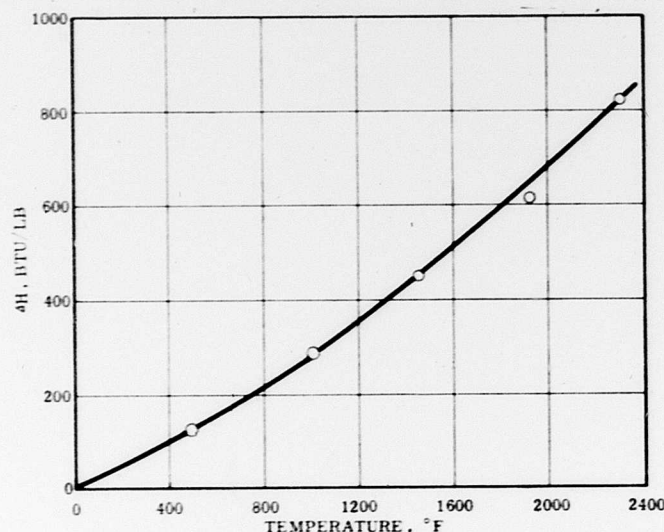
Figure 23. ΔH Versus Temperature for Composition 1.

TABLE X. DIFFERENTIAL SPECIFIC HEAT, COMPOSITION 1				
			Specific Heat	
Temperature (°F)			ΔH	dH/dT
T_2	T_1	$\overline{T}$	Btu/lb	Btu/lb °F
492	76	284	130.0	0.313
1008	492	750	160.7	0.311
1456	1008	1232	163	0.364
1922	1456	1689	160	0.343
2300	1922	2111	206	0.545

$$\overline{T} = \text{mean temperature} = \frac{1}{2}(T_2 - T_1) + T_1 = \frac{T_2 + T_1}{2}$$

38

2.11 THERMAL EXPANSION TESTS

Thermal expansion tests were conducted at temperatures from room temperature to 2300°F. The following subparagraphs describe the procedure and results of these tests.

2.11.1 Test Procedure

The thermal expansion and thermal expansion coefficient for beryllide Composition 1 were measured by an electric furnace and quartz dilatometer. A machinist's dial indicator (direct reading to 0.0001 inch) was screw-mounted to a sleeve to which a fused quartz tube was attached with epoxy cement. This allowed differential length changes to be recorded. A free-floating quartz rod inside the tube provided thermal isolation of the sample from the indicator. The cylindrical sample was inserted at the far end of the quartz tube and was held in place with a quartz pin. The resulting expansion versus temperature curve was corrected for the expansion of the fused quartz section containing the sample. The tests were conducted at temperatures from room temperature to 2300°F. The test apparatus is illustrated in Figure 24.

Figure 24. Thermal Expansion Test Apparatus.

2.11.2 Test Results

The thermal expansion and thermal expansion coefficient for beryllide Composition 1 were determined. Figure 25 depicts the thermal-expansion data obtained, while Figure 26 graphically presents the coefficient of thermal expansion.

39
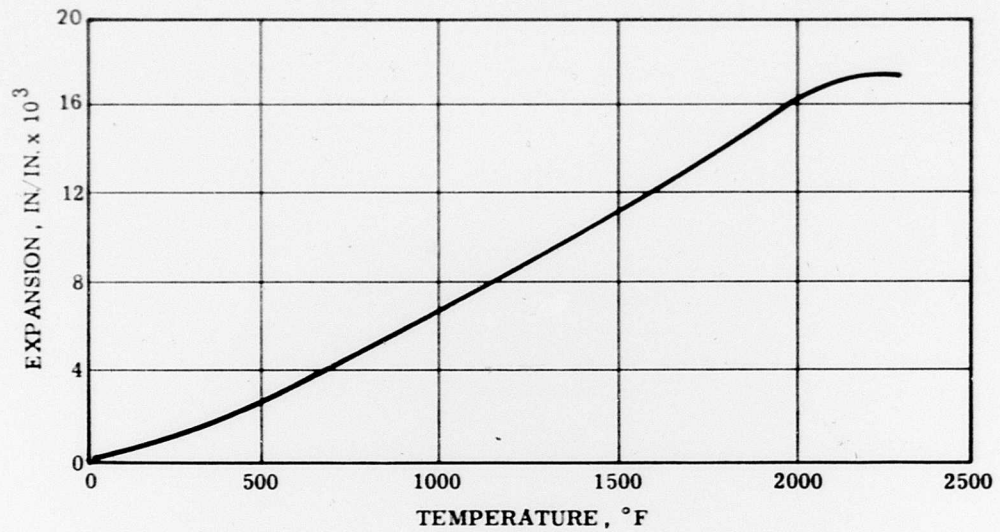
Figure 25. Thermal Expansion of Beryllide
Composition 1.
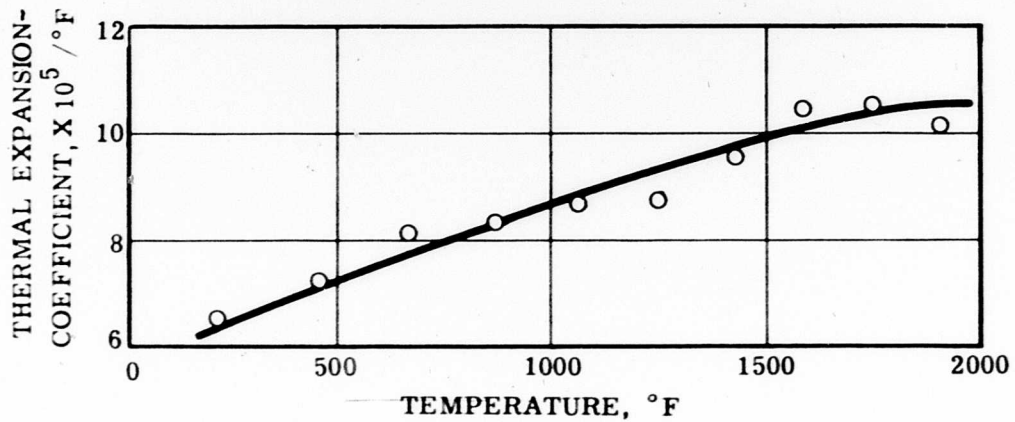
Figure 26. Thermal Expansion Coefficient
for Beryllide Composition 1.

40

2.12 RADIANT EMISSIVITY TESTS

Radiant emissivity measurements were made at room temperature, 1300°, 1500°, 1800°, and 2100°F. The following subparagraphs describe the procedure and results of these tests.

2.12.1 Test Procedure

The emissivity of beryllide Composition 1 was measured by comparing the radiant power emitted by an initially polished slab sample mounted in an electric furnace with the comparable signal from a cavity formed by an oblique surface of alumina ceramic and the side face of the beryllide. This was considered to act as a gray-body source with $\epsilon = 0.95$. Spectral measurements were made at 1300°, 1500°, 1800°, and 2100°F. In addition, room-temperature reflectivity measurements were made. The data were measured on a spectrophotometer over the wavelength region of 2.5 to 16 microns. Shortwave readings were also taken with an optical pyrometer. The test apparatus is illustrated in Figure 27.

2.12.2 Test Results

It was observed that the radiant intensity and, hence, the emissivity of beryllide Composition 1 increased progressively with the surface oxidation of the sample. After 3 or 4 hours at temperatures in excess of 1800°F, little change upon further heat aging was observed. The results of the measurements are shown in Figure 28. The abscissa increases uniformly with the integrated black-body energy curve, so the ratios of areas below the curves to the rectangular area for $\epsilon = 1$ give the total emissivity. For high emitting materials, the normal emissivity may be taken as equal to the hemispherical emissivity, which is of importance in heat-transfer calculations.

Graphical integration of the measured values resulted in the following values:

76°F (unoxidized)	$\epsilon = 0.077$
1800°F	$\epsilon = 0.81$
2100°F	$\epsilon = 0.91$
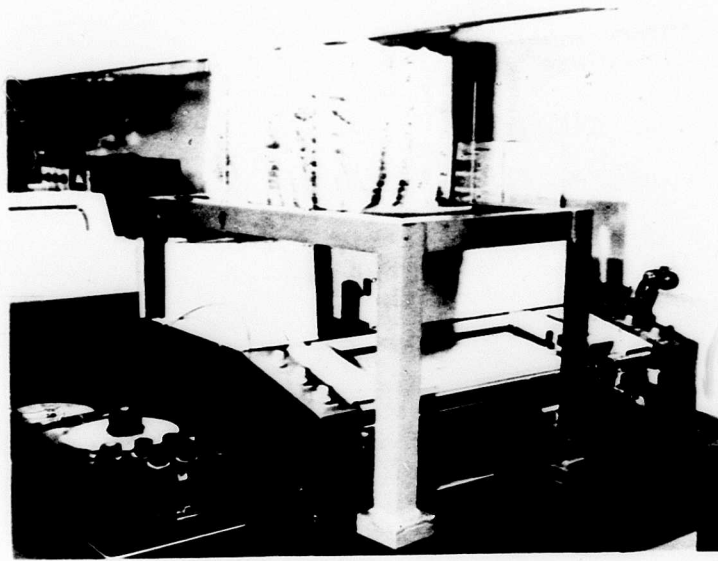
Figure 27. Radiant Emissivity Test Apparatus.
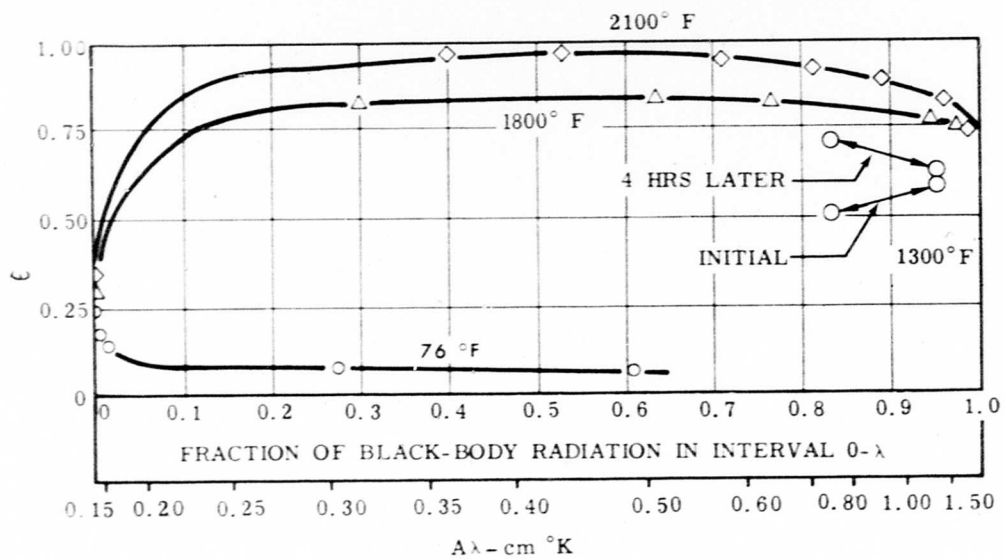
Figure 28. Radiant Emissivity of Beryllide
Composition 1.

2.13 THERMAL CONDUCTIVITY TESTS

Thermal conductivity measurements were made at temperatures ranging between room temperature and 2400°F. The following subparagraphs describe the procedure and results of these tests.

2.13.1 Test Procedure

Thermal conductivity measurements of beryllide Composition 1 were conducted. Values to 1700°F were obtained when a comparative rod apparatus with Type 316 stainless steel conductivity references was used. Basically, thermal conductivity was determined by measuring both the heat-flux density flowing axially through a cylindrical beryllide specimen and the temperature gradient along a known axial gauge length. The heat-flux density was determined with two Type 316 stainless-steel reference pieces of known thermal conductivity placed coaxially at the top and bottom of the beryllide specimen. The temperature was measured by Pt-Pt, 10-percent Rh thermocouples installed in the specimens. The Type 316 stainless-steel references and the beryllide specimens were 1 inch in diameter and length, with 0.75-inch gauge sections. Radial heat losses were carefully controlled with guard heaters. The tests were conducted in helium.

The thermal conductivity to 1700°F was calculated from the relation

$$K_s = \frac{(K_1 \Delta T_1 - K_2 \Delta T_2)}{(2 \Delta T_s)} \frac{\Delta X_s}{\Delta X_r}$$

where K_1 and K_2 are the thermal conductivities of the upper and lower reference pieces; ΔT_1, ΔT_2, and ΔT_s are the temperature gradients on the upper and lower references and the test specimen, respectively; and ΔX_s and ΔX_r are the distances between thermocouples in the specimen and the references.

A radial-inflow apparatus was employed to determine thermal conductivities at higher temperatures. The specimens were radiantly heated in a graphite furnace purged with helium. Thermal conductivities were determined from measurements of the radial heat flux and temperature gradients in the beryllide specimen. Heat flux was determined with a water calorimeter that passed along the center of the specimen. The radial temperature gradient was measured between holes drilled on different radii with the use of both thermocouples and an

43

optical pyrometer. The test specimen was placed coaxially between two guards, 1 inch in diameter by 0.50 inch in length, of the same material. Axial losses were minimized by situating the test specimen and guards between graphite cylinders packed with carbon.

The thermal conductivity values above 2000°F were computed from the relation

$$K = \frac{QL}{\Delta T A_{lm}}$$

where Q is the heat flow to the calorimeter, A_{lm} is the log mean area for the specimen, ΔT is the specimen temperature change, and L is the gauge length over which ΔT was measured.

Specimens of IN-100, a nickel-base superalloy, were included during testing. The data obtained allowed comparison of the thermal conductivity of beryllide Composition 1 with that of a superalloy.

2.13.2 Test Results

The thermal conductivity of beryllide Composition 1 was determined in helium from 82° to 1789°F with the comparative rod apparatus and from 2067° to 2379°F with the radial-inflow apparatus. Figure 29 illustrates the results of these tests. In addition, the test results for IN-100 are included for comparison. The conductivity increased linearly from 144 to 210 Btu/hr/ft³/°F/in. at 100° and 2400°F, respectively.
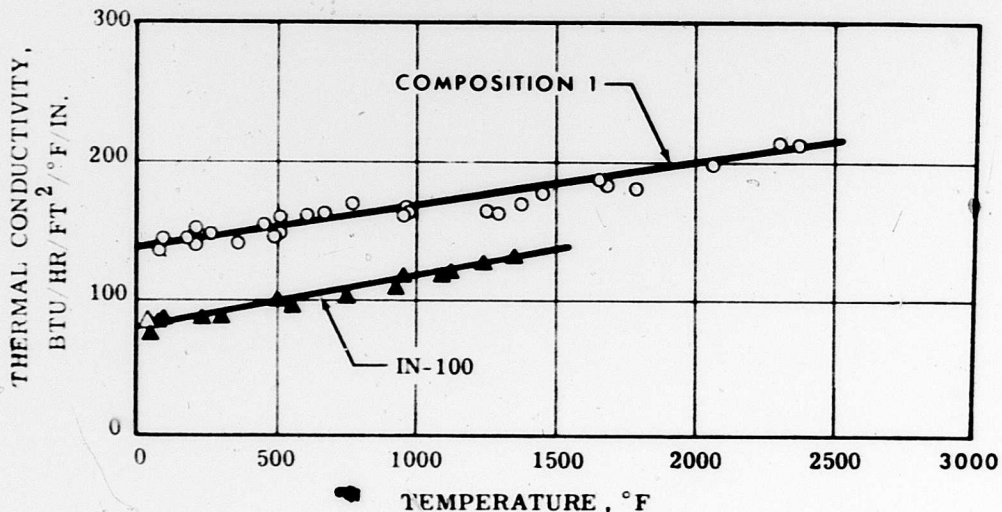
Figure 29. Thermal Conductivity of Beryllide Composition 1 and IN-100.

44

2.14 MODULUS OF ELASTICITY TESTS

The adiabatic modulus of elasticity was determined by measuring the velocity of longitudinal compression waves in a cylindrical sample of beryllide Composition 1. The modulus was measured as a function of temperature to 2350°F. The following subparagraphs describe the procedure and results of these tests.

2.14.1 Test Procedure

The mechanical resonance technique was used to determine the recorded values. The beryllide rod specimen was suspended in a horizontal position by two quartz rods which were inserted in a vertical furnace. As illustrated in Figure 30, these rods were fastened to the armatures of two phonograph cartridges, one of which was driven by an audio-oscillator through an amplifier. The resulting transverse vibration of the specimen was detected in the second cartridge, and these frequencies were measured with an EPUT counter. The test schematic is illustrated in Figure 31. The temperature of the specimen was measured both with thermocouples and with an optical pyrometer. In all cases, the temperatures measured by the two methods agreed within 30 degrees. The test apparatus setup is shown in Figure 32.

When the specimen resonated at its fundamental or first overtone mode of vibration, an increase in vibrational amplitude was noted. These frequencies are related to the modulus of elasticity by the relations

$$E = 1.26 \; (\rho \ell^4/d^2) \; f_1^2 \; Y_1 \quad \text{for the fundamental mode}$$

or

$$E = 0.17 \; (\rho \ell^4/d^2) \; f_2^2 \; Y_2 \quad \text{for the first overtone mode}$$

where
E = modulus of elasticity

ρ = density of the material

ℓ = length of the specimen

d = diameter of the specimen

f = resonant frequency

Y = a constant

45
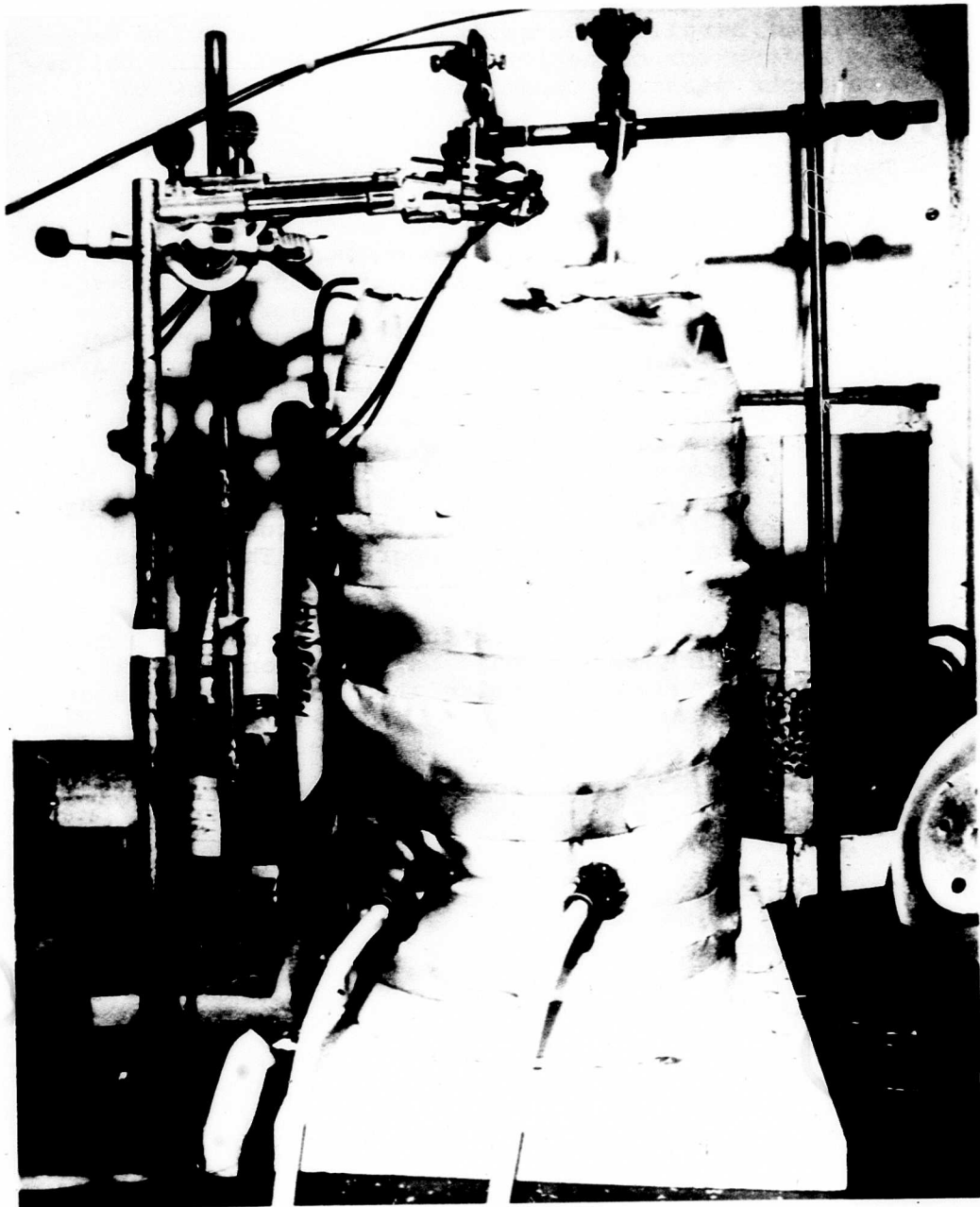
Figure 30. Furnace for Modulus of
Elasticity Measurements.
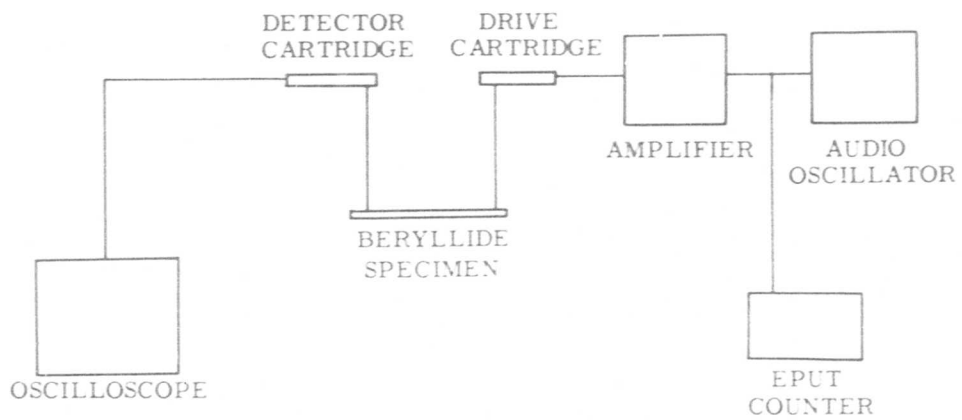
Figure 31.   Modulus of Elasticity Schematic.
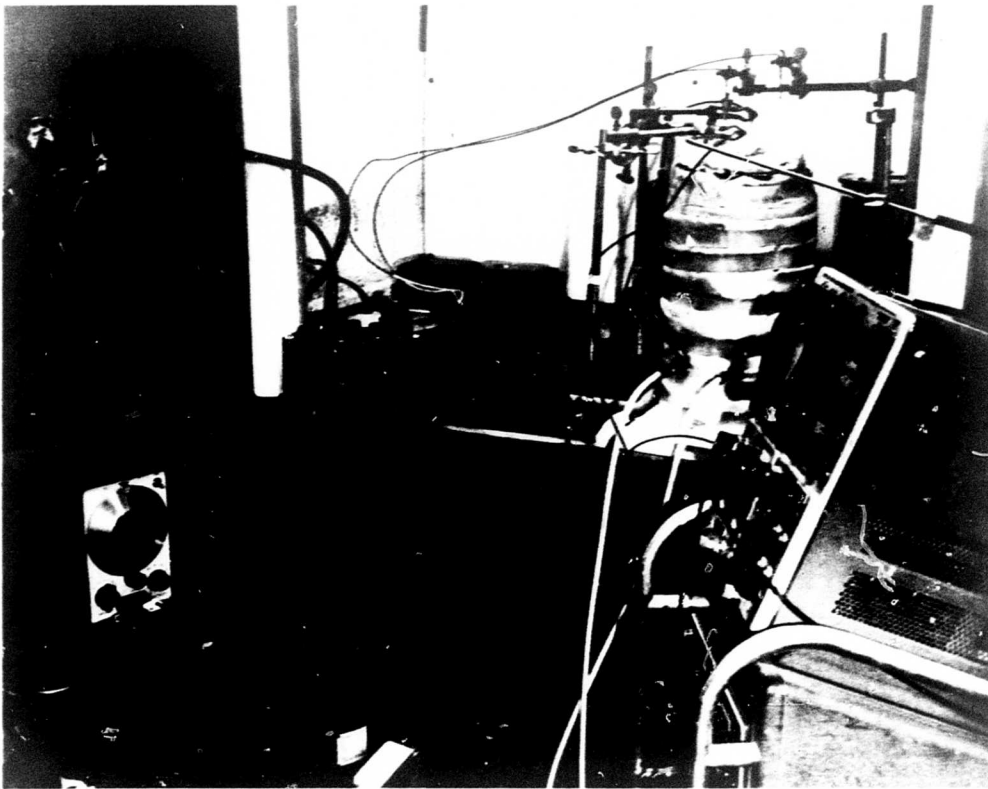
Figure 32.   Modulus of Elasticity Test Apparatus.

47

The relationship for the first overtone was used as a check on the fundamental. These expressions and the values of Y are functions of both the Poisson ratio and the d/L ratio.*

2.14.2 Test Results

The modulus decreased from a value of 44.4×10^6 psi at ambient to 35.6×10^6 psi at the maximum temperature obtainable, 2350°F. Figure 33 illustrates the variation of modulus with temperature. The modulus for beryllides is compared with that of IN-100 (Figure 34).
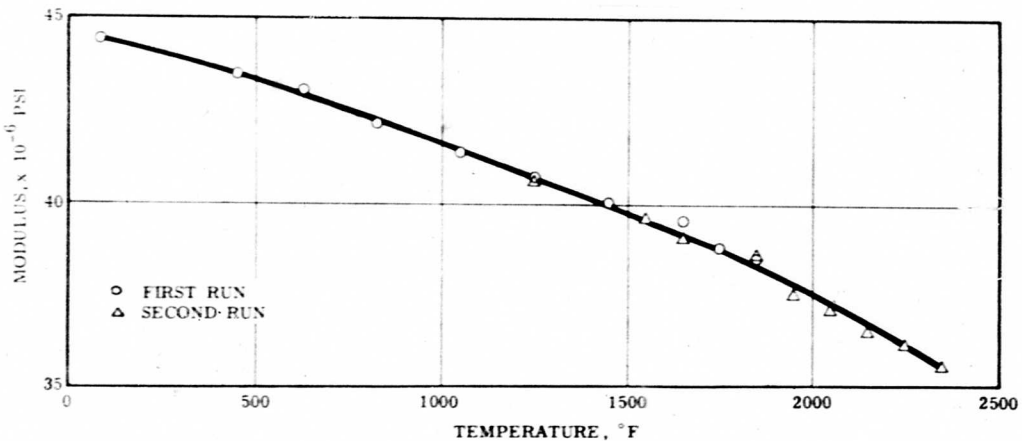
Figure 33. Modulus of Elasticity for Beryllide Composition 1.

*Spinner, S., and Tefft, W. E., A METHOD FOR DETERMINING MECHANICAL RESONANCE FREQUENCIES AND FOR CALCULATING ELASTIC MODULI FROM THESE FREQUENCIES, ASTM, Volume 61, 1961, pp. 1221-1237.
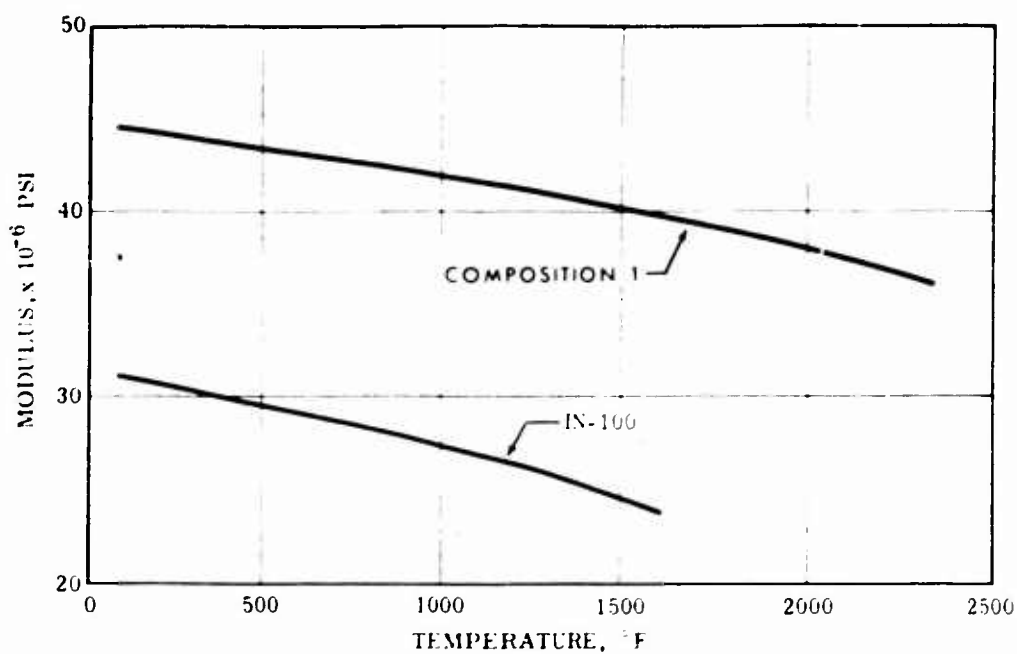
Figure 34. Comparison of Modulus of
Elasticity for Beryllide
Composition 1 and IN-100.

2.15 SUMMATION OF COMPOSITION 1 SPECI 4.N TEST RESULTS

The test data that were obtained during the Composition 1
specimen test program served three purposes:

1. Provided the physical properties information that
was necessary for the turbine design activities.

2. Established base-line material properties to
which future beryllide compositions could be
compared.

3. Defined the mechanical and physical properties
necessary to evaluate Composition 1 for appli-
cation in the 2400°F uncooled-turbine components.

49

It was apparent from the specimen test results that Composition 1 had two major property deficiencies with respect to uncooled-turbine component application:

1. Insufficient stress-rupture strength for use in the turbine rotor or stator.

2. Insufficient ductility to satisfy requirements for use in the turbine rotor or stator.

However, certain accomplishments had been achieved during the beryllide composition studies and Composition 1 specimen testing:

1. A fabrication process was developed that allowed the manufacture of beryllides of uniform and reproducible quality.

2. A number of compositional variations were evaluated, and some control of properties was established.

3. Machining techniques were developed for the fabrication of beryllide parts.

4. Ductility, although insufficient, had been obtained in Composition 1 down to 2000°F.

5. Composition 1 had demonstrated good high-temperature strength and oxidation resistance properties.

In view of these facts, two activities were determined to be appropriate to further pursue the materials investigation. Composition studies, under company sponsorship, were continued to develop a beryllide Composition 2 with increased stress-rupture strength and improved ductility over that of Composition 1. Cascade testing, under USAAVLABS sponsorship, was scheduled for stator-vane assemblies fabricated from Composition 1 to evaluate the material under a realistic engine environment.

3. CASCADE TEST PROGRAM

3.1 GENERAL

The cascade test phase of the materials research investigation comprised the following activities:

1. Design and development of a rig that would allow testing of a cascade of stator vanes at operating conditions (steady-state and transient) that simulated actual engine operation.

2. Fabrication of first-stage stator vanes from Composition 1 material to the geometry that resulted from the design activities reported in Volume II.

3. Provision of adequate high-temperature test instrumentation.

4. Hot corrosion testing of six beryllide rod specimens of three different compositions.

5. Mechanical integrity testing of Composition 1 stator-vane assemblies.

Detailed discussions of these activities are presented in the following paragraphs.

3.2 CASCADE RIG DESIGN AND DEVELOPMENT

To evaluate the integrity of beryllide compositions, a rig was conceived that would allow testing of a cascade of first-stage stator vanes fabricated from Composition 1 and having the geometry that resulted from the aerodynamic design described in Volume II. The primary requirement of the test rig was to simulate both steady-state (2400°F) and transient operating conditions that would be encountered during engine operation. The design of this rig posed several major design problems:

1. Design of a suitable configuration to support the cascade of vanes, having compatibility with the high-temperature environment.

51

2. Development of a high-temperature combustor.

3. Development of a control system to provide
    simulation of engine temperature transients.

The rig that satisfies these design requirements is shown in
Figure 35. It basically consists of:

1. A cascade test section.

2. A primary and preheat combustion system.

3. Fuel and airflow controls.

4. Inlet and discharge ducting and support
    housings.

Room-temperature air at approximately 10 atmospheres passes
through a flow-measuring orifice and enters the rig through
a flow-control valve. The preheat combustor raises the tem-
perature to approximately 700°F to simulate compressor dis-
charge temperature at a pressure ratio of 10:1. Gas flow is
then directed around the test section and into the primary
combustor, where the temperature is increased to 2400°F.
Downstream of the primary combustor, the gas enters the test
section, flows through the cascade, and is finally discharged
through a back-pressure control valve. The rig, partially
disassembled, is shown in Figure 36.

3.2.1 Cascade Test Section

The cascade test section is a structure that provides for the
installation of four stator vanes and two end walls and thus
provides a total of five gas passages. A half-section iso-
metric drawing of this component is shown in Figure 37.
Details of the vane attachment design are shown in Figure 38.

52

Figure 35. Cascade Test Assembly Sketch.

FLOW MEASURING ORIFICE

FLOW-CONTROL VALVE

FUEL IN

PREHEATER

AIR IN

FLOW ~ 0.96 LB/SEC

T 50° F

T 694° F

(MAY USE H₂O INJECTOR
TO COOL AIR PRIOR
TO ENTERING VALVE)

BACK PRESSURE
CONTROL VALVE

AIR
DISCHARGE
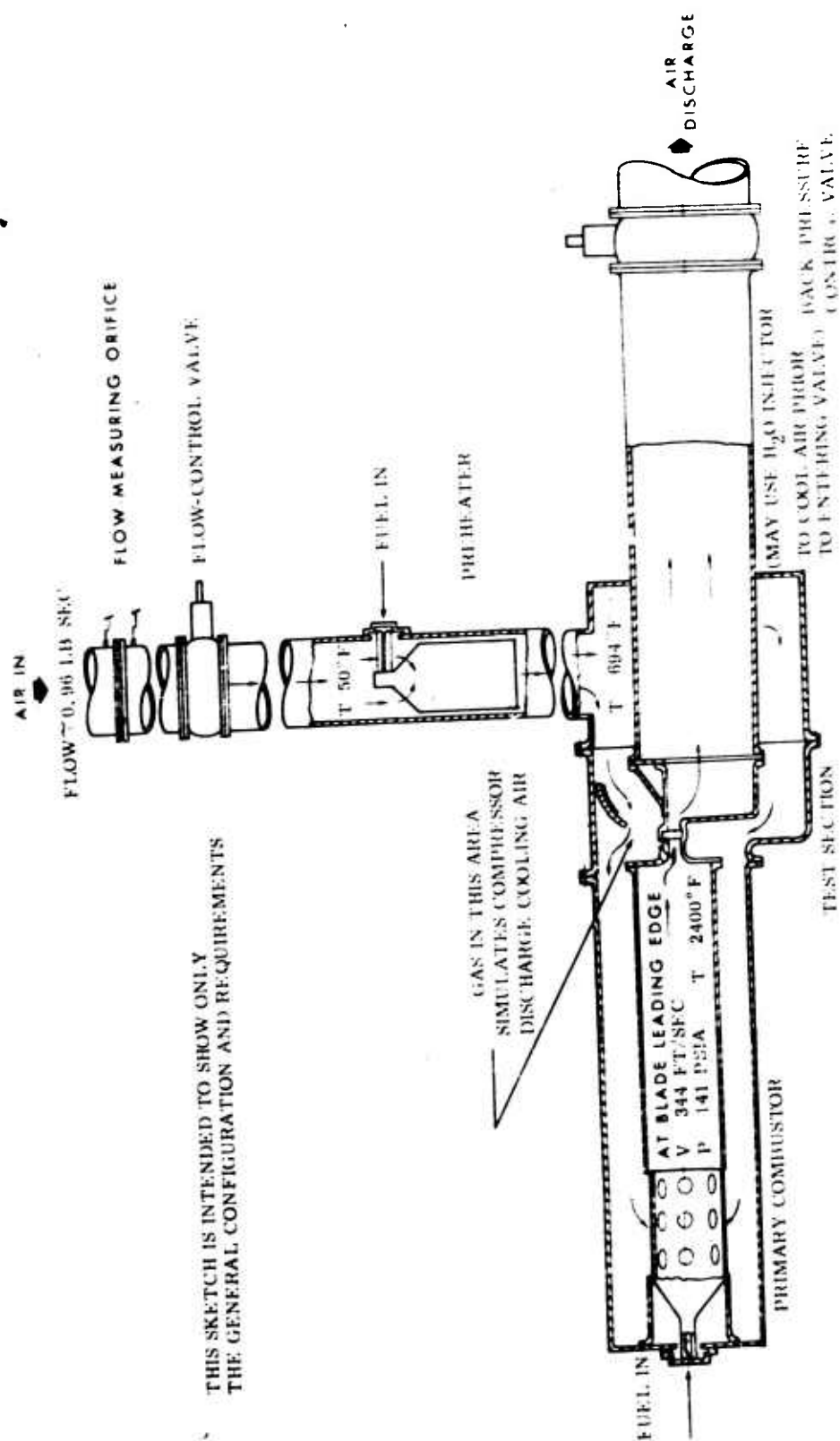
THIS SKETCH IS INTENDED TO SHOW ONLY
THE GENERAL CONFIGURATION AND REQUIREMENTS

GAS IN THIS AREA
SIMULATES COMPRESSOR
DISCHARGE COOLING AIR

TEST SECTION

AT BLADE LEADING EDGE
V   344 FT/SEC   T   2400° F
P   141 PSIA

PRIMARY COMBUSTOR

FUEL IN

53

Figure 36. Cascade Test Assembly Photograph
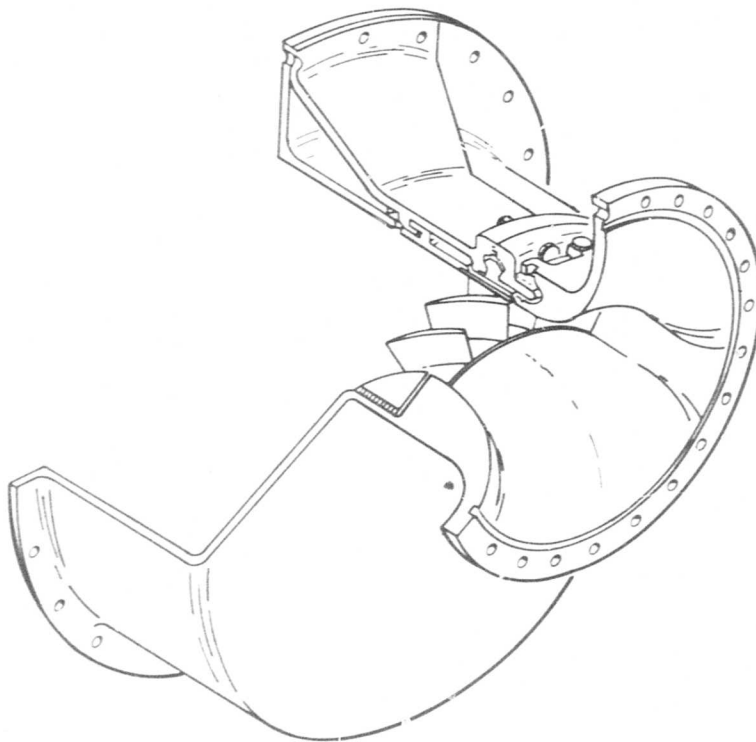
Figure 37. Cascade Test Assembly, Test Section.

54
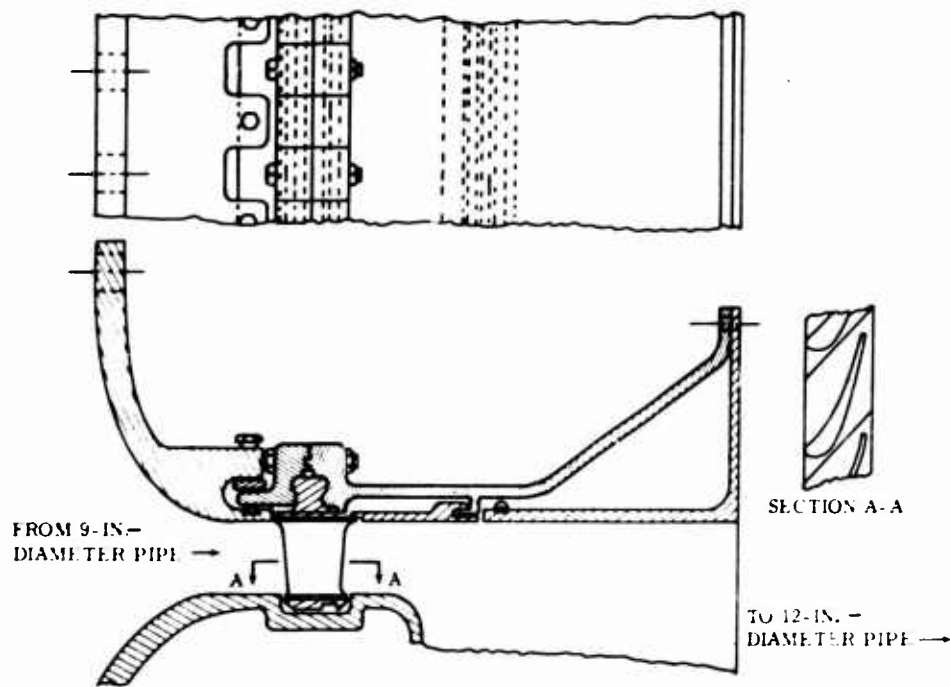
Figure 38. Cascade Test Assembly,
Vane Attachment.

Heat-transfer calculations indicated a problem area in the
transition section immediately upstream of the cascade in the
region where gas velocity increases. The resulting higher
heat-transfer coefficients in this region indicated a metal
temperature that could not be tolerated with the structural
materials that could be used. It was thus necessary to coat
this area with a nonmetallic material in order to provide a
thermal insulation. The material chosen was a zirconia oxide
coating identified as "Rokide Z." This coating was applied
by means of a spray apparatus on the critical areas to a
depth of 0.040 inch.

Heat-transfer calculations for the attachment device indi-
cated that the vane assembly would expand approximately 0.031
inch more than the supporting structure due to the temperature
gradient and thermal expansion between the two parts (Figure
39). Spanwise expansion of the vane amounts to approximately
0.004 inch for a temperature rise of 2300°F. Consideration
of these factors and the low ductility of the Composition 1
material suggested emphasis upon design details to allow for
thermal expansion and, thus, to prevent excessive loads from
developing in the vanes during rig operation.

55
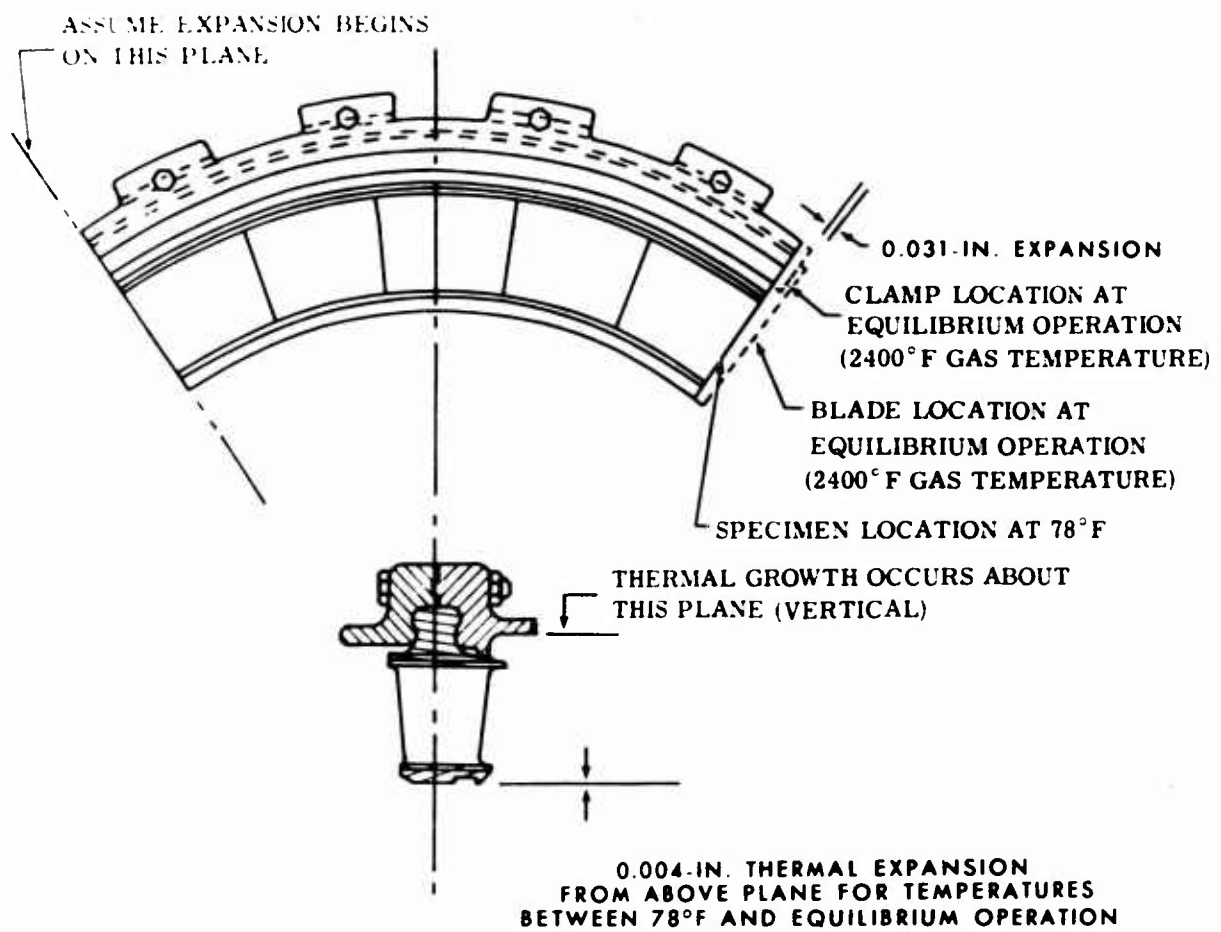
Figure 39. Cascade Test Assembly Thermal Growth Characteristics.

Figure 40 shows the inlet of the cascade test section. The
light-colored area is the "Rokide Z" coating. The three
holes in the upper surface are for high-response thermo-
couples, which are the subject of a later discussion.

Figure 40.   Cascade Test Section
Viewed From Upstream.

Figure 41 shows the cavity in the test section in which the
vanes are installed. The three small holes directly upstream
of the vane installation cavity are pressure pickups for
measurement of static pressure at the inlet to the root of the
vane.

Figure 42 illustrates the inlet nozzle and the three high-
response gas-stream thermocouples. Figure 43 is a view of
the test section housing, showing surface temperature thermo-
couples and static pressure taps.

57

Figure 41. Cascade Test Section,
Vane Installation Cavity.

Figure 42. Cascade Test Section Instrumentation,
High-Response Thermocouples.
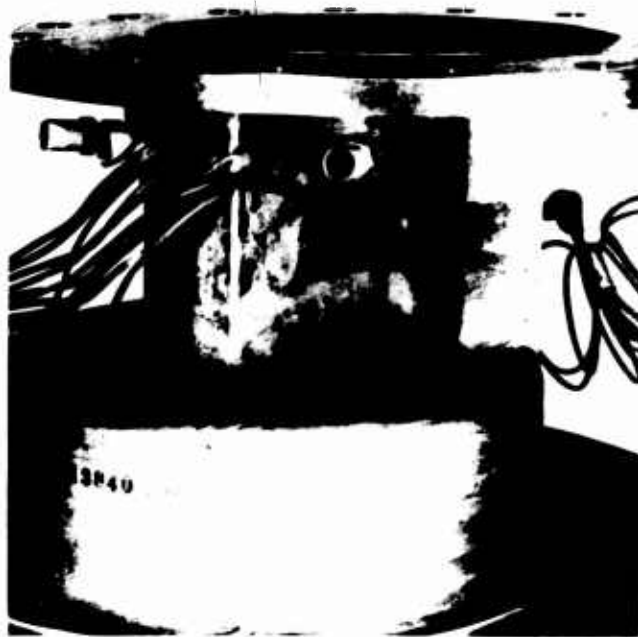
Figure 43. Cascade Test Section
Instrumentation, Surface
Temperature Thermocouples.

3.2.2 Combustor Design and Development

Development of a combustion system to provide the required
temperature at the cascade test section represents a signif-
icant portion of the overall rig development. The rig in-
corporates two combustors: (1) a preheat combustor, which
increases the system air temperature to approximately the
discharge temperature corresponding to a compressor pressure
ratio of 10:1, and (2) a primary combustor, which further
increases the temperature to that desired at the cascade
inlet. For the preheat combustor or preheater, an existing
combustor, modified for a pressure ratio of 10:1, was used
and is not discussed in this report.

The development of the primary combustor was completed after
sixteen tests, which are summarized in Table XI. A brief
discussion of the problems encountered during the development
follows.

The design-point requirements for the primary combustor are:

    1.   Airflow   0.996 lb/sec

    2.   Inlet temperature   700°F

59

TABLE XI. 2400°F COMBUSTOR DEVELOPMENT SUMMARY

Test	Configuration	Test Title	Time (hr:min)	Exit Temp (°F)	Max* Liner Temp (°F)	Fuel Nozzle (deg)	With Shroud	Bleed Flow (lb/sec)	Approx Dome Flow (%)
1	Standard, no cooling skirts	Check out	-	2400	2400±	Simplex 90	No	None	8
2	Standard, three cooling skirts	Check out	0:10	2400	2000±	Simplex 90	No	None	8
3	Standard, three cooling skirts	Temperature distribution	2:0	2400	2200±	Simplex 90	No	None	8
4	Standard, four cooling skirts	Thermocolor	0:05	1900	2200	Simplex 90	No	None	8
5	Standard, four cooling skirts	Beryllide oxidation	6:30	2400	2400±	Simplex 70	No	None	8
6	Standard, four cooling skirts	Thermocolor	0:05	1900	1350	Simplex 70	No	None	8
7	Standard, four cooling skirts	Thermocolor	0:05	2400	1700	Simplex 70	Yes	None	8
8	Rokide-coated	Thermocolor	0:05	1900	1250	Simplex 70	Yes	None	30
9	Rokide-coated	Thermocolor	0:05	2400	1650	Simplex 70	Yes	None	30
10	Rokide-coated	Endurance, temp dist	1:0	2400	1650	Simplex 70	Yes	None	30
11	Rokide-coated	Thermocolor verification	0:05	2400	1650	Simplex 70	Yes	None	30
12	Rokide-coated	Thermocolor	0:05	2400	1500	Simplex 70	Yes	1	30
13	Rokide-coated	Beryllide oxidation	10:0	2400	-	Simplex 70	Yes	1/2	30
14	Rokide-coated	Thermocolor	0:05	2600	1600	Simplex 70	Yes	1	30
15	Rokide-coated	Thermocolor	0:05	2400	1500	Simplex 70	Yes	None	40
16	Uncoated	Thermocolor	0:05	2400	1650	Simplex 70	Yes	None	40

*Max. liner temp existing in small "hot spots" only.

3.	Discharge temperature	2400°F
4.	Inlet pressure	147 psia
5.	Pressure drop	3% (minimum)
6.	Design life	40 hours (minimum)

A cylindrical liner approximately 3 inches in diameter and 8 inches long, having a design-point heat-release rate of 6.3 x 10^6 Btu/hr-ft^3-atm, was designed to satisfy the above requirements. The initial test of this configuration at 2400°F showed severe oxidation of the liner wall and suggested modifications to the design (see Figure 44).

The combustor design was modified by incorporating cooling skirts, as shown in Figures 45 and 46, to provide for film cooling of the inner surface of the liner wall. Each of the skirts provided a small annulus into which secondary air was introduced through a series of small holes in the outer liner wall. The skirts were designed to provide a flow path long enough to produce a directed flow of air along the inner wall of the liner such that film cooling was realized. Two film-cooled configurations were tested, a three-element design and a four-element design. Although significant temperature reductions were realized, neither configuration provided a liner metal temperature low enough so that the design life could be attained without extensive damage to the liner. Figure 47 shows a plot of the gas-temperature profiles at both the film-cooled primary combustor discharge and the test section inlet for various test section inlet average temperatures.

Figure 44. Primary Combustor Liner After Operation at 2400°F Discharge Temperature.

61

Figure 45. Primary Combustor Liner With
Film-Cooling Skirts.

Figure 46. Primary Combustor Liner With
Film-Cooling Skirts - Interior.
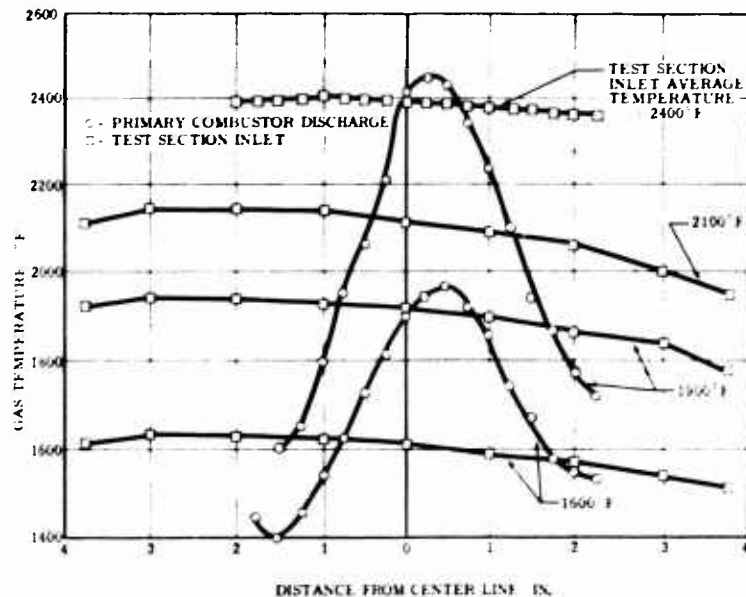
Figure 47. Gas-Temperature Profiles - Combustor
With Film-Cooling Skirts.

With evidence that the original combustor liner design would
require extensive modification in order to provide the life
required, two major alternate design approaches were initiat-
ed:

1. A shroud was designed and fabricated (Figure 48)
to fit around the liner, providing a free annulus,
0.25 inch in depth, through which the preheater
air was directed, thus providing film cooling
over the outside diameter of the liner. The
shrouded combustor liner was tested at 1900°F
and 2400°F discharge temperatures. A reduction
in liner wall temperature of approximately 250°F
was realized. Maximum metal temperature of the
liner during 2400°F operation was 1700°F.

2. In parallel with the above modification, a new
combustor was designed and was coated with "Rokide
Z." Tests of this configuration indicated a
further reduction in liner metal temperature of
at least 100°F, compared to the film-cooled,
shrouded configuration described in item 1. Fig-
ure 49 shows the combustor discharge temperature
profile obtained with this configuration at an
average test section inlet temperature of about
2400°F. Figures 50 and 51 show the combustor after
rig tests at the above temperatures.

63
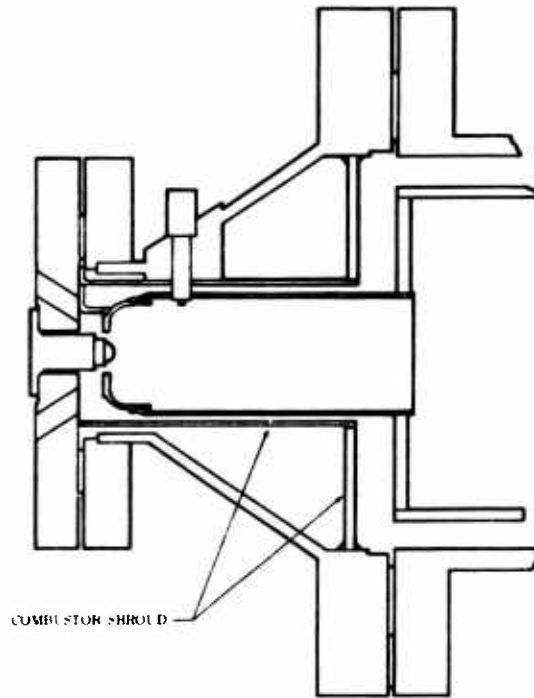
Figure 48. Shrouded Combustor Liner Configuration.
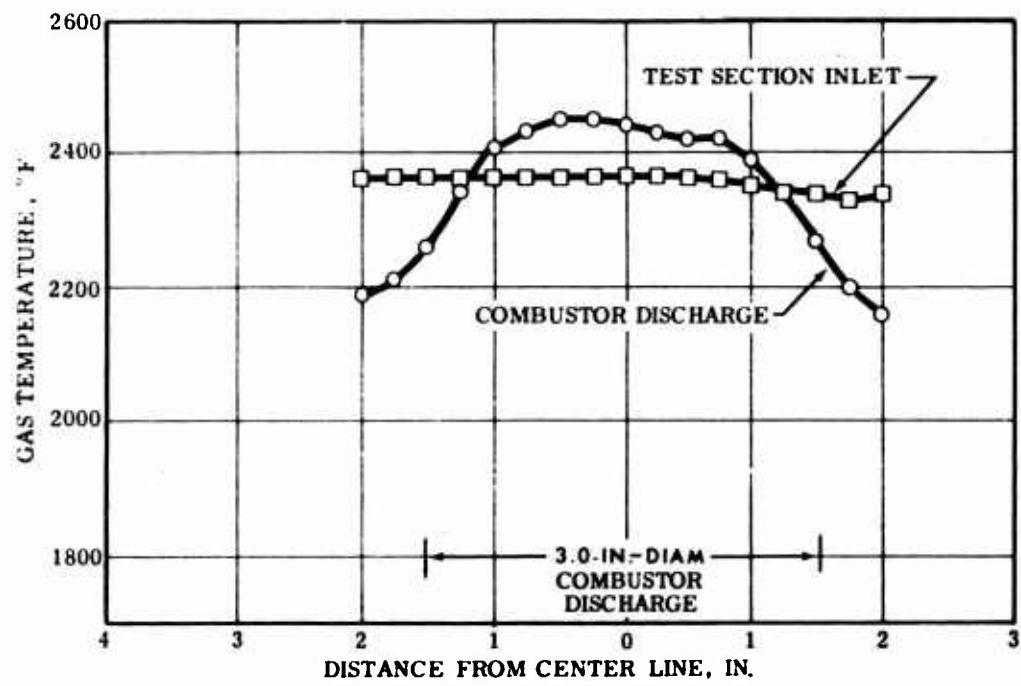
AIR MASS FLOW: 0.97 LB SEC
AIR INLET TEMPERATURE: 750°F
AIR INLET PRESSURE: 147 PSIA

Figure 49. Gas-Temperature Profiles, "Rokide Z" –
Coated Combustor Liner.

64

Figure 50. "Rokide Z"-Coated Combustor Liner After Operation at 2400°F Discharge Temperature.
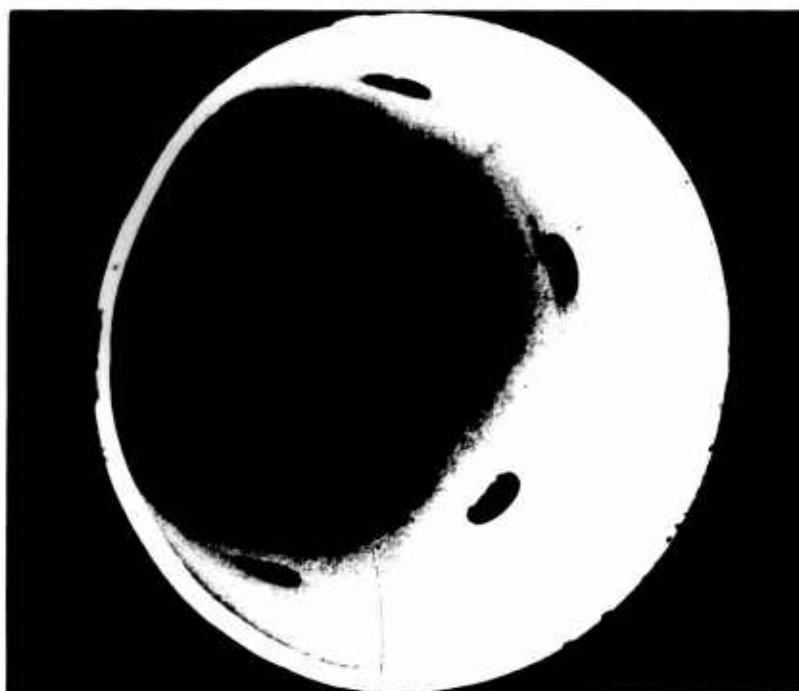
Figure 51. Inner Surface of "Rokide Z"-Coated Combustor Liner After Operation at 2400°F Discharge Temperature.

65

To further increase the reliability of the combustion system, a bleed-air system that provided additional film cooling of the combustor liner was incorporated in the rig. This was accomplished by increasing the flow through the preheater and bleeding off just prior to entry into the primary combustor. The increased flow (up to 2.3 lb/sec total) over the outside diameter of the primary combustor liner provided additional film cooling for this component. It was shown that a satisfactory liner metal temperature could be maintained at an average combustor discharge temperature of up to 2600°F by bleeding approximately 1 lb/sec. This operating condition was realized using the Rokide-coated combustor liner fully shrouded.

3.2.3 Control System

In order to simulate gas-turbine engine temperature conditions encountered during starting as well as those encountered during normal operation, a fuel-control system was designed and built enabling precise control of the fuel-flow/temperature transient. It was the objective of the subject control system to provide the fuel-flow transients depicted in Figure 52.
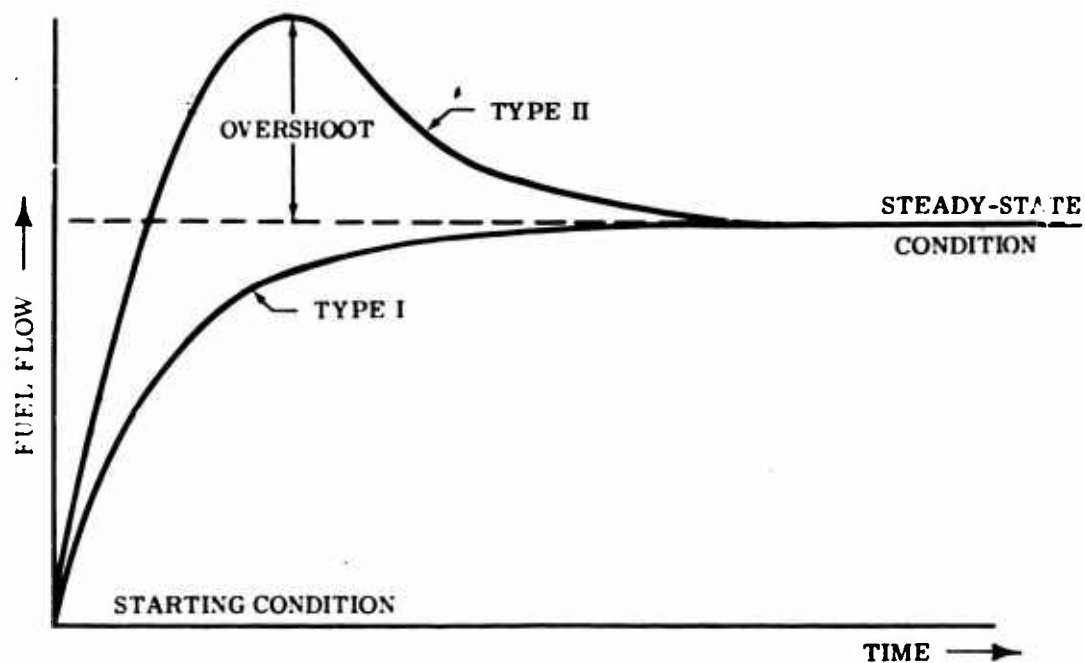
Figure 52. Fuel-Flow Transients.

The Type I transient as illustrated is classified as a first-order transient and is commonly encountered when changing engine output power conditions. The Type II transient is representative of a temperature overshoot condition, indicative of an engine start.

The fuel-control system utilized to provide the transients depicted in Figure 52 is shown in Figure 53. Fuel flow is controlled by maintaining a constant pressure drop (Δp) across a variable-area metering valve. The control system is modular in concept, with the individual components connected by external plumbing.

An electric motor drives the fuel pump that supplies fuel to both the preheater (50° to 700°F gas-temperature rise) and the primary combustor (700° to 2400°F gas-temperature rise). The servo pressure regulator maintains a constant supply pressure for the preheater flow circuit and thereby isolates it from the primary flow circuit. Regulation of the fuel flow to the preheater is achieved by the in-line Δp regulator and metering valve. The preheater gas temperature is modified by changing the needle valve area of this valve by means of an electric motor input. Fuel bypassed by the servo pressure regulator is supplied to the primary combustor flow circuit.

Constant Δp across the in-line scheduling valve is maintained by the Δp regulator valve. The minimum primary combustor fuel flow may be varied by adjustment of the minimum flow needle, which operates with the same Δp as the scheduling valve. The scheduling valve area and hence the primary fuel flow are varied by changing the pneumatic pressure in the pneumatic chamber of the in-line scheduling valve. Fuel-flow transient response is thus determined by the configuration of the pneumatic portion of the in-line scheduling valve, because fuel flow is proportional to metering valve area which, in turn, is proportional to pneumatic pressure.

The Type I transient response is achieved by utilizing only one pneumatic bleed orifice. By selection of the chamber volume, pneumatic supply pressure level, in-bleed orifice diameter, and out-bleed orifice diameter, the time required for the Type I response to attain steady-state conditions may be changed.

Controlled overtemperatures or Type II responses are achieved by incorporation of a second pneumatic bleed orifice, which is opened at a prescribed pressure level. The transient behavior in terms of response time may be modified by changing the parameters discussed in reference to Type I response.

67
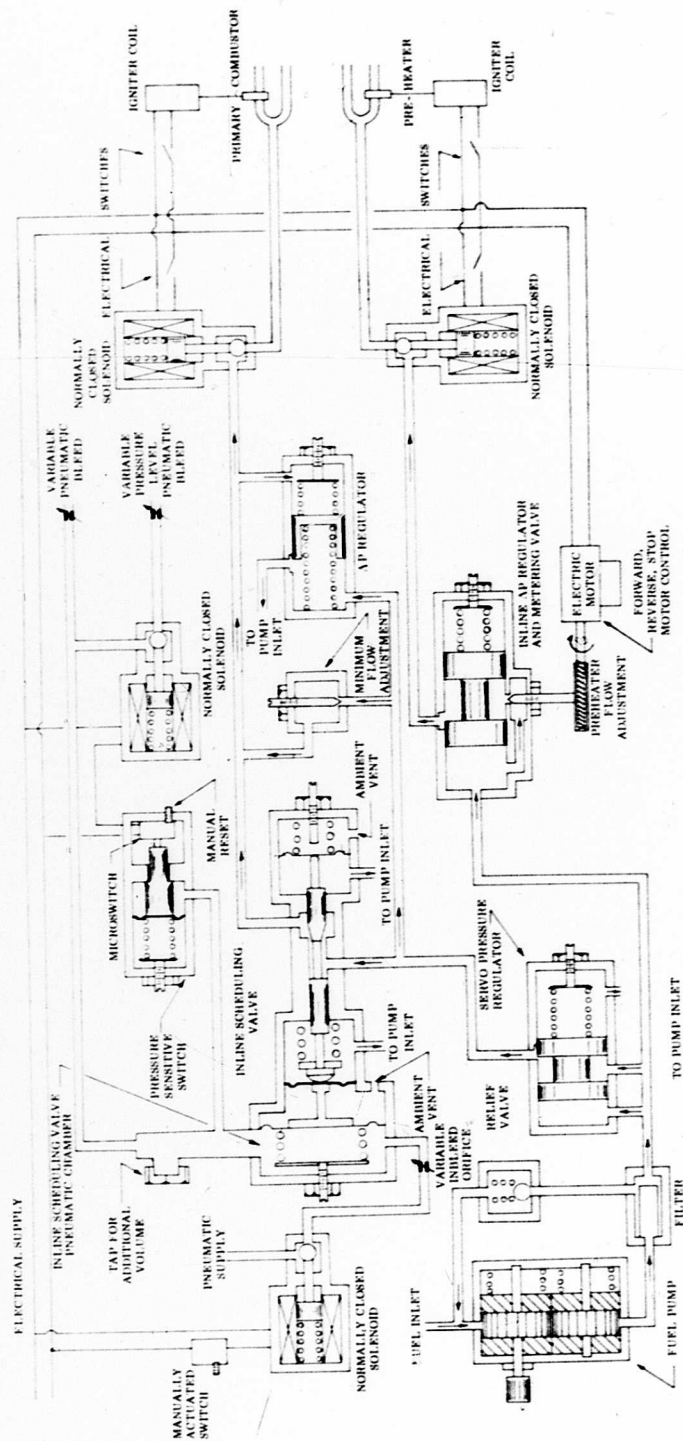
Figure 53. Fuel-Control System Schematic.

The control components were evaluated on an individual basis and were then integrated into a complete control system. The resultant system operation was excellent and satisfied all aspects of the objective without modification. The control panel is illustrated in Figure 54.

A desired temperature transient is produced by an experimental procedure in which the in-line scheduling valve pneumatic configuration is adjusted to yield the appropriate response. Typical response characteristics are shown in Figure 55.

3.3 FABRICATION OF TEST SPECIMENS

Machining of the beryllide Composition 1 material by conventional methods was difficult because of the low ductility of the material at room temperature. The subject stator vanes were particularly difficult to machine because of the long, thin, trailing-edge (approximately 0.030 inch) design. It thus became necessary to utilize a nonconventional machining process for the fabrication of these vanes. The electrical-discharge-machining process was chosen.

Microanalysis of the first vanes to be fabricated by the electrical-discharge-machining process indicated the presence of small surface cracks. The surface finish was also quite rough. It was found that the surface cracks and rough surface finish could both be eliminated by removing approximately 0.003 inch of stock from the vanes by polishing.

Nickel-aluminide was utilized throughout the test program for shroud and platform components, from which the test specimens were supported. This material lacks the strength at 2400°F required for a blade material (the goal of this program) and, as such, is not considered to be a candidate material. However, it has reasonable oxidation resistance in the temperature regime required by this test program and enough ductility to survive a thermal shock equivalent to a typical engine start. Additionally, it was found that the rate of electrical discharge machining is greater in nickel-aluminide than in beryllides, which makes it less expensive to fabricate. This material was also used in specimens for surface temperature measurement because of its greater temperature ductility, which permits the use of spot-welded attached thermocouples.

All of the cascade test components, including the vanes, shrouds, platforms, and end pieces, were electrical-discharge-machined from blanks as shown in Figure 56. Figure 57 shows finish-machined and polished vanes of both beryllide and

69

Figure 54.   Front View of Temperature Control
             System for Cascade Test Assembly.
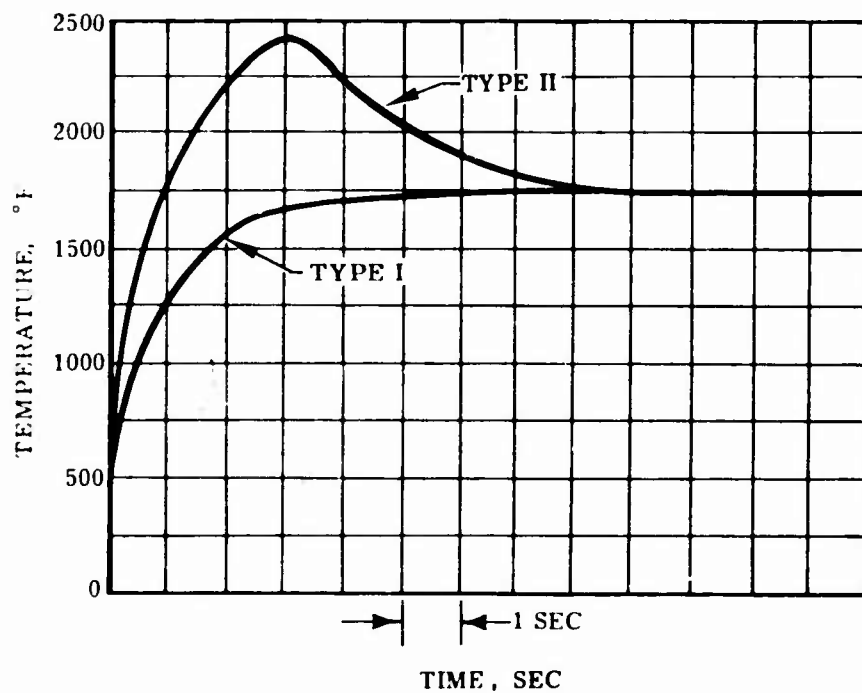
Figure 55.   Temperature/Time Transients of
             Primary Combustor.

Figure 56.   Material Blanks.
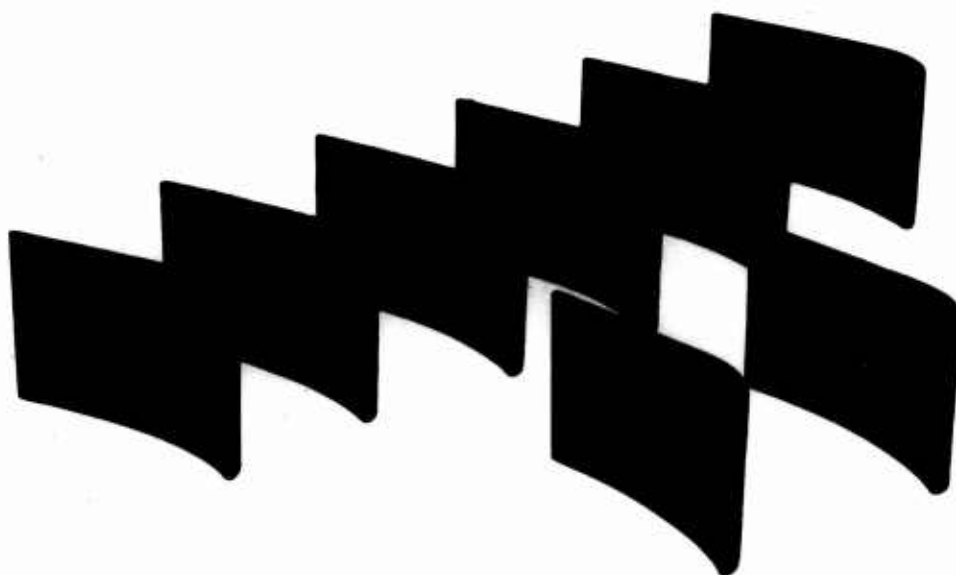
Figure 57.   Six Composition 1 and Two Nickel-
Aluminide Stator Vanes.

71

nickel-aluminide. Completed sets of Composition 1 and nickel-aluminide shrouds, platforms, and end pieces are illustrated in Figure 58.

During polishing of the Composition 1 stator vanes, trailing-edge cracks (Figure 59) were noted in the vanes, although all vanes had been X-rayed prior to polishing without detection of imperfections. Whether these cracks were present prior to, or were generated during, polishing is conjecturable. It does serve to emphasize the extreme care that must be exercised in handling these materials, because of their brittle nature at room temperature.

Figure 58. Composition 1 and Nickel-Aluminide Stator Assemblies.

Figure 59. Two Composition 1 Vanes Illustrating Cracks.

3.4 TEST INSTRUMENTATION

In order to fully evaluate the specimens in each test, provisions were made to measure the test temperatures and pressures at the location and by the methods listed below.

1. Cascade Inlet Gas Temperature - 4 platinum-rhodium aspirated thermocouples (steady state) and 3 high-response thermocouples.

2. Vane or Specimen Surface Temperature - platinum-rhodium thermocouples spot-welded to the specimens.

3. Rig Surface Temperature - 18 Chromel-Alumel thermocouples on mixing and exhaust sections and 12 Chromel-Alumel thermocouples on the cascade test section.

4. Static Pressure at Test Section Throat - 3 static taps.

To ensure completion of the cascade test activities with accurate data, it was necessary to obtain accurate temperature measurements within the rig. Several of these measurements are very difficult to obtain, primarily because of the order of magnitude of the temperature and the resultant hazard to the thermocouples:

1. Cascade test section inlet - steady state

2. Cascade test section inlet - transient

3. Stator vane skin temperature

3.4.1 Steady-State Temperature Measurement

The thermocouple utilized for measurement of the steady-state test section inlet temperature is shown in Figure 60. It is a platinum-rhodium aspirated configuration sheathed with Inconel and platinum-rhodium tubes. The combined velocity, radiation, and conduction error of this thermocouple is less than 10°F. It has proven to be reliable in service at temperatures to 2800°F. Some melting of the probes was experienced early in the program because of difficulties in the manual control that caused excessive temperatures to exist momentarily. With improved operating techniques, no additional problems of this nature were encountered.

73

STAINLESS STEEL TUBE

STAINLESS STEEL
COMPRESSION FITT·.;G

STAINLESS STEEL
BANJO FITTING

INCONEL TUBE

PLATINUM-RHODIUM
TUBE

MICROMINIATURE
THERMOCOUPLE PROBE

FOR TRANSIENT
MEASUREMENTS

PLATINUM-RHODIUM
TUBE

PLATINUM SHEATH
TYPE S THERMOCOUPLE

FOR STEADY-STATE
MEASUREMENTS
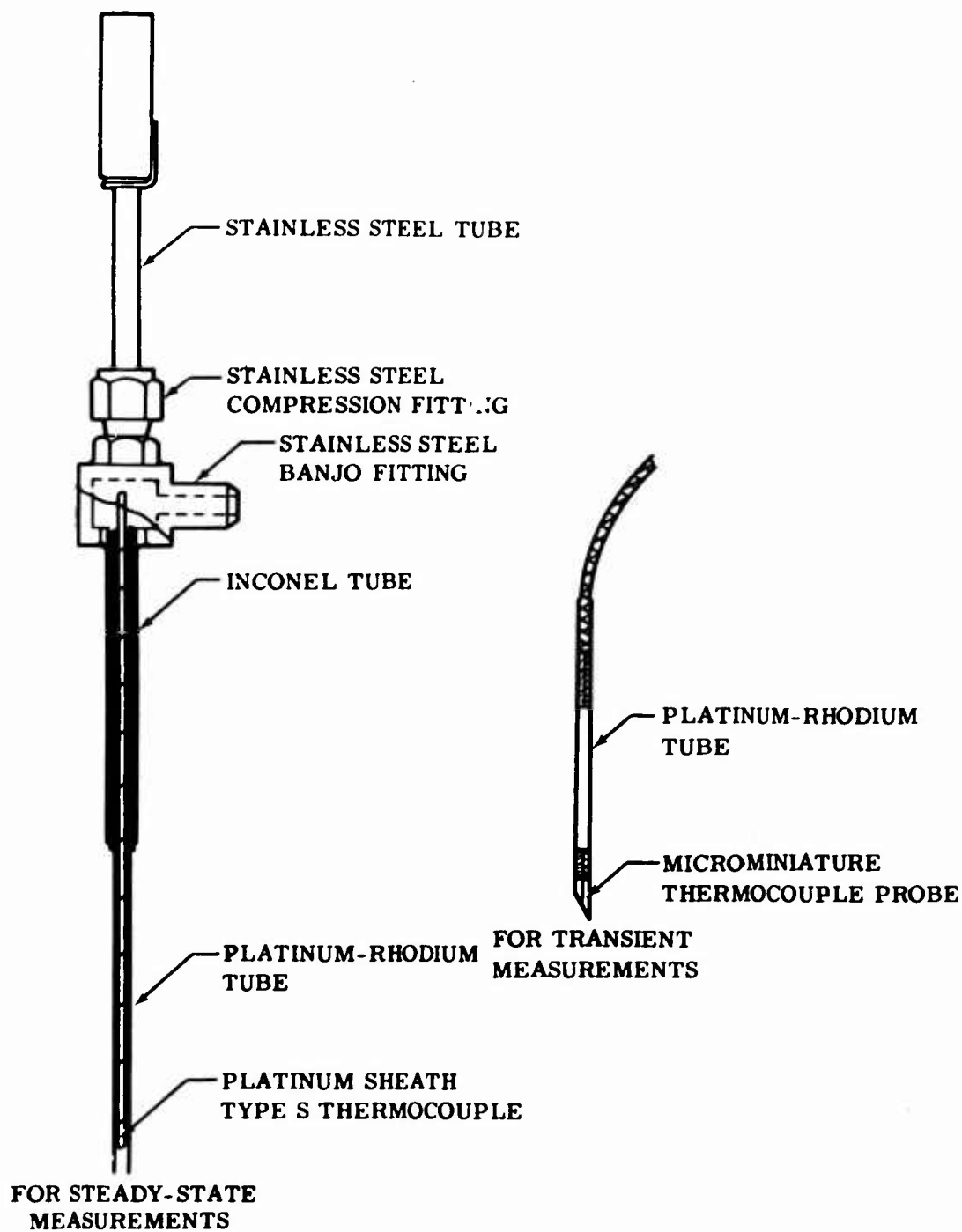
Figure 60. Thermocouples for Measurement of
Cascade Inlet Gas Temperature.

74

3.4.2 Transient Temperature Measurement

For measurement of transient temperatures, microminiature thermocouples, shown in Figure 60, were utilized.

Exposed junctions of 0.001-inch-diameter wire gave a calculated time constant of 0.005 sec. This fast response contributed to many premature failures because of overtemperature on light-offs. A few probes of this type survived several hours. Switching to enclosed junctions improved the life, but the response time was increased from 0.05 to 0.1 sec, or about the same as for the aspirated probes.

3.4.3 Blade Temperature Measurement

In order to measure the surface temperature of an object in a high-velocity gas stream it is desirable not to disturb the gas flow, which changes the convective heat-transfer to the surface. The most common method of measuring blade temperature in conventional turbines is to braze sheathed thermo-couple material in holes or grooves in the blade. This does not disturb the flow and provides good thermal contact with the blade material. To apply this technique to the beryllide materials, it was necessary to obtain a high-temperature braze alloy having compatibility with the beryllides.

Several palladium and palladium-alloy materials were tested with unsatisfactory results, primarily because of inter-metallic chemical reaction problems. Therefore, it was decided that a less desirable method of attachment would have to be utilized.

The technique used employed platinum-rhodium microminiature thermocouples with flattened junctions as shown in Figure 61. These were held to the blades with platinum foil spot-welded to the blades.
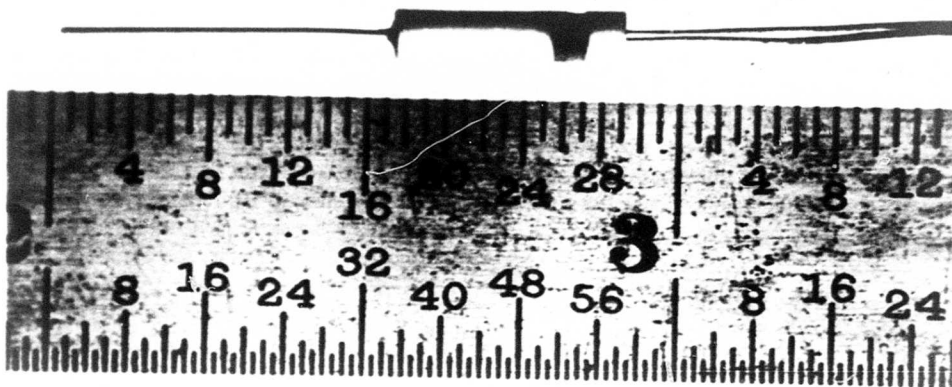
Figure 61.   Thermocouple for Measurement of
Vane Surface Temperature.

3.5 CASCADE TESTING

The cascade test series was divided into two separate activities, each of which had a specific objective.

Hot corrosion testing was conducted on rod-type specimens to determine the oxidation characteristics of Composition 1 when exposed to combustion products at 2400°F and turbine-design flow parameters.

Mechanical integrity testing was conducted on stator vanes to establish the mechanical integrity characteristics of Composition 1 during steady state (2400°F) and during simulated engine transient operating conditions.

The following subparagraphs present the results of the cascade testing.

3.5.1 Hot Corrosion Tests (Cascade Rig)

Two test runs were conducted on the cascade test rig to determine the corrosion resistance characteristics of three different beryllide compositions in a high velocity combustion gas stream and also to evaluate the cascade test rig capabilities under continuous operation. The beryllide compositions tested were:

1. Composition 1

2. $CbBe_{10}$

3. $CbBe_{10}$ plus 0.5-percent Al and 0.5 percent Ti

The oxidation test specimens were approximately 1 inch in length and were both square (0.13 x 0.13 inch) and circular (0.13-inch diameter) in shape.

3.5.1.1 Hot Corrosion Test No. 1

One square-section specimen and one circular-section specimen from each composition were installed in the cascade rig (see Figure 62) and were exposed to combustion products at 2400°F for 6.5 hours. These specimens were held in the rig test section with nickel-aluminide shrouds and platforms. The surface temperature of the specimens was then monitored by a thermocouple spot-welded to a nickel-aluminide specimen of the same configuration as that of the beryllide

77

circular-section specimens. Traces of molten HS-25 from a combustor liner failure* were deposited on the test specimens and, thus, invalidated the results to some degree.

At the completion of the 6.5 hours of testing, all of the beryllide specimens had broken. The nickel-aluminide specimen was in one piece but was bent. It is conjectured that bending was the result of a load imposed by differential expansion of the test section boundaries or of the specimen and shroud. This theory would also explain fracture of the beryllide specimens.

A microscopic examination revealed a depleted region of approximately 0.001-inch depth on both the beryllide specimens and the nickel-aluminide reference specimen. Both materials showed a thin film of oxidation products on the surface. These products were identified by X-ray diffraction as C_0O and Cr_2O_3 that came from the HS-25 combustor liner.
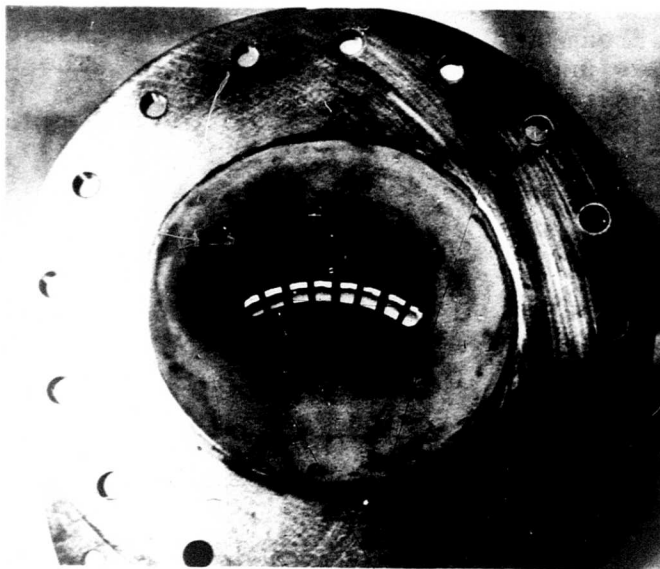
Figure 62. Cascade Test Section With Beryllide Specimens Installed Before Test No. 1.

---

*During this test, development of the combustor liner was still being pursued.

78

3.5.1.2 Hot Corrosion Test No. 2

Following development of the cascade combustion liner (reported in 3.2.2), six beryllide specimens of the same geometry and material compositions as those used in test No. 1 were installed in the rig test section. During installation, two of the square-section specimens (Composition 1 and $CbBe_{10}$) were broken. In addition to the beryllide specimens, one nickel-aluminide circular-section specimen was installed that had two surface-temperature thermocouples spot-weld-attached. Sufficient clearance was provided between the specimens and their support members to ensure that differential thermal growth would not generate high stresses in the specimens.

The rig operating parameters were set as in test No. 1 in order to subject the specimens to 2400°F combustion products. After 2 hours of running, the one remaining square-section specimen ($CbBe_{10}$ plus 0.5-percent Al and 0.5-percent Ti) was found broken. After 7 hours, the $CbBe_{10}$ circular-section specimen showed signs of erosion. At the completion of 10 hours of testing, the $CbBe_{10}$ plus 0.5-percent Al and 0.5-percent Ti circular-section specimen was found broken and only the Composition 1 and nickel-aluminide circular-section specimens were intact. Figure 63 illustrates the beryllide specimens and the test section at the completion of the test.

Inspection of the specimens revealed the following:

1. The Composition 1 circular-section specimen was intact and showed negligible oxidation.

2. The $CbBe_{10}$ plus 0.5-percent Al and 0.5-percent Ti circular-section and square-section specimen were both broken, but the pieces (a total of four) were nearly free of oxides.

3. The $CbBe_{10}$ circular-section specimen showed signs of erosion, which was believed to have been caused by the severe oxidation attack on the nonstoichiometric composition nickel-aluminide specimen holder.

4. The nickel-aluminide instrumented circular-section specimen also showed poor resistance to oxidation. However, this specimen was fabricated from off-chemistry material.

5. The fractures that occurred in the test specimens were believed to have been the result of a combination of factors--namely, the severe oxidation attack on the nonstoichiometric composition nickel-aluminide holders, thermal shock, and possibly mechanical stresses occurring in thermal expansion mismatch.

Figure 63. Cascade Test Section Specimens After Oxidation Test No. 2.

3.5.2 Stator Vane Mechanical-Integrity Test

As reported in the following subparaoraphs, two test runs were conducted to determine the mechanical integrity of stator vanes that were fabricated·from beryllide Composition 1.

3.5.2.1 Stator Vane Test No. 1

Three Composition 1 vanes and one nickel-aluminide vane were positioned in a cascade as shown in Figure 64. Two of the beryllide vanes were provided with beryllide platform and shroud elements. The other shrouds and platforms for this assembly were fabricated from nickel aluminide. A trial assembly was made, as shown in Figure 65, prior to assembly in the cascade test section in order to verify the existence of sufficient clearance to provide for thermal expansion. The vane assembly installed in the cascade test section is shown in·Figures 66

and 67. It should be noted that the nickel-aluminide vane was broken during installation of instrumentation.

The first test was intended to evaluate the stator vanes at steady-state conditions; therefore, precautions were taken to minimize the temperature transient during primary combustor light-off. The peak observed combustor discharge temperature during light-off was 1900°F, which represented a ΔT of about 1300°F in approximately 2 sec (primary combustor inlet temperature = 600°F). This peak dropped to approximately 1500°F, after which it was raised to approximately 2300°F in about 4 minutes. This temperature corresponds to a cascade test section inlet temperature of 1900° to 1950°F and was maintained for 30 minutes. Temperatures and pressures existing throughout the rig during this 30-minute test are shown in Figure 68. The rig was then disassembled. Visual inspection of the stator assembly showed that all of the beryllide vanes were cracked, with large sections of the trailing edges of the No. 4 and No. 5 vanes missing. The nickel-aluminide vane showed no signs of cracking or deterioration (see Figure 69). Figure 70 shows the disassembled stator components arranged in the same order in which they were assembled in the test section (Figure 64).

THREE-PIECE STATOR DESIGN

ARRANGEMENT OF STATOR ASSEMBLIES

1	2	3	4	5	6
NiAl	Beryl.	NiAl	Beryl.	NiAl	NiAl

NiAl	Beryl.	NiAl	Beryl.	Beryl.	NiAl

NiAl	Beryl.	NiAl	BeryL	NiAl	NiAl
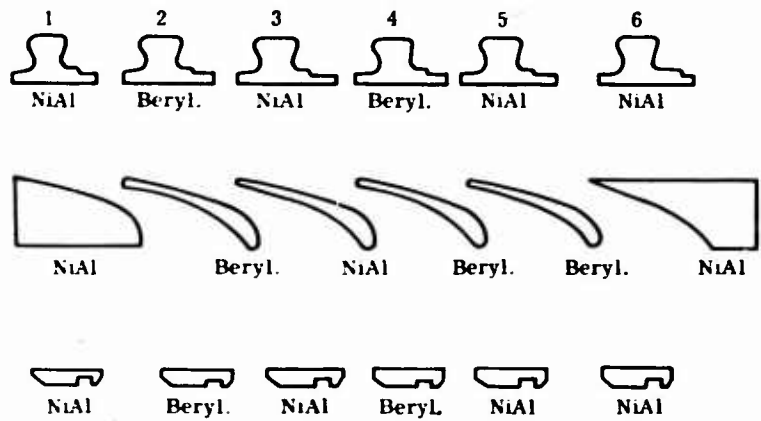
Figure 64.   Cascade Test Components,
Test No. 1.

Figure 65.   Stator Assembly Before Installation.

82

Figure 66. Stator Assembly Installation,
Viewed From Upstream.

Figure 67. Stator Assembly Installation,
Viewed From Downstream.

83
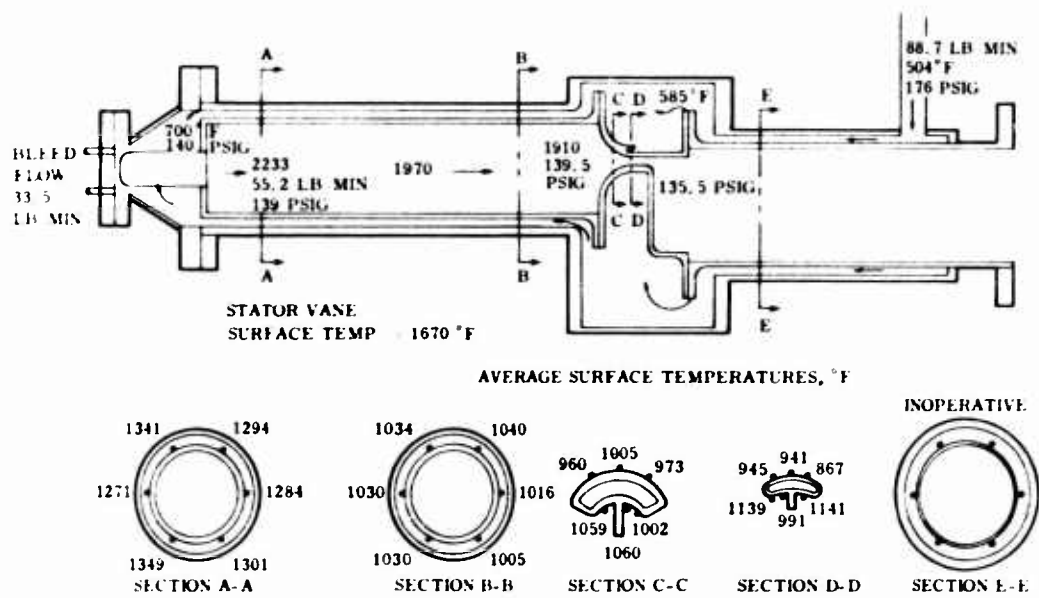
Figure 68.   Test Rig Operating Conditions,
Test No. 1.

Figure 69.   Stator Assembly Condition
After Test No. 1.
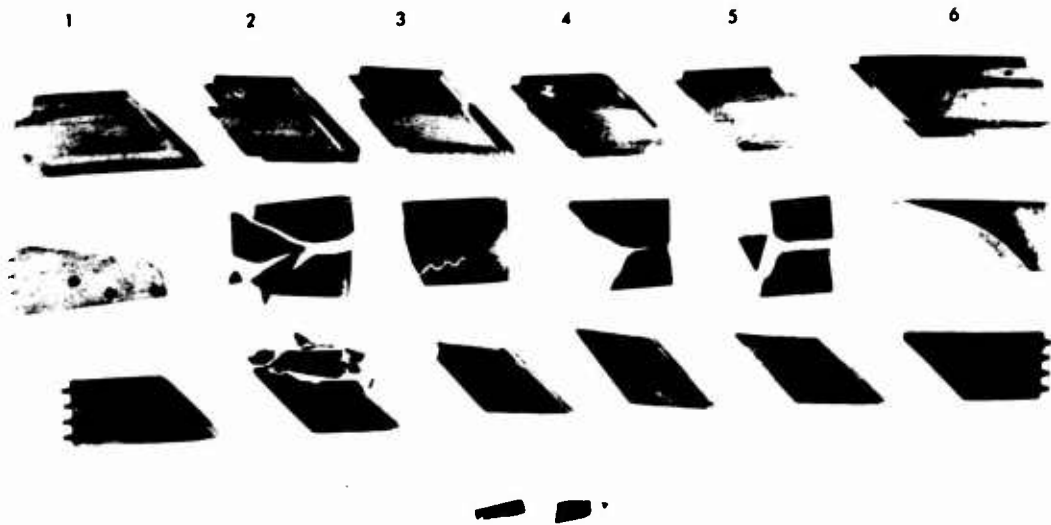
Figure 70. Stator Cascade Components
Condition After Test No. 1.

A description of the condition of the component parts
as they appeared after test follows (refer to Figures 64
and 70):

1. Nickel-aluminide end section assembly,
   convex. These components showed no signs
   of deterioration.

2. Beryllide vane assembly. The vane was
   fractured in several places. Severe
   shattering of the platform indicated that
   compressive stresses existed in the vane.
   The hole in the trailing-edge section of
   the shroud also indicated compressive
   loading between the vane and the shroud.

3. Nickel-aluminide vane assembly. The shroud
   and platform were in good condition except
   for a small piece broken from the trailing
   edge of the platform.

4. Beryllide vane assembly. The platform
    showed signs of oxidation, the leading-
    edge corner of the shroud was broken, and
    a hole was broken through the trailing-
    edge corner (similar to vane assembly No. 2).
    The vane was fractured (similar to vane
    assembly No. 2).

5. Beryllide vane with nickel-aluminide shroud
    and platform. The platform was in good
    condition, a corner was broken from the
    leading edge of the shroud, and the vane
    failed in the same fracture pattern as did
    the other two beryllide vanes.

6. Nickel-aluminide end assembly, concave. No
    indications of oxidation or cracking were
    found on this assembly.

3.5.2.2 Stator Vane Test No. 2

Four stator vanes were positioned in a cascade as shown
in Figure 71. The four test vanes included one
Composition 1, one aluminum-nitride, another high-
temperature candidate material included for comparison,
and two nickel-aluminide vanes (one instrumented).
The Composition 1 vane was supported with beryllide
shroud and platform elements; all other vanes were
supported with nickel-aluminide components. Small
sections of the trailing edges of both the nickel-
aluminide and the aluminum-nitride vanes were broken
inadvertently prior to installation.

The failure mode of the first set of stator vanes sug-
gested that spanwise compressive stresses may have
developed during the test and could have contributed
to the vane failures. To minimize the occurrence of
this failure mode during the second test, the vane-to-
shroud clearance was set at 0.015 inch. This clearance
was considered to be sufficient to prevent contact
between the vane ends and shroud elements and, thus,
should have prevented compressive loading from develop-
ing due to thermal expansion of the vanes against the
shrouds and platforms.

86

THREE-PIECE STATOR DESIGN

ARRANGEMENT OF STATOR ASSEMBLIES

1	2	3	4	5	6
NiAl	NiAl	NiAl	NiAl	Beryl.	NiAl

NiAl	Al Nitride	NiAl (Instru.)	NiAl	Beryl.	NiAl

NiAl	NiAl	NiAl	NiAl	Beryl.	NiAl
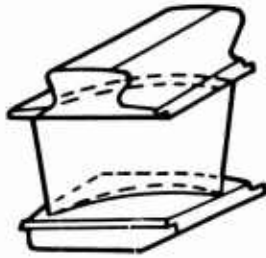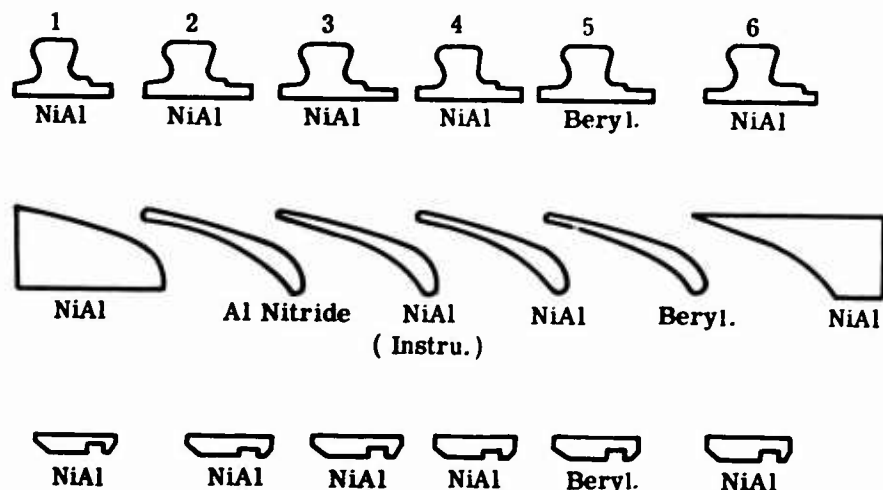
Figure 71. Cascade Test Components, Test No. 2.

As in the first test of the vane assembly, emphasis was placed upon minimizing the start transient. Again the peak observed combustor discharge temperature at light-off was 1900°F, and the rate of change of temperature was approximately as before. Combustor discharge temperature was increased from 1500°F to 2833°F in 15 minutes to provide 2500°F at the test section inlet. This condition was then maintained for 35 minutes, after which the temperature was slowly decreased, the rig was shut down, and the cascade test section was disassembled. Figure 72 shows the temperatures and pressures existing throughout the rig during this test.

87

AVERAGE SURFACE TEMPERATURES, F

| SECTION A-A | SECTION B-B | SECTION C-C | SECTION D-D | SECTION E-E |
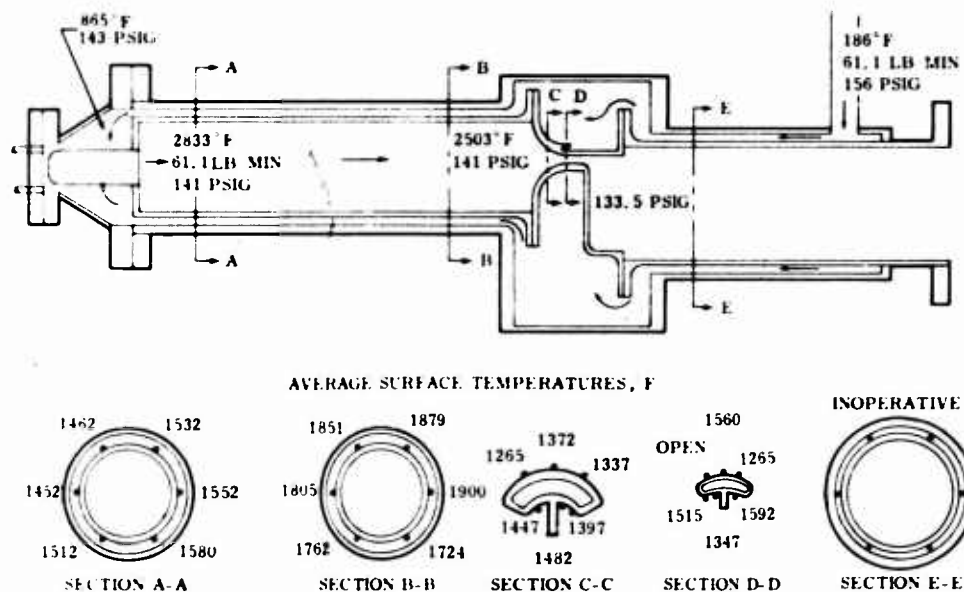
Figure 72. Test Rig Operating Conditions,
Test No. 2.

The beryllide assembly was fractured in several places,
as shown in Figure 73. No major damage to the other
test pieces was incurred. Fracture modes of the beryl-
lide vane appeared to be similar to those noted in the
first test except that indications of high compressive
loads from the vane ends to the shroud and platform were
not apparent as in the first test.

Figure 73. Beryllide Stator Assembly
After Test No. 2.

88

3.6 SUMMATION OF CASCADE TEST PROGRAM

While Composition 1 exhibited good oxidation resistance dur-
ing a 10-hour hot-corrosion cascade rig test, the poor duc-
tility of Composition 1 was emphasized by the cascade tests,
in which all of the beryllide vanes tested cracked in a
characteristic pattern. Analysis revealed that the crack
pattern in the vanes was similar to that produced in beryl-
lide wedge-shaped specimens, which failed by thermal cycling
in the laboratory. The beryllide material has a yield
strength of less than 55,000 psi at temperatures below 1900°F
and lacks ductility in this temperature regime. It is
probable that the vanes cracked from the thermal stresses
induced during light-off of the primary combustor. Propaga-
tion of these cracks may have occurred quite rapidly there-
after, because of the brittle material characteristics and
the aerodynamic loading on the vane.

4. COMPOSITION 2 STUDIES AND SPECIMEN TESTING

4.1 GENERAL

Under company sponsorship, a development program was conducted in an attempt to define means by which the stress-rupture strength and ductility available in Composition 1 could be improved.

The specific goals of the Composition 2 development program were to define a beryllide material that would meet the following requirements:

1. Ultimate tensile strength:

    30,000 psi minimum at 1800° and 2000°F

2. Tensile elongation:

    1.0 percent minimum at 1800°F

3. Stress rupture:

    8000 psi for 200 hours at 2200°F (based on specific gravity of 3.03 gm/cm^3)

4. Oxidation resistance:

    Less than 50 $mg/in.^2$ weight gain at 1700° and 2400°F for 200 hours

4.2 COMPOSITION STUDIES

Various compositions, fabrication parameters, and alloying additions were evaluated. Since Composition 1 was based on the columbium-beryllide system, additional studies were performed to determine if compositions within this system could be modified to increase stress-rupture strength. Approaches taken included increasing grain size, additions of alloying elements, and changes in basic composition and processing parameters.

Tantalum beryllides, in the compositional regions of interest, possess higher melting points than do the columbium beryllides of similar crystal structure. This could indicate the existence of greater atomic bonding forces and a potentially greater resultant stress-rupture strength. Effects of minor additions of aluminum and boron on the tantalum beryllides were evaluated.

Mixtures of columbium and tantalum beryllides, formed by pressing and sintering of mixed powders, were also evaluated.

The compositions selected for the specimen test evaluations are identified in the individual test descriptions presented in 4.3.

4.3 SPECIMEN TESTING

Specimen testing of Composition 2 candidate compositions comprised stress-rupture, oxidation, and tensile tests. The following subparagraphs describe the test specimens, test procedures, and test results.

4.3.1 Test Specimens

The specimens that were used for the stress-rupture testing and for the tensile testing that was conducted above 2000°F were machined in accordance with Figure 74. This specimen design, with minor modifications, was also used for tensile testing below 2000°F, as described in the tensile test discussion. The oxidation test specimens were identical to the Composition 1 oxidation test specimens shown in Figure 4.

4.3.2 Stress-Rupture Tests

The stress-rupture specimen testing was conducted at 2400°F with the same test equipment and instrumentation that was used for the Composition 1 stress-rupture specimen testing described in 2.5. The four basic compositions subjected to the stress-rupture specimen testing (excluding alloying elements) were:

1. $CbBe_{12}$

2. 50-percent $CbBe_{12}$ and 50-percent $TaBe_{12}$

3. $TaBe_{10.6}$

4. $TaBe_{10.6}$ with 0.5-percent B

91

(DIMENSIONS, IN.)
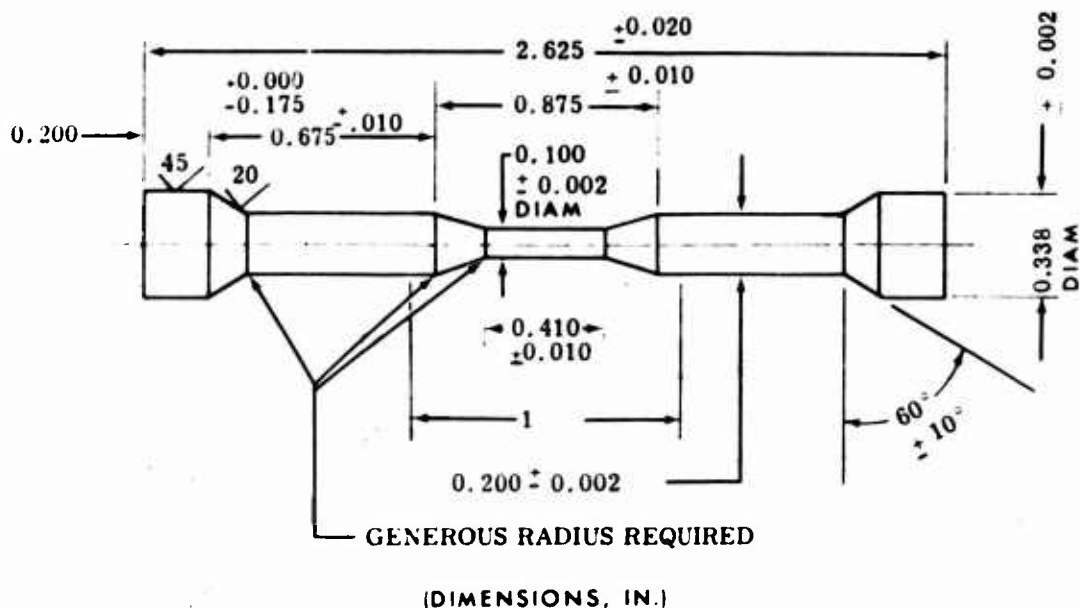
Figure 74. Beryllide Composition 2 (Candidates) Stress-Rupture and Tensile Test Specimen.

The percentage of elongation was determined by measuring the distances between the gauge marks on the fractured specimen and comparing these values to the original dimensions.

Figure 75 is a plot of the more pertinent data points, along with data for Composition 1 material. It should be noted that the constant used in the Larson-Miller parameter was 30.7 for the beryllides, rather than the usual 15 to 20 that is used for most superalloys. This value was calculated as the constant that would give the best curve fit for the beryllide data.

It can be seen in Figure 75 and Table XII that the Composition 2 candidates indicate stress-rupture lives that exceed the minimum of 200 hours at 2400°F and 2500 psi, as required by the uncooled-turbine stator vane design.

In general, the data showed that a gain in stress-rupture strength resulted in a reduction in elongation in stress rupture. Of importance were the apparent effects of the ternary alloying additions, aluminum and boron, on stress-rupture properties. The general effect of aluminum additions was one of reducing stress-rupture strength but increasing ductility, while boron additions appeared to have the reverse effect of increasing stress-rupture life and reducing elongation.

92

$(T + 460) (30.7 + \log t) \times 10^{-3}$
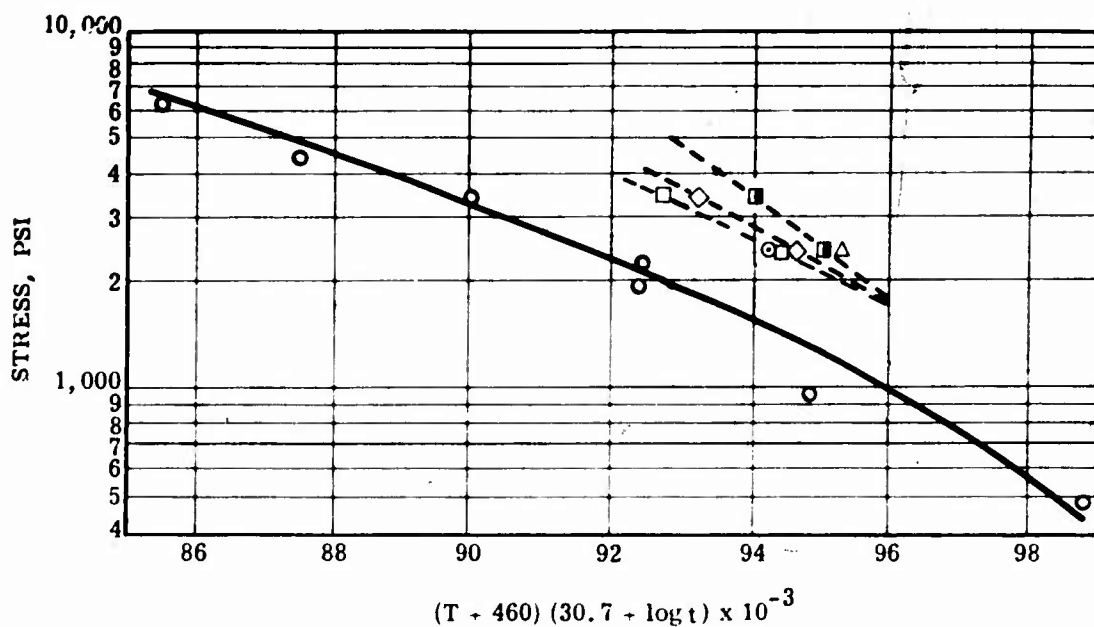
o : COMPOSITION 1

⊙ : MINIMUM REQUIREMENTS FOR STATOR MATERIAL
     (200 HRS AT 2500 PSI AND 2400 °F)

COMPOSITION 2 CANDIDATES

□ : Ta Be $_{10.5}$
◇ : Cb Be $_{12}$
◘ : Ta Be $_{10.5}$ +0.5 % B
△ : 50% Cb Be $_{12}$ +50% Ta Be $_{12}$

Figure 75. Stress-Rupture Test Results.

TABLE XII. STRESS-RUPTURE LIVES AND ELONGATION AT 2400°F AND 2500 PSI, BERYLLIDE COMPOSITION 2 STUDIES		
Basic Composition (Excluding Alloying Elements)	Life (hr)	Elongation (%)
$CbBe_{12}$	253.6	8.1
$TaBe_{10.5}$	225.4	27.2
$TaBe_{10.5}$ + 0.5% B	318.9	12.5
50% $CbBe_{12}$ + 50% $TaBe_{12}$	457.0÷*	6.2÷*
*Test discontinued; specimen did not rupture.		

4.3.3 Oxidation Testing

Oxidation specimen testing was conducted in static air at
1600°, 1700°, 1800°, and 2400°F with the same test equipment
and instrumentation that was used for the Composition 1
oxidation specimen testing described in 2.8. The nine
basic compositions subjected to the oxidation specimen test-
ing (excluding minor alloying elements) were:

1. $CbBe_{10.6}$ plus 0.5-percent Al

2. $TaBe_{10.6}$

3. $TaBe_{10.6}$ plus 1.0-percent Al

4. $TaBe_{10.6}$ plus 0.5-percent B

5. $TaBe_{12}$

6. $TaBe_{12}$ plus 1.0-percent Al

7. $TaBe_{12}$ plus 0.5-percent B

8. $CbBe_{12}$ plus 0.5-percent B

9. $CbBe_{12}$ plus 1.0-percent Al

Following completion of the 300-hour test, the specimens were
photographed as shown in Figure 76. The TaBe compositions
showed very good oxidation resistance at all temperatures
and met the Composition 2 program objective of less than
50 mg per sq in. weight gain in a 300-hour period. The
$CbBe_{12}$ composition with the 0.5-percent B and 1.0-percent
Al additions showed good oxidation resistance at 1600°,
1700°, and 1800°F but was badly oxidized at 2400°F. The
$CbBe_{10.6}$ composition with 0.5-percent Al showed poor
oxidation resistance at all temperatures, with the poorest
results being at the 1700°F test point.

4.3.4 Tensile Testing

The tensile testing consisted of two phases as described in
the following subparagraphs.

4.3.4.1 Phase I

The Phase I tensile testing was conducted at tempera-
tures between 2000°F and 2400°F with the same test
equipment and instrumentation that was used for the
Composition 1 tensile specimen testing described

94

CbBe $_{10.5}$ + 0.5% Al

TaBe $_{10.5}$

TaBe $_{10.5}$ + 1.0% Al

TaBe $_{10.5}$ + 0.5% B

TaBe $_{12}$

TaBe $_{12}$ + 1.0% Al

TaBe $_{12}$ +0.5% B

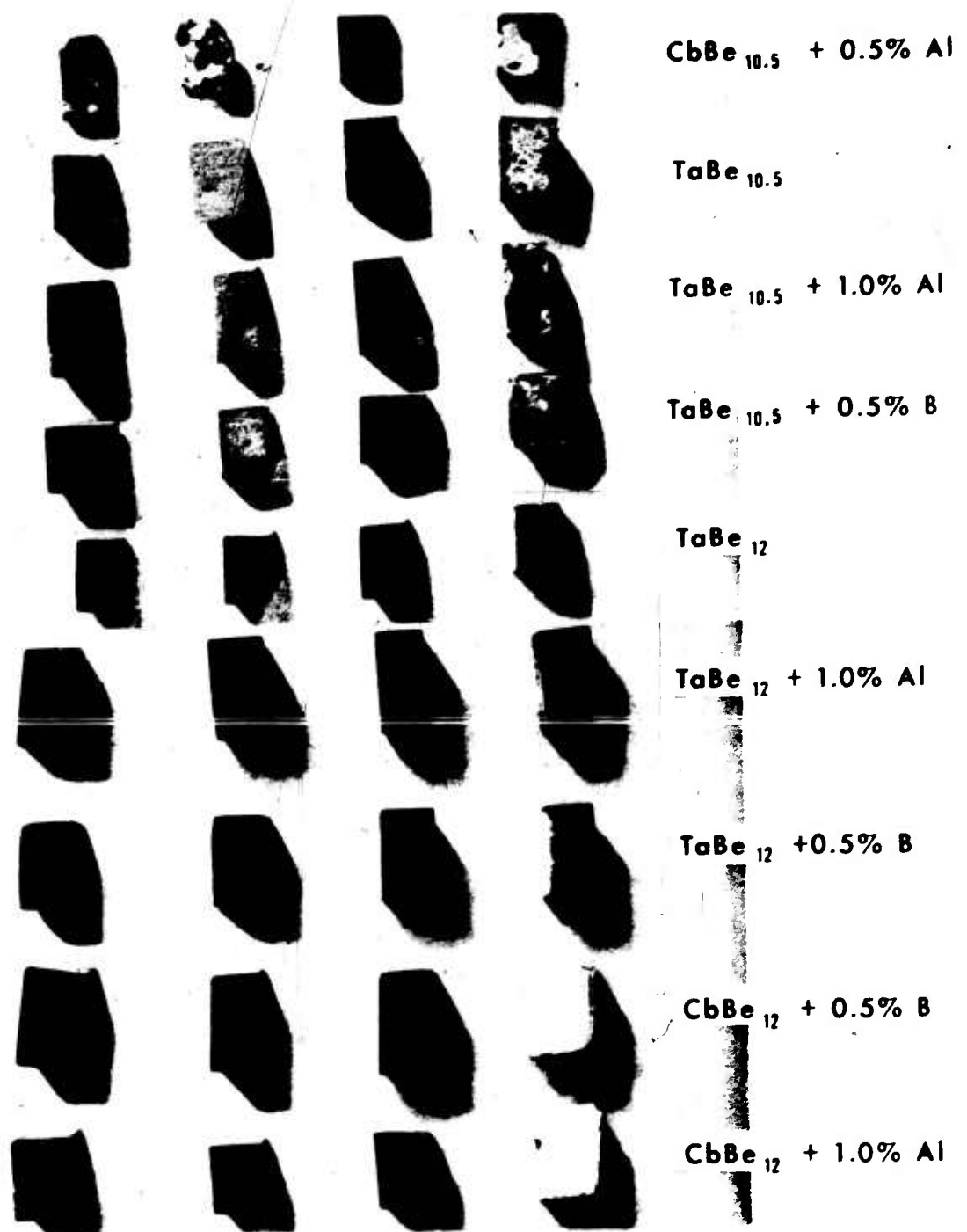CbBe $_{12}$ + 0.5% B

CbBe $_{12}$ + 1.0% Al

Figure 76. Beryllide Composition 2
Oxidation Test Specimens
After 300 Hours' Exposure.

in 2.3. The compositions and the test specimen con-
figuration that were subjected to the tensile testing
were identical to those tested in the Composition 2
stress-rupture testing reported in 4.3.

The compositions that were tensile-tested had exhibited
higher stress-rupture strength values than those of
Composition 1. The results of the tensile testing
revealed that these compositions also had greater
tensile strength than Composition 1. However, duc-
tility of these compositions did not show substantial
improvement over that of Composition 1. Therefore,
additional beryllide compositions were tensile-
tested (Phase II) in an attempt to develop a composi-
tion that showed ductility improvements.

4.3.4.2 Phase II

The Phase II tensile testing was conducted at 1800°F
by a materials-testing vendor with an Instron
testing machine. This instrument was calibrated to
record load-time information so that a conversion
could be made to load-elongation and, thus, record
indications of plastic deformation. The configura-
tion of the test specimens was identical to that
of the specimen design that was used for Phase I
testing (Figure 35) except that the test-section
diameter was reduced from 0.100 inch to 0.080 inch.
This modification was necessary to assure failure
in the test section rather than the "button head"
ends. The compositions (excluding alloying elements)
that were tested were:

1. Composition 1
2. 50-percent $CbBe_{10.5}$ and 50-percent $TaBe_{10.5}$
3. $CbBe_{10.5}$ plus 0.25-percent Y
4. $CbBe_{10.5}$ plus 1.0-percent Y
5. $CbBe_{10.5}$ plus 5.0-percent Y
6. $CbBe_{10.5}$ plus 10.0-percent Ta
7. Equal $CbBe_{10.5}$ and $TaBe_{10.5}$ plus 1.0-percent Al
8. $TaBe_{10.5}$ plus 1.0-percent Al

The task of the Phase II testing was to evaluate the
tensile strength and elongation of the above-listed
beryllide compositions at 1800°F. Then, as originally
planned, those compositions that displayed an indica-
tion of ductility at 1800°F would be further tested

96

to evaluate stress-rupture and oxidation properties. However, none of the compositions tested gave sufficient evidence of ductility to warrant further testing.

4.4 SUMMATION OF COMPOSITION 2 STUDIES

In reviewing the data collected during this investigation, a number of conclusions were reached:

1. The minimum stress-rupture requirements for the uncooled-turbine stator vane design (200 hours at 2400°F and 2500 psi) can be met with various beryllide compositions.

2. Tensile elongation was not measurable at 1800°F for any of the beryllide compositions tested.

3. Ternary alloying additions have definite effects on stress-rupture strength, ductility, and oxidation resistance; specifically,

   a. Aluminum additions improved oxidation resistance of the columbium beryllides.

   b. Boron additions were harmful to the oxidation resistance of the columbium beryllides but did not affect the resistance of the tantalum beryllides.

   c. Aluminum additions decreased the stress-rupture and tensile strength but tended to increase the ductility of both columbium and tantalum beryllides.

   d. Boron additions increased the stress-rupture and tensile strength of the tantalum beryllides.

Results from the beryllide Composition 2 study and specimen test program indicate that although beryllides can now be produced that exhibit both good oxidation resistance and stress-rupture strengths that exceed the minimum requirements for the uncooled-turbine stator design, the beryllides do not display sufficient ductility at the lower temperatures for stator or rotor designs. As a result of lack of indications of ductility, it was not possible to recommend a Composition 2 material for application in the uncooled-turbine components.

97

5. IN-100 AND AIRESIST 13 SPECIMEN TESTING

5.1 GENERAL

Part of the uncooled-turbine materials investigation consisted of material properties testing conducted on IN-100 and AiResist 13 alloy specimens. This testing included tensile, stress-rupture, notch-fatigue, creep, oxidation, oxidation-sulfidation, mechanical-fatigue, and thermal-fatigue tests.

IN-100 and AiResist 13 materials were intended for use in the uncooled-turbine components of the final stage(s). The purpose of the material properties testing was to provide the turbine design activities (reported in Volume II) with substantiated IN-100 and AiResist 13 material-property values.

Subsequent paragraphs (a) describe the preparation of the alloys and fabrication of the test specimens, (b) define the material properties test procedures, and (c) present summations of the test results for each type of test that was conducted.

5.2 ALLOY PREPARATION AND TEST SPECIMEN FABRICATION

Vendors were selected to prepare master heats and cast the required test bars for each alloy. Test specimen fabrication was accomplished in-house. The following subparagraphs discuss the melting, casting, and fabrication activities for each of the two materials.

5.2.1 AiResist 13 - Melting

Since AiResist 13 was a new alloy with a more reactive chemistry than normal cobalt-base alloys, it was decided to introduce as many variables into the melting process as a program of this nature would permit. This enabled a more complete determination of the melting practices that may be detrimental to the performance of the alloy. Therefore, three different material vendors were selected, each to prepare a 500-pound heat.

The good corrosion-resistant properties of AiResist 13 depend
upon the presence of aluminum and yttrium in the alloy. How-
ever, the reactive nature of the yttrium with crucible mate-
rials and the atmosphere necessitated investigation of the
benefit of maintaining the required composition under varying
melting conditions. Therefore, each of the three selected
vendors was requested to melt its alloy heat by standard
in-house practices. Tables XIII, XIV, and XV present the
"Alloy Development Record," which shows the basic melting pro-
cedures followed by the three vendors. It should be noted
that one vendor declined to reveal certain aspects of the
melting information that he considered to be proprietary.

The heat sizes of the three vendors are listed below:

Vendor	Heat Weight (lbs)	Ingot Size
No. 1	2200	2-3/4 inches in diameter
No. 2	1000	2-3/4 inches in diameter
No. 3	500	3-1/2 inches in diameter

Due to furnace minimums, both the No. 1 and the No. 2 vendor
melted larger charges. Both larger heats were within the
chemistry specification limits.

Each melting vendor reported the source of its master alloys
used to produce each alloy heat. A chemical analysis per-
mitted the evaluation of each master alloy for "tramp" ele-
ments that might be deleterious to AiResist 13 properties.
All were found to be of high purity, with no known harmful
contamination. The chemical analysis of the three alloy heats
is presented in Table XVI.

TABLE XIII. VENDOR NO. 1 ALLOY DEVELOPMENT RECORD

Development Alloy Designation__AiResist 13

Master Heat No.__65V 3411   Date__6/1/64__

Weight of Heat__2200 lbs   Size__2-3/4-in. diam

Melting Log (Master Heat Only)

Prime Alloy Charge   Crucible Mold__Nortons P.M. 1170

Refining Time__98 minutes after__

__all additions__

Refining Temp, °F__2820__

Pouring Temp, °F__2825__

Metal

1. Co
2. Cr
3. W
4. Al
5. C
6. Y
7. FeCb

Alloying Sequence

Metal   Time of Addition

1. C   ⎫
2. Cr   ⎪
3. Fe   ⎬ Added to crucible cold
4. Co   ⎪ and melted in it.
5. W   ⎪
6. FeCb ⎭
7. Al   Added 76 minutes after charge was molten.
8. Y   Added 45 minutes after aluminum addition.
            Charge poured 98 minutes after adding
            yttrium misch metal.

TABLE XIV. VENDOR NO. 2 ALLOY DEVELOPMENT RECORD

Development Alloy Designation __AiResist 13__

Master Heat No. __6-3581__   Date __7/8/64__

Weight of Heat __1000 lbs__   Size __2-3/4-in. diam x R/L__

Melting Log (Master Heat Only)

Prime Alloy Charge   Crucible Mold____ Proprietary

                                  Refining Time____ Proprietary

                                  Refining Temp, °F__ Proprietary

                                  Pouring Temp, °F__ Proprietary

Metal

1. C
2. Cr
3. Co
4. W
5. FeCb
6. Al
7. Y

Alloying Sequence

Metal	Time of Addition
1. C	
2. Cr	Charged in crucible and melted
3. Co	down and refined in accordance
4. W	with established procedures.
5. FeCb	
6. Al	Added at 1402 hours
7. Y	Added at 1416 hours

TABLE XV. VENDOR NO. 3 ALLOY DEVELOPMENT RECORD

Development Alloy Designation__AiResist 13

Master Heat No.__T2759   Date__7/6/64

Weight of Heat__500 lbs   Size__3-1/2-in. diam

Melting Log (Master Heat Only)

Prime Alloy Charge   Crucible Mold__Lamag 32H with
                                                    __ceramic shell

                                      Refining Time__25 minutes____

                                      Refining Temp, °F__2620 - 3000

                                      Pouring Temp, °F___3000_____

Metal

  *1.
   2.
 **3.
   4.
   5.
   6.
   7.
***8.

 *AGSR Graphite
 **Ancor Sponge E.
***70-percent yttrium misch metal

Alloying Sequence

Metal	Time of Addition
1. C	In cold charge
2. Cr	In cold charge
3. Fe	In cold charge
4. Co	In cold charge
5. W	In cold charge
6. Cb	In cold charge
7. Al	25 minutes after cold charge all melted
8. Y	31 minutes after cold charge all melted
	Poured 25 minutes after yttrium addition

102

TABLE XVI. CHEMISTRY OF THREE MASTER HEATS OF AIRESIST 13

						Composition, Weight Percent						
	C	Si	Mn	Co	Ni	Cr	Fe	W	Al	Cb + Ta	Y
Vendor No. 1	0.48	0.13	0.10	Bal	0.20	21.20	1.37	10.80	3.30	2.14	0.42
Vendor No. 2	0.47	0.10	0.10	Bal	0.18	21.10	1.25	10.70	3.30	2.20	0.50
Vendor No. 3	0.48	0.10	0.10	Bal	0.20	21.60	1.27	11.60	3.50	1.95	0.15
EMS 598 Specification	0.40 0.50	0.50 max	0.50 max	Bal	1.00 max	20.00 22.00	2.50 max	10.00 12.00	3.00 3.40	1.50 2.50	0.30 0.60

It was established that substantial yttrium can be lost
during melting, and this loss must be compensated. It is
believed that the yttrium loss can occur from any of the
following reactions:

1. Atmosphere (vacuum) $4Y + 3O_2 = 2Y_2O_3$ (slag)

2. Crucible reaction $aY + b \begin{Bmatrix} MgO \\ ZrO_2 \\ Al_2O_3 \end{Bmatrix} = mY_2O_3$

$+ n \begin{Bmatrix} Mg \\ Zr \\ Al \end{Bmatrix}$ (stays in master heat)

3. Entrapped gaseous impurities $4Y + 3 \begin{Bmatrix} O_2 \\ N_2 \\ S_2 \end{Bmatrix} = 2 \begin{Bmatrix} Y_2O_3 \\ Y_2N_3 \\ Y_2S_3 \end{Bmatrix}$
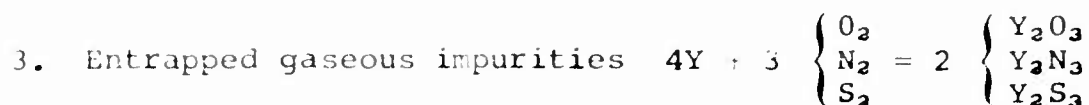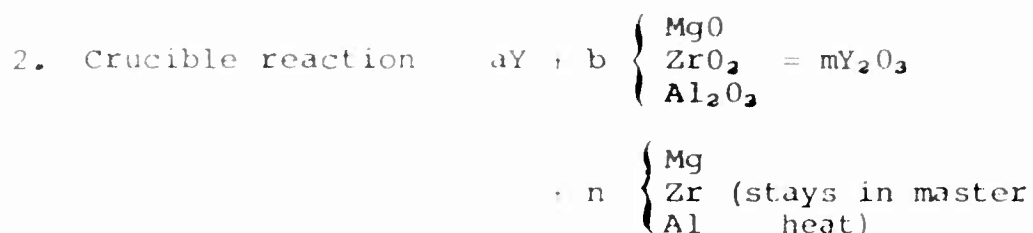
On the basis of the response of the materials in both the
casting operations and the mechanical-property tests, all
three sources proved their capability of handling the
preparation of AiResist 13. The three different melting
procedures used revealed that AiResist 13 requires close
control during melting but is not sensitive to any particular
melting formula.

5.2.2 AiResist 13 - Casting

One vendor was selected to cast all AiResist 13 test speci-
mens for use in the test program. With one casting vendor
using one set of casting procedures, the elimination of cast-
ing variables was realized, permitting a better evaluation of
the three different master heats. Each type of specimen
casting included castings from each of three different master
heats. One hundred seventy test bars were cast.

The data obtained during the casting operation are presented
in Table XVII. As can be seen in Table XVII, each casting
variable was closely controlled. The mold preheat tempera-
ture was 1800°F, while the pouring temperature varied from
2850° to 2900°F, depending on the size of the charge and the
configuration of the test bar being cast. All metal tempera-
tures were measured by an immersion thermocouple. Optical
temperature-measuring devices could not be used because of
the cloudy surface common with molten AiResist 13.

The cast test-bar molds were allowed to cool for 8 hours
before removal of the cast test bars. The test-bar molds are
shown in Figures 77, 78, 79, and 80. Table XVIII presents

104

TABLE XVII. CASTING DATA OF THREE AIRESIST 13 MASTER HEATS

Specimen	Charge Wt (lb)	Order of Casting	Melt Temp (°F)	Pour Temp (°F)	Vacuum at Pour (microns)
Fatigue B-2406	12	6	2900	2900	7
		7	2900	2900	15
		14	2900	2900	8
		15	2900	2900	6
		21	2900	2900	7
		22	2900	2900	5
Tensile/Stress-Rupture B-2402	12	2	2900	2870	12
		3	2870	2870	10
		10	2870	2870	12
		11	2885	2885	3
		18	2870	2870	8
		19	2870	2870	8
Thermal Fatigue B-2483	11	1	2865	2865	5
		9	2870	2870	10
		17	2860	2860	20
Notched Rupture/Creep B-2399	12	4	2890	2880	7
		5	2870	2870	10
		12	2870	2870	9
		13	2870	2870	5
		20	2870	2870	8
Oxidation Sulfidation Bar	7	8	2850	2850	10
		16	2850	2850	7
		23	2850	2850	8

NOTE: Casting Furnace: Continuous casting type
        Crucible: Zirconia base (17 lb)
        Mold Material: Zirconia base

Figure 77. Mold Pattern Used for Casting AiResist 13
Tensile and Stress-Rupture Test Bars.

106

Figure 78. Mold Pattern Used for Casting AiResist 13
Notch-Rupture and Creep Test Bars.

107
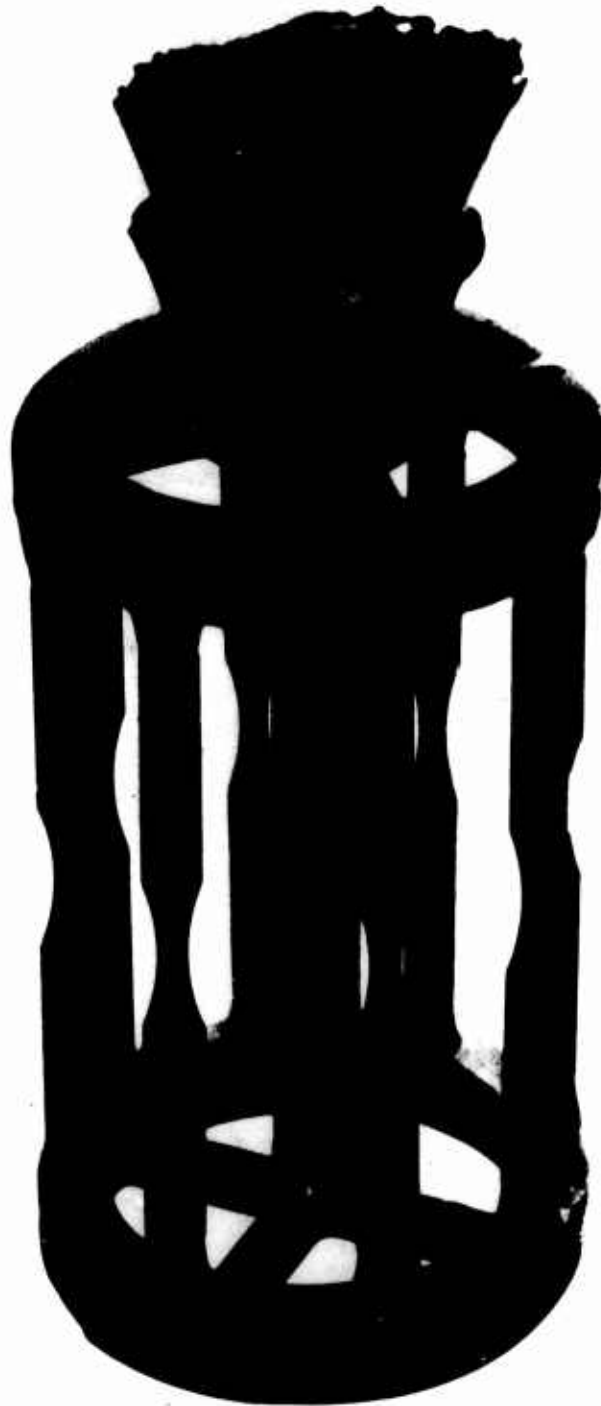
Figure 79.   Mold Pattern Used for Casting AiResist 13
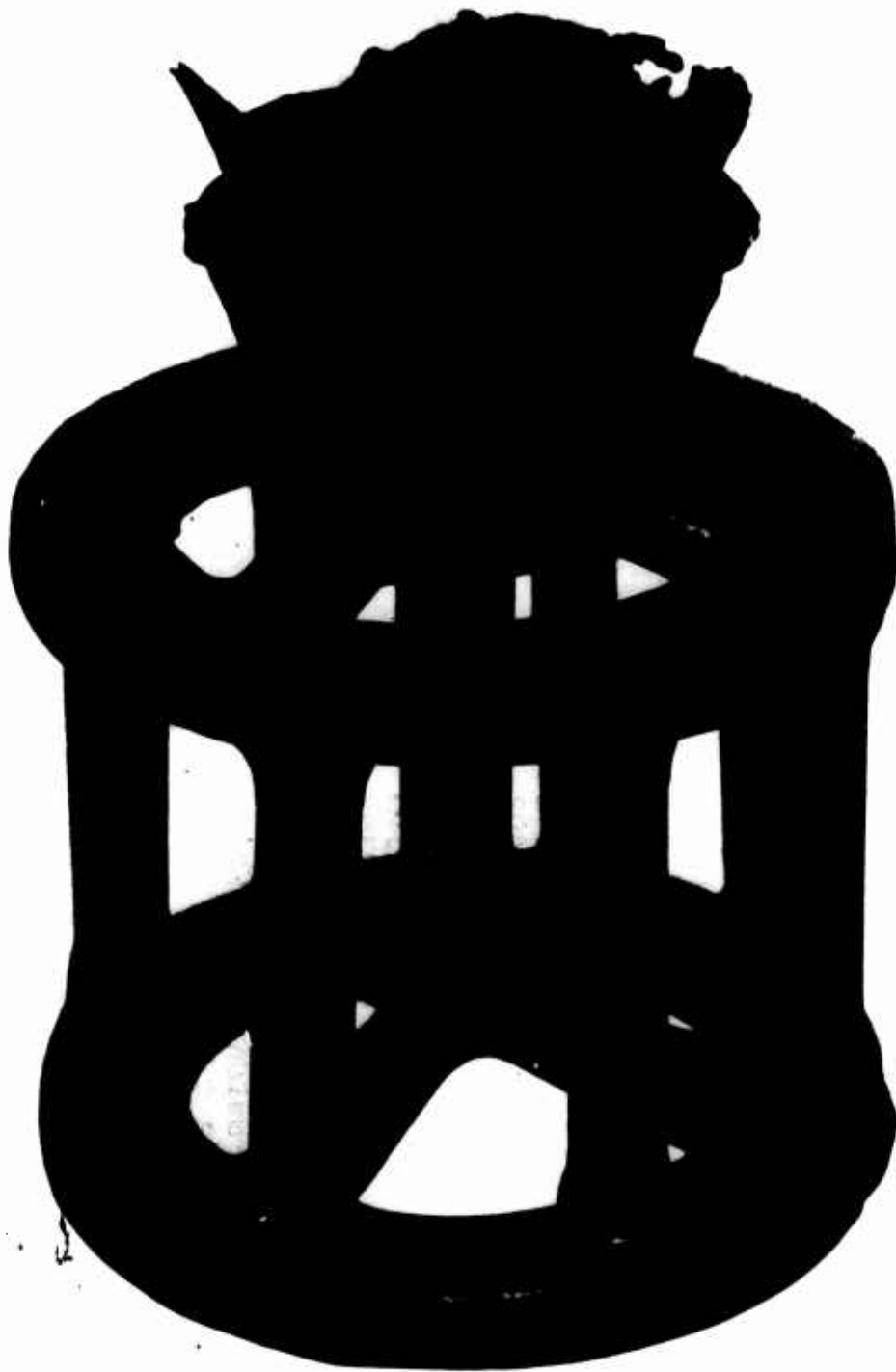Mechanical Fatigue Test Bars.

Figure 80.   Mold Pattern Used for Casting AiResist 13
             Oxidation and Oxidation-Sulfidation Test Bars.

TABLE XVIII. SPECIMEN SUMMARY SHEET

Flask No.	Heat No.	Type	Part Number	Grain Size (in.)	Quantity	Quantity Shipped	Quantity Rejected*
186	65V3411	Fatigue bar	B2406	1/16	8	7	1
187	65V3411	Fatigue bar	B2406	1/32	8	6	2
194	63581	Fatigue bar	B2406	1/16	8	7	1
195	63581	Fatigue bar	B2406	1/32 - 1/16	8	7	1
201	T2759	Fatigue bar	B2406	1/16	8	7	1
202	T2759	Fatigue bar	B2406	1/32 - 1/16	8	7	1
182	65V3411	Cast to size	B2402	1/8 - 3/16	16	10	6
183	65V3411	Cast to size	B2402	1/32 - 1/16	16	10	6
190	63581	Cast to size	B2402	1/64	16	10	6
191	63581	Cast to size	B2402	1/64	16	11	5
198	T2759	Cast to size	B2402	1/16	16	10	6
199	T2759	Cast to size	B2402	1/8	16	15	1
184	65V3411	Shoulder fed	B2399	1/64	16	11	5
185	65V3411	Shoulder fed	B2399	1/64	16	9	7
192	63581	Shoulder fed	B2399	1/32	16	9	7
193	63581	Shoulder fed	B2399	1/64	16	9	7
200	T2759	Shoulder fed	B2399	1/32 - 1/16	16	9	7
181	65V3411	Erosion bars	B2483	1/32 - 1/16	12	9	3
189	63581	Erosion bars	B2483	1/32	12	8	4
197	T2759	Erosion bars	B2483	1/16	12	9	3
188	65V3411	1/2 D bar	-	<1/64	-	7	0
196	63581	1/2 D bar	-	1/16	-	6	0
203	T2759	1/2 D bar	-	1/8	-	6	0

*Scrapped because of excessive visual and/or Zyglo indications.

the specimen summary sheet showing the yield of each test-bar mold. It was noted that a large number of test specimens were rejected by visual and/or fluorescent-penetrant inspection due to surface defects.

All molds were prime-dip-inoculated to provide proper grain-size control. The grain size of each cluster is shown in Table XVIII and was found to be very consistent.

Each test bar was X-ray-inspected in the as-cast condition. Following this inspection, the gauge diameters of the tensile, creep, and stress-rupture test bars were ground approximately 0.003 inch below the cast surface to remove any mold-metal surface defects. The ground specimens and all remaining cast test bars then were subjected to fluorescent-penetrant and radiographical inspection to determine if any surface defects were present. As shown in Table XVIII, approximately 20 percent of the cast specimens were rejected as a result of these inspection procedures. Figure 81 illustrates the AiResist 13 cast specimens.

The configuration of the thermal-fatigue test specimen was changed after completion of the casting program. Therefore, it was necessary for a new specimen design to be cast. The revised thermal-fatigue specimens are shown as cast in Figure 82.

5.2.3 AiResist 13 - Specimen Fabrication

The cast bars were machined in-house to the final test specimen configurations. The tensile and stress-rupture test specimens were machined in accordance with Figure 83. Approximately 0.020 inch was machined from the gauge diameter of each specimen to conform to the dimensions of Figure 83. The machined notch-rupture test specimens conformed to the illustration presented as Figure 84. The creep test specimens were machined in accordance with Figure 85. Figure 86 illustrates the configuration of the final-machined mechanical-fatigue test specimens. The machined thermal-fatigue test specimens conformed with the specimen illustrated in Figure 87. The oxidation and oxidation-sulfidation test specimens were prepared by cutting 1/4-inch-thick samples from the cast 1/2-inch-diameter bars.

After completion of the final machining, each test specimen was subjected to fluorescent-penetrant inspection prior to testing.
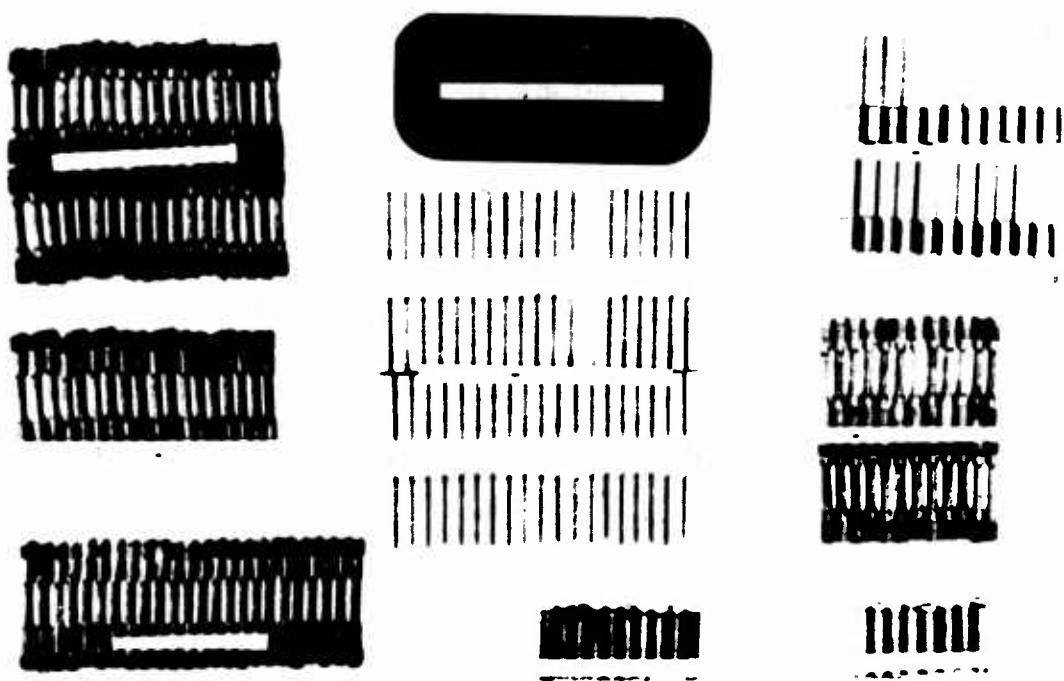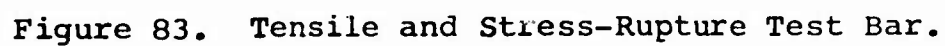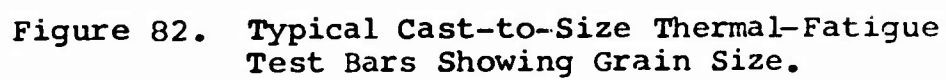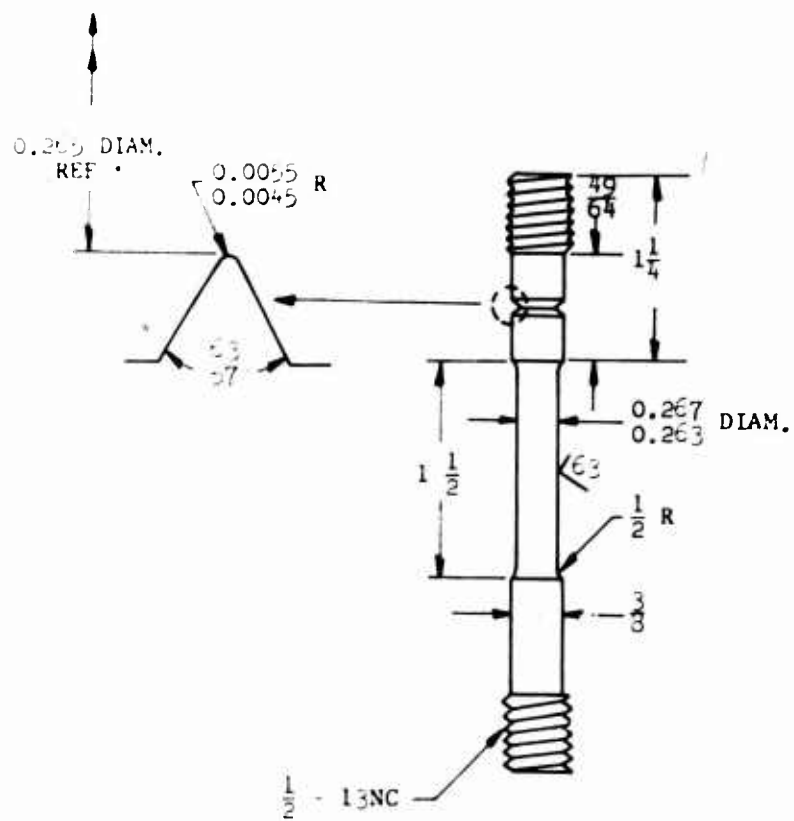
111

Figure 81.   Test Bars in the As-Cast Condition.

Figure 82.   Typical Cast-to-Size Thermal-Fatigue
Test Bars Showing Grain Size.

(DIMENSIONS, IN)

Figure 83.   Tensile and Stress-Rupture Test Bar.

113

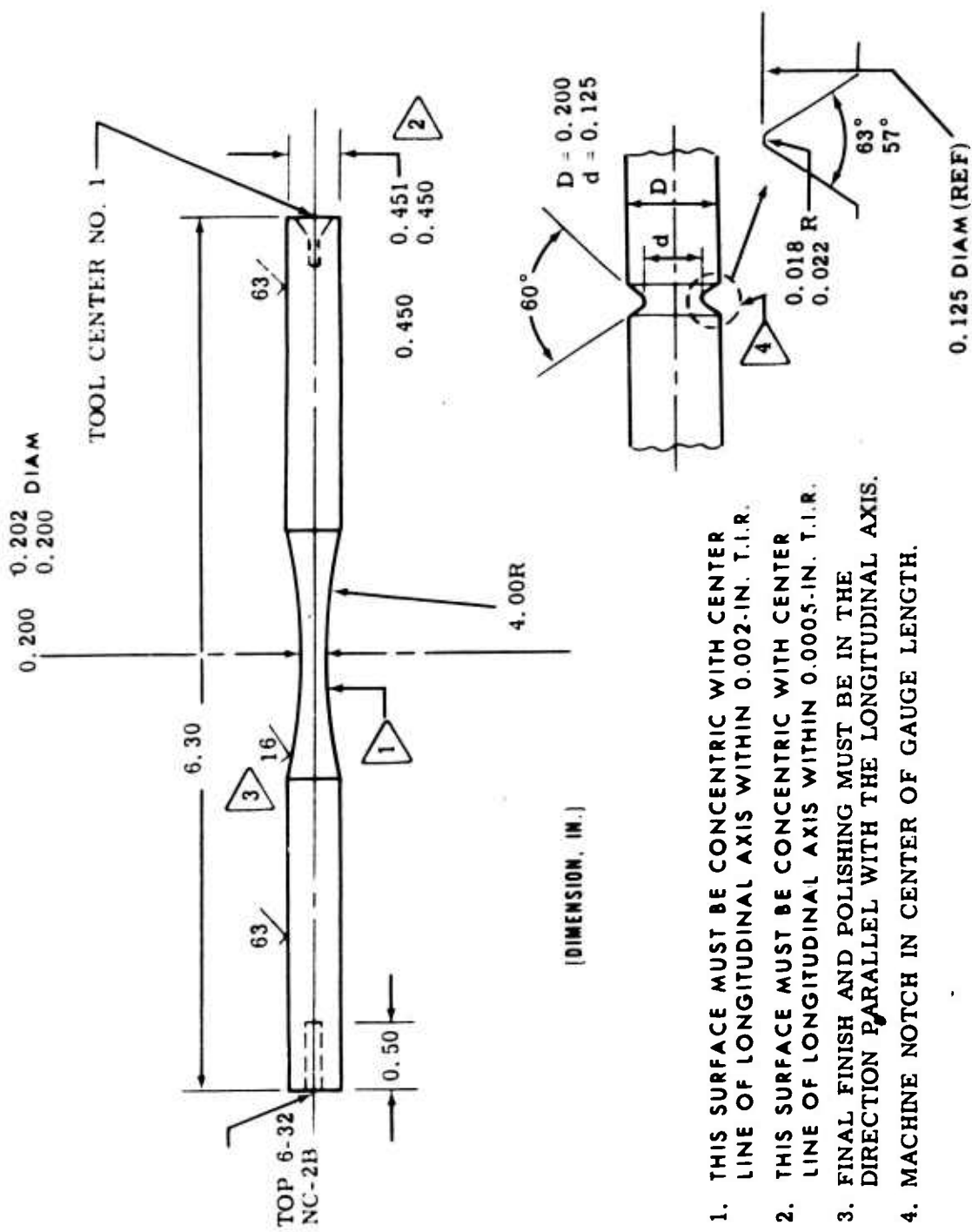*THIS DIAMETER MUST BE WITHIN 0.0005 INCH OF GAUGE DIAMETER.

(DIMENSIONS, IN.)

Figure 84.   Notch-Rupture Bar.

FOUR HOLES NO. 48 DRILL, $\frac{1}{16}$ INCH MAX. DRILL DEPTH

$\frac{1}{2}$ - 13 NC

$\frac{1}{2}$ R

$\frac{17}{64}$

$\frac{3}{8}$

$\frac{1}{2}$ -13 NC

$1\frac{1}{2}$

$1\frac{1}{2}$

$\frac{1}{2}$

$1\frac{1}{4}$

(DIMENSIONS, IN.)

PARALLEL SECTION OF DIAMETERS TO BE CONCENTRIC WITH CENTER LINE WITHIN 0.0005 INCH T.I.R. FOR DISTANCE.

Figure 85.   Machined Creep Specimen.

TOOL CENTER NO. 1

0.202
0.200 DIAM

0.200

0.451
0.450

0.450

4.00R

6.30

0.50

TOP 6-32
NC-2B

[DIMENSION, IN.]

D = 0.200
d = 0.125

60°

63°
57°

0.018
0.022 R

0.125 DIAM (REF)

1. THIS SURFACE MUST BE CONCENTRIC WITH CENTER
   LINE OF LONGITUDINAL AXIS WITHIN 0.002-IN. T.I.R.

2. THIS SURFACE MUST BE CONCENTRIC WITH CENTER
   LINE OF LONGITUDINAL AXIS WITHIN 0.0005-IN. T.I.R.

3. FINAL FINISH AND POLISHING MUST BE IN THE
   DIRECTION PARALLEL WITH THE LONGITUDINAL AXIS.

4. MACHINE NOTCH IN CENTER OF GAUGE LENGTH.

Figure 86. Mechanical-Fatigue Test Specimen.

116

(DIMENSION, IN.)
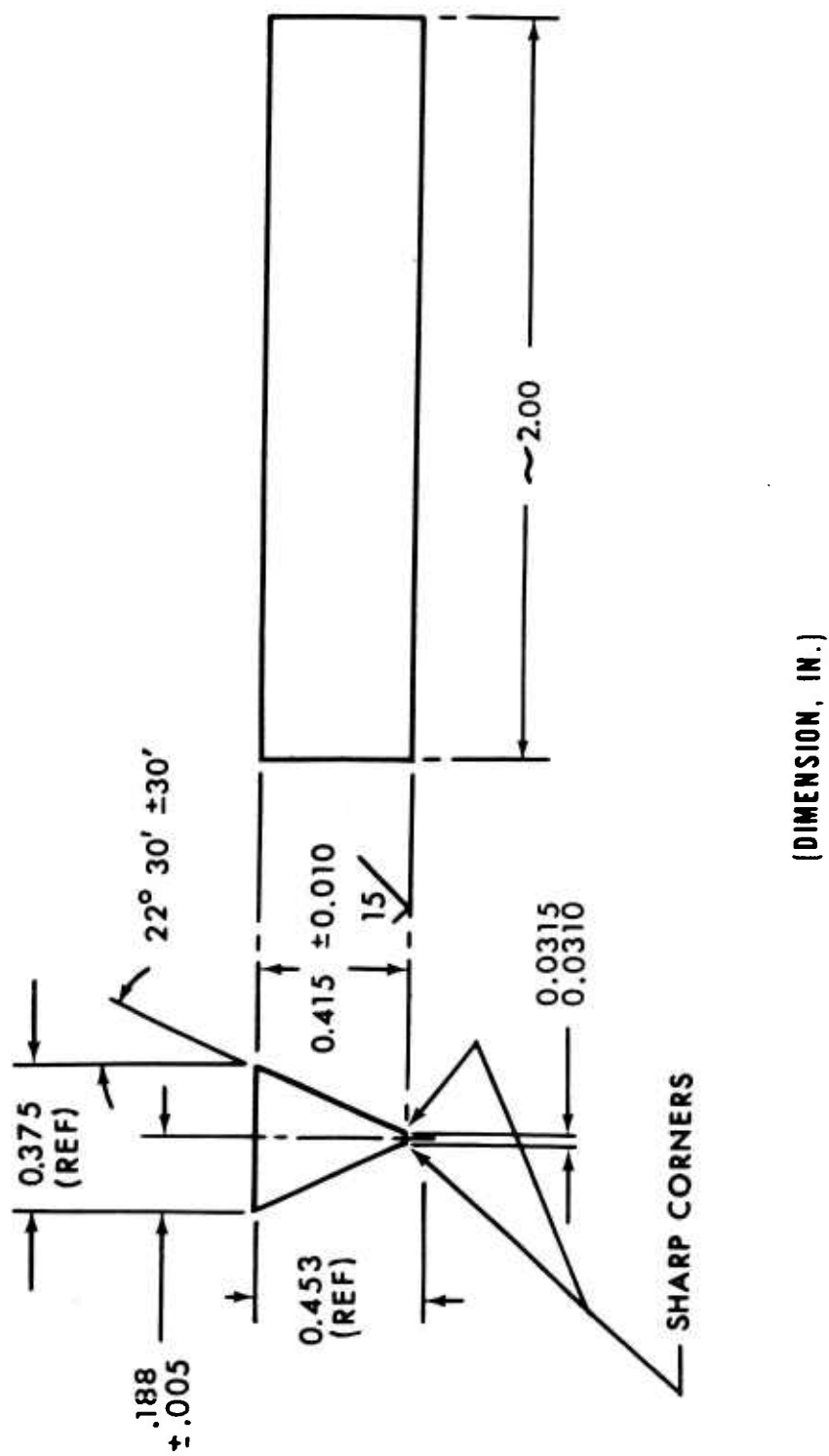
Figure 87. Thermal-Fatigue Test Specimen.

117

5.2.4 IN-100 - Melting

One vendor was selected to melt and cast the IN-100 material. The melting and casting operations were performed in a partial vacuum. Table XIX presents the "Alloy Development Record," which shows the basic melting procedure that was followed by the vendor.

Three 500-pound master heats were prepared as follows:

1. 100-percent prime material

2. 50-percent prime material plus 50-percent revert material

3. 100-percent revert material

Only IN-100 revert material was used during preparation of the 50- and 100-percent revert master heats.

The materials used in preparing the prime IN-100 master heat, the sources of procurement, and the chemical analysis of each material are listed in Table XX. The chemical compositions of the three master heats are presented in Table XXI.

5.2.5 IN-100 - Casting

Conditions during casting of the disks and thermal-fatigue specimens were closely controlled in order to obtain uniform grain size. The zirconium mold preheat temperature was 1900°F. The IN-100 charge was melted at 3080°F, held at that temperature for 45 minutes, cooled to 2650°F, and then cast. All metal temperatures were measured by optical means.

Three disks and one bar (thermal-fatigue specimen) were cast from each of the three master heats. The outline shown in Figure 88 was followed during the casting operation.

The shape of the cast disks, shown in Figure 89, was chosen for the following reasons:

1. Ease of castability.

2. The disk shape closely duplicates blanks from which turbine wheels are machined.

3. More representative material properties can be obtained from disks than from cast-to-size test bars.

118

TABLE XIX.   ALLOY DEVELOPMENT RECORD

Development Alloy Designation: IN-100

Master Heat No. T2700, Source - 100% Prime,   Date: 6-26-64
Size - 450 lb

Melting Log (Master Heat Only)

Prime Alloy Charge

Crucible__Lamag 32H
Ingot__1020 iron pipe
Refining Time__45 min.
Refining Temp, °F__3080
Pouring Temp, °F__2650

Metal		Alloying Sequence	
1.	Cr	Metal	Time of Addition
2.	Mo	1. Cr	In cold charge
3.	Co	2. Mo	In cold charge
4.	Ni	3. Co	In cold charge
*5.	C	4. Ni	In cold charge
6.	Al	***5. C	When cold charge just melted
7.	V	6. Al (Bal)	45 minutes after cold charge all melted
8.	Ti	7. V	45 minutes after cold charge all melted
9.	Zr	8. Ti	53 minutes after cold charge all melted
**10.	B	9. Zr	81 minutes after cold charge all melted
		10. B	81 minutes after cold charge all melted

*AGSR Graphite
**Nickel Boron
***Plus 1/2% Al.

TABLE XX. MATERIALS USED TO PREPARE THE PRIME IN-100 MASTER HEAT

Element	Elements Found		
	>1.0%	0.1 - 1.0%	<0.1%
Carbon	C	-	-
Chromium	Cr	Al	Ca, Co, Cu, Mn, Si, and Fe
Cobalt	Co	Cu and Ni	Al, Mn, Si, Fe
Molybdenum	Mo	-	Ca, Co, Cr, Cu, Fe, Mg, Mn, Si, Ti
Titanium	Ti	Co and Si	Al, Cr, Ca, Cu, Mn, Mg, Fe, Sn, Ni, Mo
Aluminum	Al	Si, Fe, Mg	Cu, Mn, Ca
Vanadium	V	Co	Cu, Fe, Mn, Mo, Ni, Cr
Boron	Ni, B	Ca, Fe, Mg, Si	Al, Co, Cu, Cr, Mn, Co, P
Zirconium	Zr	-	Cu, Fe
Nickel	Ni	B, Mg	Ca, Cr, Cu, Mn, Mo, Si, Sn

TABLE XXI. CHEMISTRY OF THE THREE IN-100 MASTER HEATS

Heat Number	C	S	Si	Mn	Cr	Mo	Fe	Ti	Al	Co	V	Zr	B	Ni
T2700 (100% Prime)	.19	.004	.057	.02	9.60	3.01	.20	4.82	5.53	14.90	1.00	.069	.015	Bal
T2761 (50% Prime 50% Revert)	.16	.004	.069	.02	9.00	2.96	.34	4.88	5.37	14.00	.88	.065	.013	Bal
T2762 (100% Revert)	.18	.005	.051	.02	9.40	2.96	.29	4.79	5.37	14.50	.94	.065	.014	Bal

NOTE: Quantities are percent by weight.

121

```
┌─────────────────┐      ┌─────────────────┐      ┌─────────────────┐
│   100% PRIME    │      │   50% PRIME     │      │  100% REVERT    │
│  MASTER HEAT    │      │   50% REVERT    │      │  MASTER HEAT    │
│                 │      │  MASTER HEAT    │      │                 │
└─────────────────┘      └─────────────────┘      └─────────────────┘
```
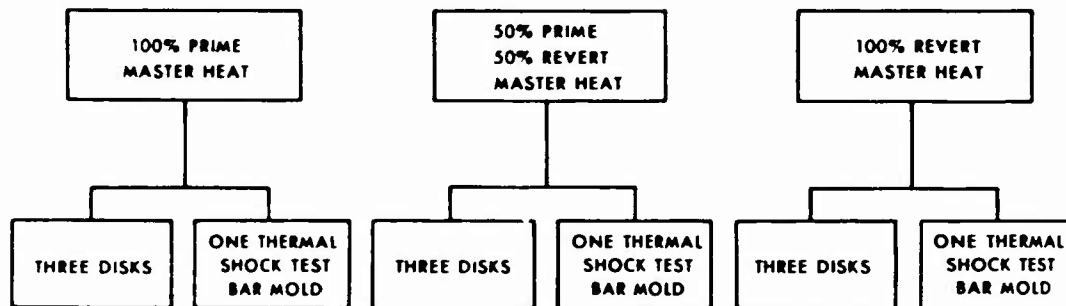
Figure 88. Casting Outline.

Figure 89. Cast IN-100 Disks.

However, it was decided that the thermal-fatigue test specimens should be cast to size. This was done in order to more closely duplicate a cast turbine rotor blade and, thus, to obtain more representative thermal-fatigue results.

After completion of the casting operations, all cast disks
and thermal-fatigue specimens (bars) were radiographically
inspected.

5.2.6 IN-100 - Specimen Fabrication

The cast disks were machined in-house to the final test
specimen configurations. The first operation was to electro-
chemically machine samples from the cast disks. The
machining and identification were in accordance with the
sketch shown in Figure 90. Following the electrochemical
machining and prior to final machining, the samples, along
with the cast-to-size thermal-fatigue specimens, were heat-
treated at 1600°F for 50 hours. IN-100 is a complex, multi-
phase alloy, and it has been found that less scatter in
mechanical test data is realized when the above heat treat-
ment is used to stabilize the microstructure.

The samples were machined to the final test specimen con-
figurations following heat treatment. The tensile test
specimens were machined in accordance with Figure 91. The
final stress-rupture test specimen configuration is depicted
in Figure 83. The machined notch-rupture test specimens
conformed with the illustration presented in Figure 92. The
creep test specimens were machined in accordance with the
sketch presented in Figure 93. The configuration of the
final-machined mechanical-fatigue test specimens is shown in
Figure 86. The machined thermal-fatigue test specimens
conformed with the specimen illustrated in Figure 87. The
oxidation and oxidation-sulfidation test specimens were pre-
pared by cutting 1/4-inch-thick samples from 1/2-inch-
diameter bars electrochemically machined from the cast disks.

After completion of the final machining, each test specimen
was subjected to fluorescent-penetrant inspection prior to
testing.

5.3 AIRESIST 13 AND IN-100 TEST PROCEDURES

Identical test procedures were used in the material
properties testing conducted on the AiResist 13 and IN-100
material test specimens. The following subparagraphs detail
the procedures that were used for each test.

5.3.1 Tensile Test Procedures

Tensile testing was performed in accordance with ASTM E21-58T
standard specification. A constant strain rate of 0.005
±0.002 inch per inch per minute was used during application
of the load. Approximately 0.6-percent strain offset from

123

SPECIMEN IDENTIFICATION CODE:

X   X

└── LOCATION OF TEST BAR

└───── MASTER HEAT IDENTIFICATION
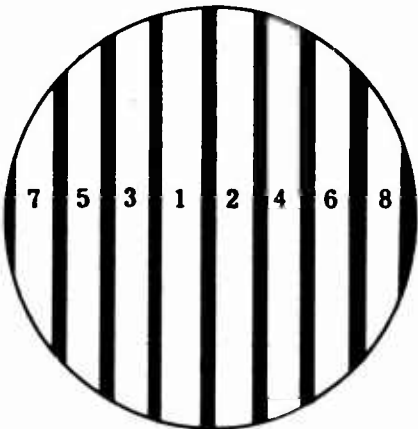
LOCATION OF TEST BARS
IN THE IN-100 WHEEL BLANKS

MASTER HEAT IDENTIFICATION

NUMBER	DESCRIPTION
1	100% PRIME
2	100% PRIME
4	100% PRIME
5	50% PRIME, 50% REVERT
7	50% PRIME, 50% REVERT
8	50% PRIME, 50% REVERT
3	100% REVERT
6	100% REVERT
9	100% REVERT

Figure 90.   IN-100 Specimen Identification.

124

Figure 91. Tensile Specimen.

Figure 92. Notch-Rupture Bar.

125
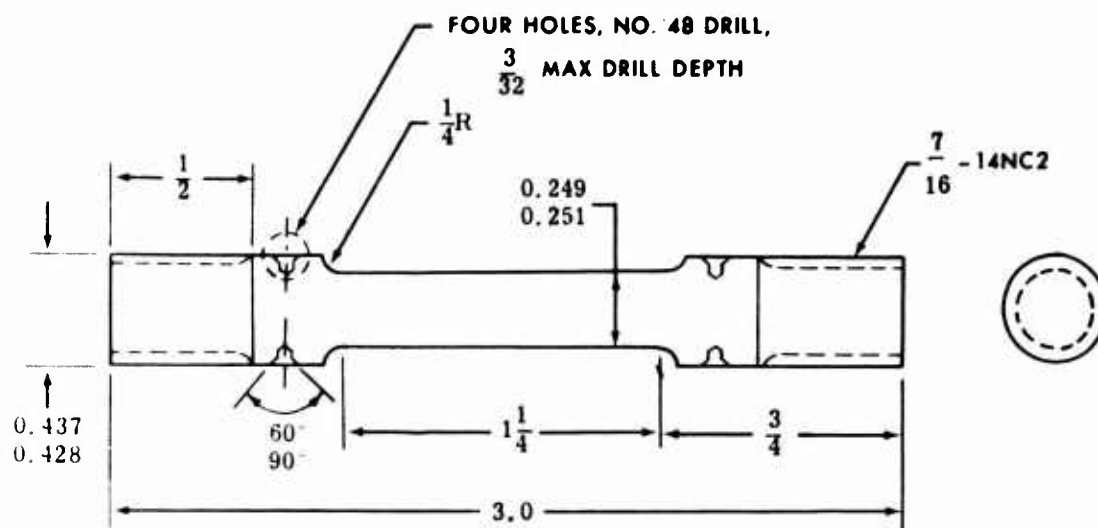
NOTE: PARALLEL SECTION OF DIAMETERS TO BE CONCENTRIC
WITH CENTER LINE WITHIN 0.0005 T.I.R. FOR DISTANCE
(DIMENSIONS, IN.)

Figure 93. Machined Creep Specimen.

126

the straight-line portion of the load-strain curve was used. This offset was measured by extensometers attached to gauge meters. A strain rate of 0.10 ±0.02 inch per inch per minute was used from the 0.6-percent strain offset until the test specimen fractured.

The ultimate strength of each of the test bars was determined. The 0.2-percent offset yield strength was determined from the stress-strain curve. For measuring elongation, the ends of the fractured specimen were fitted together, and the distance between gauge marks was measured. The elongation was reported as the increase in length of the gauge section expressed as a percentage of the original gauge length. For determining the reduction of area, the minimum diameter was measured while the ends of the fractured specimen were fitted together. The difference between the area of this cross section and the original area was reported as the percentage of reduction of area.

The test temperature was measured by three 24-gauge Chromel-Alumel thermocouples attached and equally spaced along the specimen gauge length. Temperature control was in accordance with ASTM E21-38T, Section 5. The test temperature was maintained for 15 minutes prior to performance of each tensile test.

Two specimens from each alloy heat (six specimens of each material) were subjected to short-time tensile tests at each of the following test temperatures: room temperature, 1200°, 1400°, 1600°, 1800°, and 2000°F. Ultimate tensile strength, 0.2-percent yield strength, percentage of elongation, and percentage of reduction in area results were recorded for each test.

5.3.2 Stress-Rupture Test Procedures

Stress-rupture tests were performed in accordance with the ASTM E139-587 standard specification.

The test temperature was measured by Chromel—Alumel thermo-couples that were equally spaced and attached along the specimen gauge length.

Percentage of elongation was determined in accordance with ASTM E139-58T, Section 10. Gauge marks equivalent to 4D (4 times diameter) length were located in the gauge length of each specimen prior to testing. When oxidation during long times at elevated temperature precluded the use of the gauge marks, elongation after fracture was determined by using the specimen total length.

The stress levels utilized during the stress—rupture tests were selected to produce times-at-temperature of approximately 100 hours. At the completion of each test, the rupture time and percentage of elongation were recorded, along with the applied stress and test temperature. Larson-Miller curves were prepared showing the relation between stress and rupture time obtained from the tests conducted at 1400°, 1600°, 1800°, and 2000°F. Two test bars cast from each heat of each material were tested at each of the indicated temperatures.

5.3.3   Notch-Rupture Test Procedures

The notch-rupture tests were conducted in the same manner as the stress-rupture tests of Paragraph 5.3.2. The same equipment was used for both tests. Notch-rupture tests were performed on two specimens from each heat of each material at test temperatures of 1200° and 1400°F. Larson-Miller curves were prepared from the data obtained. The test results were compared with the results of the stress-rupture investigation.

5.3.4   Creep Test Procedures

Creep tests were conducted in accordance with ASTM E139-587 standard specification on two specimens from each heat of each material. The selected test temperatures were 1800°, 1900°, 2000°, and 2100°F. The initial creep stress levels

were chosen to produce 1-percent creep in approximately 100 hours. The stress levels then were varied to determine creep curves at various stress conditions.

Creep during each test was measured by extensometers attached to the specimen shoulders. Data were recorded every 2 hours until completion of the test.

The test results were reported as the time required to obtain the indicated creep. Larson-Miller curves were used to present the data. Creep curves also were prepared indicating creep rate at various stress-temperature conditions.

5.3.5 Oxidation Test Procedures

Small disk samples of both materials were subjected to oxidation corrosion tests in static air at 1900°, 2000°, and 2100°F. One specimen from each heat of each material was utilized during the tests at each temperature and for each exposure time. Specimens of WI-52, a cobalt-base alloy, were included in the tests for comparison with the AiResist 13 specimens. Specimens of INCO 713C, a standard nickel-base alloy, also were included in the tests for means of comparison for the IN-100 specimens.

Prior to testing, each test specimen was properly weighed and its surface area was accurately determined. The specimens were placed in an in-house laboratory furnace that was used exclusively for these tests and that allowed precise temperature control. Coors porcelain crucibles were used to contain each sample during testing.

Tests were conducted at the established temperatures for 50, 150, and 250 hours. The net weight change per initial unit surface area was calculated for each specimen and was recorded along with the test exposure time. The data obtained were presented in graphical form—weight change versus time. The WI-52 and INCO 713C test results also were included for comparison. Photomicrographs of the specimens were prepared to provide pictorial results for correlation with the oxidation corrosion data.

129

5.3.6 Oxidation-Sulfidation Test Procedures

Disk-shaped specimens of each heat of both materials were exposed to synthetic atmospheres containing gaseous sulfur compounds to establish the resistance of the alloy to oxidation-sulfidation corrosion.

The test apparatus used in the oxidation-sulfidation tests is illustrated in Figure 94. A special silica retort used as the test chamber was installed in a heat-muffle furnace and was held in place by firebrick. The test specimens were placed in Alundum "combustion boats" and were positioned in the controlled hot zone of the silica retort. The specimens then were exposed to an atmosphere that simulated gas turbine combustion products and that consisted of air, N_2, CO_2, H_2O, SO_2, and H_2S. The SO_2 and H_2S gas content was increased to 100 times the normal turbine combustion-product content to obtain an accelerated test. The flow of each gas was controlled separately by flowmeters to maintain the desired gas mixture.

Prior to testing, each specimen was weighed and its surface area was measured. Duplicate tests, with specimens from each heat of each material, were conducted at 1800°, 1900°, and 2000°F. Specimens of HS-31 and WI-52 (representative cobalt-base alloys) and INCO 713C (representative nickel-base alloy) were also included during each test as comparison materials. Initially, the specimens were exposed to a reducing atmosphere consisting of N_2, H_2O, CO_2, and H_2S gases for 2 hours. Following the reducing atmosphere, the test specimens were subjected to an oxidizing atmosphere for 20 hours. The oxidizing atmosphere consisted of a mixture of air, H_2O, CO_2, and SO_2. The use of these two cycles during each test closely duplicated a gas turbine start when H_2S is present in the initial combustion gases and continuous operation when SO_2 is found in the combustion gases.

After completion of the two test cycles, the specimens were removed from the retort, allowed to cool, and cleaned. The specimens were scraped to remove any loose scale, boiled in a solution of NaOH, and then scraped again to remove any scale loosened during the caustic soak. The specimens then were placed in boiling concentrated HNO_3, removed, and again wire-brushed for final cleaning. After cleaning, the specimens were reweighed, and the net weight change per initial unit surface area was calculated and recorded. The data obtained were presented as graphs. Photomicrographs illustrating the results were prepared. HS-31, WI-52, and INCO 713C test results were also included.

130
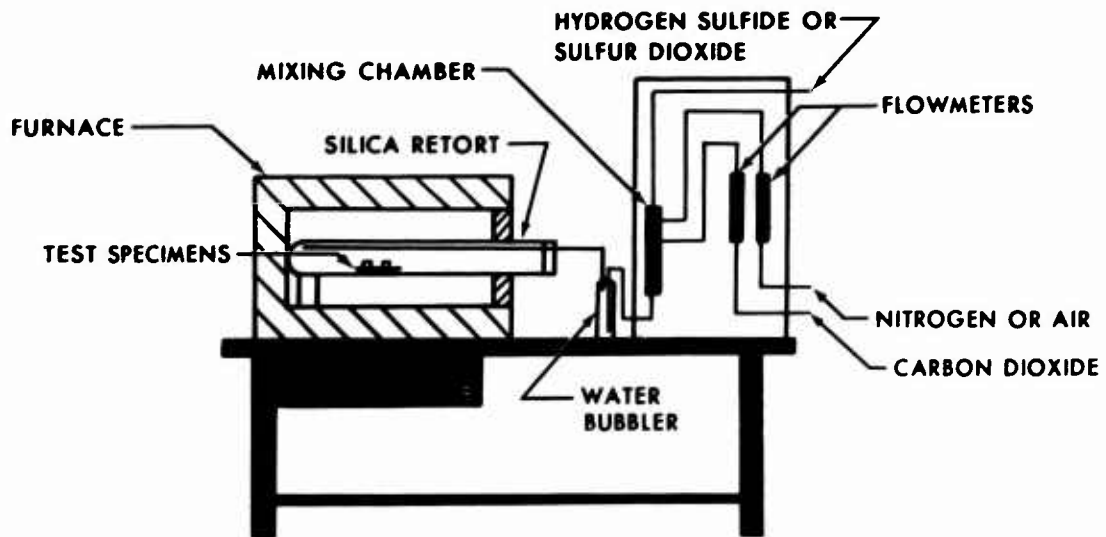
Figure 94. Oxidation-Sulfidation
Test Apparatus.

5.3.7 Mechanical-Fatigue Test Procedures

Mechanical-fatigue testing was conducted in accordance with ASTM Special Technical Publication No. 91. The tests were performed on a 10,000-pound-capacity axial-loaded fatigue machine which employed a rigid friction grip fixture and a radiant heat furnace. This machine is shown in Figure 95. The tests utilized tension-compression loading at zero mean stress.

Twelve specimens of each material were tested at 1800 cycles per minute at each of the test temperatures--1400° and 1700°F. The specimens were heated at a rate of approximately 500°F per minute to 1400°F and at a rate of 100°F per minute from 1400°F to 1700°F. The specimens were soaked for 15 minutes at the indicated temperatures prior to testing. Both smooth and notched specimens were subjected to the tests at each temperature to establish typical S-N curves, stress versus cycles to failure, to a maximum of 10^8 cycles.

131
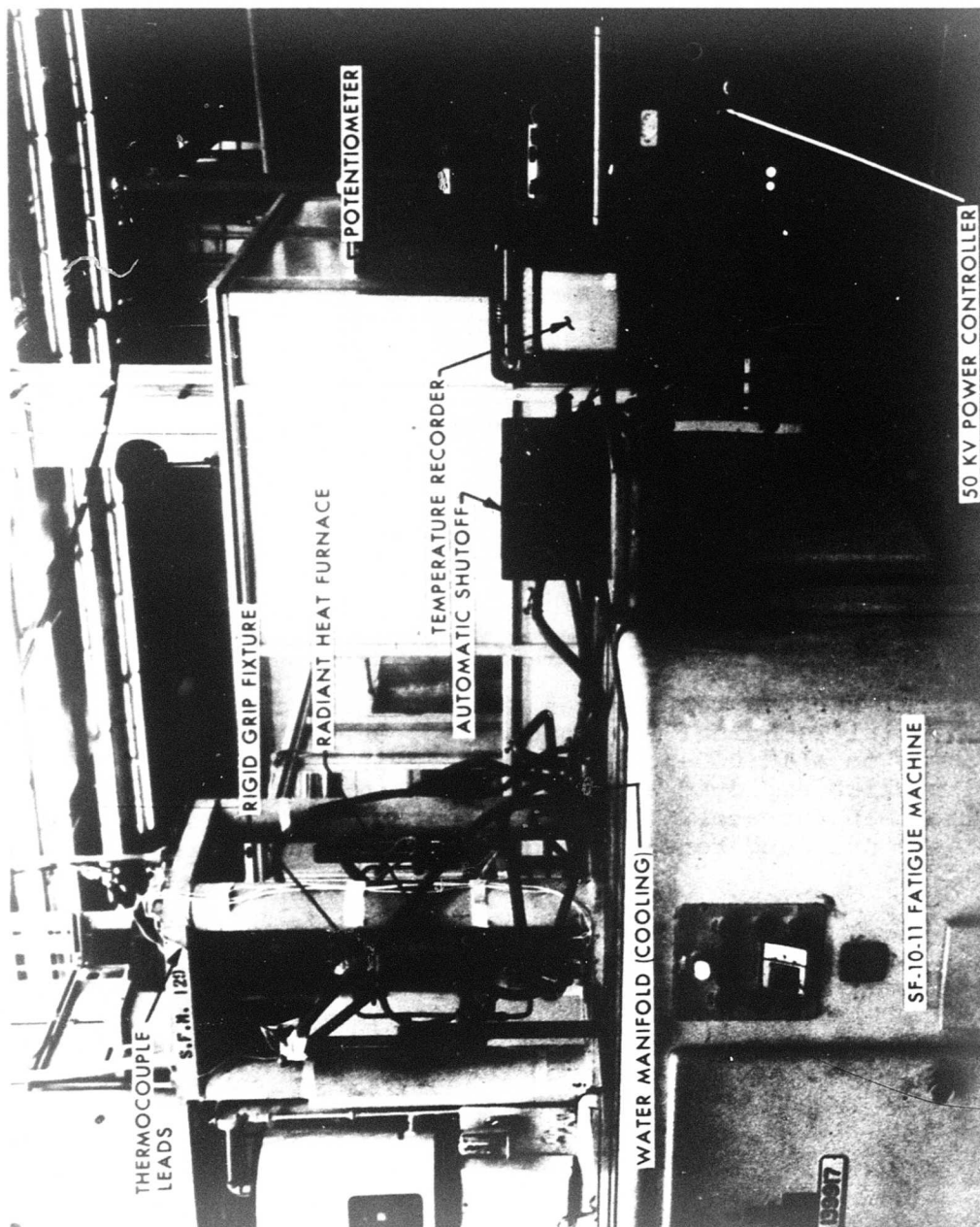
Figure 95. Mechanical-Fatigue Test Setup.

132

5.3.8 Thermal-Fatigue Test Procedures

Thermal-fatigue testing was conducted in accordance with the procedure outlined in a 1957 ASTM paper.*

The test bars were cast oversize and machined to size. After the specimens were cast, and prior to machining, the test bars were etched for grain-size determination and were photographed. The photographs were used to correlate grain size and grain orientation with thermal-fatigue cracking.

The test specimens were heated by an oxygen-acetylene flame and were cooled by a room-temperature air blast. A test cycle included heating a specimen for approximately 30 seconds in the oxygen-acetylene flame, followed by subjecting the specimen for approximately 30 seconds to an air blast directed at the leading edge of the specimen. Only the leading edge of each specimen was allowed to reach the test temperature. No time was allowed for holding at the test temperature.

Prior to each test, the temperature at a specified position in the apparatus was standardized with a common test bar of INCO 713C alloy.

Testing was continued until the first appearance of a crack was observed by examination under X25 magnification. Interruptions of the tests were made every 100 cycles during the first 500 cycles and then every 50 cycles to failure. The obtained test data were reported graphically (cycles to failure versus temperature). The test temperatures were 2000°, 2100° and 2000°F. Microexaminations of each test specimen were performed to confirm cracking and to evaluate the nature of the cracking.

5.4 AIRESIST 13 AND IN-100 TEST RESULTS

The following subparagraphs present summations of the results yielded by each test conducted on the AiResist 13 and IN-100 material.

5.4.1 Tensile Test Results

Tensile testing was accomplished as described in 5.3.1. Yield strength, ultimate strength, percentage of elongation, and percentage of reduction-in-area results were tabulated and plotted versus temperature.

---

*Muscatell, Reynolds, Dyrkacz, and Dalkeim, THERMAL SHOCK RESISTANCE OF HIGH-TEMPERATURE ALLOYS, ASTM, 1957.

1. **AiResist 13** - The tensile test data are presented in Table XXII and on Figures 96 through 99. The test results revealed a small degree of data scatter among the three heats. The alloy heat prepared by Vendor No. 3 showed slightly higher ductility at the elevated temperatures.

2. **IN-100** - The tensile test data are presented in Table XXIII and on Figures 100 through 103. No definite differences in the short-time tensile properties of the three IN-100 heats were observed. The test results revealed a small degree of data scatter.

5.4.2 Stress-Rupture Test Results

Stress-rupture testing was accomplished as described in 5.3.2. The test results were tabulated and are graphically depicted on Larson-Miller curves.

1. **AiResist 13** - The stress-rupture test data are presented in Table XXIV and on Figure 104. A small degree of data scatter was observed in the results from the three master heats.

    Examination of the prepared Larson-Miller curve (Figure 104) revealed a nonstandard slope. Most Larson-Miller curves exhibit a convex curve instead of the concave or dip condition of the resulting AiResist 13 curve. It is believed that this indicates the presence of an aging reaction at 1400° and 1600°F. This is shown by the higher stress-rupture properties during the tests at these temperatures. Thus, specimens tested at 1400° and 1600°F aged during the test. It is anticipated that if the specimens that were tested at 1800°F and 2000°F had been subjected to a heat treatment at 1400° to 1600°F, the stress-rupture properties at these higher temperatures would have been improved, and a more normal Larson-Miller curve would have resulted.

    The established stress-rupture properties that result in a life of 100 hours are as follows:

Temperature, °F	Stress, psi
1400	37,500
1600	17,750
1800	8 200
2000	5 000

134

Specimen No.	Test Temp (°F)	0.2% YS (psi)	UTS (psi)	Elong (%)	RA (%)
2	RT	81,700	83,400	1.5	--
23	RT	79,400	86,400	1.5	--
113	RT	76,100	87,000	1.5	--
130	RT	77,000	85,000	2.0	--
217	RT	75,500	88,900	1.5	--
218	RT	75,500	92,600	2.5	--
18	1200	57,800	67,500	3.0	2.4
27	1200	57,900	66,800	4.0	2.4
116	1200	57,300	66,300	4.0	4.1
136	1200	54,300	65,900	3.0	3.3
214	1200	53,000	71,600	6.0	6.3
215	1200	55,000	74,200	8.0	5.7
22	1400	49,900	59,900	1.0	1.6
28	1400	52,500	64,400	4.0	5.8
124	1400	46,900	61,000	6.0	6.2
125	1400	45,800	56,500	4.0	3.6
213	1400	44,000	70,300	12.0	45.0
228	1400	45,750	62,300	7.0	8.1
21	1600	37,400	42,100	5.0	5.8
31	1600	37,250	40,800	18.0	30.4
114	1600	40,600	42,100	24.0	27.7
126	1600	39,920	42,000	23.0	29.0
223	1600	42,000	44,100	30.0	34.3
225	1600	40,300	43,500	25.0	33.5
25	1800	23,830	26,520	22.0	35.4
26	1800	27,000	28,620	32.0	41.8
110	1800	24,250	26,780	33.0	46.0
117	1800	22,900	26,200	25.0	24.8
212	1800	24,820	27,600	29.0	40.0
227	1800	25,650	27,580	30.0	33.2
4	2000	13,760	14,380	50.0	63.8
32	2000	13,610	14,260	42.0	68.0
123	2000	9260	9560	5.0	3.0
133	2000	12,840	14,830	45.0	51.7
221	2000	12,600	14,270	50.0	61.5
222	2000	13,020	14,770	55.0	64.6

NOTES:

1. Specimen Numbers: 1 to 100, Vendor No. 1
                                         100 to 200, Vendor No. 2
   200 to 300, Vendor No. 3
2. RT = room temperature
3. RA = reduction in area
4. UTS = ultimate tensile strength
5. YS = yield strength

135
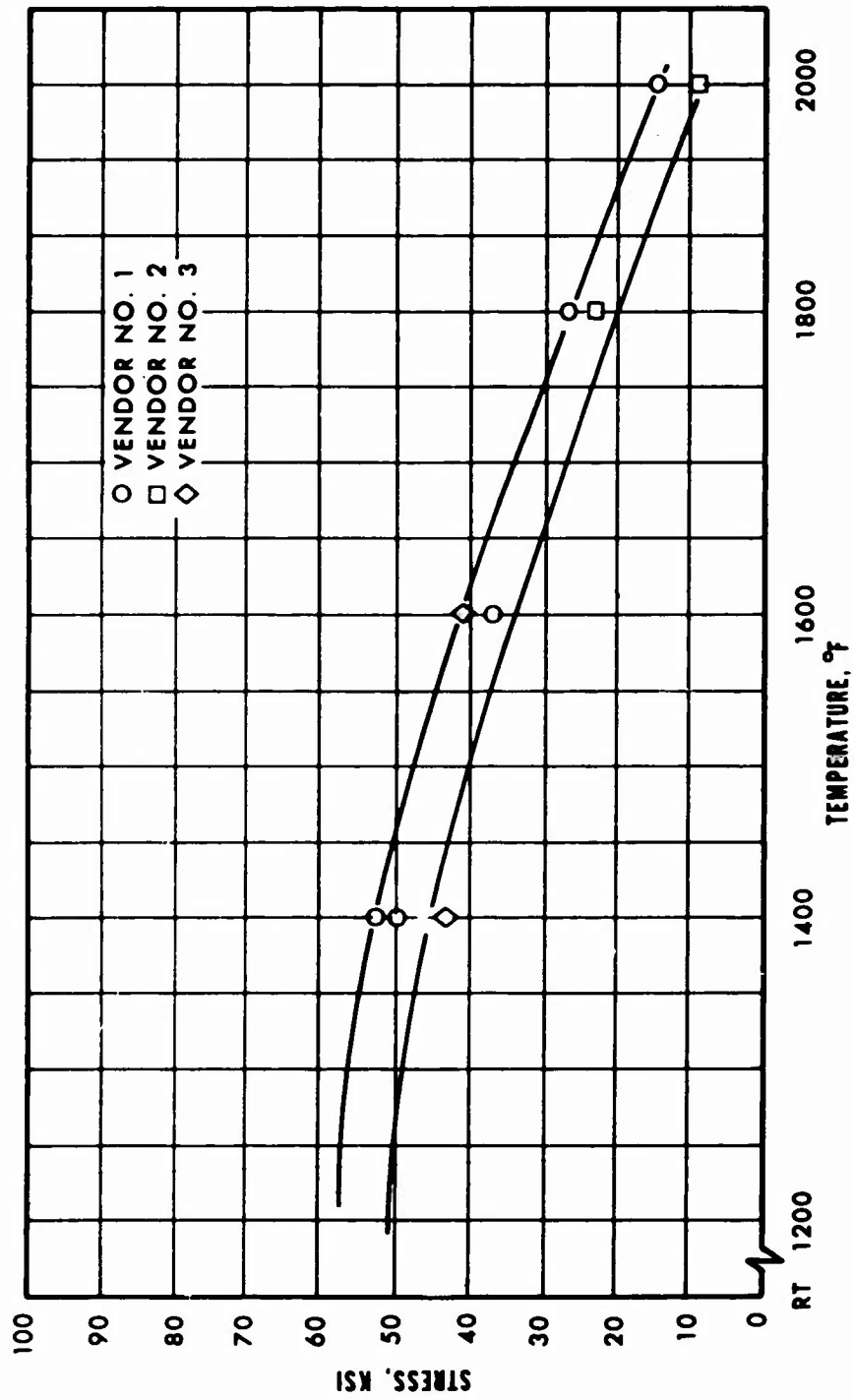
Figure 96. 0.2-Percent Yield Strength Results of Three Heats of AiResist 13.
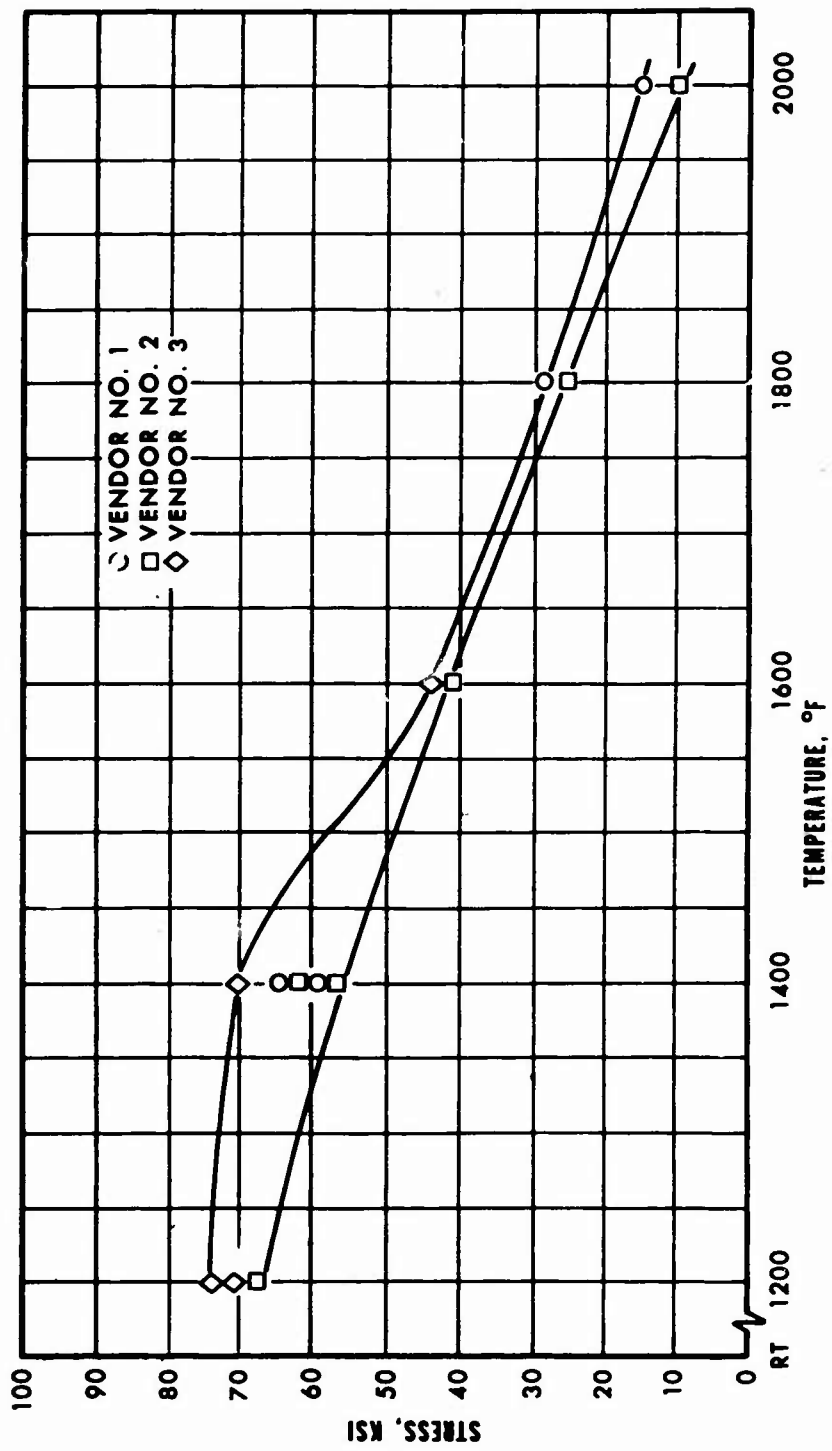
Figure 97. Ultimate Tensile Strength Results of Three Heats of AiResist 13.

137
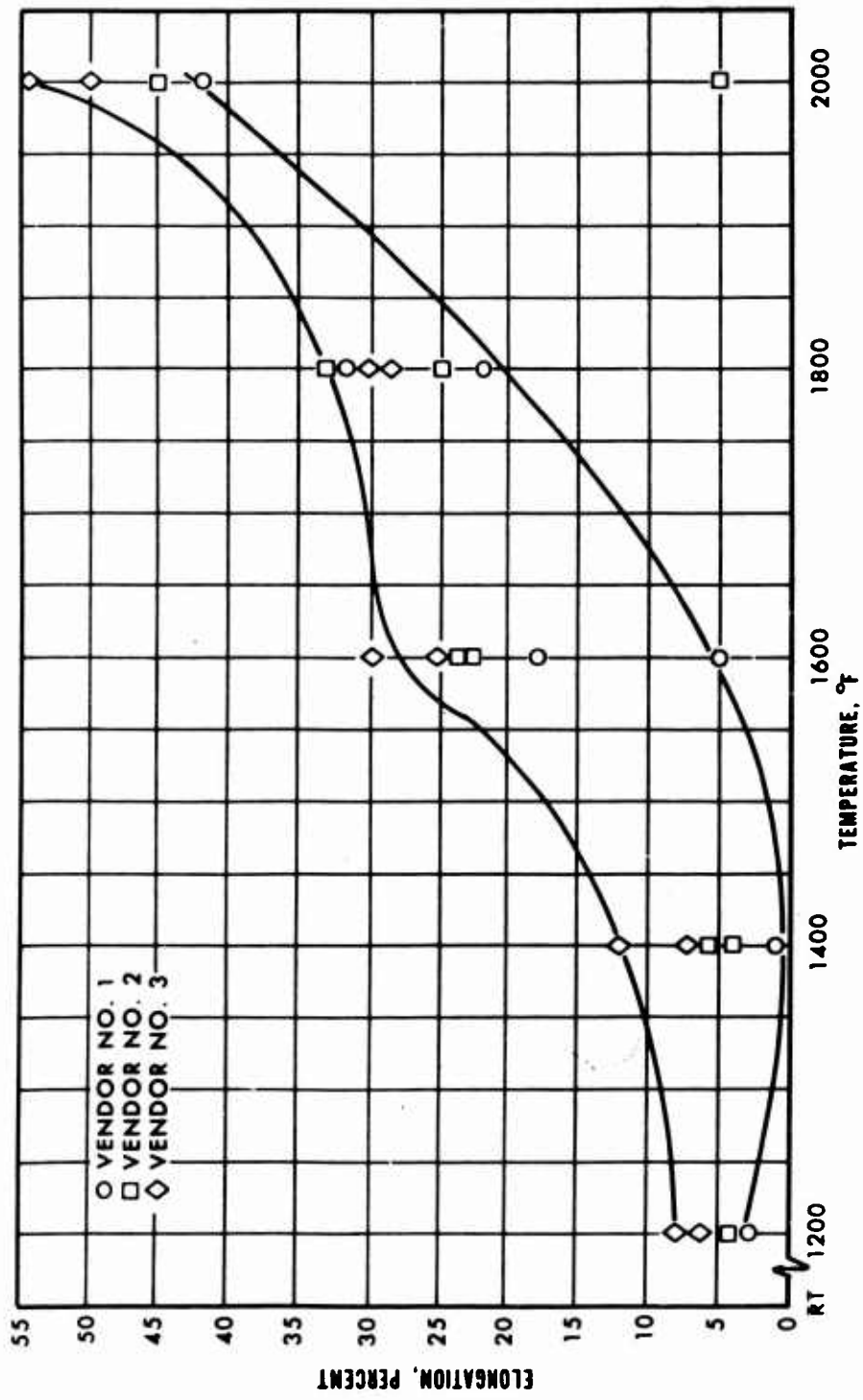
Figure 98. Tensile Elongation Results of Three
Heats of AiResist 13.
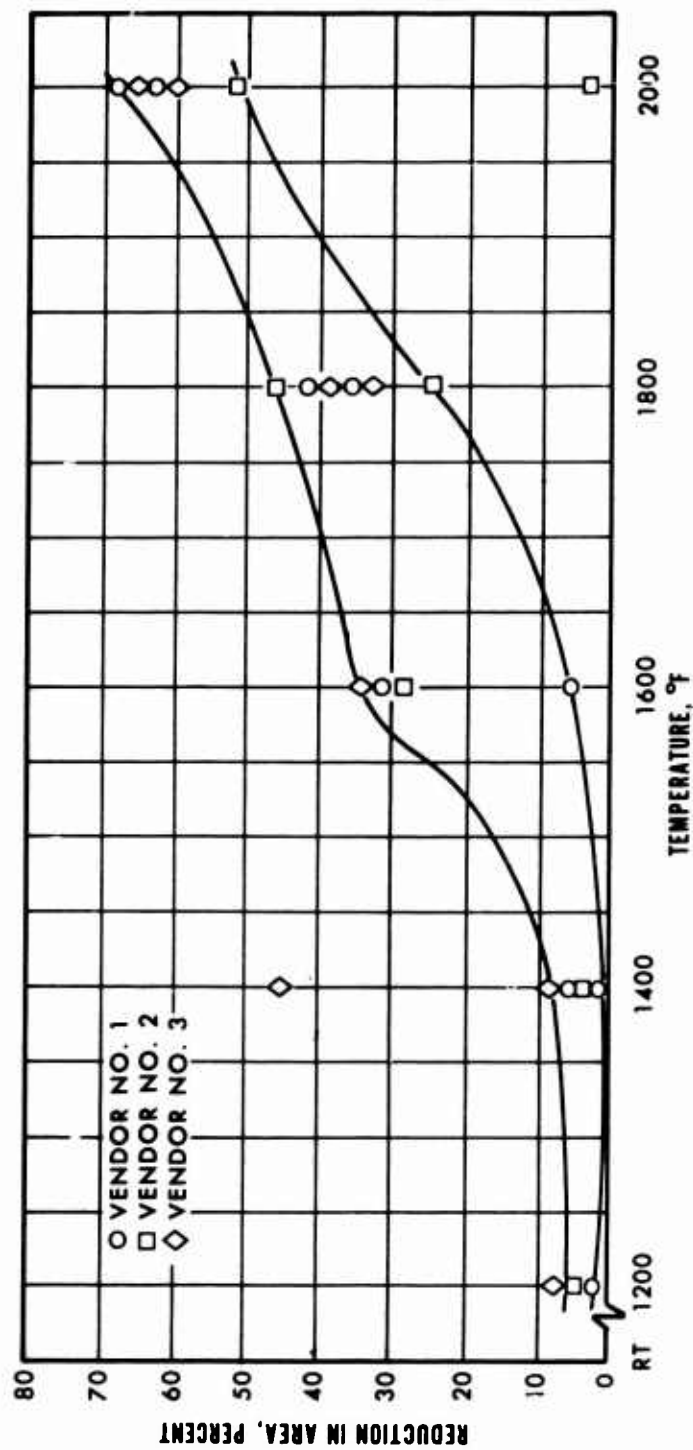
Figure 99. Tensile Reduction-in-Area Results of Three Heats of AiResist 13.

TABLE XXIII. TENSILE RESULTS FOR IN-100

Specimen No.	Test Temp (°F)	0.2% Yield Strength (psi)	Ultimate Tensile Strength (psi)	Elong (%)	RA (%)
1-1	RT	98,500	113,500	7.0	7.5
4-3	RT	104,000	110,000	7.0	10.0
5-1	RT	105,000	114,000	6.0	9.0
7-6	RT	93,200	101,000	8.0	17.5
3-1	RT	96,000	105,200	5.0	6.5
6-●	RT	99,600	108,000	6.0	6.5
1-3	1200	98,480	118,180	5.0	8.7
2-1	1200	97,980	121,210	6.0	10.1
7-1	1200	96,230	125,760	7.0	9.4
8-1	1200	96,740	118,630	4.0	8.0
3-3	1200	90,400	117,680	6.0	9.3
6-●	1200	91,140	102,850	4.0	4.7
2-3	1400	101,830	127,290	4.0	4.1
4-1	1400	106,110	133,020	7.0	6.4
7-3	1400	98,270	126,270	6.0	9.4
8-3	1400	94,190	126,780	6.0	7.9
6-●	1400	93,690	119,140	6.0	6.3
9-●	1400	98,270	123,730	6.0	6.3
1-5	1600	86,560	103,360	4.0	5.5
4-5	1600	88,590	105,910	8.0	16.9
5-3	1600	89,250	108,560	5.0	8.8
8-5	1600	86,760	104,720	9.0	11.7
3-5	1600	86,560	102,850	5.0	7.9
9-●	1600	78,410	98,780	3.0	1.6
2-5	1800	61,610	73,320	11.0	13.8
4-7	1800	51,430	73,320	10.0	8.6
5-5	1800	56,010	71,280	9.0	11.0
7-5	1800	51,930	73,830	11.0	13.8
3-7	1800	56,420	69,250	9.0	10.2
9-●	1800	62,120	73,320	8.0	9.4
1-7	2000	30,710	35,350	11.0	16.2
2-7	2000	29,090	30,950	11.0	11.0
4-6	2000	30,040	32,380	11.0	9.4
5-7	2000	29,330	34,010	12.0	10.2
8-7	2000	28,310	32,690	11.0	11.6
6-●	2000	23,510	34,620	10.0	11.6
9-●	2000	27,330	32,920	9.0	8.7

●Specimen location not known.

NOTES:

1. Specimen numbers are listed in order of heats.
   1-, 2-, 4- = 100% prime
   5-, 7-, 8- = 50% revert - 50% prime
   3-, 6-, 9- = 100% revert
2. RT = room temperature.
3. RA = reduction in area.
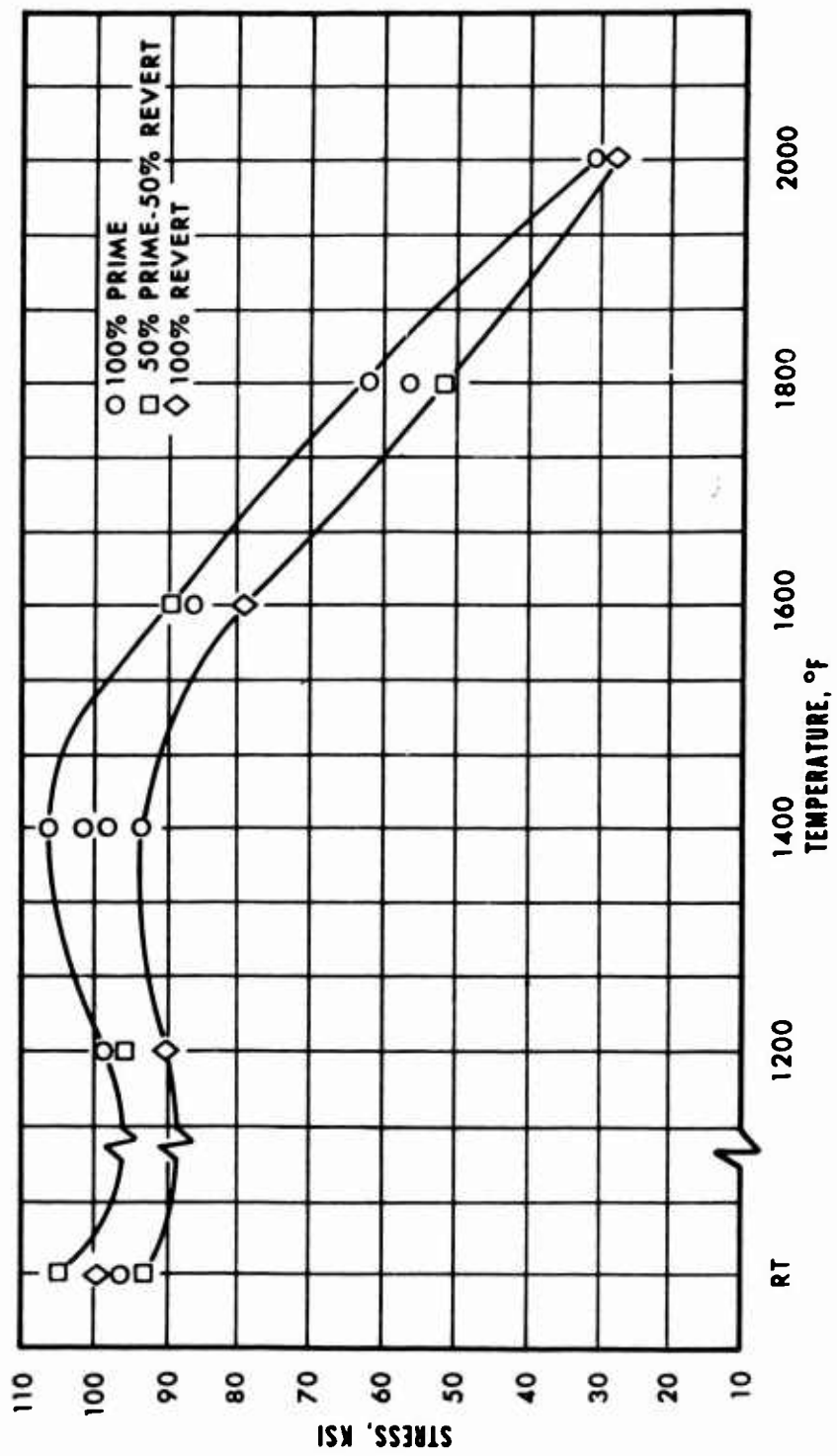
Figure 100. 0.2-Percent Yield Strength Results for Three Heats of IN-100.
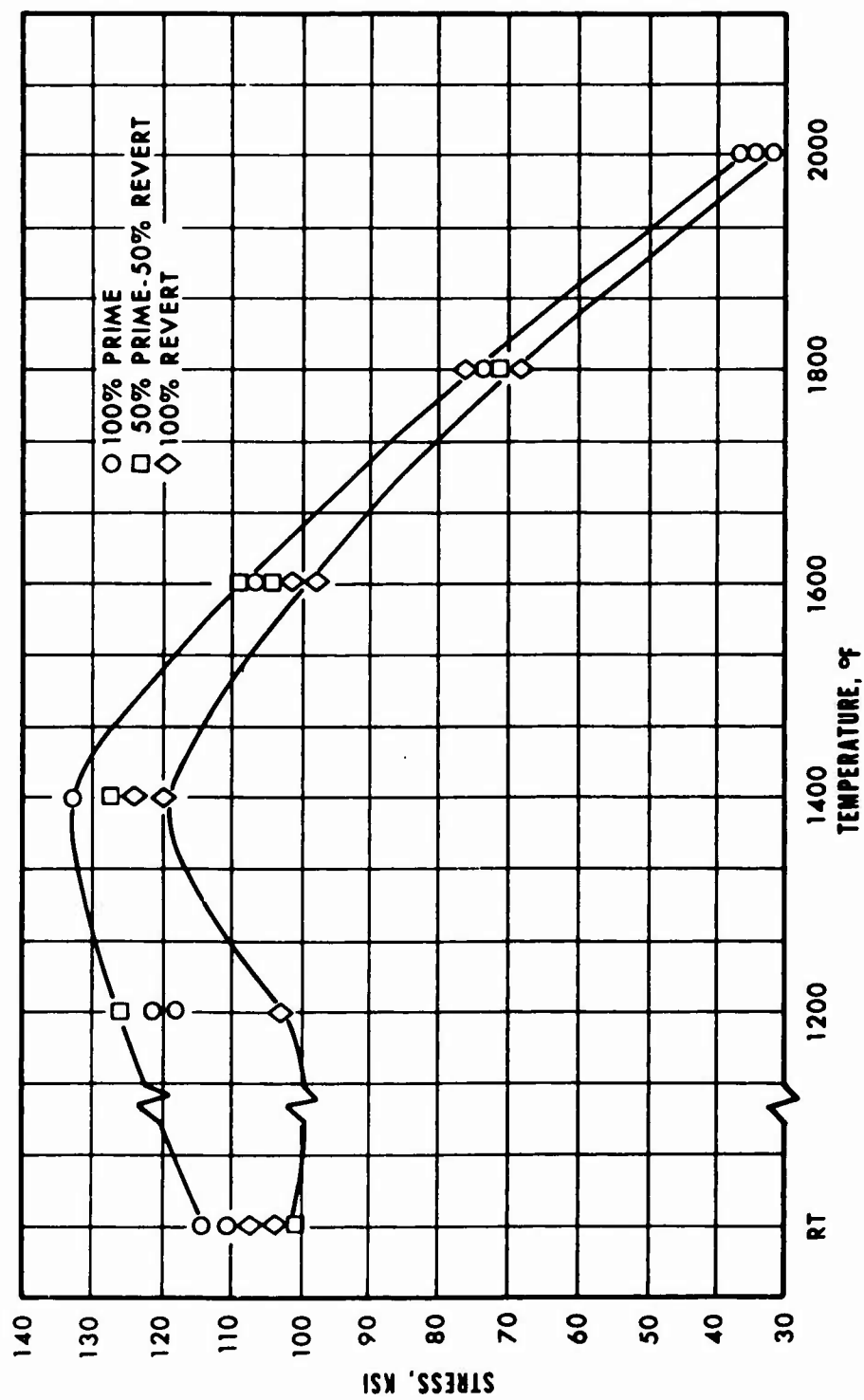
Figure 101. Ultimate Tensile Strength Results for Three Heats of IN-100.

142
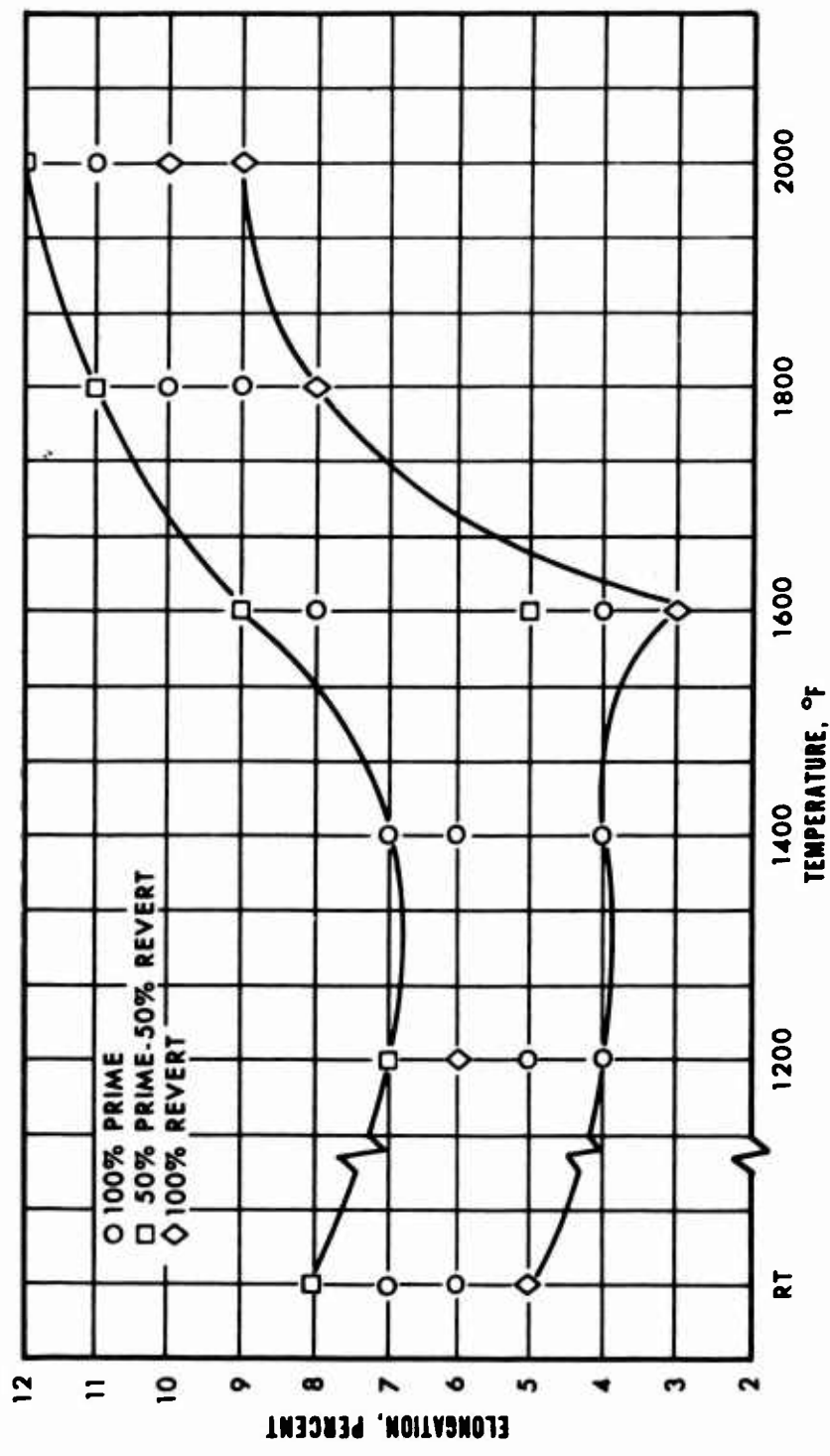
Figure 102. Tensile Elongation Results for Three Heats of IN-100.

143
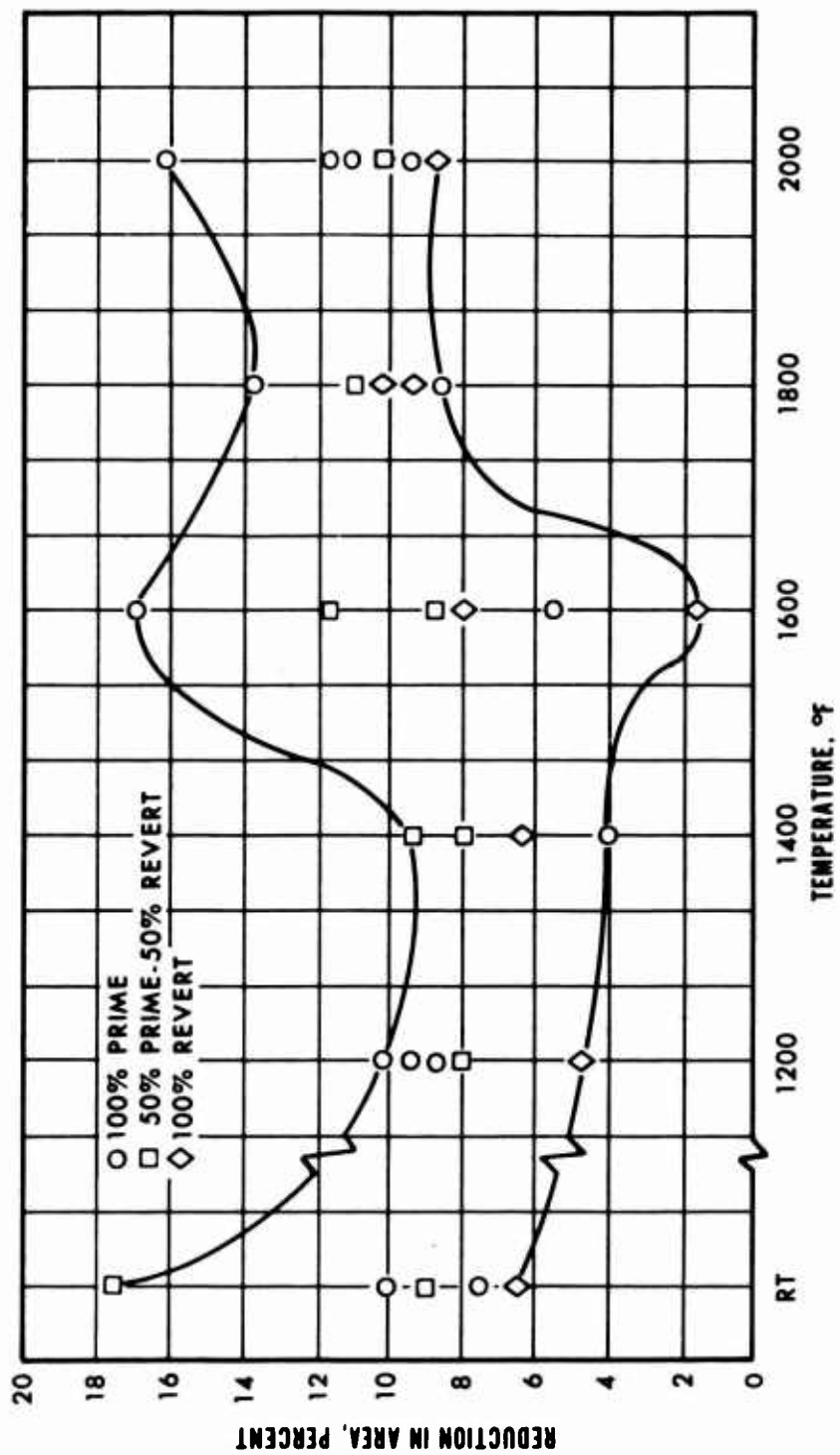
Figure 103. Tensile Reduction-in-Area Results for Three Heats of IN-100.

144

Specimen No.	Test Temp (°F)	Stress (psi)	Time (hr)	Elong (%)
	TABLE XXIV. STRESS-RUPTURE RESULTS FOR AIRESIST 13			
11	1400	39,000	87.3	11.5
12	1400	39,000	1.0 min	2.5
119	1400	35,000	181.5 (D)	-
129	1400	40,000	63.0	17.0
230	1400	39,000	65.4	24.0
232	1400	39,000	117.7	24.0
5	1600	17,500	93.3 (D)	-
9	1600	19,500	91.9	28.0
128	1600	15,000	193.2 (D)	-
132	1600	20,000	62.5	35.0
231	1600	19,500	66.6	32.0
233	1600	19,000	167.1	24.0
8	1800	8200	7.5	25.0
13	1800	8200	73.8	32.0
137	1800	9000	46.3	23.0
140	1800	7500	162.3	34.0
234	1800	8100	109.9	35.0
235	1800	8100	113.9 (D)	-
6	2000	5000.	117.9	20.0
15	2000	5000	84.8	35.C
139	2000	5000	108.9	28.0
141	2000	5000	60.5	25.0
236	2000	5000	84.7	17.0
239	2000	5000	38.9	25.0

NOTES:

1. Specimen Numbers: 1 to 100, Vendor No. 1
   100 to 200, Vendor No. 2
   200 to 300, Vendor No. 3

2. D = run discontinued; bar not broken.

145
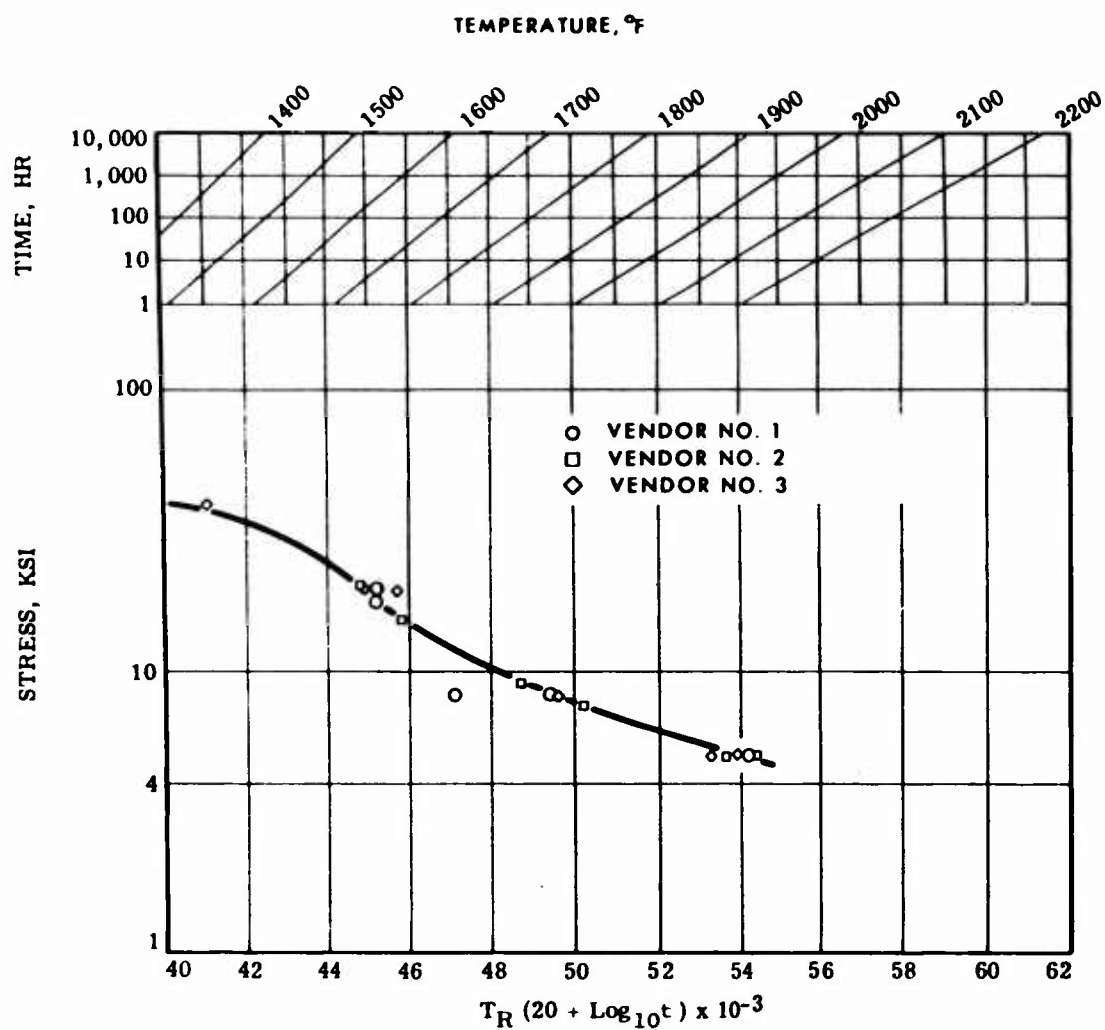
Figure 104. Larson-Miller Stress-Rupture
Curves for Three Heats of
AiResist 13.

146

2.   IN-100 – The stress-rupture test data are pre-
sented in Table XXV and on Figure 105.

Although some data scatter was observed, it was
believed to be normal for cast specimens. Only
the test result from specimen No. 3-5 was dis-
counted because it was abnormally low. A micro-
examination of the fracture area of this spectrum
revealed slight material shrinkage which caused
the low rupture time.

The established stress-rupture properties that
result in a life of 100 hours are as follows:

Temperature, °F	Stress, psi
1400	83,000
1600	51,000
1800	22,000
2000	6,200

5.4.3   Notch-Rupture Test Results

The notch-rupture testing, described in 5.3.3, was conducted
at 1200° and 1400°F to evaluate the effects of notch failure
at these temperatures. This was expected to be the most
critical temperature range for notch brittleness of the
alloys. The test data were tabulated and evaluated.

1.   AiResist 13 – As shown in Table XXVI, the only
tests that gave significant notch ruptures were
long periods (>125 hours) of exposure at 1200°F
with the load greatly increased. The test
results indicate that AiResist 13 is notch-
ductile at 1200° and 1400°F except when sub-
jected to a rapid increase in stress after a
lengthy exposure at 1200°F. No notch failures
were experienced at 1400°F.

2.   IN-100 – As shown in Table XXVII, one notch
failure, specimen No. 1-4, occurred at 1400°F,
which made it appear that IN-100 was susceptible
to notch brittleness at this temperature. How-
ever, further investigation (four rerun tests)
showed no further specimen failure in the notch
for either test temperature. An examination of
the test results revealed that IN-100 is not
notch-sensitive at 1200°F and 1400°F.

147
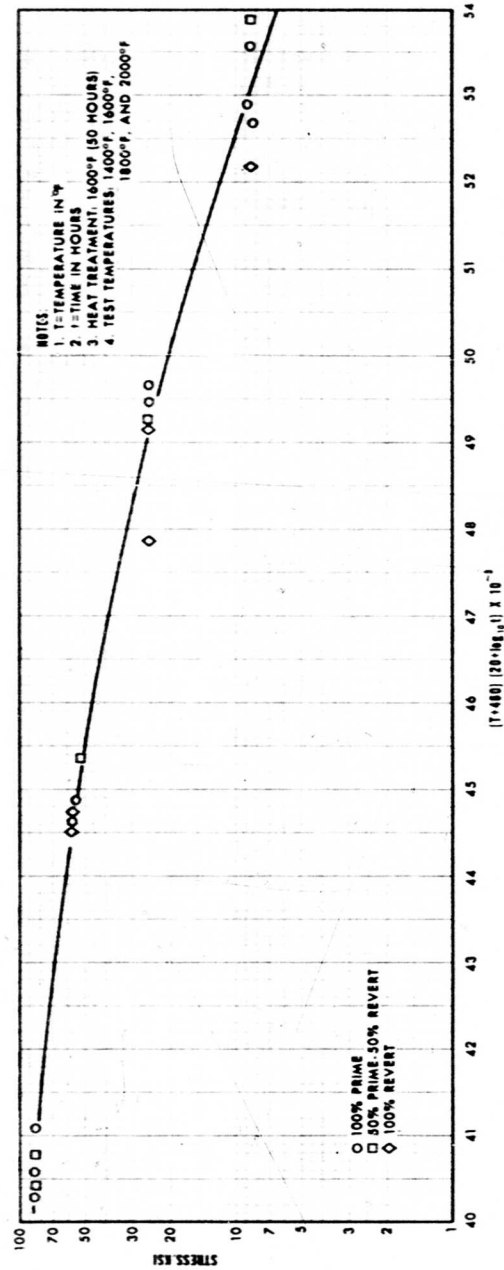
Figure 105. Larson-Miller Stress-Rupture
Curve for IN-100.

Specimen No.	Test Temp (°F)	Stress (psi)	Rupture Time (hr)	Elong (%)
TABLE XXV. IN-100 STRESS-RUPTURE RESULTS				
1-6	1400	85,000	133.5	4.0
5-4	1400	85,000	60.5	5.0
2-6	1400	85,000	55.5	6.0
4-2	1400	85,000	63.1	5.0
5-6	1400	84,000	88.4	7.0
2-2	1600	55,000	44.5	5.0
1-4	1600	55,000	62.5	7.0
3-4	1600	55,000	49.1	6.5
6-*	1600	55,000	40.5	6.8
6-*	1600	55,000	41.1	6.9
7-2	1600	52,500	50.5	5.3
7-6	1600	52,500	90.9	7.5
8-6	1600	52,500	107.1	8.3
3-5	1800	25,000	14.1	8.0
2-4	1800	25,000	93.5	11.2
4-4	1800	25,000	73.2	10.4
5-2	1800	25,000	68.6	9.0
8-4	1800	25,000	64.0	8.1
9-*	1800	25,000	58.8	10.3
9-*	1800	25,000	59.0	9.7
1-2	2000	8500	61.3	5.0
7-4	2000	8500	76.1	11.0
8-2	2000	8500	34.5	7.0
9-*	2000	8400	30.2	5.0
6-2	2000	8400	17.0	5.0
2-2	2000	8200	23.9	8.0

*Location of specimen in the disk is unknown.

TABLE XXVI. RESULTS OF NOTCH-RUPTURE TESTING ON AIRESIST 13

Specimen No.	Test Temp (°F)	Stress (psi)	Time to Failure (hr)	Elong (%)	Remarks
37	1200	55,000	147.8		Load increased to 60,000 psi
		60,000	24.0		Load increased to 70,000 psi
		70,000	8.3		Load increased to 79,000 psi
		79,000	0		Ruptured in notch
35	1200	57,000	134	2.0	Load increased to 75,000 psi
		75,000	0		Ruptured in notch
168	1200	60,000	0.05	3.0	Ruptured in smooth section
152	1200	58,000	143.2		Increased load to 81,000 psi
		81,000	0	4.0	Ruptured in smooth section
252	1200	55,000	162.4		Did not fail, discontinued
251	1200	65,000	0.2	3.0	Ruptured in smooth section
40	1400	39,000	103.2		Did not fail, discontinued
34	1400	39,000	81.7	8.0	Ruptured in smooth section
159	1400	39,000	140.3	7.0	Increased load to rupture Ruptured in smooth section
154	1400	39,000	103.2		Did not fail, discontinued
243	1400	39,000	104.7	24.0	Ruptured in smooth section
244	1400	39,000	85.0	23.0	Ruptured in smooth section

NOTE:

SPECIMEN NUMBERS:

    1 to 100, Vendor No. 1
    100 to 200, Vendor No. 2
    200 to 300, Vendor No. 3

Specimen No.	Test Temp (°F)	Stress (ksi)	Test Time (hrs)	Elong (%)	Remarks
					TABLE XXVII. RESULTS OF IN-100 NOTCH-RUPTURE TESTING AT 1200°F AND 1400°F
1-2	1200	87.5	102.4	5.0	Superloaded to 101.5 ksi; broke in 126.5 hours.
2-4	1200	95.0	132.6	-	Superloaded to 121.0 ksi; broke in gauge mark.
3-2	1200	110.0	0.1	7.0	
4-4	1200	100.0	122.4	3.5	Superloaded to 124.9 ksi; ruptured at 122.6 hours.
7-4	1200	105.0	137.6	6.0	Superloaded to 122.3 ksi; ruptured at 137.9 hours.
8-4	1200	105.0	216.3	5.0	Superloaded to 129.4 ksi; ruptured at 216.6 hours.
1-4	1400	85.0	138.8	-	Superloaded to 93.0 ksi, broke in notch.
2-5	1400	85.0	87.0	3.5	
3-4	1400	85.0	56.8	4.0	
4-5	1400	91.0	1.2	8.0	
5-5	1400	85.0	118.7	6.0	Superloaded to 105.5 ksi; ruptured at 118.9 hours.
6-	1400	84.0	75.0	6.0	Location unknown.
7-2	1400	85.0	137.3	5.0	Superloaded to 125.2 ksi.
7-5	1400	90.0	55.3	7.0	Temperature control erratic.
8-2	1400	85.0	106.5	4.5	
8-5	1400	85.0	107.7	5.0	

5.4.4 Creep Test Results

The creep testing, described in 5.3.4, was conducted at 1800°, 1900°, 2000°, and 2100°F. The tests were performed at various stress levels for each temperature to evaluate the effect on the creep rate and to establish the stress that produces 1 percent creep in 100 hours. The test data were tabulated and plotted on curves that present time versus percent elongation for various stress levels at each of the test temperatures. Larson-Miller diagrams were also prepared from the test data.

1. AiResist 13 - The creep test data are presented in Table XXVIII and on Figures 106 through 110. The Larson-Miller diagram (Figure 110) includes a stress-rupture curve to show comparison of the 1-percent creep properties of AiResist 13 with its stress-rupture properties.

    The approximate stress values that result in a 1.0-percent creep in 100 hours were established as follows:

Temperature, °F	Stress, psi
1800	6500
1900	5500
2000	4000
2100	2300

    As was stated in the stress-rupture test procedure discussion, 5.3.4, it is likely that the creep properties of AiResist 13 could be improved by heat treating in the 1400° to 1600°F temperature range.

2. IN-100 - The creep test data are presented in Table XXIX and on Figures 111 through 115. It should be noted that a slight inconsistency in the 100-hour stress-rupture and 1-percent creep values at 2000°F exists. The established value for stress-rupture at 2000°F was 6200 psi. However, as is indicated in Figure 115, the creep results showed 1 percent creep at 2000°F to be 8300 psi. The stress values for creep cannot be higher than the stress values for stress-rupture. It is believed that this inconsistency was due to data scatter. This indicates further that 1 percent creep is the maximum strain prior to failure (with stress-rupture and creep values almost identical).

152

Specimen No.	Test Temperature (°F)	Stress (psi)	Test Duration (hr)	Final Deformation (%)
	TABLE XXVIII. RESULTS OF CREEP TESTING ON AIRESIST 13			
C42	1800	4500	214.7	0.353
C45	1800	4500	214.8	0.379
C169	1800	6000	143.1	0.717
C256	1800	6500	113.5	1.039
C149	1800	7000	79.0	1.000
C43	1900	3000	216.0	0.211
C46	1900	3000	214.9	0.340
C147	1900	4500	143.2	0.704
C173	1900	5000	132.6	1.010
C257	1900	5500	103.9	1.025
C50	2000	2000	113.8	0.285
C52	2000	3000	134.0	0.559
C145	2000	4000	97.7	1.048
C150	2000	4000	100.0	1.172
C254	2000	4000	100.0	1.101
C47	2100	1000	161.4	0.176
C151	2100	2000	137.3	0.767
C44	2100	2300	100.0	1.198
C146	2100	3000	27.3	2.013

NOTE:

SPECIMEN NUMBERS:

    1 to 100, Vendor No. 1
  100 to 200, Vendor No. 2
  200 to 300, Vendor No. 3
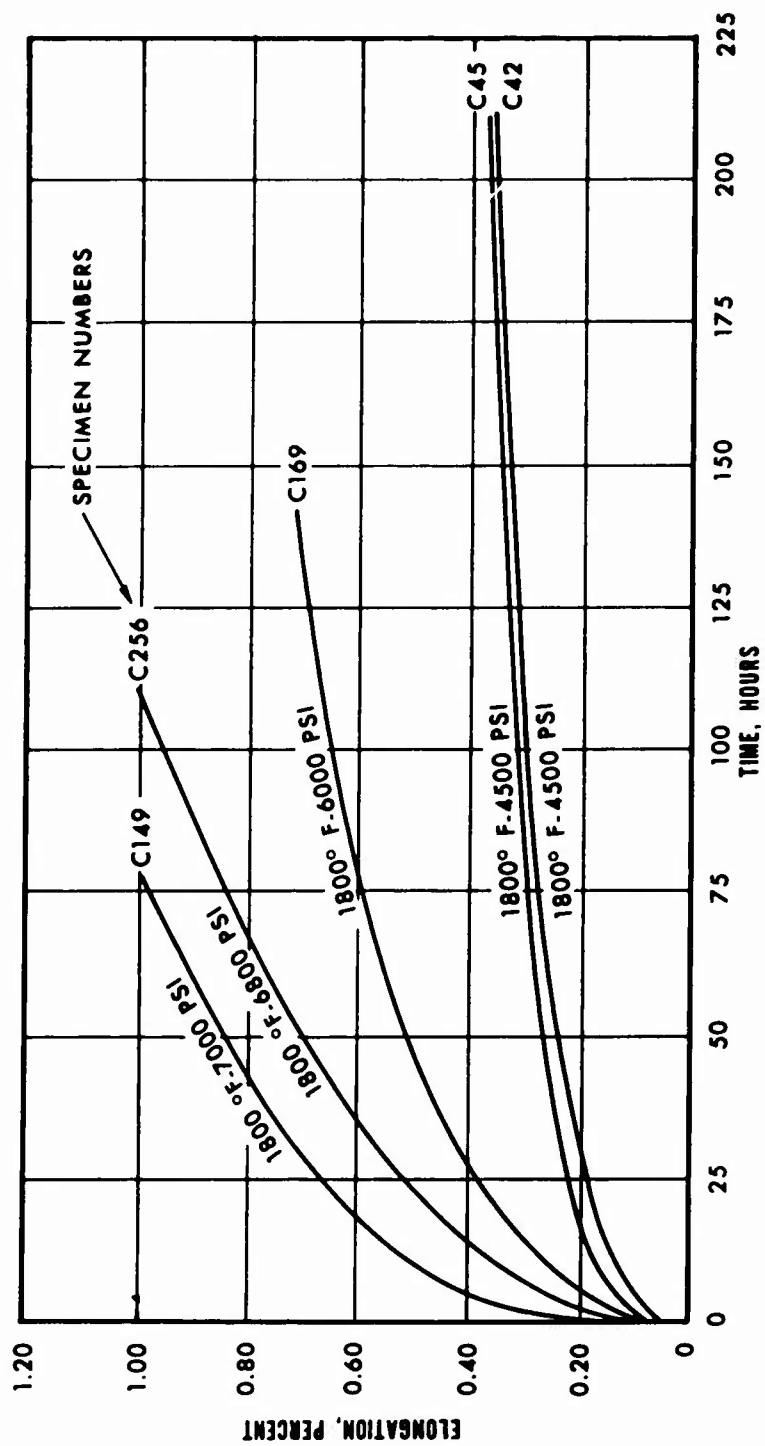
Figure 106. Creep Curves for AiResist 13 at 1800°F and Various Stress Levels.
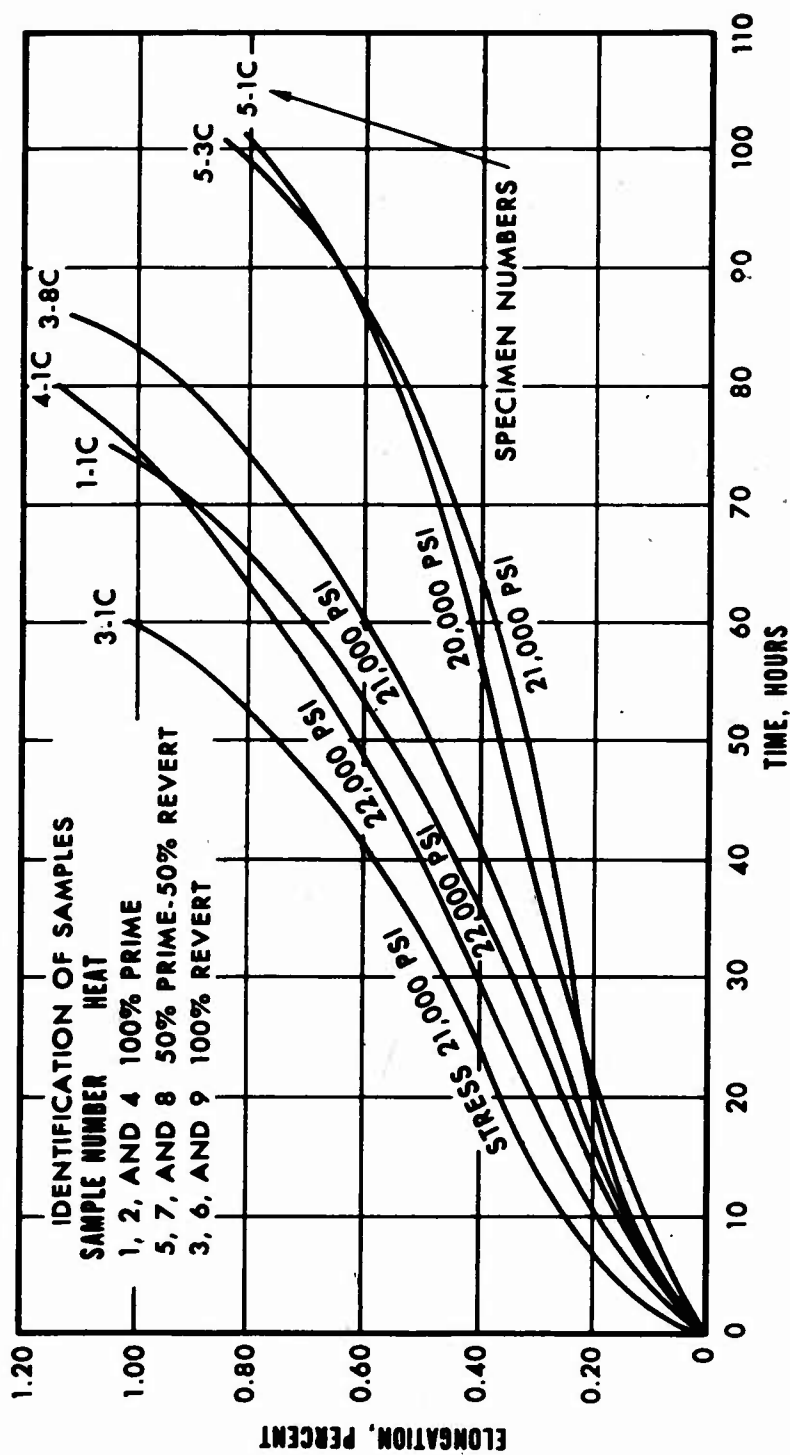
154
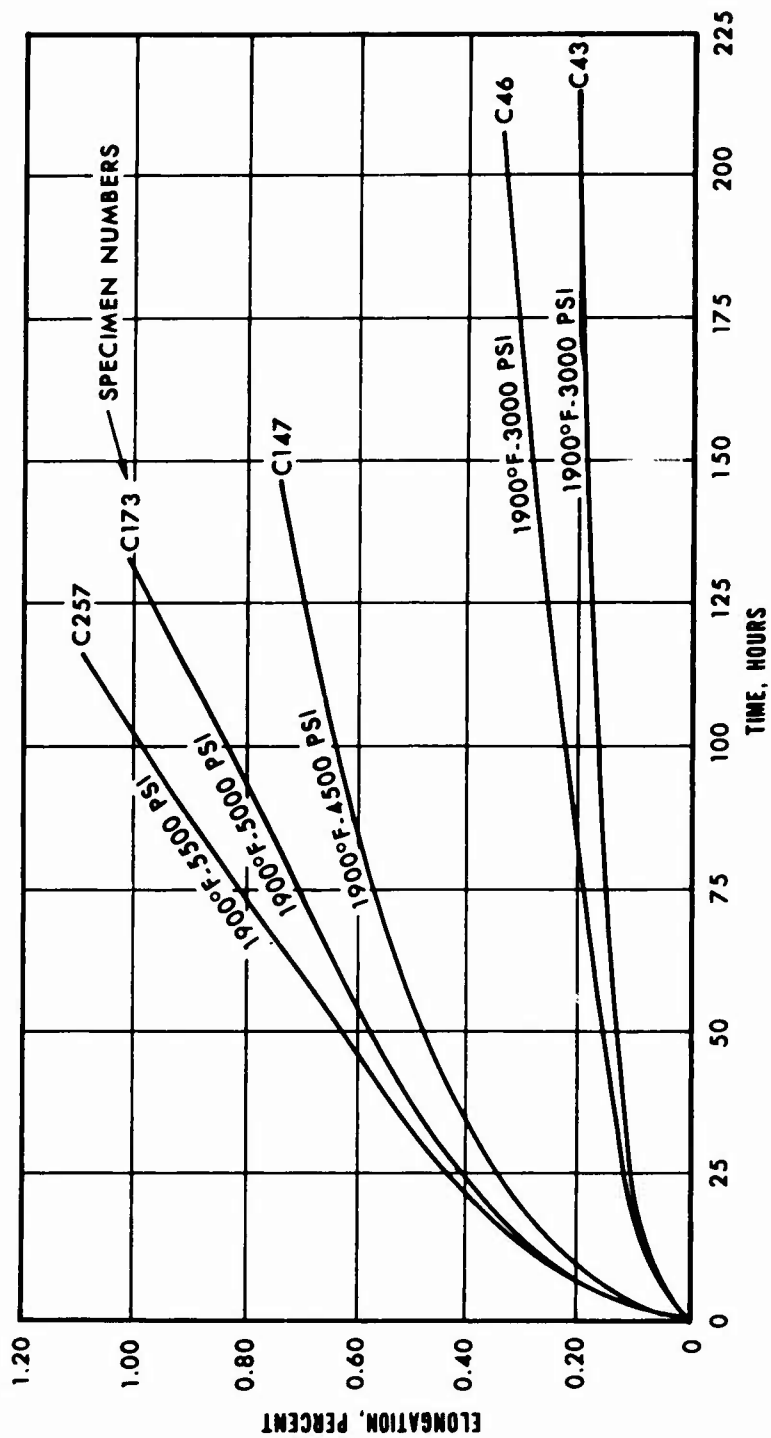
Figure 107. Creep Curves for AiResist 13 at 1900°F and Various Stress Levels.
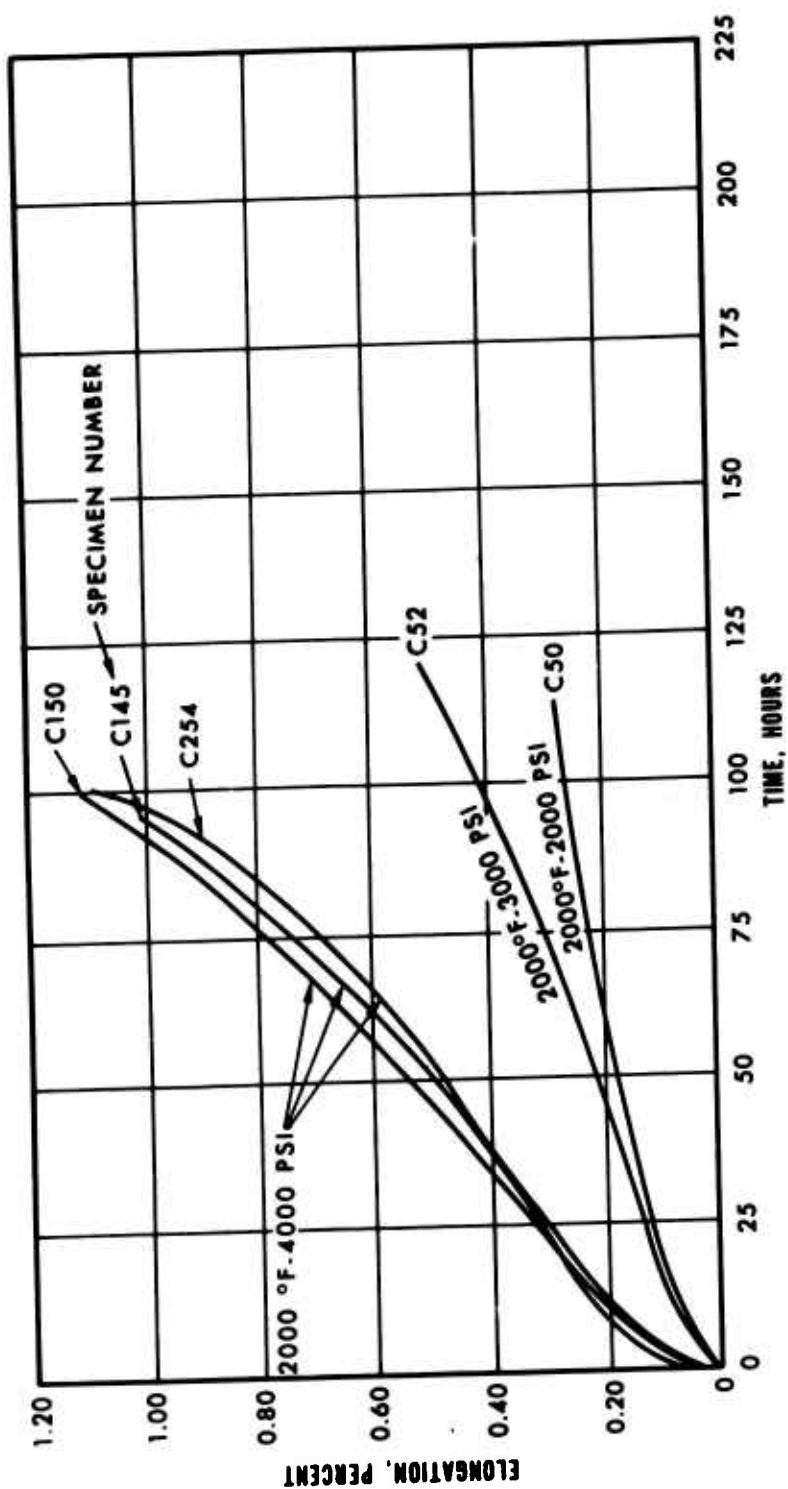
Figure 108. Creep Curves for AiResist 13 at 2000°F and Various Stress Levels.

156
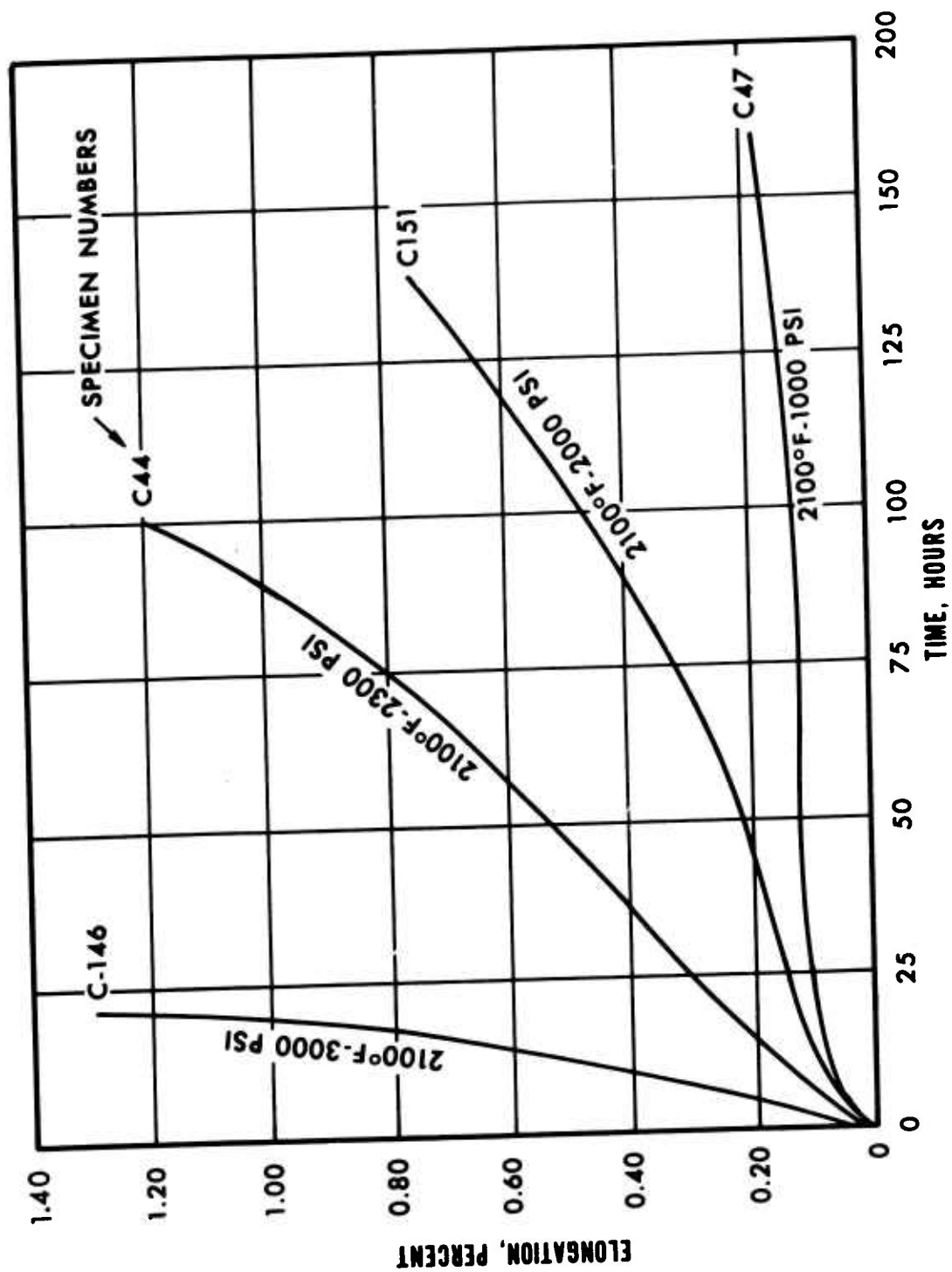
Figure 109. Creep Curves for AiResist 13 at 2100°F and Various Stress Levels.

157
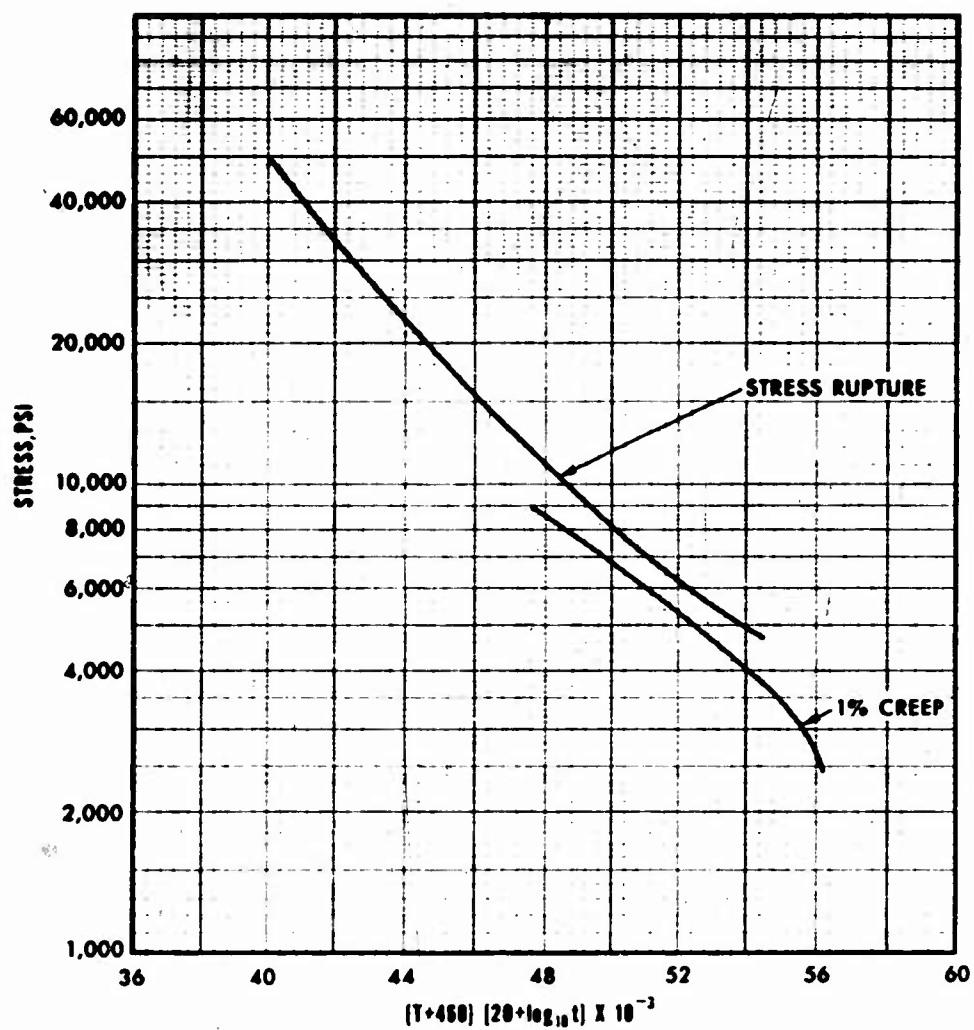
Figure 110. Larson–Miller Curves
for AiResist 13.

158

The approximate stress values that result in 1 percent creep in 100 hours were established as follows:

Temperature, °F	Stress, psi
1800	21,500
1900	14,500
2000	8300
2100	3750

5.4.5 Oxidation Test Results

The oxidation testing, described in 5.3.5, was conducted in static air at 1900°, 2000°, and 2100°F for 50, 150, and 250 hours. Upon completion of the tests, microexaminations were performed on each test specimen to determine the depth of the oxidation attack. Representative photomicrographs were prepared to provide pictorial results for correlation with the tabulated test data.

1. AiResist 13 - The oxidation test data are presented in Table XXX and on Figures 116 through 124. As shown in Figures 116, 117, and 118, AiResist 13 revealed superior oxidation resistance to a similar cobalt-base alloy, WI-52, at 1900° and 2000°F but showed little improvement at 2100°F. The test specimens after being subjected to the high-temperature oxidation tests are shown in Figures 119, 120, and 121.

    Figures 122, 123, and 124 illustrate the sub-surface condition of the AiResist 13 specimens after extended periods of exposure at 1900°, 2000°, and 2100°F, respectively. As can be seen in Figure 122, AiResist 13 exhibits a fine, needle-like phase, while the WI-52 material reveals a more general-type attack with deeper penetration. The needle-like phase was found with all AiResist 13 oxidation specimens examined. In general, this needle-like phase was found to penetrate deeper with higher temperatures and/or longer exposure times.

			Test	Final Creep	Time to
Specimen No.	Test Temp (°F)	Stress (psi)	Duration (hr)	Reading (%)	1% Creep (hr)
1-1	1800	22,000	75.3	1.134	69.5
5-1	1800	20,000	100.0	0.780	-
4-1	1800	22,000	87.8	1.357	72.5
5-3	1800	21,000	100.0	0.828	-
3-1	1800	21,000	59.6	1.002	59.5
3-8	1800	21,000	83.6	1.058	82.0
2-1	1900	13,000	100.0	0.764	-
2-3	1900	14,000	97.7	1.051	95.0
3-3	1900	14,000	61.0	1.036	59.5
4-3	1900	15,000	64.8	1.031	64.0
6-*	1900	14,000	59.7	1.322	52.0
8-1	1900	14,000	58.9	1.096	56.0
8-3	1900	14,000	83.4	1.371	71.0
1-3	2000	6000	100.0	0.409	-
4-8	2000	10,000	36.5	1.351	28.5
6-*	2000	7500	93.9	1.119	89.5
7-1	2000	7500	93.3	1.219	86.5
8-8	2000	7500	100.0	1.002	100.0
9-*	2000	7500	100.0	1.012	99.5
1-8	2100	3000	100.0	0.680	-
2-8	2100	4000	74.0	1.134	71.0
5-8	2100	4000	49.6	0.374	-
7-3	2100	4000	82.8	1.193	81.0
9-*	2100	4000	57.5	0.426	-

TABLE XXIX.   IN-100 CREEP RESULTS

*Location of specimen in the disk is unknown.

160

Figure 111. Creep Curves for IN-100 at 1800°F and Various Stress Levels.

161

Figure 112. Creep Curves for IN-100 at 1900°F and Various Stress Levels.
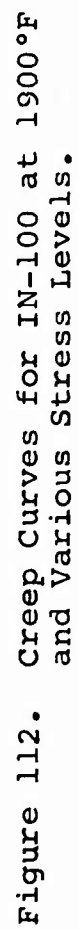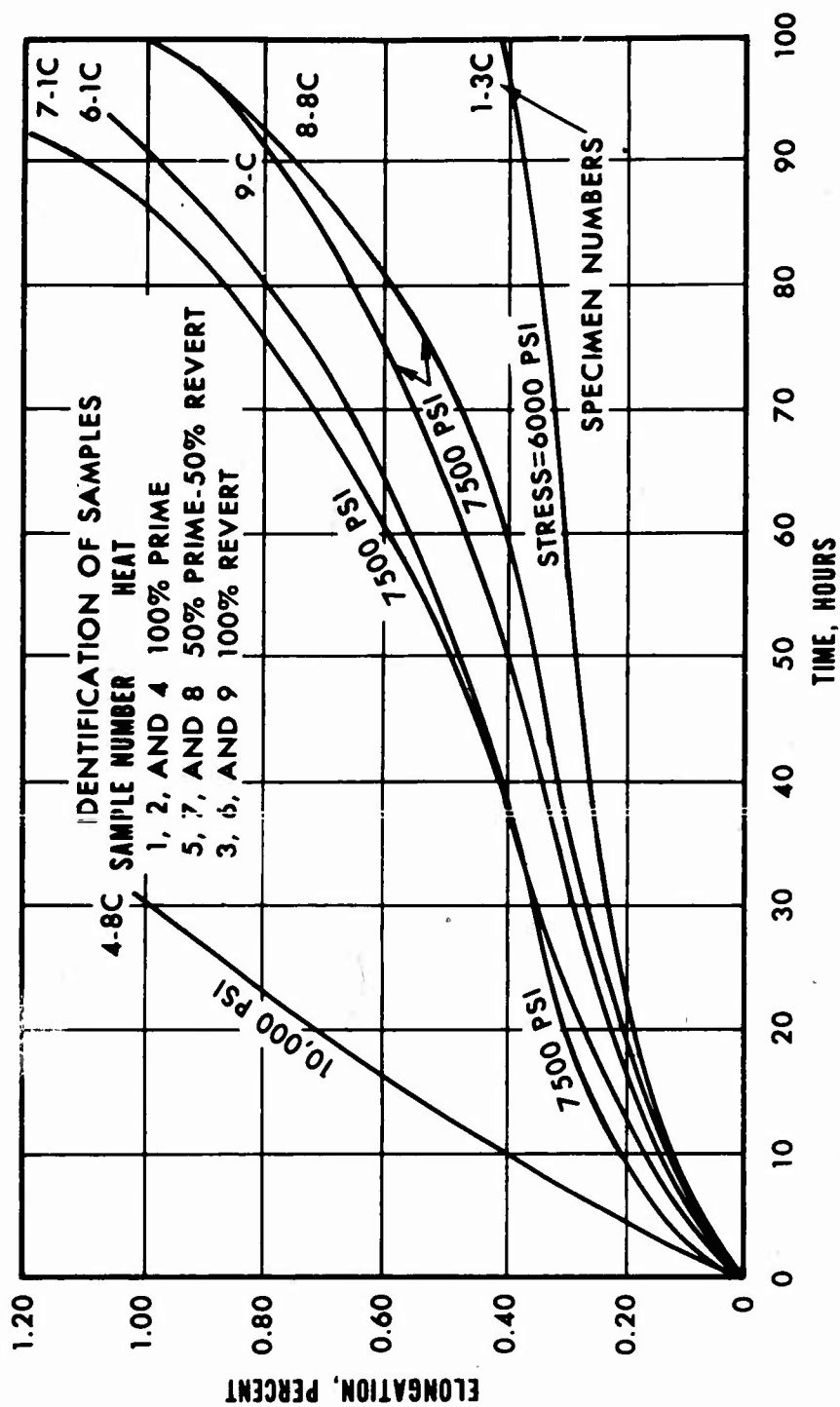
Figure 113. Creep Curves for IN-100 at 2000°F and Various Stress Levels.

163
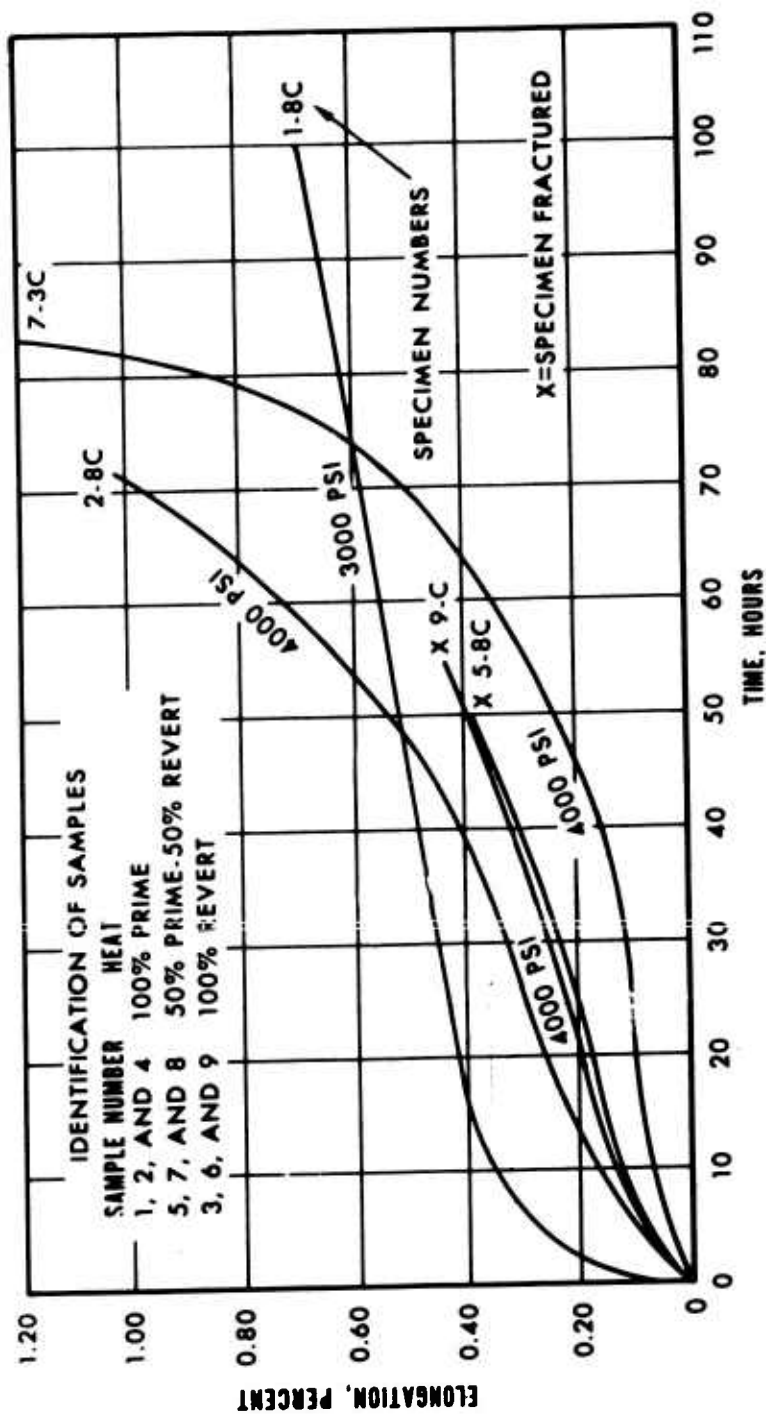
Figure 114. Creep Curves for IN-100 at 2100°F and Various Stress Levels.

164
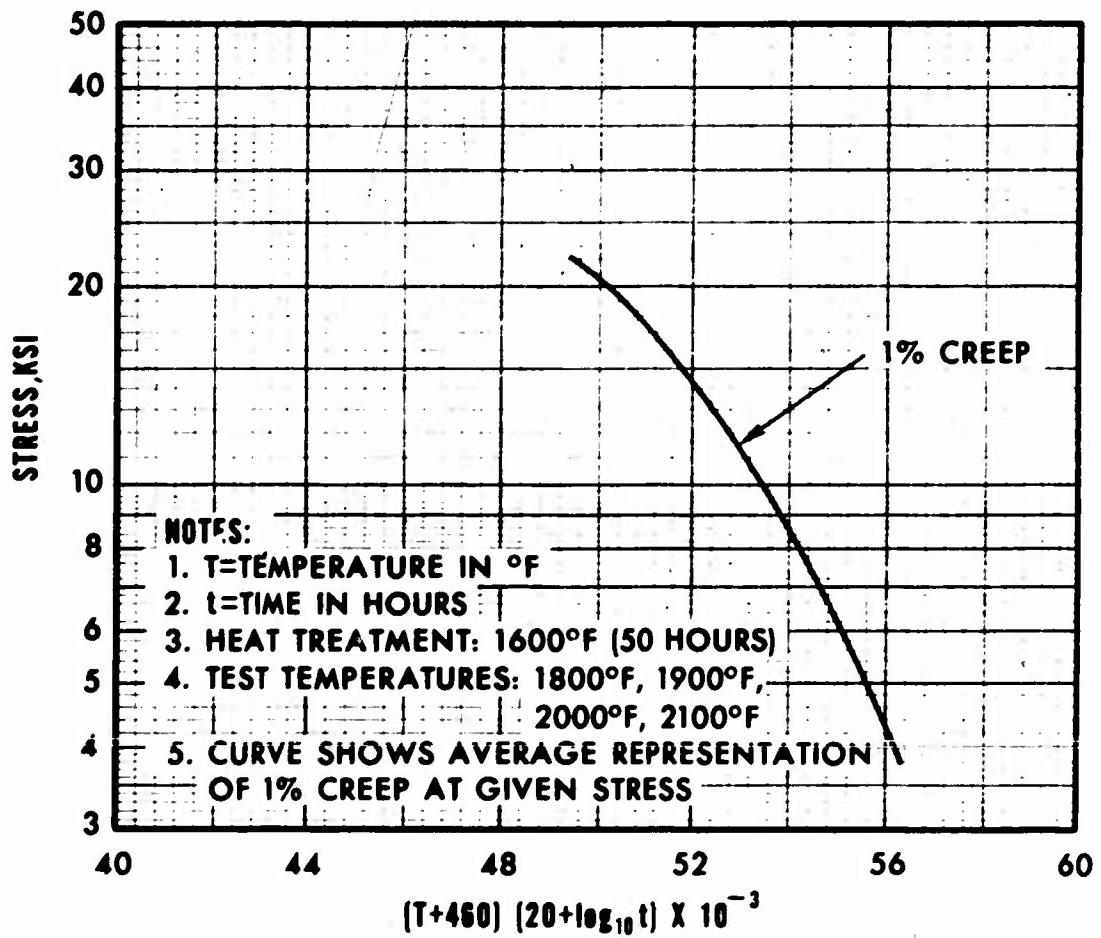
Figure 115. Larson–Miller 1-Percent
Creep Curve for IN–100.

Alloy	Test Temp (°F)	WEIGHT CHANGE (MG/SQ IN.) (LESS SPALLED-OFF SCALE) Exposure Time		
		50 Hrs	150 Hrs	250 Hrs
AiResist 13 (Vendor No. 1)	1900	+6	+9	+12
	2000	−3	−29	−377
	2100	−610	−895	−3656
AiResist 13 (Vendor No. 2)	1900	+6	+10	+14
	2000	−35	−146	−472
	2100	−404	−727	−3324
AiResist 13 (Vendor No. 3)	1900	+6	+7	+11
	2000	−5	−50	−535
	2100	−536	−821	−3805
WI−25	1900	+9	−35	−110
	2000	−191	−617	−859
	2100	−1018	−1766	−3325

TABLE XXX.   RESULTS OF OXIDATION TESTING ON AIRESIST 13 AND WI-52
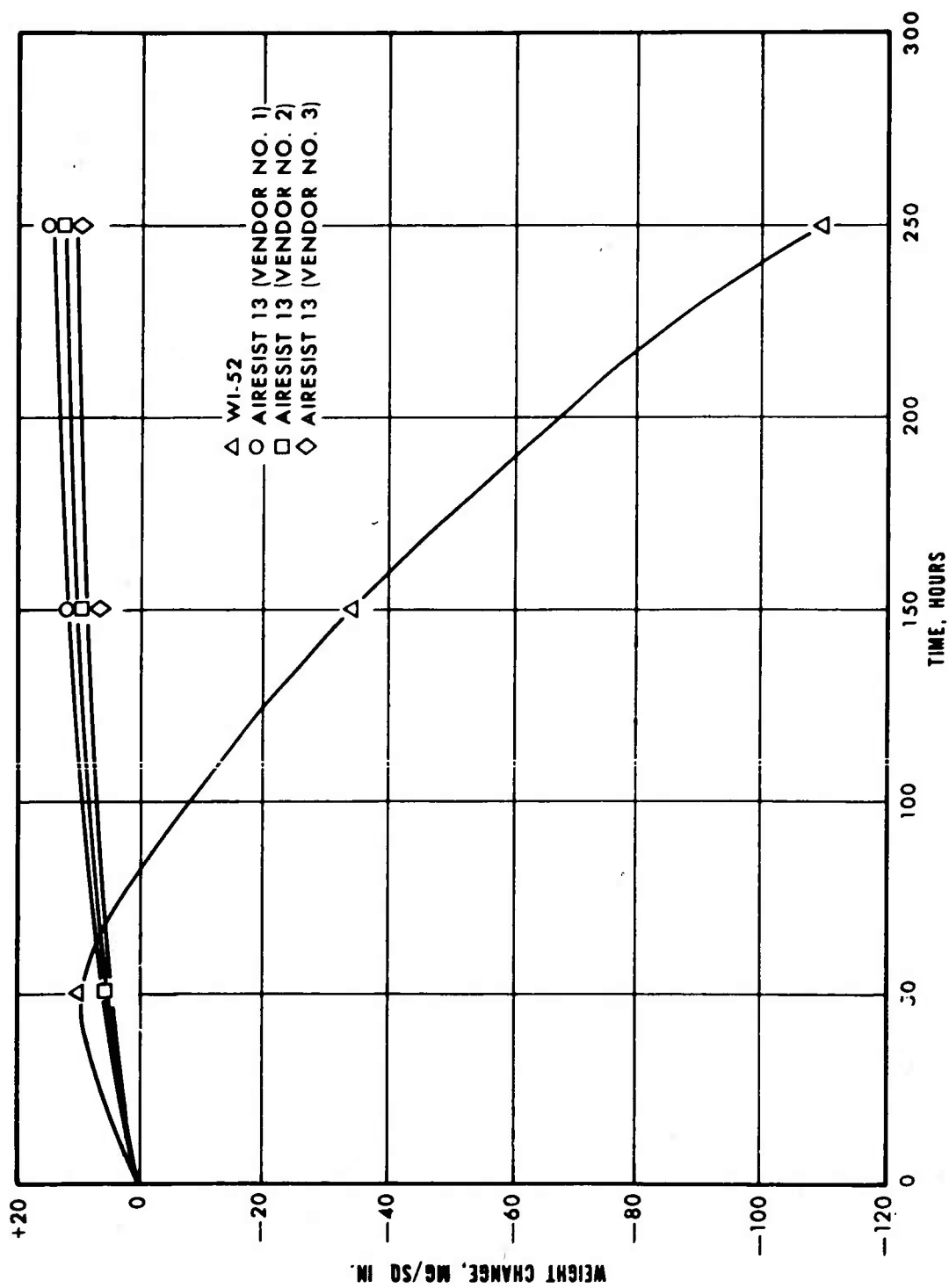
Figure 116.   Oxidation Results at 1900°F
(Weight Change Less Spalled-Off Scale).

167
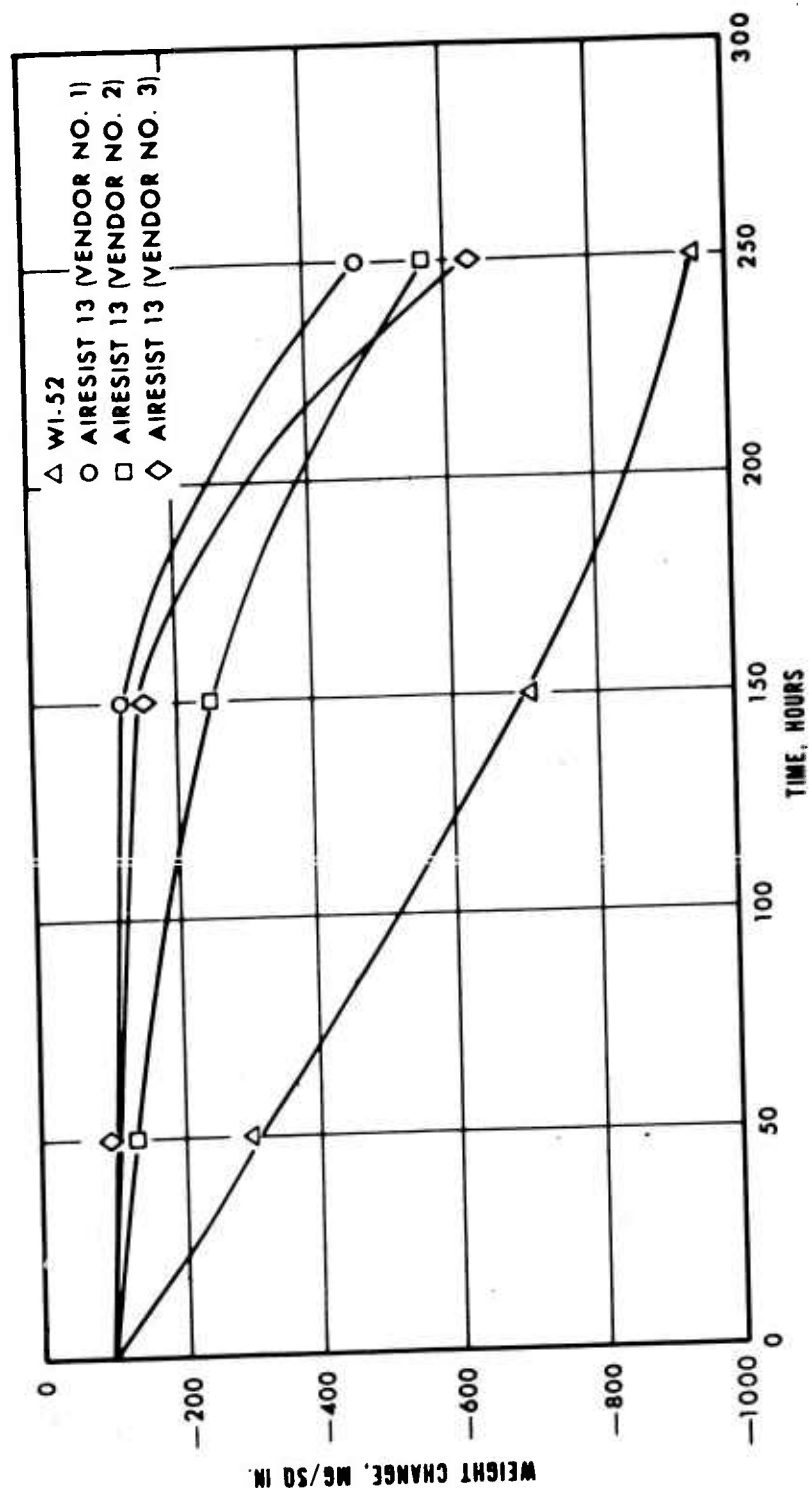
Figure 117. Oxidation Results at 2000°F (Weight Change Less Spalled-Off Scale).

168
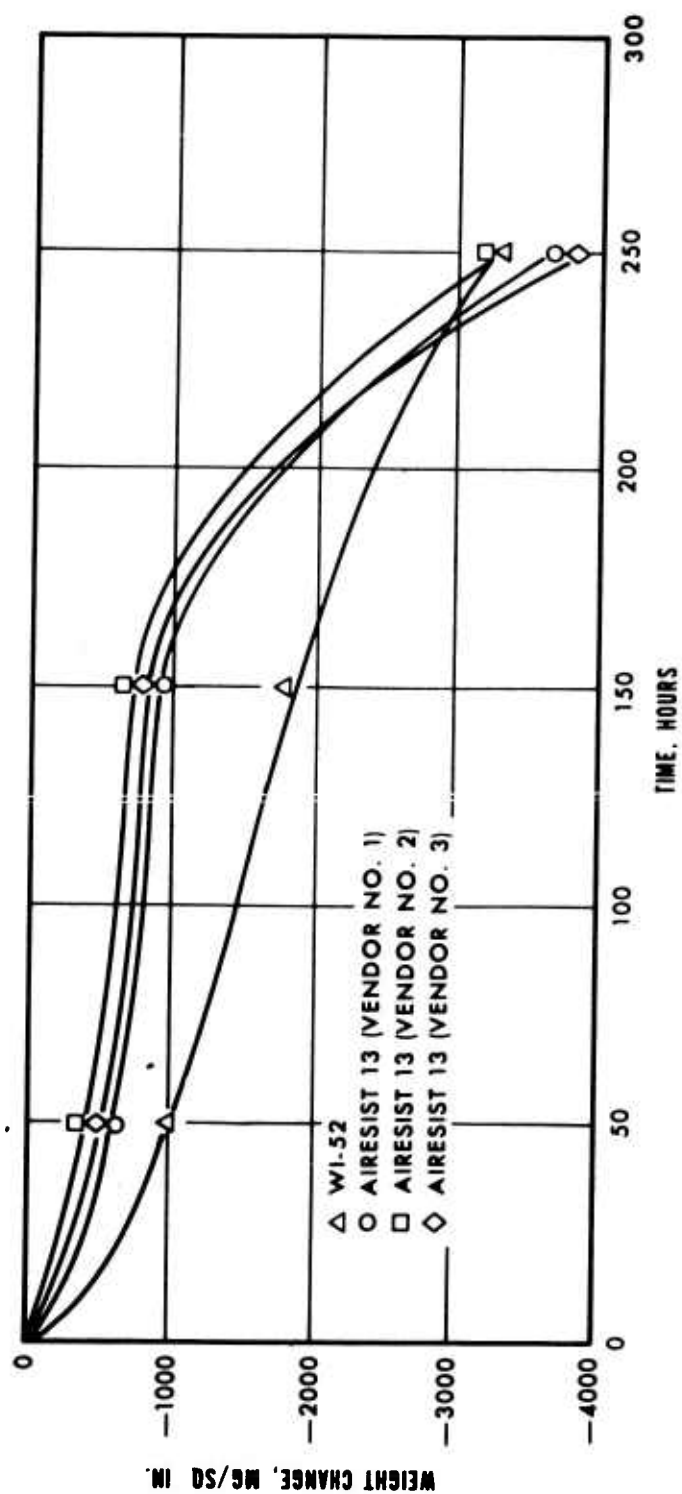
Figure 118. Oxidation Results at 2100°F (Weight Change Less Spalled-Off Scale).
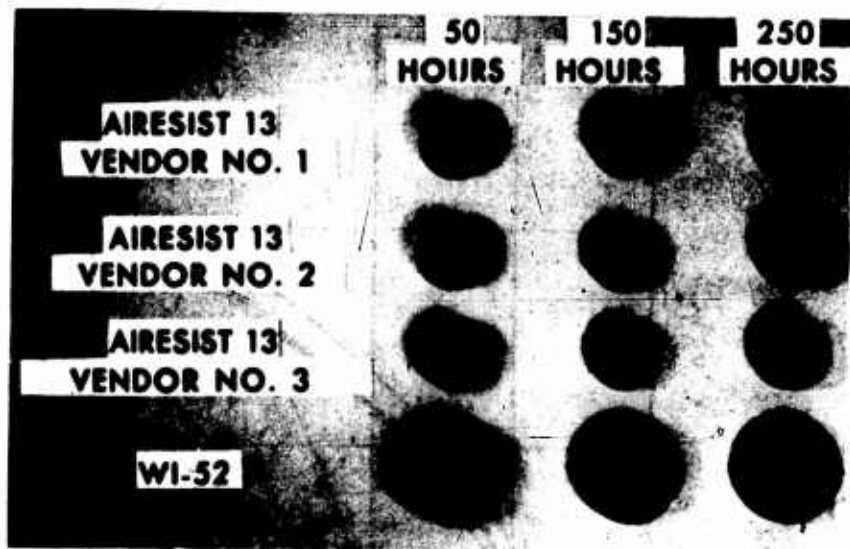
Figure 119.   Results of AiResist 13
              Oxidation Tests at 1900°F.
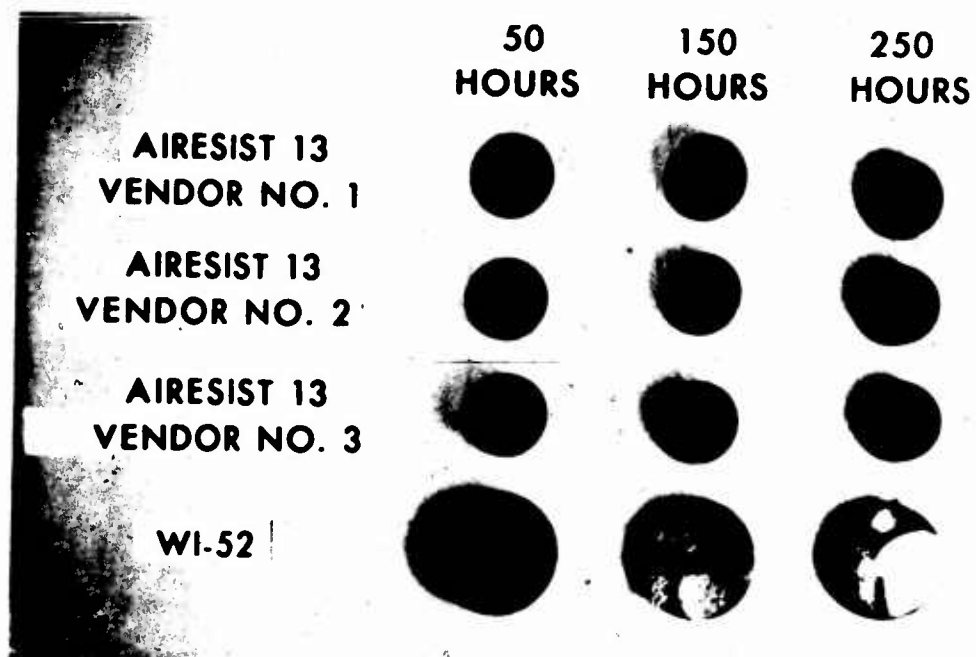
Figure 120.   Results of AiResist 13
              Oxidation Tests at 2000°F.

170
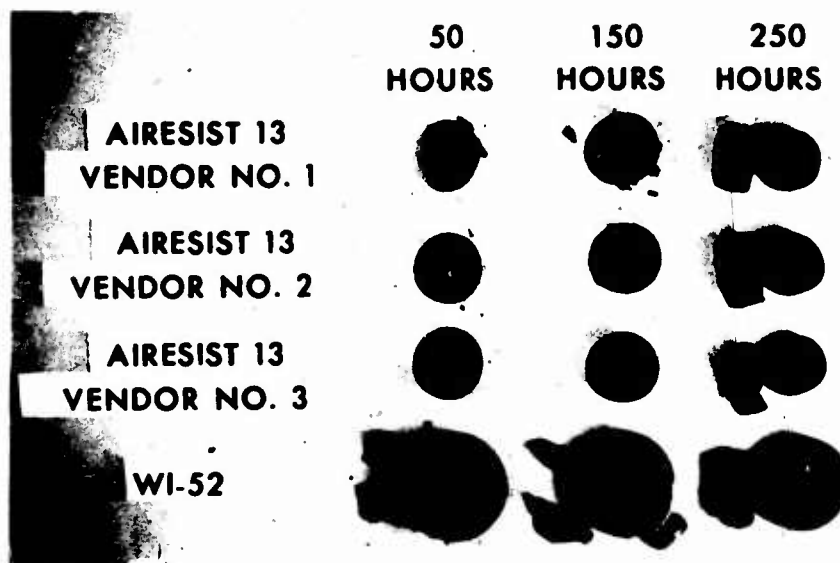
Figure 121. Results of AiResist 13
Oxidation Tests at 2100°F.
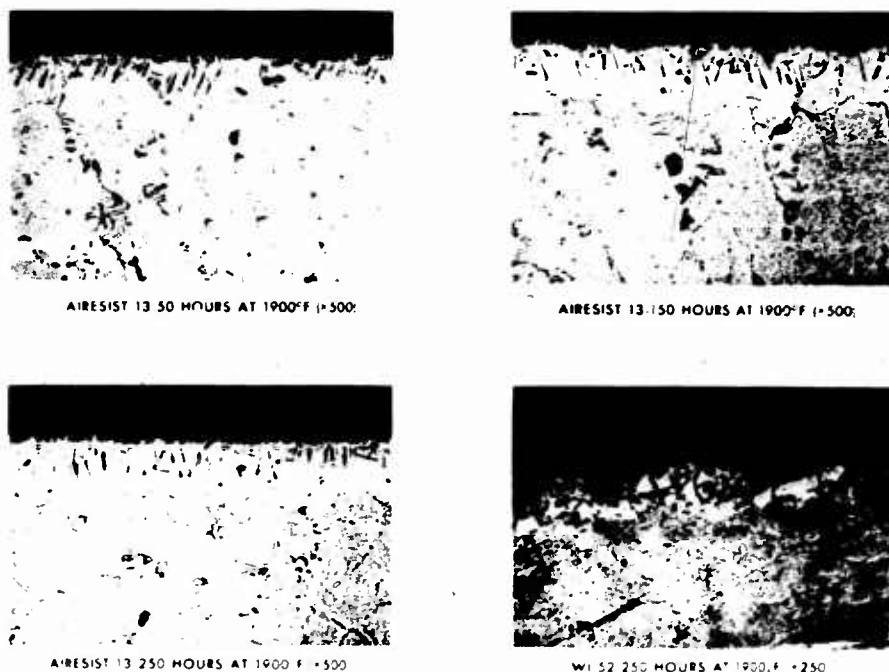
Figure 122. Photomicrographs Showing 1900°F
Oxidized Surface.
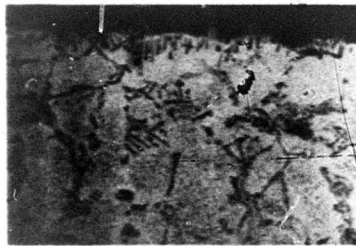
AIRESIST 13-50 HOURS AT 2000°F (×500)
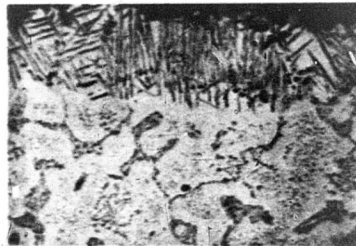
AIRESIST 13-150 HOURS AT 2000°F (×500)

AIRESIST 13-250 HOURS AT 2000°F (×500)

Figure 123.   Photomicrographs Showing 2000°F
Oxidized Surface (X500).
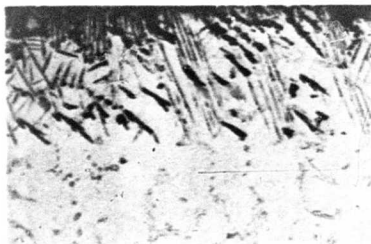
AIRESIST 13-50 HOURS AT 2100°F (×500)
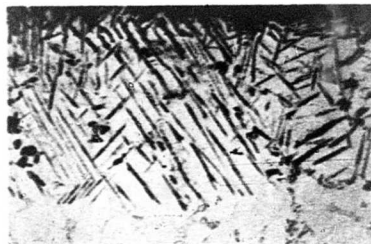
AIRESIST 13-150 HOURS AT 2100°F (×500)
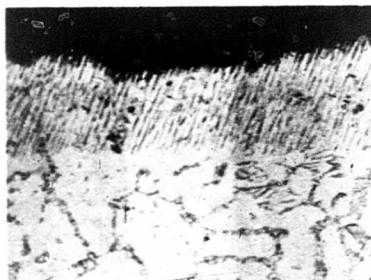
AIRESIST 13-250 HOURS AT 2100°F (×250)

Figure 124.   Photomicrographs Showing 2100°F
Oxidized Surface.

172

2. __IN-100__ - The oxidation test data are presented in Table XXXI and on Figures 125 through 133. As shown in Figures 125, 126, and 127, INCO 713C exhibits oxidation resistance superior to that of IN-100 at 2100°F. Also, a difference in the oxidation resistance of the three IN-100 heats was observed, with the 100-percent revert heat showing the least resistance to oxidation at each of the test temperatures. The test specimens after they were subjected to the high-temperature oxidation tests are shown in Figures 128, 129, and 130.

Figures 131, 132, and 133 show the oxidized surface condition of the 100-percent prime, 50 percent prime plus 50-percent revert, and 100-percent revert specimens, respectively, after 50, 150, and 250 hours at an exposure temperature of 1900°F.

It was apparent from microscopic examinations that grain-boundary attack of the IN-100 100-percent revert material was quite severe, while the 50-percent revert material showed a lesser degree of oxidation attack. The 100-percent prime material showed almost no grain-boundary attack. The micro-examinations substantiated the test data which revealed that the 100-percent revert heat exhibited the least oxidation resistance of the three material heats tested.

Alloy	Test Temp (°F)	WEIGHT CHANGE, MG/SQ IN. (LESS SPALLED-OFF SCALE) Exposure Time		
		50 Hrs	150 Hrs	250 Hrs
IN-100 (100% prime)	1900	+5	+8	+2
	2000	-5	-26	-30
	2100	-10	-32	-674
IN-100 (100% revert)	1900	-5	-20	-33
	2000	-7	-90	-293
	2100	-33	-78	-1010
IN-100 (50% revert, 50% prime)	1900	+4	+1	-1
	2000	-14	-10	-21
	2100	-44	-63	-553
INCO 713C	1900	+2	+6	+5
	2000	-2	-2	-4
	2100	-11	-13	-19

TABLE XXXI. RESULTS OF OXIDATION TESTS ON IN-100 AND INCO 713C
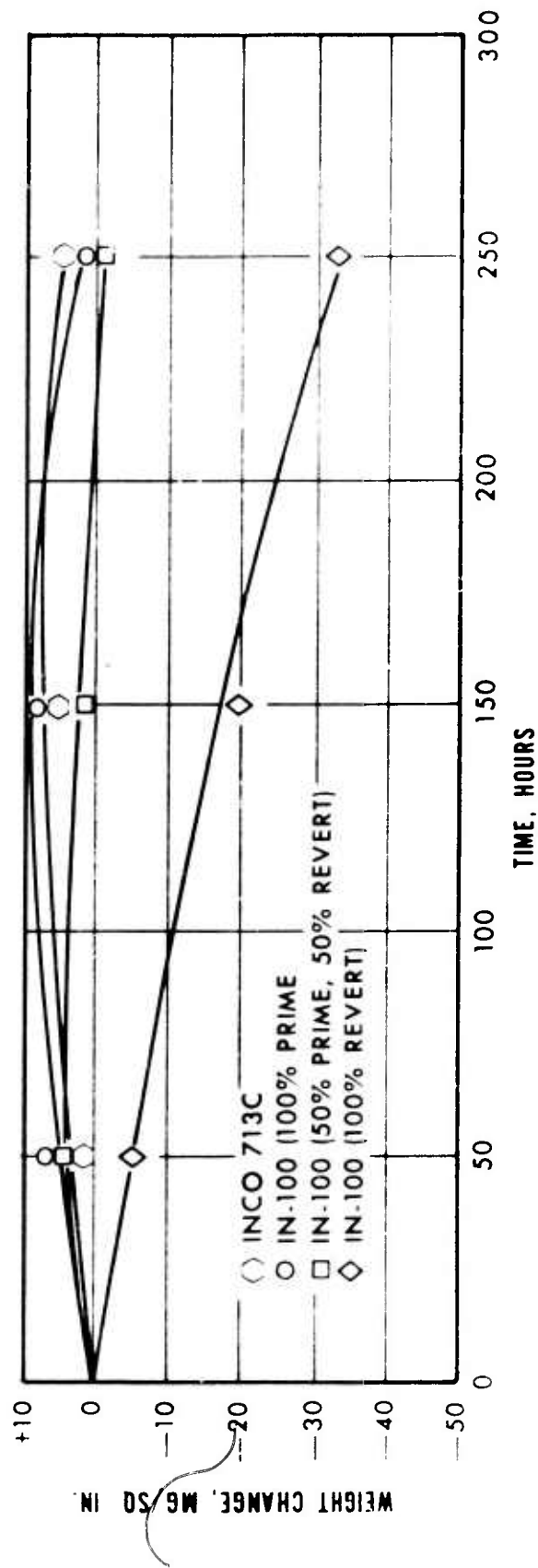
Figure 125. Oxidation Results at 1000°F (Weight Change Less Spalled-Off Scale).

175
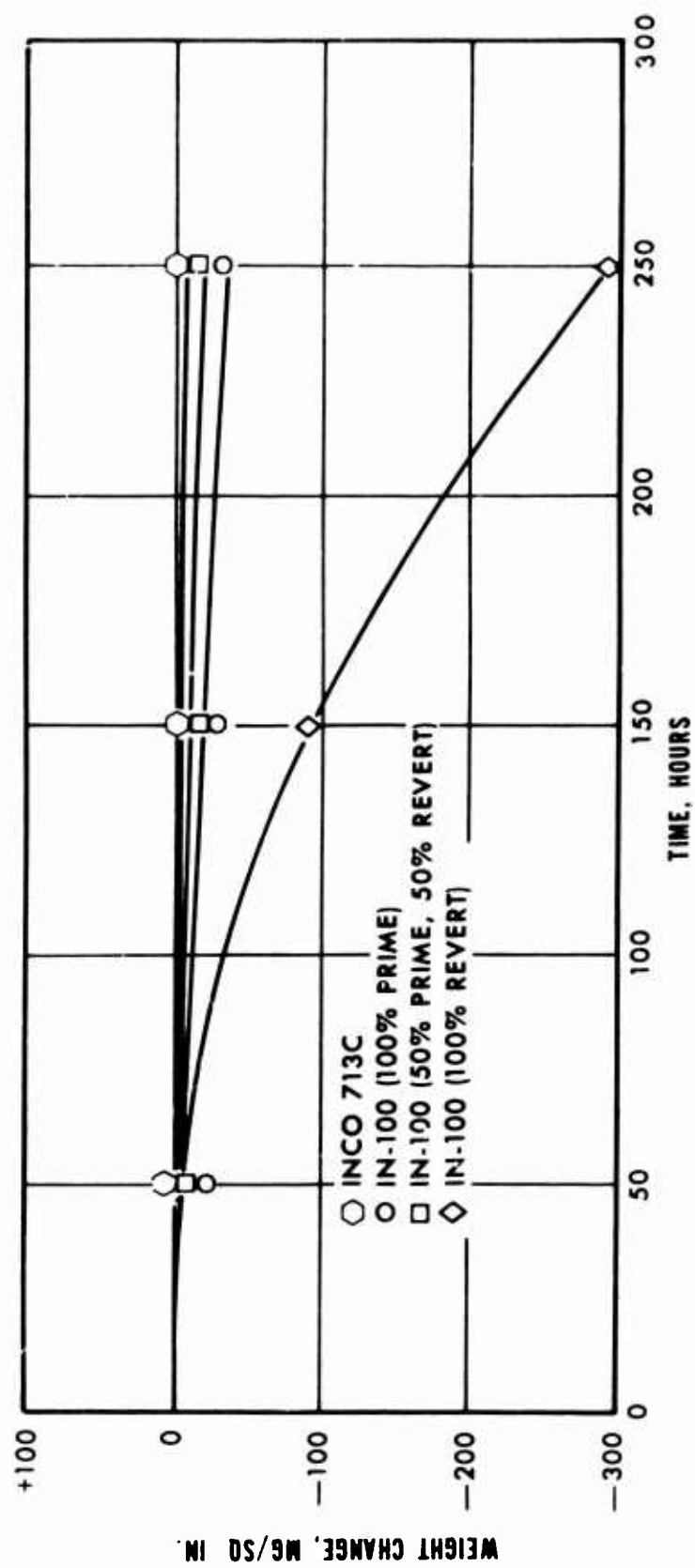
Figure 126. Oxidation Results at 2000°F (Weight
Change Less Spalled-Off Scale).

176
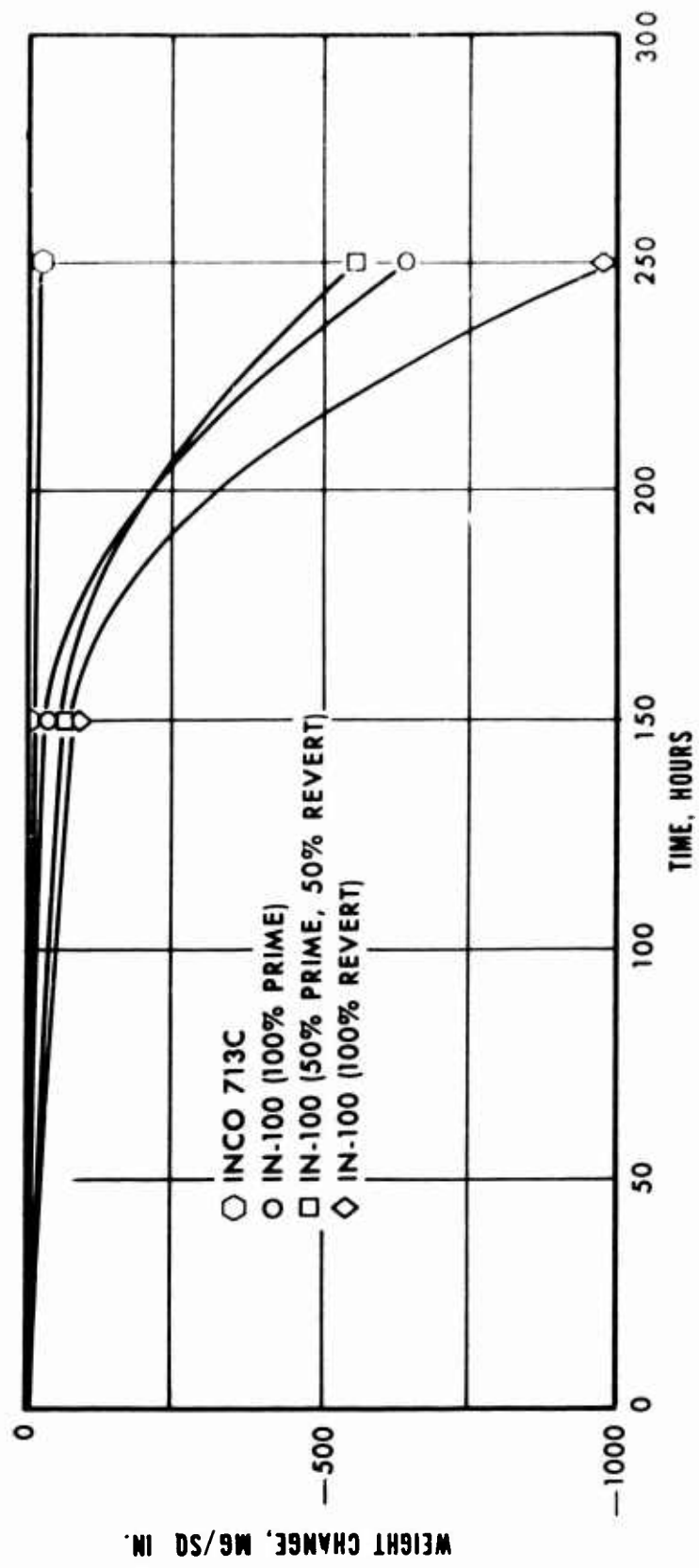
Figure 127. Oxidation Results at 2100°F (Weight Change Less Spalled-Off Scale).

177
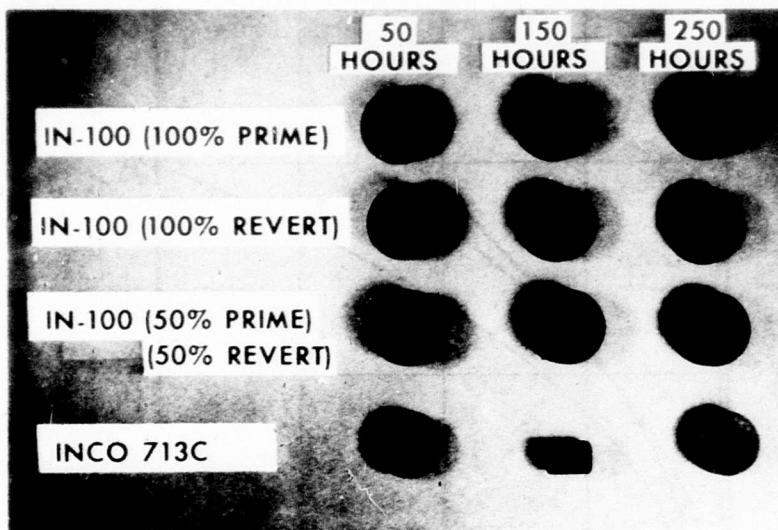
Figure 128. IN-100 Specimens After
Oxidation Tests at 1900°F.
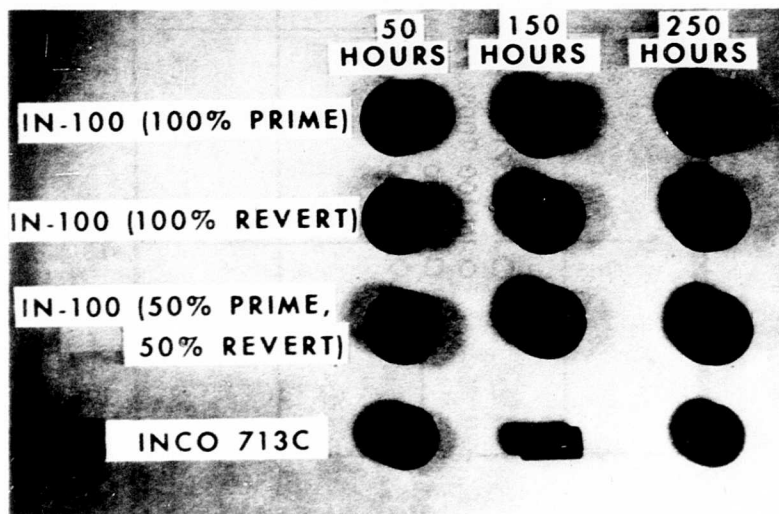
Figure 129. IN-100 Specimens After Oxidation
Tests at 2000°F.

178
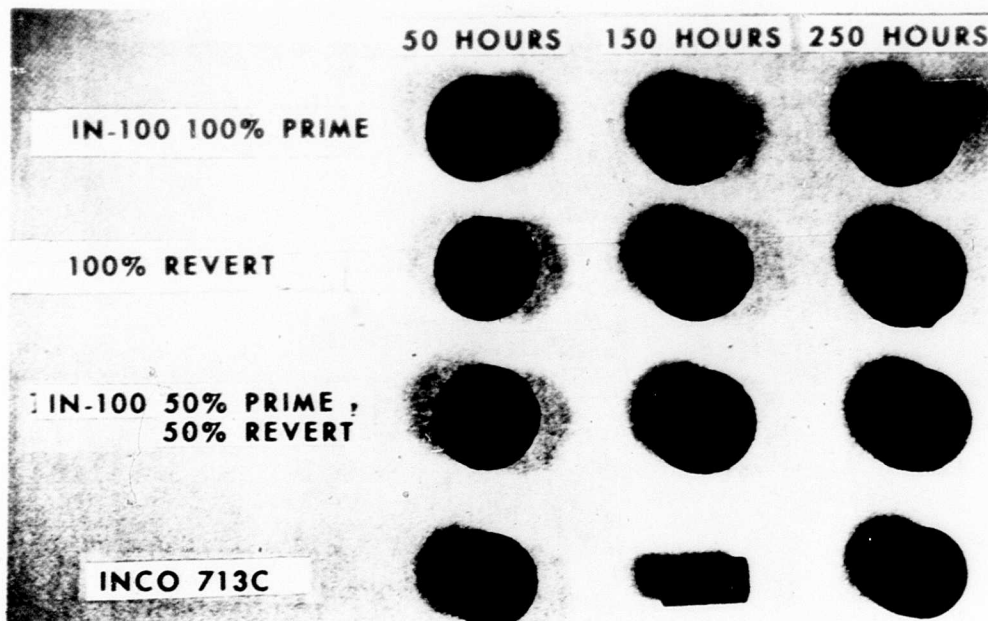
Figure 130.   IN-100 Specimens After
Oxidation Tests at 2100°F.
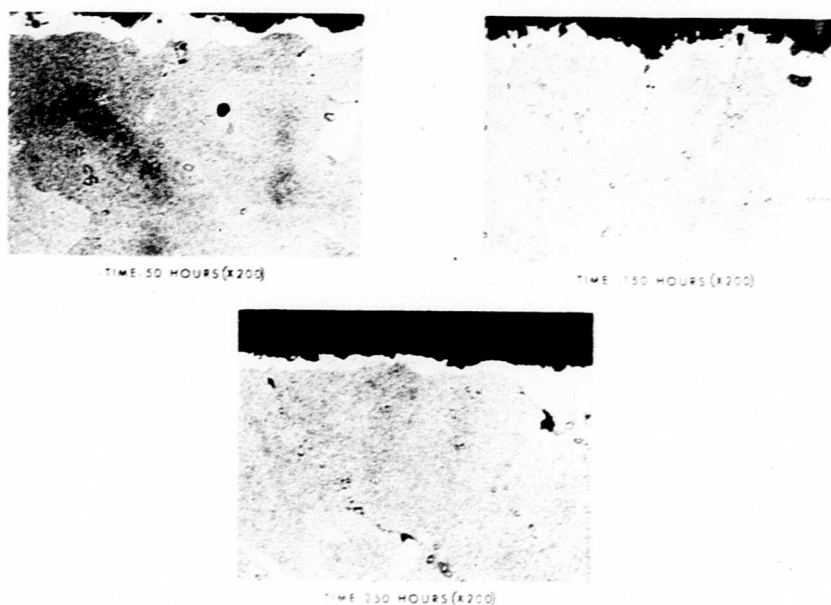
Figure 131.   Photomicrographs of IN-100 (100% Prime)
After Oxidation Testing at 1900°F.

179
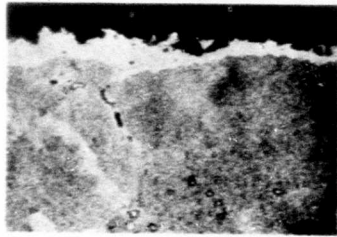
TIME-50 HOURS (X200)

TIME-150 HOURS (X200)

TIME-250 HOURS (X200)

Figure 132. Photomicrographs of IN-100
(50% Prime-50% Revert) After
Oxidation Testing at 1900°F.
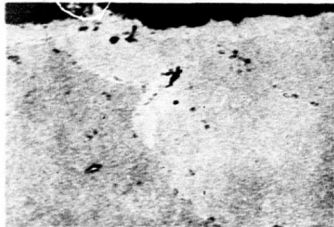
TIME-50 HOURS (X200)
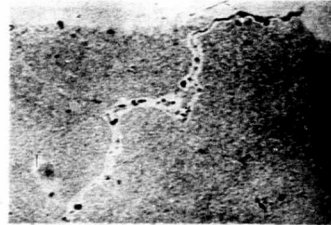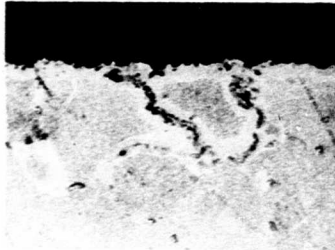
TIME-150 HOURS (X200)

TIME-250 HOURS (X200)

Figure 133. Photomicrographs of IN-100
(100% Revert) After Oxidation
Testing at 1900°F.

180

5.4.6 Oxidation-Sulfidation Test Results

The oxidation-sulfidation testing, described in 5.3.6, was conducted at 1800°, 1900°, and 2000°F. Upon completion of the tests, microexaminations were performed on each test specimen. Representative photomicrographs were prepared to provide pictorial results for correlation with the tabulated test data.

1. AiResist 13 -- The oxidation-sulfidation test data are presented in Table XXXII and Figures 134 through 138. The test results showed AiResist 13 to be far superior to WI-52 or HS-31 in resistance to oxidation-sulfidation corrosion. It is believed that the formation of a highly stable yttrium sulfide, Y_3S_3, enables AiResist to exhibit its excellent oxidation-sulfidation corrosion resistance. The test results also showed a good degree of similarity among the three different AiResist 13 heats.

    As shown in Table XXXII and Figure 134, AiResist 13 compares with WI-52, a standard turbine cobalt-base alloy, in oxidation-sulfidation resistance as follows:

    1800°F -- AiResist 13 superior by factor of 3

    1900°F -- AiResist 13 superior by factor of 10

    2000°F -- AiResist 13 superior by factor of 12

    Figures 135, 136, and 137 show the various specimens after completion of the tests.

    A microexamination of each of the specimens was conducted after exposure to the sulfur-bearing atmosphere. Representative photomicrographs (Figure 138) were prepared to provide pictorial results for correlation with the tabulated data. It was observed that the carbide phase of the WI-52 exhibited very poor resistance to the sulfur attack, while the AiResist 13 showed almost complete resistance in both the carbide and the matrix areas.

181

|		Weight Loss (MG/SQ IN.)		
TABLE XXXII. RESULTS OF OXIDATION-SULFIDATION TESTING OF AIRESIST 13, HS-31, AND WI-52		1800°F	1900°F	2000°F
WI-52		1250	4100	4650
		1150	3000	4300
	Avg.	1200	3550	4475
HS-31		1680	1435	3360
AiResist 13		372	465	253
		330	320	300
(Vendor No. 1, 0.42Y)	Avg.	351	393	277
AiResist 13		324	303	340
		300	310	394
(Vendor No. 2, 0.50Y)	Avg.	312	307	367
AiResist 13		296	322	312
		320	300	350
(Vendor No. 3, 0.13Y)	Avg.	308	311	331

NOTE: 22 hours at test temperature.
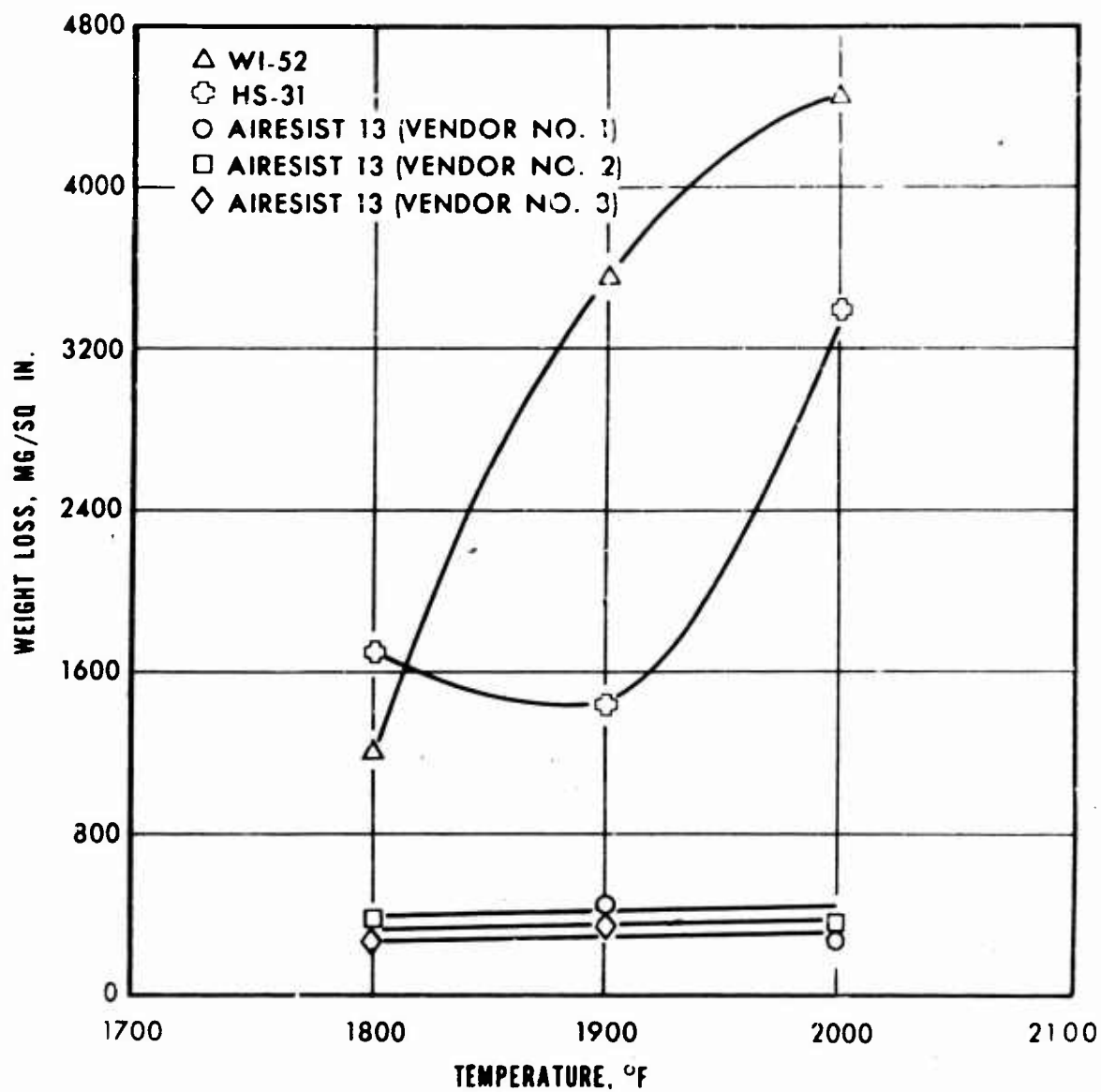
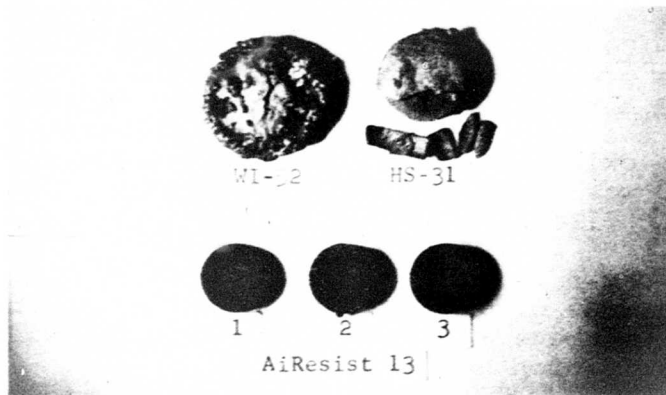Figure 134. Average Values of Sulfidation Test
Results, 22 Hours at Temperature.

183
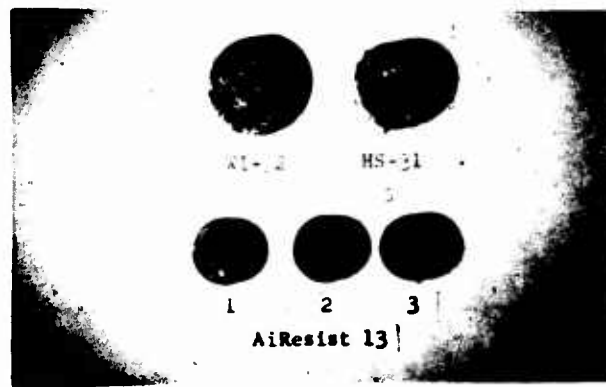
1-AIRESIST 13 (VENDOR NO. 1)
2-AIRESIST 13 (VENDOR NO. 2)
3-AIRESIST 13(VENDOR NO 3)

Figure 135. Results of Sulfidation Tests
at 1800°F (22 Hours).
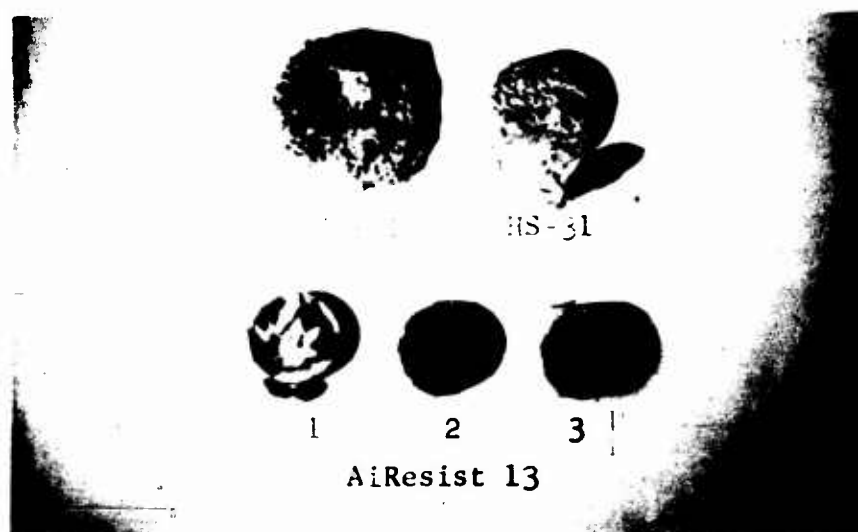
1-AIRESIST 13 (VENDOR NO. 1)
2-AIRESIST 13 (VENDOR NO. 2)
3-AIRESIST 13 (VENDOR NO. 3)

Figure 136. Results of Sulfidation Tests
at 1900°F (22 Hours).

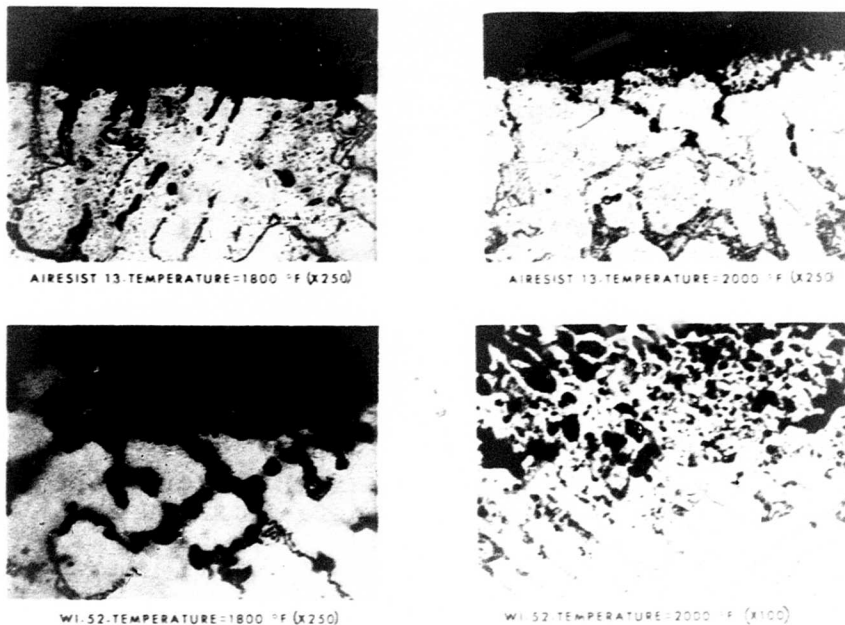1-AIRESIST 13 (VENDOR NO. 1)
2-AIRESIST 13 (VENDOR NO. 2)
3-AIRESIST 13 (VENDOR NO. 3)

Figure 137. Results of Sulfidation Tests
at 2000°F (22 Hours).

AIRESIST 13-TEMPERATURE=1800 °F (X250)

AIRESIST 13-TEMPERATURE=2000 °F (X250)

WI-52-TEMPERATURE=1800 °F (X250)

WI-52-TEMPERATURE=2000 °F (X100)

Figure 138. Photomicrographs of AiResist 13
and WI-52 After 22-Hour
Sulfidation Tests.

185

2. <u>IN-100</u> - The oxidation-sulfidation test data are presented in Table XXXIII and on Figures 139 through 143. No appreciable differences in the three heats of IN-100 were observed. The oxidation-sulfidation resistance of IN-100 was found to be superior to that of INCO 713C.

As shown in Table XXXIII and Figure 139, IN-100 compares with INCO 713C, a standard turbine nickel-base alloy, in resistance to oxidation-sulfidation as follows:

1800°F - IN-100 superior by factor of 2

1900°F - IN-100 superior by factor of 3

2000°F - IN-100 superior by factor of 1.2

Figures 140, 141, and 142 show the various specimens after completion of the tests

A microscopic examination of each of the specimens was conducted after exposure to the sulfur bearing test atmosphere. Representative photomicrographs were prepared to provide pictorial results for correlation with the tabulated data. Figure 143 depicts the surface condition of the IN-100 specimens after 22 hours' exposure at 1800°, 1900°, and 2000°F. These photomicrographs reveal the severe attack of IN-100 by sulfur-bearing atmospheres.

5.4.7 Mechanical-Fatigue Test Results

The mechanical-fatigue testing, described in 5.3.7, was conducted on both smooth and notched specimens at 1400° and 1700°F. The test results were tabulated and plotted on curves.

1. AiResist 13 - The mechanical-fatigue test results are presented in Table XXXIV and in Figures 144 and 145.

186

	WEIGHT LOSS (MG/SQ IN.)		
Alloy	1800°F	1900°F	2000°F
IN-100	896	528	1268
(100% prime	699	573	1210
IN-100	588	494	1290
(100% revert	472	544	1050
IN-100	544	465	1040
(50% revert, 50% prime)	472	463	980
INCO 713C	1080	1854	1290
	1284	1566	1458

TABLE XXXIII. RESULTS OF OXIDATION-SULFIDATION TESTING ON IN-100 AND INCO 713C

NOTE: 22 hours at test temperature.
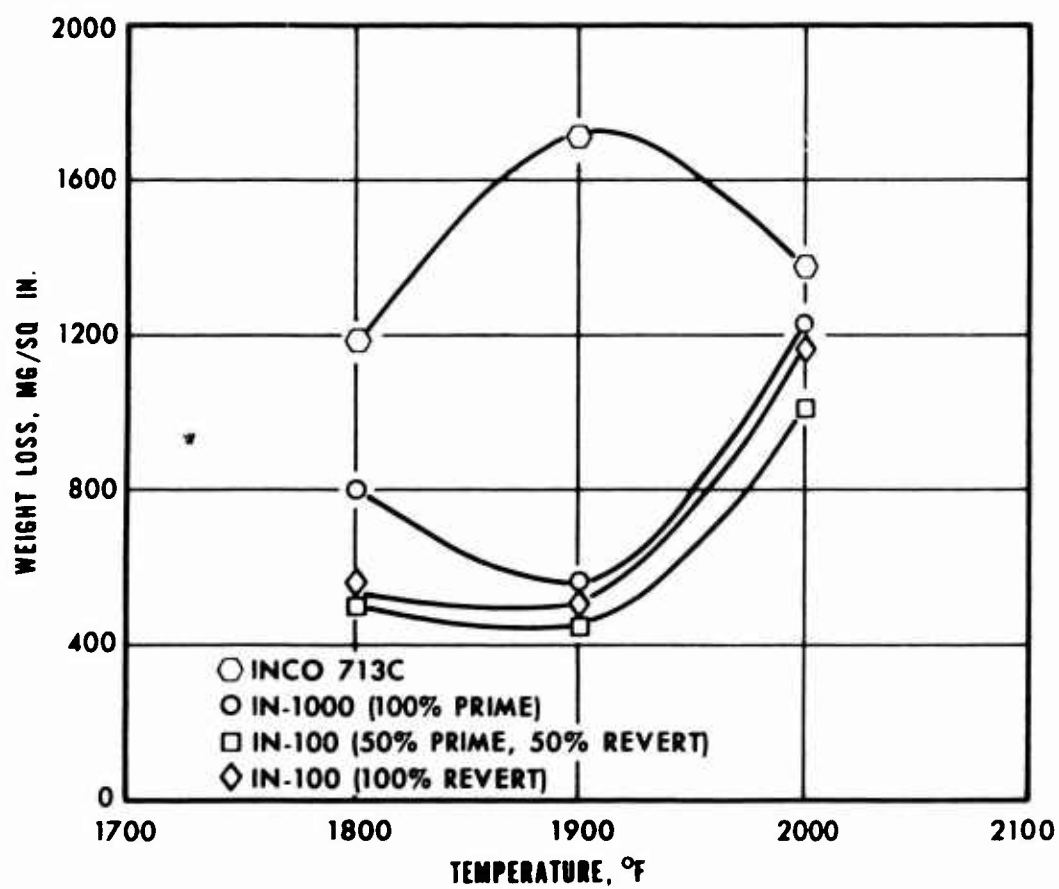
Figure 139. Average Values of Sulfidation
Test Results (22 Hours at
Temperature).

IN-100
100% PRIME

IN-100
50% PRIME,
50% REVERT

IN-100
100% REVERT
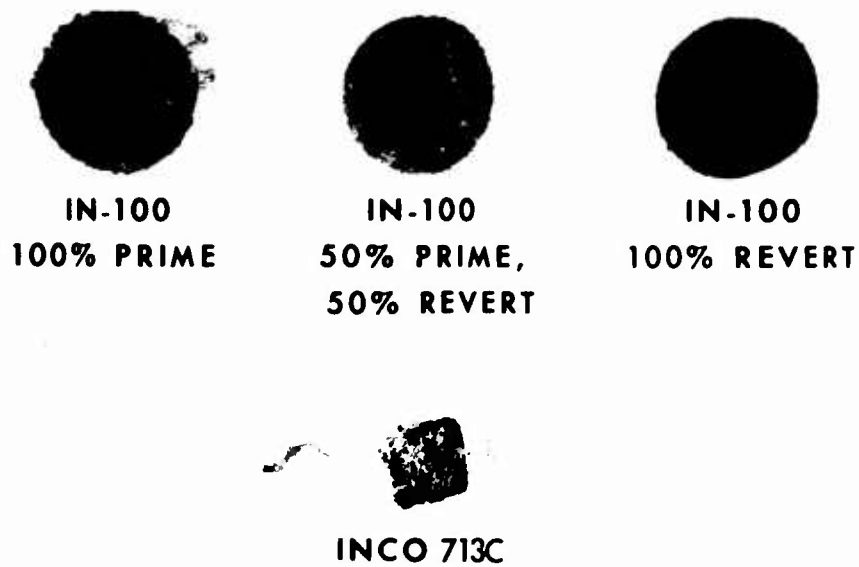
INCO 713C

Figure 140. IN-100 Specimens After
Oxidation-Sulfidation Tests
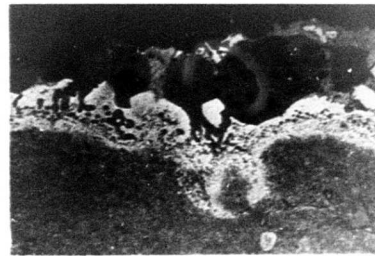at 1800°F (22 Hours).

IN-100
100% PRIME
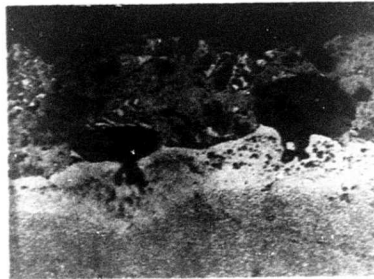
IN-100
50% PRIME
50% REVERT

IN-100
100% REVERT
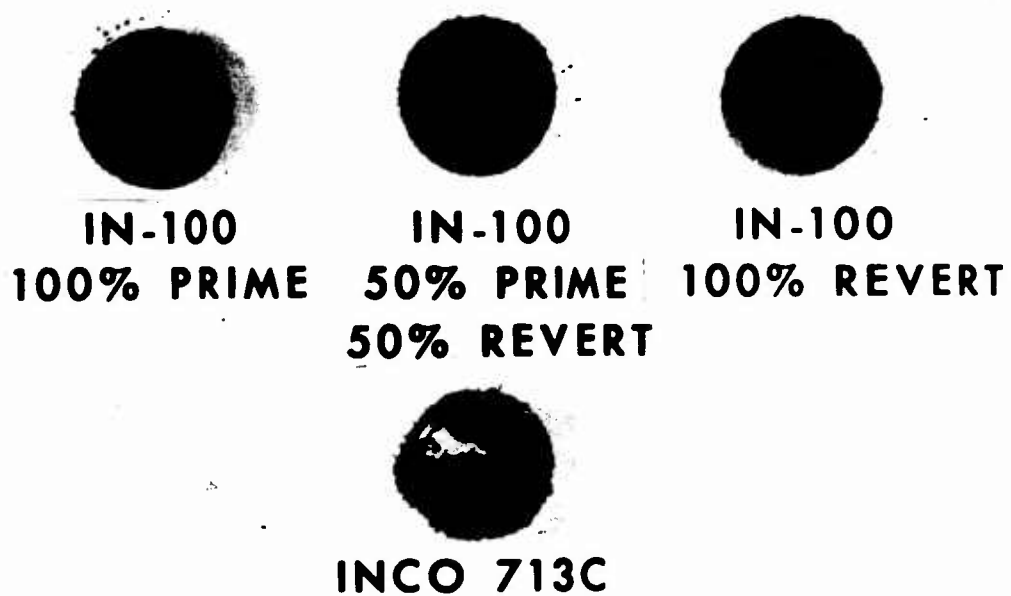
INCO 713C

Figure 141. IN-100 Specimens After
Oxidation-Sulfidation Tests
at 1900°F (22 Hours).

189

IN-100
100% PRIME

IN-100
50% PRIME
50% REVERT

IN-100
100% REVERT

INCO 713C

Figure 142. IN-100 Specimens After
Oxidation-Sulfidation Tests
at 2000°F (22 Hours).

TEMPERATURE=1800 °F (×250)

TEMPERATURE=1900 °F ×250

TEMPERATURE=2000 °F ×250

Figure 143. Photomicrographs of IN-100 Specimens
After 22-Hour Oxidation-Sulfidation
Test (X250).

190

TABLE XXXIV. AIRESIST 13 MECHANICAL-FATIGUE RESULTS

Sample No.	Test Temperature (°F)	Stress (psi)	Number of Cycles to Failure
1-1	1400	44,000	3.8×10^4
1-2	1400	42,000	1.2×10^4
1-3	1400	38,000	3.328×10^6 (n.f.)
1-4	1700	40,000	1.4×10^4
1-5	1700	35,000	1.5×10^4
1-6	1700	30,000	1.644×10^6
1-7	1700	32,500	9.25×10^5
1-8	1700	36,000	1.2×10^4
1-9	1700	34,000	3.3×10^4
2-1	1400	40,000	6.67×10^5
2-2	1400	46,000	4.513×10^6 (n.f.)
2-3	1400	48,000	1.93×10^6 (n.f.)
2-4	1400	52,000	2.0×10^3
2-5	1400	46,000	1.3×10^4
2-6	1400	54,000	2.0×10^3
2-7	1400	52,000	3.0×10^3
2-8	1400	50,000	6.0×10^3
2-9	1400	48,000	2.9×10^4
3-1	1700	33,000	1.252×10^6
3-2	1700	29,000	6.0×10^3
3-3	1700	28,000	2.312×10^6
3-4	1700	40,000	0.5×10^3
3-5	1700	32,000	1.0×10^4
3-6	1700	31,000	2.7×10^4
****1-1N***	1400	25,000	4.315×10^6 (n.f.)
1-2N	1400	40,000	9.0×10^3
1-3N	1400	27,000	3.433×10^6 (n.f.)
1-4N	1700	30,000	1.9×10^4
2-1N	1400	35,000	1.6×10^4
2-2N	1400	30,000	7.2×10^4
3-1N	1700	25,000	8.4×10^4
3-2N	1700	22,500	5.59×10^5
3-3N	1700	21,000	2.345×10^6 (n.f.)**
3-4N	1700	22,500	8.37×10^5
3-5N	1700	21,000	3.0×10^3 *

* Sample failed outside of notch.

** (n.f.) - Sample did not fail; test discontinued.

*** (1-) - Series cast by Vendor No. 1.
    (2-) - Series cast by Vendor No. 2.
    (3-) - Series cast by Vendor No. 3.
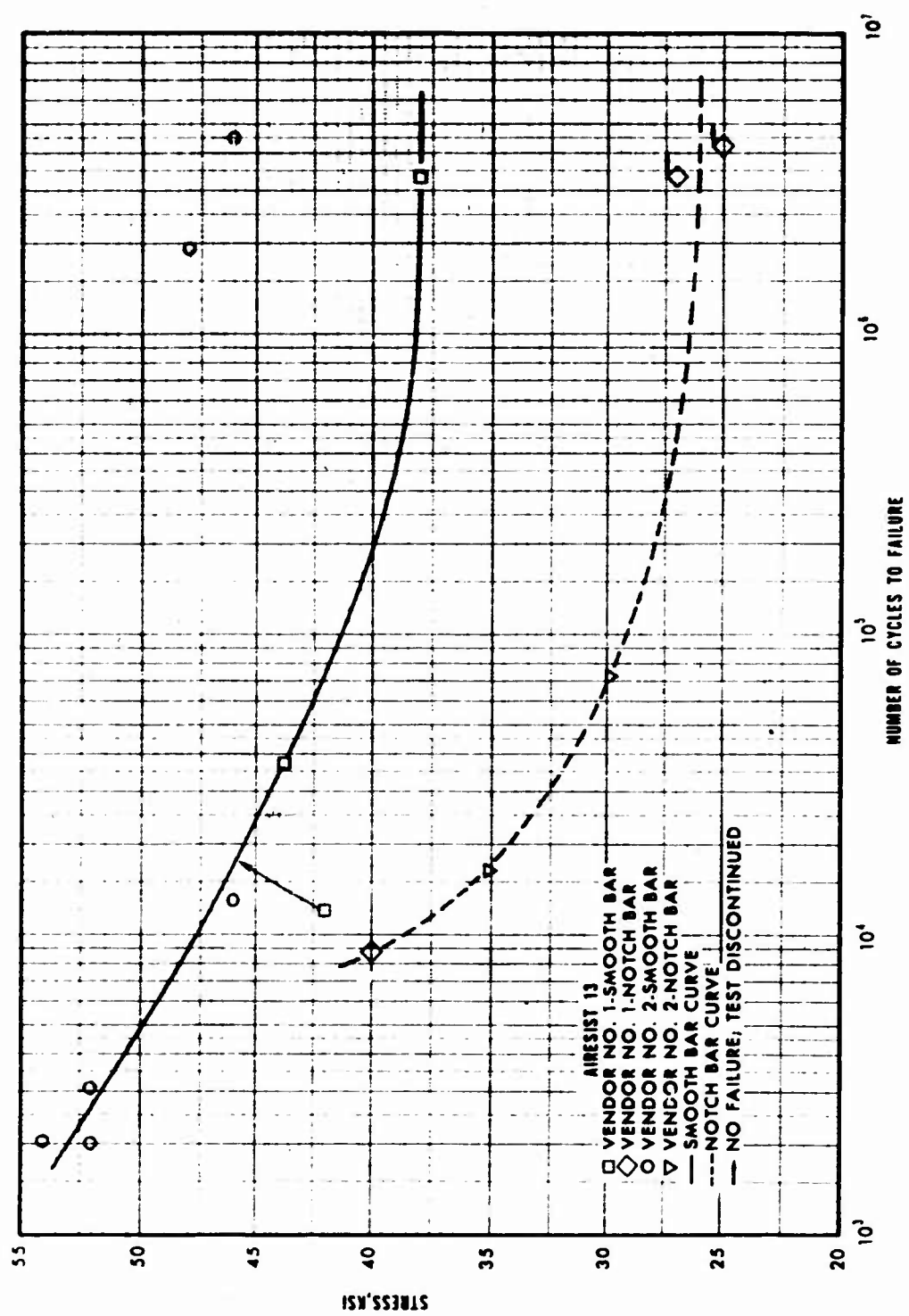
**** 1-IN - Denotes notched mechanical-fatigue bar.

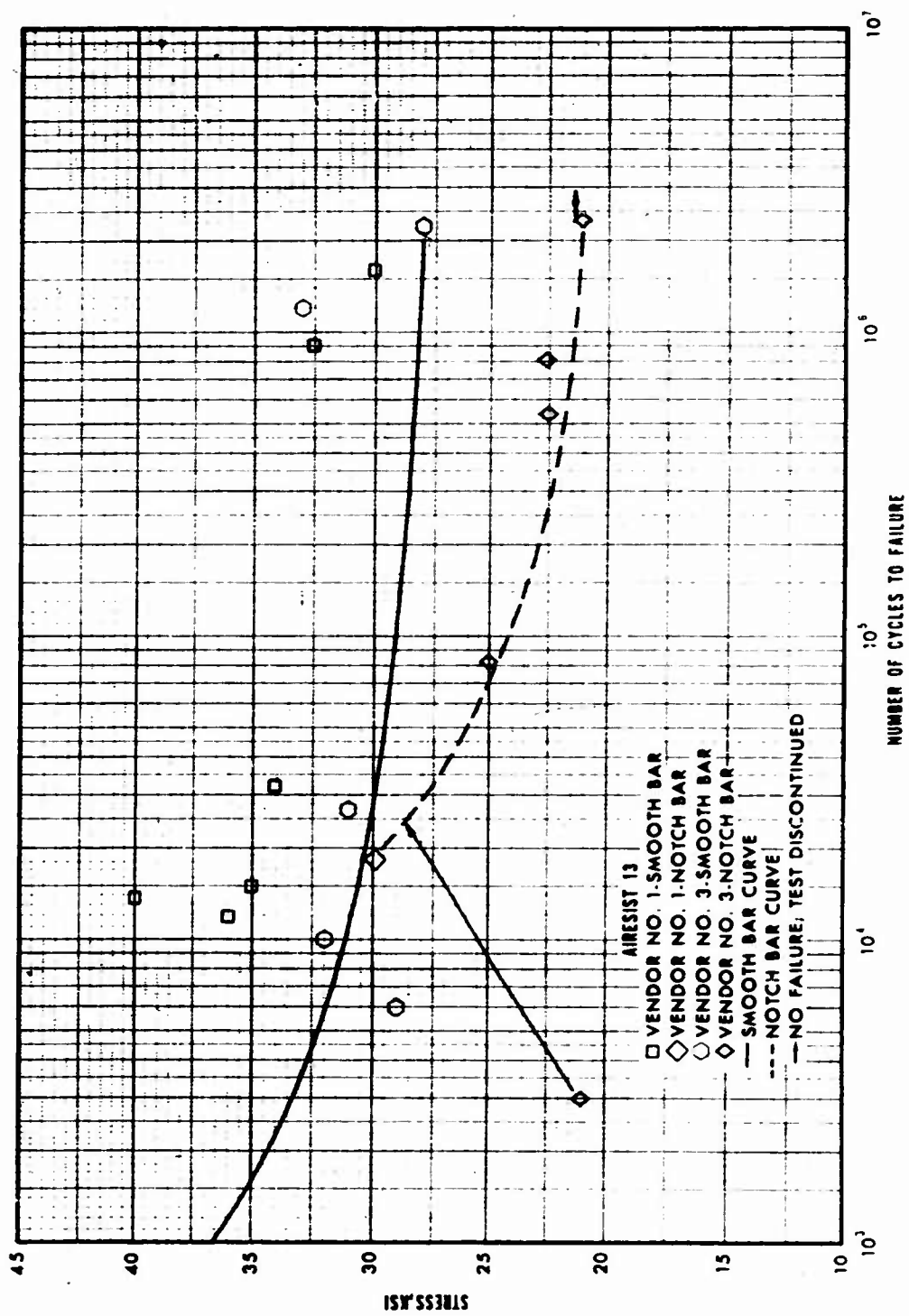Figure 144. Mechanical-Fatigue Results for AiResist 13 at 1400°F.

192

Figure 145. Mechanical-Fatigue Results for AiResist 13 at 1700°F.

193

These test results are the first known results of mechanical-fatigue testing of a cast cobalt-base alloy utilizing tension-compression loading at zero mean stress. Therefore, it is not known whether the observed data scatter can be considered abnormal. No reasons for the data scatter can be advanced. Stress loads and heat-up time were maintained with consistency throughout the testing. The test temperature deviation was within ±2 percent. After completion of the tests, the specimen finishes were examined and were found to be uniform. Occasional nicks on the surface of the test bars were observed, but the failures did not occur at those locations.

Since it is not known whether the obtained data scatter can be considered normal, the values of the endurance limit given below may be considered only as close approximations.

Test Temperature (°F)	Test Bar Configuration	Endurance Limit for 10^6 Cycles (psi)	Tensile Strength (psi)	Endurance Ratio
1400	Smooth	38,000	62,500	0.61
	Notched	26,000	62,500	0.42
1700	Smooth	28,000	35,000	0.80
	Notched	21,000	35,000	0.60

2. IN-100 – The mechanical-fatigue test results are presented in Table XXXV and in Figures 146 and 147.

The curves of Figures 146 and 147 were generated through the lowest test results. The results at both test temperatures exhibited a normal degree of scatter for the cast IN-100 alloy. Stress loads and heat-up times were consistently maintained throughout the testing. The test-temperature deviation was within ±2 percent. After completion of the tests, the specimen finishes were examined and were found to be uniform. Occasional nicks on the surface of the test bars were observed, but the failures did not occur at those locations.

194

TABLE XXXV.   IN-100 MECHANICAL-FATIGUE RESULTS

Sample No.	Test Temperature (°F)	Stress (psi)	Number of Cycles to Failure
N1-1	1700	25,250	2.174×10^6 (n.f.) *
N1-2	1700	50,000	3.0×10^4
N1-3	1700	35,000	1.877×10^6
N1-4	1700	60,000	5.0×10^3
N1-5	1700	40,000	8.31×10^5
N1-6	1700	40,000	4.3×10^6
N2-1	1400	40,000	2.161×10^6
N2-2	1700	35,000	2.648×10^6
N2-3	1700	45,000	2.84×10^5
N2-4	1700	50,000	8.3×10^4
N2-5	1700	55,000	5.0×10^4
N2-6	1700	45,000	1.33×10^5
N2-7	1700	37,000	3.051×10^6
N3-1	1400	50,000	2.22×10^5
N3-2	1400	54,000	2.15×10^5
N3-3	1400	58,000	5.4×10^4
N3-4	1400	64,000	1.9×10^4
N3-5	1400	46,000	7.85×10^5
N3-6	1400	68,000	2.0×10^4
N3-7	1400	42,000	1.903×10^6
N3-8	1400	74,000	3.1×10^4
N3-9	1400	78,000	6.0×10^3
N3-10	1400	74,000	7.0×10^3
N3-11	1400	38,000	3.071×10^6 (n.f.)
N3-12	1400	40,000	8.27×10^5
N1-1N	1400	30,000	1.18×10^5
N1-2N	1400	40,000	3.3×10^4
N1-3N	1400	29,000	3.043×10^6 (n.f.)
41-4N	1400	50,000	6.0×10^3
N1-5N	1700	45,000	8.0×10^3
N1-6N	1700	35,000	2.5×10^4
N1-7N	1700	30,000	2.356×10^6 (n.f.)
N1-8N	1700	32,500	3.6×10^4
N1-9N	1700	31,000	1.199×10^6
N2-1N	1400	50,000	1.1×10^4
N2-2N	1400	29,000	1.47×10^5
N2-3N	1400	45,000	1.4×10^4
N2-4N	1400	35,000	5.0×10^4
N2-5N	1700	32,000	2.243×10^6 (n.f.)
N2-6N	1700	40,000	1.2×10^4
N2-7N	1700	35,000	2.3×10^4
N3-1N	1400	40,000	3.2×10^4
N3-2N	1400	30,000	1.1×10^5
N3-3N	1400	25,000	2.668×10^6 (n.f.)
N3-4N	1400	28,000	2.189×10^6 (n.f.)
N3-5N	1700	32,500	6.4×10^4
N3-6N	1700	31,000	5.9×10^4
N3-7N	1700	45,000	6.0×10^3
N3-8N	1700	40,000	1.4×10^4

*   (n.f.) - Sample did not fail; test discontinued.

**   (N1-) - 100% prime.
   (N2-) - 50% revert - 50% prime.
   (N3-) - 100% revert.

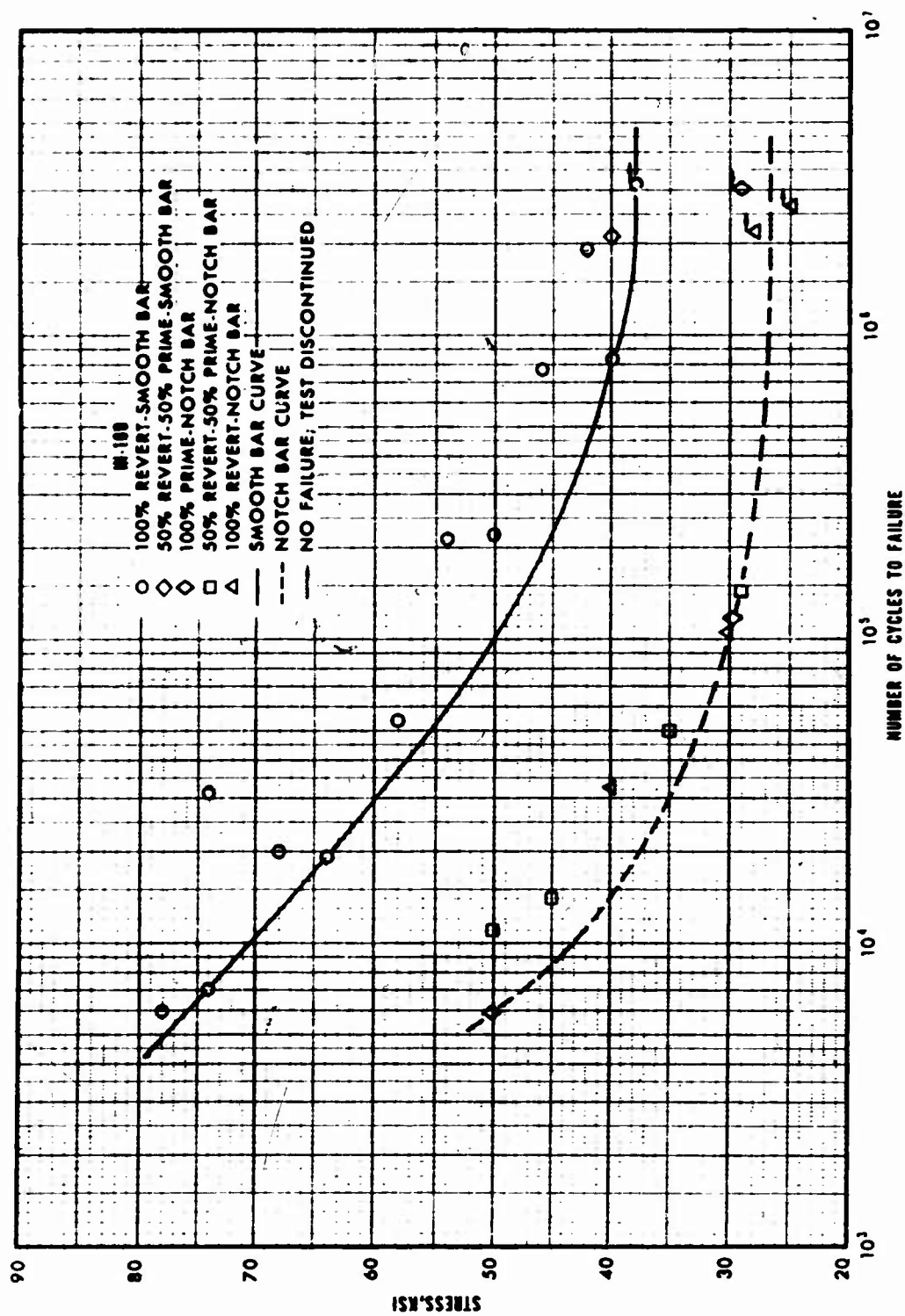***   N1-1N - Denotes notched mechanical-fatigue bar.

Figure 146. Mechanical-Fatigue Results
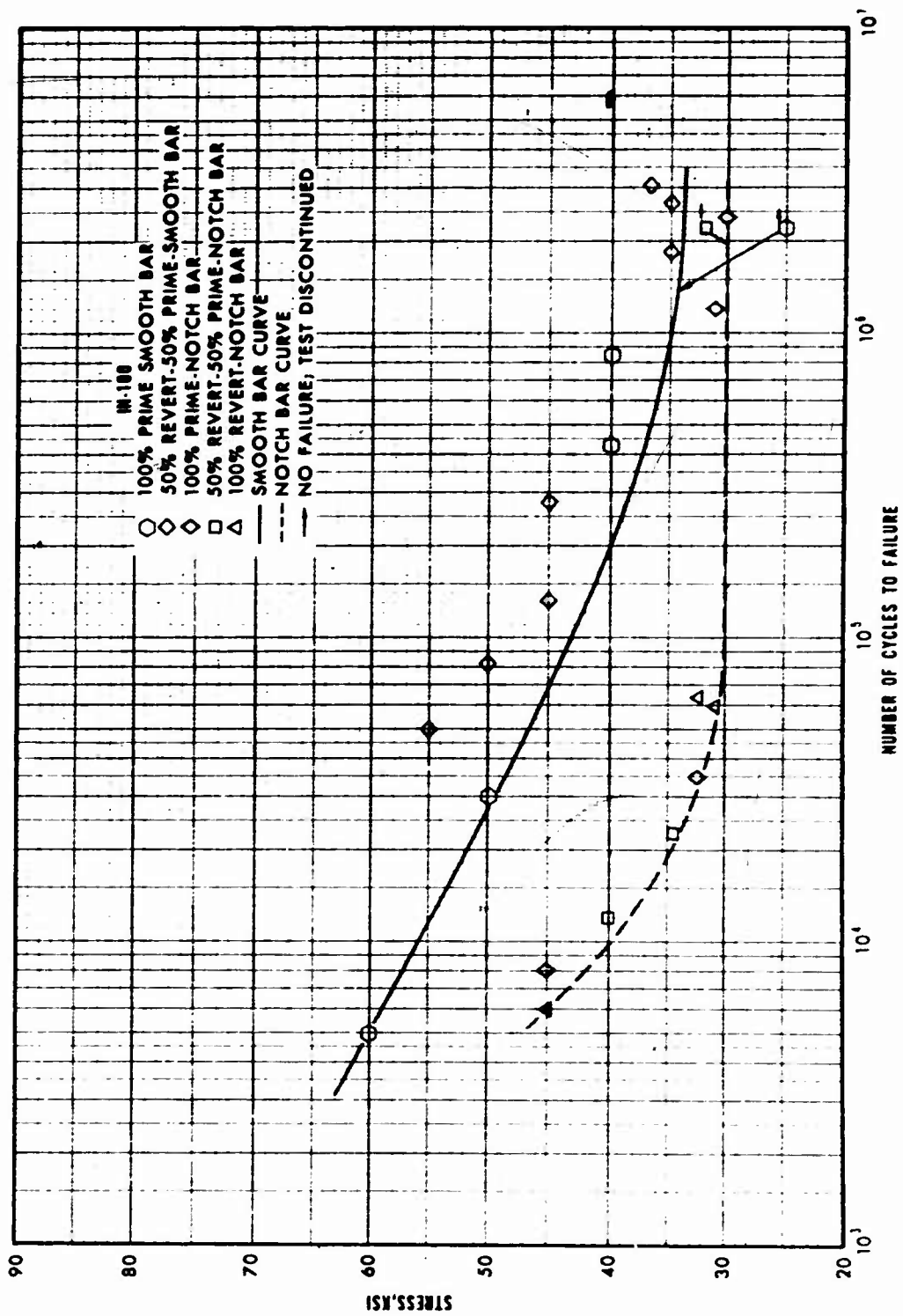for IN-100 at 1400°F.

196

Figure 147. Mechanical-Fatigue Results for IN-100 at 1700°F.

197

The smooth- and notched-bar endurance limit values determined during this test program are shown below:

Test Temperature (°F)	Test Configuration	Endurance Limit for 10^6 Cycles (psi)	Tensile Strength (psi)	Endurance Ratio
1400	Smooth	38,000	126,000	0.30
	Notched	26,000	126,000	0.21
1700	Smooth	34,000	88,500	0.38
	Notched	30,000	88,500	0.34

5.4.8 Thermal-Fatigue Test Results

The thermal-fatigue testing was conducted as described in 5.3.8. Results of the tests are presented in the following subparagraphs.

1. AiResist 13 - The thermal-fatigue tests were conducted at 2000°, 2100°, and 2200°F. The test results presented in Table XXXVI show that AiResist 13 and WI-52 have quite similar thermal-fatigue properties. The data scatter that was observed was considered abnormal and necessitated reruns of particular tests. The scatter in results was not significantly influenced by the test temperature.

   It should be noted that two thermal-fatigue tests were performed on each specimen—one test on each end. It was found that in only two instances was the number of cycles to crack initiation for Test No. 2 lower than that for Test No. 1. Thus, it was evident that more cycles were required to initiate cracking once a test specimen had been subjected to thermal cycling on the opposite end. This phenomenon is unexplainable, since the opposite end of the test bar never reached 600°F during thermal-fatigue testing.

198

TABLE XXXVI. THERMAL-FATIGUE TEST RESULTS

Material	Heat	Spec. No.	Test Temp (°F)	Test No.	Cycles to Initial Crack	Cycles to Failure*	No. of Adjacent Cracks
AiResist 13	Vendor No. 1	F	2000	1	1180	1540	1
		F	2000	2	1230	1770	1
	Vendor No. 3	D	2000	1	1178	2228	2
		D	2000	2	898	1374	0
	Vendor No. 2	BB	2000	1	367	607	2
		BB	2000	2	480	980	1
		CC**	2000	1	597	1197	5
WI-52		Y	2100	1	918	1227	-
		Y	2100	2	192	327	-
AiResist 13	Vendor No. 1	D	2100	1	641	941	4
		D	2100	2	405	585	1
	Vendor No. 3	C	2100	1	283	824	3
		C	2100	2	359	1079	8
	Vendor No. 2	AA	2100	1	282	642	4
		AA	2100	2	300	840	6
WI-52		Z	2200	1	322	700	-
		Z	2200	2	295	475	-
AiResist 13	Vendor No. 1	C	2200	1	123	183	4
		C	2200	2	245	544	3
	Vendor No. 3	A***	2200	1	61	181	1
		A***	2200	2	182	482	2
	Vendor No. 2	A	2200	1	120	300	2
		A	2200	2****	120	480	4

*Failure = when crack propagated across the leading edge of the test specimen.

**Test reruns.

***Specimen had large columnar grains.

****Specimen overheated.

199

AiResist 13 specimens cast from the material
prepared by Vendor No. 1 showed slightly better
resistance to crack initiation than the AiResist
13 from Vendors Nos. 2 and 3. This is shown in
Figures 148 and 149, which present cycles to
crack initiation and cycles to failure versus
temperature, respectively.

Figures 150, 151, and 152 illustrate the grain
size in the test specimens prior to testing.
All of the test bars were cast with identical
gating designs, invested in the same manner,
preheated to identical temperatures, and poured
at the same temperature. However, it was ob-
served that the specimens cast from the material
prepared by Vendor No. 3 were not as fine-grained
as those cast from the material prepared by
Vendors No. 1 and 2.

All specimens were examined by X-ray and
fluorescent-penetrant methods prior to testing.
No indications of material defects were found.

Specimen failure was established as the number
of cycles for propagation of a crack across
the leading edge of the test specimen. Smaller
cracks in the leading edge were observed in
addition to the main crack which determined
the failure. The presence of these smaller
cracks appeared to increase the number of cycles
required for failure. When only one crack
formed on the leading edge, it propagated more
rapidly and caused an early failure. This is
reasonable, since the thermal stress buildup
in the test bar during thermal cycling would
be less for test specimens with a greater
number of cracks. Thus, it is believed that
the criterion of "cycles to initial cracking,"
Figure 148, is more significant than the
number of cycles required for failure. The
number of additional or secondary cracks ob-
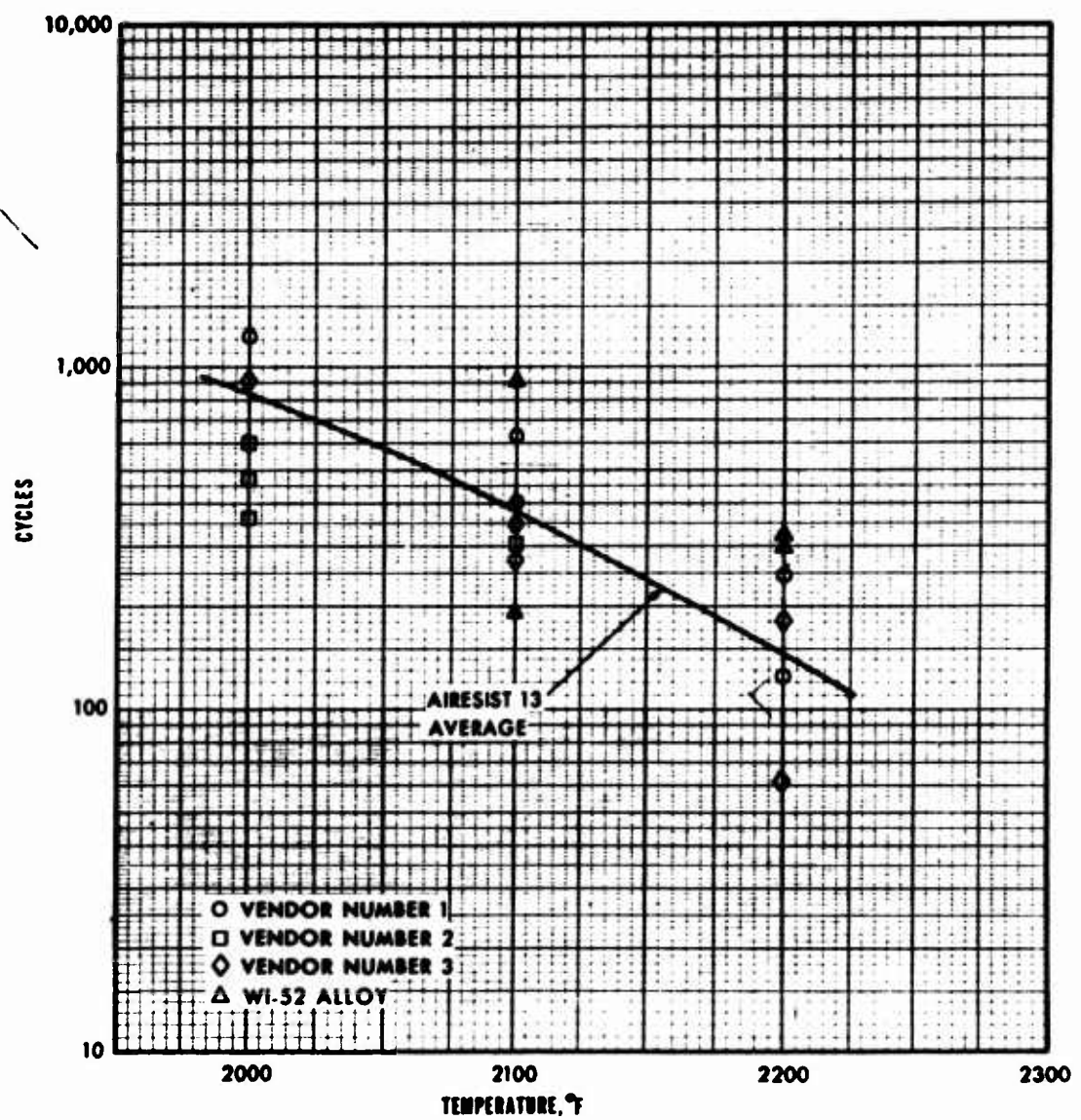served after completion of each test is pre-
sented in Table XXXVI.

200

Figure 148. AiResist 13 - Thermal-Fatigue
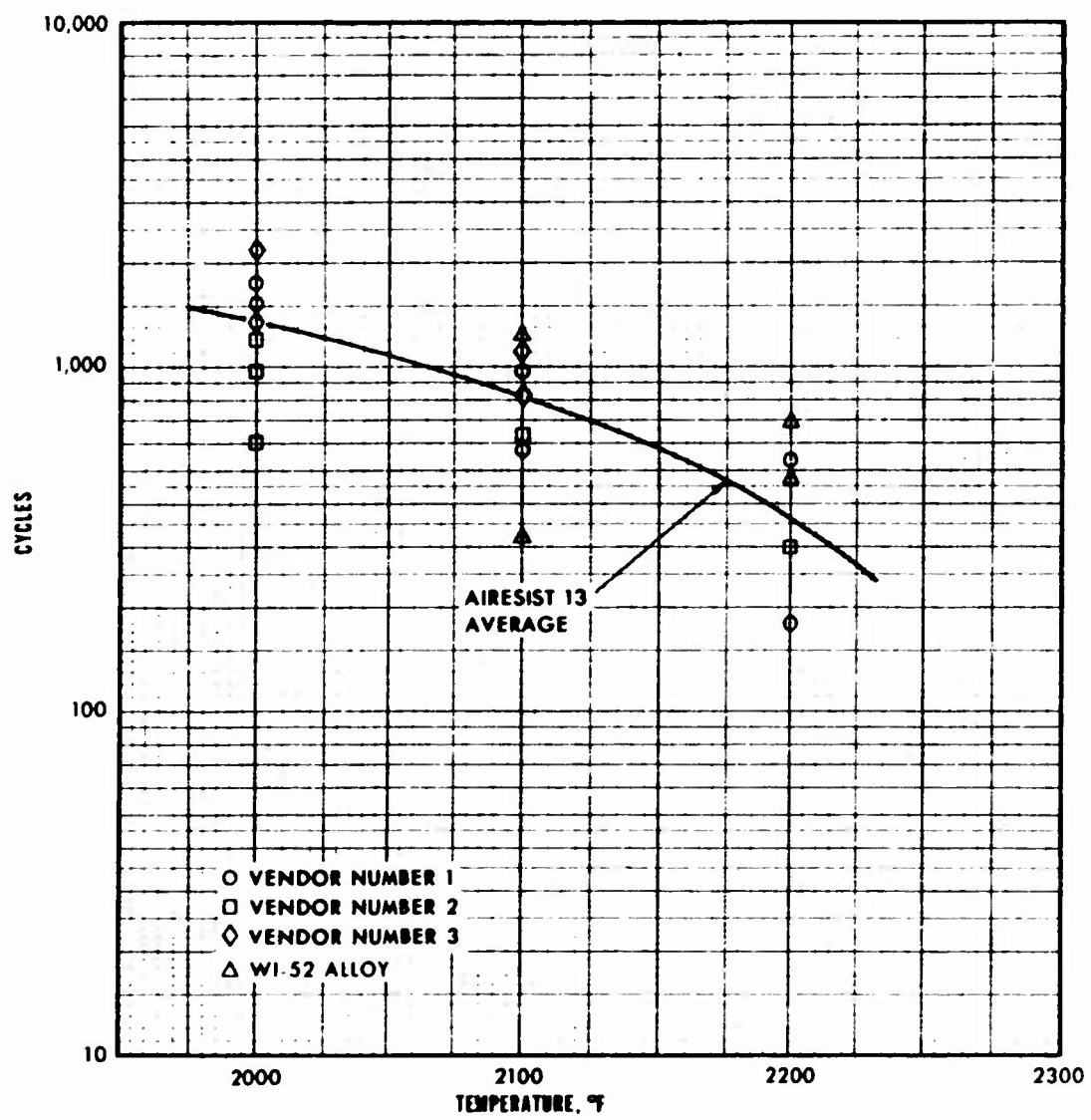Cycles to Initial Cracking.

201

Figure 149. AiResist 13 – Thermal-Fatigue
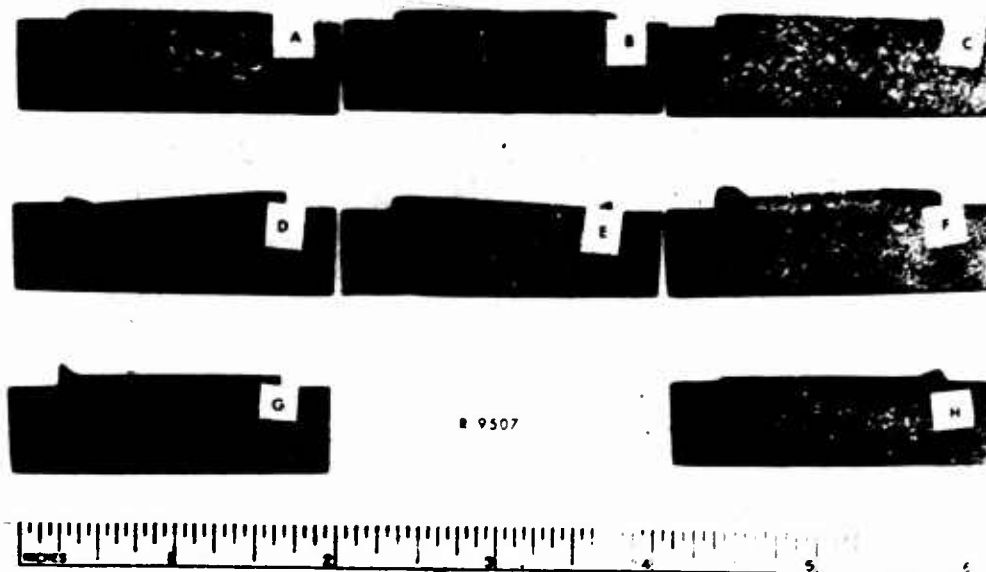Cycles to Failure.

Figure 150. Grain Size of Cast Thermal-
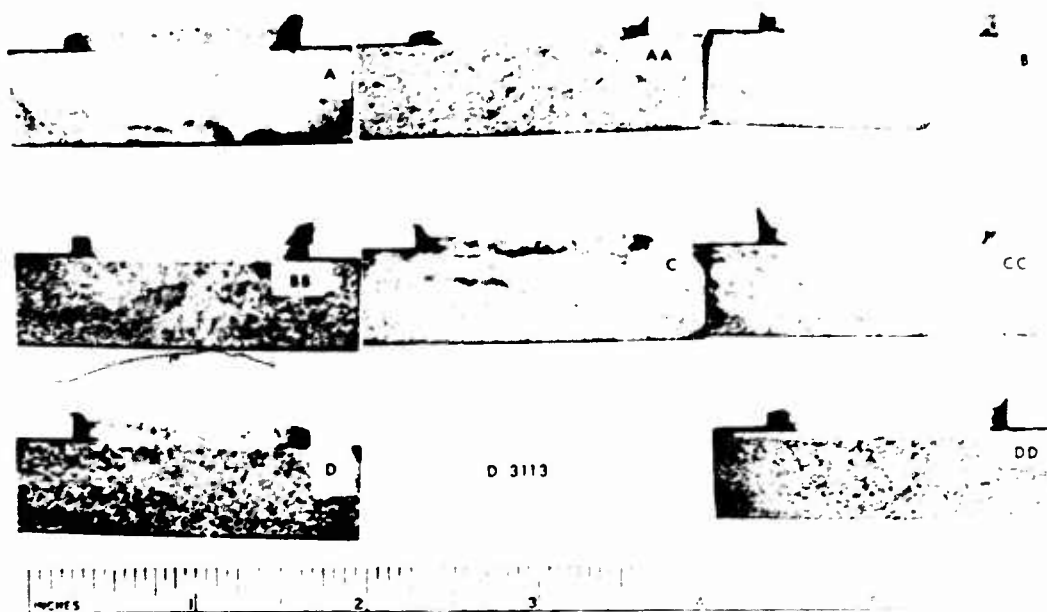Fatigue Specimens, Vendor No. 1
AiResist 13 Material.

Figure 151. Grain Size of Cast Thermal-
Fatigue Specimens, Vendor No. 2
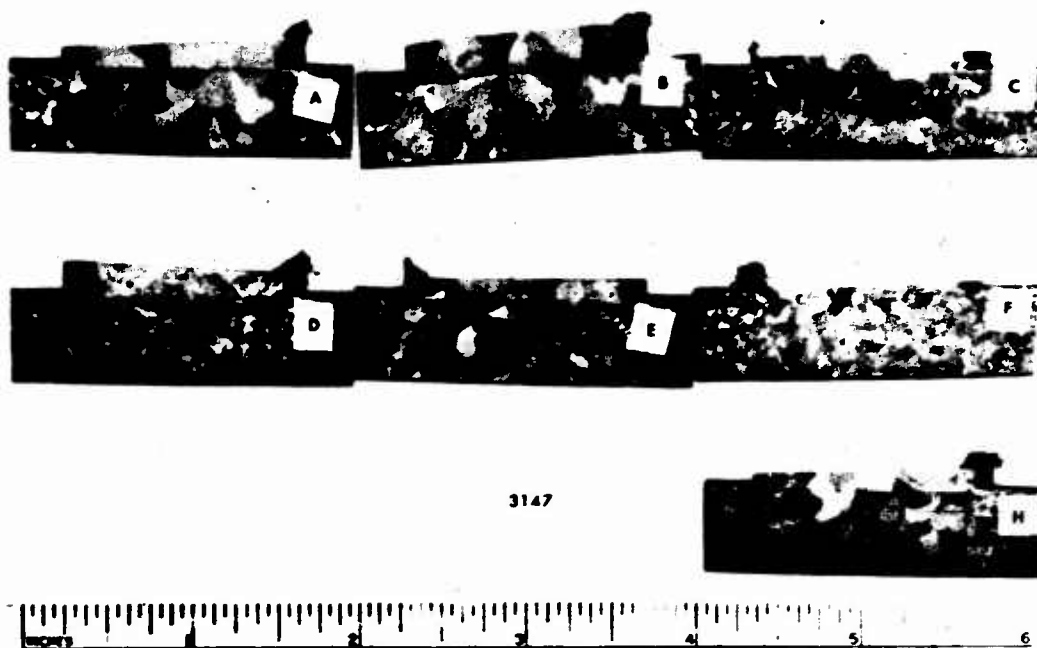AiResist 13 Material.

203

Figure 152. Grain Size of Cast Thermal-Fatigue
Specimens, Vendor No. 3
AiResist 13 Material.

2.   IN-100 - IN-100 thermal-fatigue tests were
     conducted at 2000°, 2100°, and 2200°F. The
     test results are presented in Table XXXVII.
     Test results for INCO 713C also were included
     as a basis for comparison. The results showed
     that IN-100 and INCO 713C have similar thermal-
     fatigue properties. The data scatter that was
     observed was considered to be abnormal and
     necessitated reruns of certain tests in an
     attempt to gain more consistent values. The
     scatter in the recorded data was not signif-
     icantly influenced by the test temperature.
     Only one test was completely discounted:
     Specimen No. C, Test No. 2 (50-percent prime,
     50-percent revert) at 2000°F, which showed very
     low cycles to failure.

| | | | Test | | Cycles to | |
Material	Heat	Specimen No.	Temp (°F)	Test No.	Initial Crack	Cycles to Failure*
IN-100	100% prime	C	2000	1	897	1497
	50% prime, 50% revert	C	2000	1	1179	2469
		C	2000	2	59	59
		D**	2000	1	1439	1798***
	100% revert	G	2000	1	659	1377
		G	2000	2	954	2394
INCO 713C		C	2000	1	1197	1677
		C	2000	2	777	¹497
IN-100	100% prime	D	2100	1	463	1607
		D	2100	2	134	1612
	50% prime, 50% revert	B	2100	1	120	240
		B	2100	2	1164	1405
	100% revert	E	2100	1	465	1048
		E	2100	2	278	278
INCO 713C		B	2100	1	1004	1375
		B	2100	2	1150	1610
IN-100	100% prime	A	2200	1	61	61
		A	2200	2	310	375
		C**	2200	1	57	117
	50% prime, 50% revert	A	2200	1	122	302
		A	2200	2	62	62
	100% revert	A	2200	1	62	62
		A	2200	2	70	375
		H**	2200	1	60	60
		H**	2200	2	60	60
INCO 713C		A	2200	1	127	505
		A	2200	2	292	292

*Failure = when crack propagated across the leading edge of the test specimen.
**Test reruns.
***Test discontinued; 3/4 cracked.

205

Except for the preceding case, it was observed
that the IN-100 specimens from the 50-percent
prime, 50-percent revert heat exhibited slightly
better resistance to thermal fatigue than the
specimens from the 100-percent prime and 100-
percent revert IN-100 heats. This is shown in
Figures 153 and 154, which present cycles to
crack initiation and cycles to failure versus
temperature, respectively.

Figures 155 and 156 illustrate the grain size
of each of the test specimens prior to testing.
The grain size is fairly uniform from test bar
to test bar in each alloy heat. All of the
test specimens were cast under identical con-
ditions.

All specimens were examined by X-ray and
fluorescent-penetrant methods prior to testing.
No material defects were found.
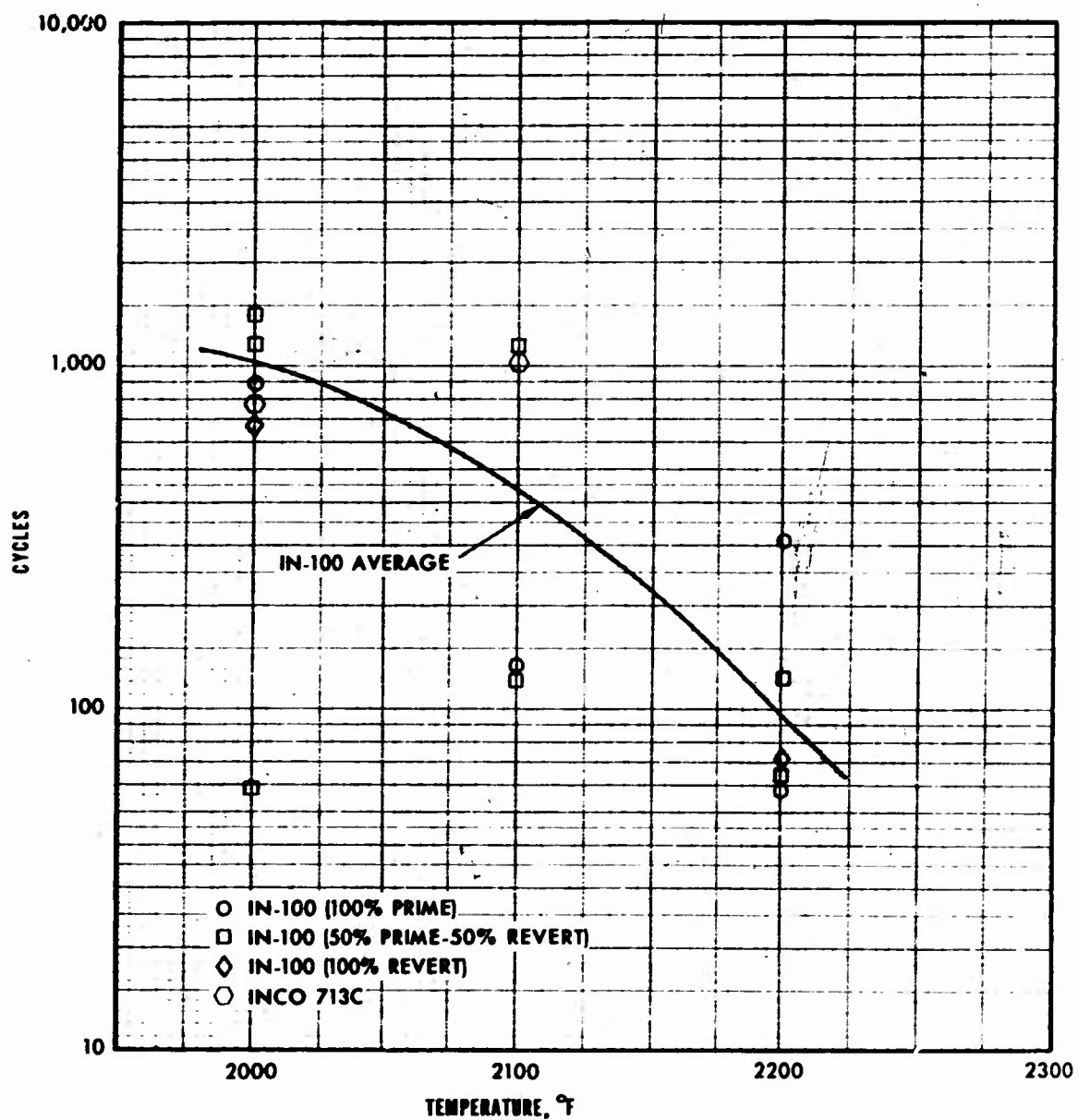
Figure 153. IN-100 – Thermal-Fatigue
Cycles to Initial Cracking.

207
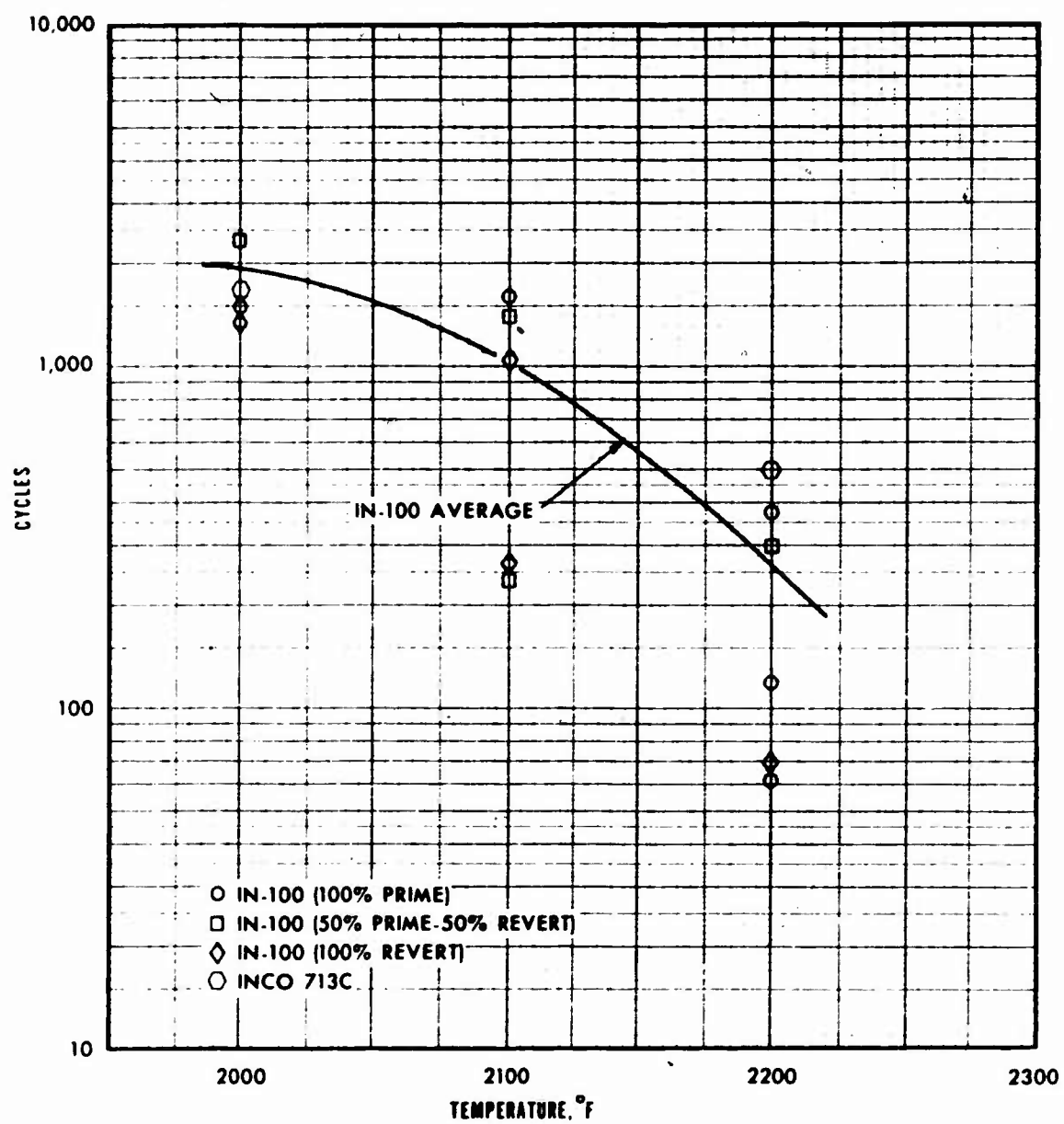
Figure 154.   IN-100 - Thermal-Fatigue
Cycles to Failure.

208
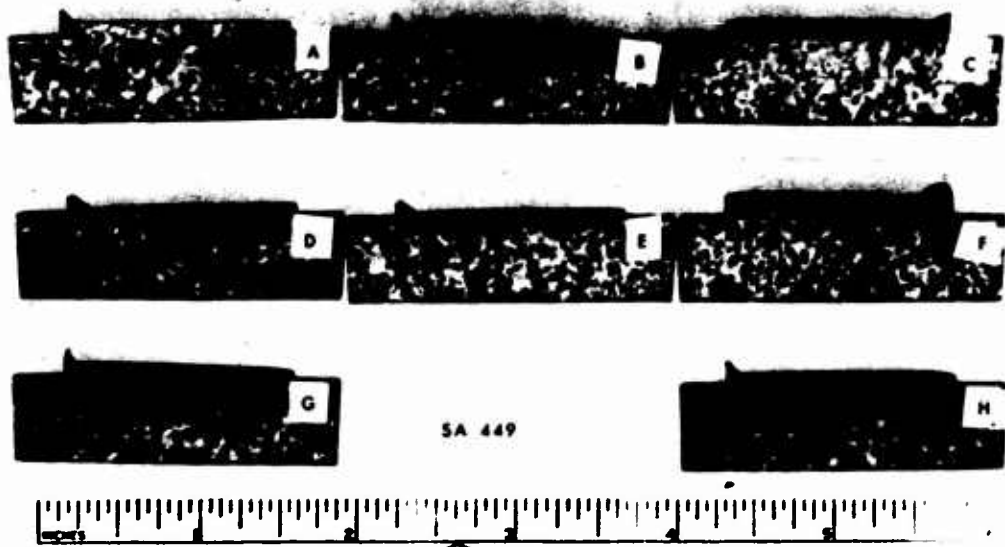
Figure 155. Grain Size of Cast Thermal-
Fatigue Specimens, IN-100
100-Percent Prime.
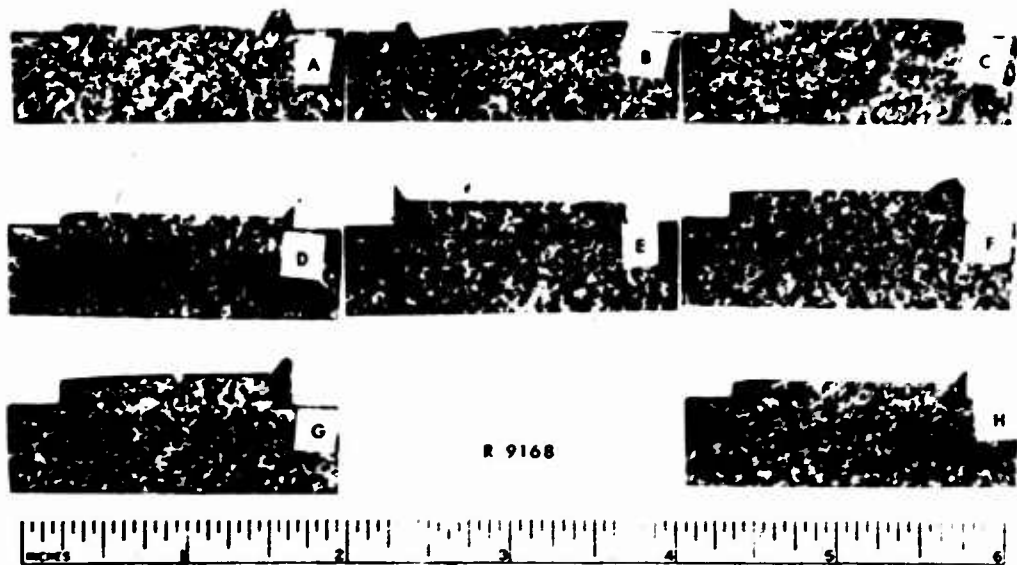
Figure 156. Grain Size of Cast Thermal-
Fatigue Specimens, IN-100
50-Percent Prime, 50-Percent
Revert.

209
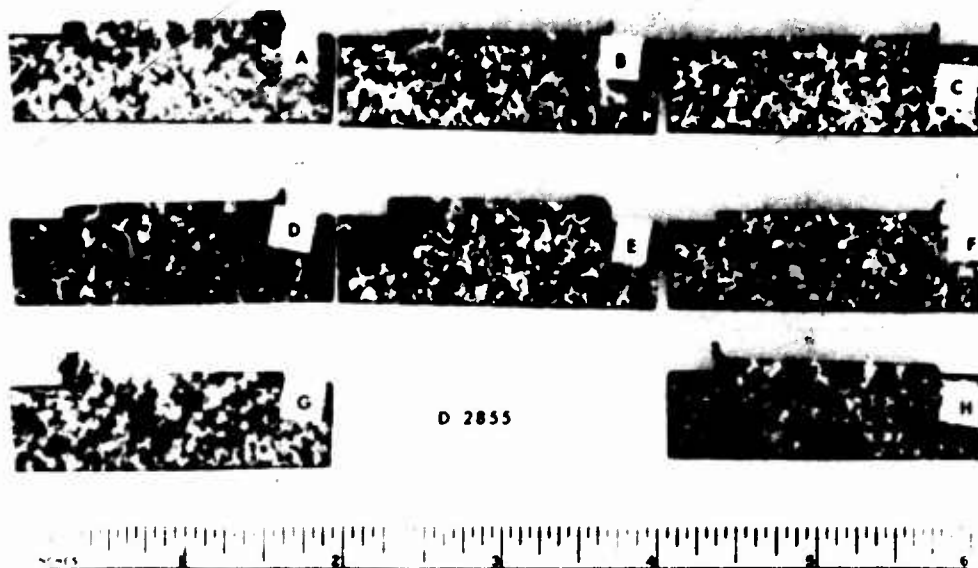
Figure 157. Grain Size of Cast Thermal-
Fatigue Specimens, IN-100
100-Percent Revert.
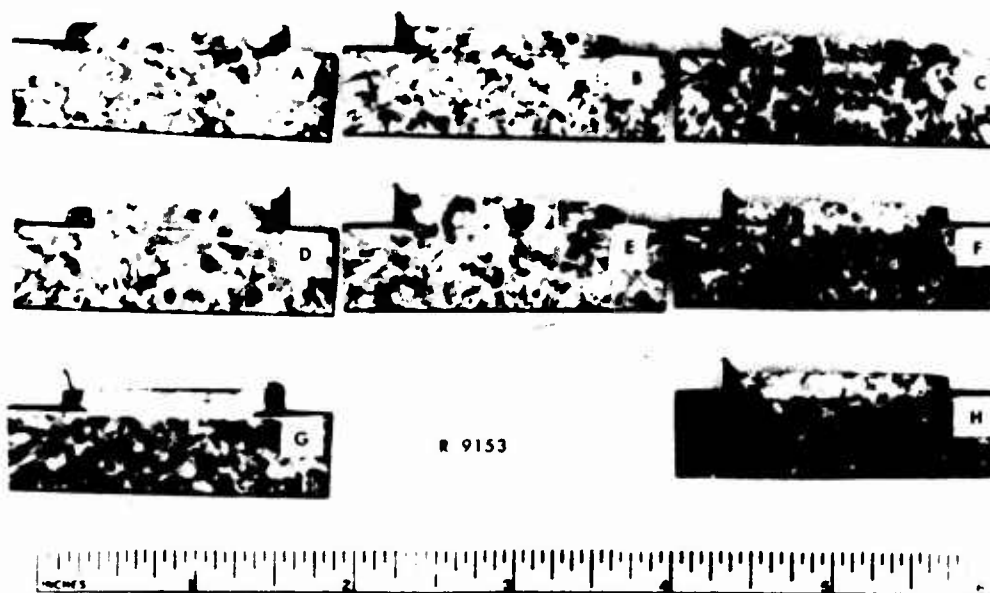
Figure 158. Grain Size of Cast Thermal-
Fatigue Specimens, INCO 713C.

5.5   SUMMATION OF AIRESIST 13 AND IN-100 SPECIMEN TEST RESULTS

The extensive material properties specimen test program that
was conducted served to document the temperature capabilities
of both AiResist 13 and IN-100 materials.

The test results of AiResist 13 demonstrate the extended tem-
perature capability of this relatively new cobalt-base alloy.
Although there are a few cast cobalt-base alloys that have
greater strength, AiResist 13 exhibits a vast improvement
in corrosion resistance with equally good castability. In
addition, it was found that AiResist 13 can be heat-treated
for improved strength. Thus, AiResist 13 has established its
usefulness as a high-temperature turbine alloy for stationary
turbine components in the 2000°F range.

The test results of IN-100 demonstrate the excellent elevated-
temperature mechanical properties of this nickel-base alloy.
Good high-temperature strength along with a relatively low
density makes IN-100 an attractive alloy to use for rota-
tional turbine components in the 2000°F range.

6. CONCLUSIONS

The objective of the materials research investigation, namely, to develop a material that could be used for turbine components with application in a 2400°F uncooled, small gas turbine, was not accomplished. Three major items were unresolved, which precluded the realization of the program goal:

1. Insufficient ductility in the beryllides for use in either the stator or rotor components. The turbine design required a minimum of 1.0 percent elongation at 1800°F. Measurable ductility in Composition 1 was not achieved below 2000°F, and efforts to increase ductility in Composition 2 candidates were not successful.

2. Insufficient stress-rupture strength in the beryllides for use in the rotor component. While four Composition 2 candidates displayed adequate stress-rupture strength for the stator design (200 hours at 2500 psi and 2400°F), they did not approach the rotor design requirement of 200 hours at 8000 psi and 2200°F.

3. Prohibitive fabrication and machining costs of the beryllides. While methods of fabricating and machining were developed that were sufficient for this program, manufacturing beryllide turbine components on any type of production basis by these methods would be extremely costly.

Certain work was accomplished, however, that could have an influence on future material research programs of a similar nature:

1. Development of sufficient test data to substantiate that IN-100 is a suitable material for rotational turbine components in the 2000°F operational range.

2. Development of sufficient test data to substantiate that AiResist 13 is a suitable material for stationary turbine components in the 2000°F operational range.

3. Development of fabrication processes that allowed the manufacture of beryllides of uniform and reproducible quality.

4. Development of machining techniques for the fabrication of beryllide parts.

5. Development and test of beryllide compositions that (a) exhibited good oxidation resistance (less than 50 mg per sq in. weight change at 1600°, 1700°, 1800°, and 2400°F for 200 hours) and minimal "pest" reaction; (b) displayed measurable ductility down to 2000°F; and (c) displayed stress-rupture strength in excess of 200 hours at 2500 psi and 2400°F.

6. Development of sufficient test data on a beryllide composition (Composition 1) to facilitate turbine design activities.

7. Development of a cascade test rig, including instrumentation, combustors, and a control system, that simulated temperature conditions encountered during starting and normal operation of a 2400°F turbine with the design parameters of the subject uncooled turbine.

213

7. RECOMMENDATIONS

Although the general suitability of beryllides for high-temperature turbine component application has not yet been demonstrated, the intermetallic system should not be considered ineligible for continued research efforts. Requirements for increasingly higher turbine operating temperatures force material selection into the areas of ceramics, refractory metals, composites, and intermetallics. Each of these material classes is characterized by one or more serious limitations which research must resolve before practical high-temperature structural application can be investigated. However, it is believed that a review of the possible advantages and limitations revealed by this program indicate that the intermetallics afford enough potential to warrant continued material research.

Therefore, while it is not recommended at this time that further effort be expended on utilizing the beryllides as high-temperature turbine component material, it is recommended that material programs researching the intermetallics be continued to determine means by which low-temperature ductility can be increased. With the occurrence of such a technical breakthrough, it is believed that the oxidation resistance and long-time strength qualities of the intermetallics could also be further increased to the extent that a promising high-temperature turbine component program could be instituted.

DOCUMENT CONTROL DATA - R & D

(Security classification of title, body of abstract and indexing annotation must be entered when the overall report is classified)

1. ORIGINATING ACTIVITY (Corporate author)	2a. REPORT SECURITY CLASSIFICATION
AiResearch Manufacturing Company 402 S. 36th Street Phoenix, Arizona	Unclassified
	2b. GROUP

3. REPORT TITLE

2400°F UNCOOLED TURBINE/MATERIAL PROGRAM
VOLUME I - MATERIALS INVESTIGATION

4. DESCRIPTIVE NOTES (Type of report and inclusive dates)

Final Technical Report

5. AUTHOR(S) (First name, middle initial, last name)

Milt S. Roush
Fritz Weber

6. REPORT DATE	7a. TOTAL NO. OF PAGES	7b. NO. OF REFS
July 1970	238	3

8a. CONTRACT OR GRANT NO.	9a. ORIGINATOR'S REPORT NUMBER(S)
DA 44-177-AMC-183(T)	
b. PROJECT NO.	USAAVLABS Technical Report 70-32A
Task 1G162204A01409	
c.	9b. OTHER REPORT NO(S) (Any other numbers that may be assigned this report)
d.	

10. DISTRIBUTION STATEMENT

This document is subject to special export controls, and each transmittal to foreign governments or foreign nationals may be made only with prior approval of U. S. Army Aviation Materiel Laboratories, Fort Eustis, Virginia 23604.

11. SUPPLEMENTARY NOTES	12. SPONSORING MILITARY ACTIVITY
Volume I of a 3-volume report	U.S. Army Aviation Materiel Laboratories Fort Eustis, Virginia

13. ABSTRACT

This report describes a materials investigation conducted to select, evaluate, and develop materials for application in the turbine component of a 2400°F turbine inlet temperature uncooled gas turbine. Additional turbine parameters of the turbine design (Volume II) included a compressor pressure ratio of 10:1, an airflow rate of 5 lb per sec, a rotational speed of 38,000 rpm, and a predicted total-to-total efficiency of 88 pct. Mechanical and physical property tests of a beryllide intermetallic developed under company sponsorship showed insufficient stress-rupture strength at 2400°F for stator or rotor application and insufficient ductility below 2000°F. Studies conducted to improve these properties were not successful, although stress-rupture properties were improved to exceed the minimum stator requirement. Tests of beryllide oxidation specimens and stator vanes in a 2400°F cascade rig simulating engine transient and steady-state conditions verified that stress-rupture strength and ductility were inadequate. It was concluded that extensive experimental materials research on the beryllide compositions is required before they can be applied in the 2400°F uncooled turbine. Mechanical and physical property tests were also conducted on high-temperature alloys IN-100 and AiResist 13. Results showed that IN-100 was suited for rotating turbine components in the 2000°F range and that AiResist 13 was suited for stationary turbine parts in the 2000°F range.

14. KEY WORDS	LINK A		LINK B		LINK C	
	ROLE	WT	ROLE	WT	ROLE	WT
2400°F Uncooled Turbine						
Beryllide Turbine Material						
AiResist 13						
IN-100						
Material Specimen Testing						